Nanovectorisation de la curcumine sous forme liposomale : interactions biomolécule / membrane, transferts et cytotoxicité dans des systèmes in vitro

Mahmoud Hasan

UNIVERSITE DE LORRAINE

Ecole Doctorale Ressources Procédés Produits Environnement

Laboratoire d'Ingénierie des Biomolécules

THÈSE

Présentée à l'Université de Lorraine par

Mr Mahmoud HASAN

En vue d'obtenir le grade de

DOCTEUR DE L'UNIVERSITE DE LORRAINE

Spécialité : Procédés Biotechnologiques et Alimentaires

Nanovectorisation de la curcumine sous forme liposomale : interactions biomolécule / membrane, transferts et cytotoxicité dans des systèmes *in vitro*

Soutenue publiquement le 17 Novembre 2015 devant la commission d'examen

Rapporteurs	Mr B. Frisch	Directeur de Recherche au CNRS, Strasbourg
	Mr P. Villeneuve	Professeur au CIRAD, Montpellier
Examinateurs	Mme A. Girard-Egrot	Professeur à l'Université de Lyon 1, Lyon
	Mme C. Frochot	Directeur de Recherche au LRGP, Nancy
	Mme E. Arab Tehrany	Professeur à l'Université de Lorraine, Nancy
	Mr M. Linder	Professeur à l'Université de Lorraine, Nancy

REMERCIEMENTS

Ce travail a été réalisé au laboratoire d'ingénierie des biomolécules (LIBio) de l'Ecole Nationale Supérieure d'Agronomie et des Industries Alimentaires (ENSAIA) - Université de Lorraine, sous la direction du Professeur Michel Linder et sous la co-direction du Professeur Elmira Arab-Tehrany.

Je tiens tout d'abord à remercier Monsieur Michel Fick, Directeur de l'ENSAIA, pour m'avoir sélectionné en Syrie et de m'avoir accueilli à l'ENSAIA.

Je tiens également à remercier Monsieur Michel Linder pour m'avoir confié ce travail, guidé tout au long de ces années, et pour avoir contribué à la qualité des raisonnements et des interprétations.

De la même façon, je tiens à adresser à Madame Elmira Arab-Tehrany, mes remerciements pour avoir co-encadré avec justesse et exigence ce travail. Je tiens ici à lui adresser un merci tout particulier pour sa disponibilité et ses conseils lors de l'interprétation des résultats et son apport scientifique.

Je suis très honoré par la présence dans le jury de Monsieur Benoit Frisch, directeur de recherche au CNRS, à l'Université de Strasbourg, de Monsieur Pierre Villeneuve, professeur au CIRAD, à Montpellier, de Madame Céline Frochot, directrice de recherche au CNRS (LRGP) à Université de Lorraine, ainsi que de Madame Agnès Girard-Egrot, professeur à l'Institut de Chimie et Biochimie Moléculaires et Supramoléculaires de l'Université Lyon 1.

Je souhaiterais aussi remercier Mademoiselle Nabila Belhaj, pour son aide, pour toutes ses explications qui ont permis une meilleure interprétation des résultats obtenus notamment avec l'appareil Xcelligence.

Je souhaiterais également remercier Monsieur Cyril Khan, pour son aide concernant l'étude statistique et la génération des figures sur le logiciel MATLAB.

Je remercie également Madame Muriel Barberi-Heyob de nous avoir permis d'effectuer les manipulations *in vitro* dans son laboratoire, ainsi que Monsieur Hamanou Benachour (post doctorant au CRAN) pour nous avoir assisté pendant les manipulations sur l'appareil Xcelligence.

Je tiens aussi à remercier Monsieur Cédric Paris, ingénieur de recherche au LIBio, pour les analyses structurelles sur LC-MS afin de déterminer les différentes espèces moléculaires des classes lipidiques.

Je remercie également les permanents de l'ENSAIA qui ont contribué d'une manière ou d'une autre dans la réalisation de ce travail : Carole Jeandel, Carole Perroud, Cécile Mangavel, Aurélie Chapé et bien d'autres personnes à l'ENSAIA et ailleurs qui méritent mes remerciements pour leur aide et / ou leur soutien.

Je tiens également à remercier Monsieur Jaafar Ghanbaja pour sa disponibilité concernant les travaux en microscopie électronique à transmission (Service Commun de Microscopie, Université de Lorraine).

Je souhaiterais aussi remercier les personnes qui m'ont aidé pour mieux comprendre les résultats obtenus : Monsieur Florentin Michaux, Maître de Conférences à l'ENSAIA, pour les manipulations sur le SAXS, Monsieur Jordane Jasniewski, Maître de Conférences à l'ENSAIA, pour les manipulations sur l'appareil Zetasizer, Monsieur Ghazi Ben Messaoud, doctorant, pour les manipulations sur le rhéomètre et Monsieur Adrien Jacquot, doctorant, pour les marquages du chitosane et des liposomes.

Mes remerciements s'adressent également à toute l'équipe du laboratoire, notamment aux doctorants et post-doctorants, Abdulhadi, Charlotte, Jennifer, Mohammed, Marie, Mouna, Magda, Yoana, Rana, Nadine, Hind et tous ceux que je n'ai pas pu citer.

Je n'oublierai pas mon épouse Reem Mathbout pour sa patience, sa compréhension pendant la rédaction et son aide pour la préparation à la soutenance. Je pense aussi à ma petite princesse Maryam.

Un ENORME merci à ma famille : mes parents, mes frères et mes sœurs, qui n'ont jamais cessé de croire en moi et m'ont soutenu avec beaucoup d'amour et de confiance tout au

long de ma vie. Merci pour votre soutien inconditionnel. Et je n'oublierai pas mes beaux parents, beaux frères et belles sœurs, pour leur aide, leur confiance et leur soutien.

Toute la communauté syrienne à Nancy, résidents et étudiants avec qui j'ai passé de grands moments de joie, d'amitié et de partage est aussi remerciée.

Enfin, je remercie toutes les personnes qui m'ont aidé de près ou de loin, tout au long de ces années.

PUBLICATIONS et COMMUNICATIONS

Publication de rang A

Publications acceptées

1. Hasan, M., Belhaj, N., Benachour, H., Barberi-Heyob, M., Kahn, C.J.F. Jabbari, E., Linder, M., Arab-Tehrany, E. 2014. Liposome encapsulation of curcumin: Physico-chemical characterizations and effects on MCF7 cancer cell proliferation. International Journal of Pharmaceutics. Volume 461, 1–2, 519–528.
2. Bouarab, L., Maherani, B., Kheirolomoom, A., Hasan, M., Aliakbarian, B., Linder, M., Arab-Tehrany, E. 2014. Influence of lecithin–lipid composition on physico-chemical properties of nanoliposomes loaded with a hydrophobic molecule. Colloids and Surfaces B: Biointerfaces, Volume 115, 197–204.

Publications soumises

3. Hasan, M., Belhaj, N., Kahn, C., Tamayol, A., Arab-Tehrany, E., Linder, M. 2015. Enhancing anti-cancer activity of curcumin on MCF7 cells through O/W nanoemulsions based on marine and plant lipids.
4. Hasan, M., Arab-Tehrany, E. , Belhaj, N., EL-Reffaei, W. H., Benachour, H., Kahn, C.J.F., Tamayol, A., Barberi-Heyob, M., Linder, M. 2015.Chitosan-coated liposomes encapsulation of curcumin for enhanced cancer MCF7 cell destruction.
5. Hasan, M., Latifi, S., Kahn, C., Tamayol, A., Linder, M., Arab-Tehrany, E. 2015. Curcumin-loaded natural salmon nanoliposomes with high effect on primary cortical neurons in vitro.
6. Hasan, M., Ben Messaouad, G., Michaux, F., Tamayol, A., Kahn, C., Belhaj, N., Linder, M., Arab-Tehrany, E. 2015. Chitosan-coated liposomes encapsulating curcumin: Study lipid-polysaccharide interactions and nanovesicles behavior.

Publications en cours de rédaction

7. Hasan, M., Tamayol, A., Kahn, C., Belhaj, N., Linder, M., Arab-Tehrany, E. Chitosan-coated liposomes encapsulating curcumin: physicochemical characterizations and study the release kinetics of encapsulated curcumin in simulated environment.

Communications Internationales

1. Hasan, M., Arab-Tehrany, E., Barberi-Heyob, M., Kahn, C., Jabbari, E., Linder, M. 2015. Influence of curcumin-loaded chitosan liposome on MCF7 cytotoxicity. 106rd AOCS Annual Meeting & Expo. May 3-6, 2015, Orlando, Florida, USA.
2. Arab-Tehrany, E. Hasan., M., Belhaj, N., Linder, M. 2013. Curcumin encapsulated in nanoliposome as drug delivery for cancer treatment. Drug Discovery and Therapy World Congress 2013, Boston. 3-6 June.
3. Linder, M., Hasan, M., Arab-Therany, E. 2014. Oméga 3 à longue chaîne, de la Production à la Consommation : Quelle Balance Aujourd'hui et Demain? SFEL, 17 octobre Paris.
4. Aliakbarian, B., Hasan, M., Painia, M., Casazza, A.A., Comotto, M., Perego, P., Arab-Tehrany, E. (2014). Nanoliposome encapsulation of apigenin. The 3rd International Congress on Natural Sciences and Engineering, May 7-9, 2014, Kyoto, Japan.

ABBREVIATIONS

AA	Acide arachidonique
AAPH	2,2′-azobis (2-amidinopropane) hydrochloride
ABTS°⁺	Acide 2,2'–azinobis (3-éthylbenzothiazoline-6-sulfonique)
ADN	Acide désoxyribonucléique
AGMI	Acides gras monoinsaturés
AGPI	Acides gras polyinsaturés
AGPI-LC	Acides gras polyinsaturés à longue chaîne
AGS	Acides gras saturés
ANOVA	Analyse de la variance
APR	Activité de réduction de puissance
ATP	Adénosine tri-phosphate
ATR	Attenuated Total Reflectance
ALA	Acide α-linolénique
B-27	Serum-free supplement for neural cell culture
BF_3	Trifluorure de bore
BSA	Bovine serum albumin
$CaCl_2$	Chlorure de calcium
°C	Degré celsius
CCM	Chromatographie sur couche mince
CDAI	Crohn's Disease Activity Index
CH-LP	Chitosan-coated liposome
CHO	Cholesterol
CI	Cell Index
CI50	Concentration inhibitrice médiane
COX-2	Cyclooxygénase 2
CPG	Chromatographie en phase gazeuse
CRP	Protéine C réactive
CS	Chitosan
CUR	Curcumin
Da	Dalton
DA	Degré d'acétylation

d	Distance de répétition ou distance de Bragg
DD	Degré de désacétylation
DAG	Diacylglycérols
DGLA	Acide di-homo-y-linoléique
DHA	Acide docosahexaénoïque
DIV	Days *in vitro*
DMSO	Diméthylsulfoxyde
DLS	Dynamic Light Scattering
DMPD°$^{+}$	N, N, dichlorhydrate de N-diméthyl-p-phénylènediamine
DO	Densité optique
DPA	Acide docosapentaénoïque
DPH	Diphenylhexatriene
DPPH°	1,1-diphenyl-2-picrylhydraxyl
DTGS	Deuterated-Triglycine Sulfate
Dz	Z-average mean
E/H	Emulsion eau dans huile
ENSAIA	École Nationale Supérieure d'Agronomie et des Industries Alimentaires
EPA	Acide eicosapentaénoïque
ETA	Acide eicosatétraénoïque
FAMEs	Fatty acid methyl esters
FCS	Fetal calf serum
Fe $^{2+}$	Ions ferreux
Fe^{3+}	Ions ferriques
FFA	Free fatty acid
FID	Détecteur à ionisation de flamme
FTIR	Fourier Transform Infrared Spectroscopy
FITC	Fluorescein isothiocyante
g	Gramme
GI	Gastro-intestinal
GMO	Glyceryl monoleate
GLA	Acide y-linolénique
GSH	Glutathion réduit

GUV	Giant unilamelar vesicles
H^+	Hydrogen ion
H/E	Emulsion huile dans eau
HCL	Acide chlorhydrique
He/Ne	Helium–neon
HPLC	Chromatographie liquide à haute performance
HO°	Hydroxyle
Hz	Hertz
IF	Immunofluorescence
IR	Infra-rouge
K^+	Ion de potassium
KDa	Kilodalton
Kg	Kilogramme
KHz	Kilohertz
L	Liter
LA	Acide linoléique
LiBio	Laboratoire d'Ingénierie des Biomolécules
LN	Lipides neutres
Log P	Coefficient de partage
LOX	Lipoxygénase
LP	Lipide polaire
L-PC	Lysophosphatidylcholine
LUV	Large unilamelar vesicles
M	Molaire
MCF7	Human breast cancer cell line
MDA	Malondialdéhyde
MICI	Maladies inflammatoires chroniques de l'intestin
min	Minute
ml	Milliliter
MLV	Multilamellar vesicles
mg	Milligramme
mm	Millimeter

mM	Millimolaire
MPTP	1-methyl-4-phenyl-1,2,3,6-tetrahydropyridine
mV	Millivolts
mW	Milliwatt
n-3	Oméga-3
n-6	Oméga-6
NaCl	Chlorure de sodium
NCI	Normalized cell index
nd	Non déterminé
NF-κB	Nuclear factor kappa-light-chain-enhancer of activated B cells
ng	Nanogramme
$NH3^+$	Protonated amino groups
NIPAAm	N-isopropylacrylamide
nm	Nanométre
NO	Oxyde nitrique
NTA	Nanoparticle tracking analysis
$O2^{\circ-}$	Superoxyde
OH^-	Hydroxide ions
O/W	Oil-in-water emulsions
P	Polarization value
PBS	Phosphate-buffered saline
PC	Phosphatidylcholine
PDI	Polydispersity index
PE	Phosphatidylétanolamine
PEG	Polyethylene glycol
PEG-PEI	Polyethylene glycol-poly (ethylene imine)
PFA	Paraformaldehyde
pH	Potentiel hydrogène
PHEMA	Poly (2-hydroxyethyl methacrylate)
PG	Phosphatidylglycérol
PI	Phosphatidylinositol
PKa	Constante d'acidité

PL: Phospholipides

PLGA Polylactic-co-glycolic acid

$PO2^-$ Hypophosphite ion

PS Phosphatidylsérine

PUFA Polyunsaturated fatty acids

R° Radical libre

RBF Round bottomed flask

RI Refractive index

RH Acide gras insaturé

Rh Hydrodynamic radius

RO° Radical alcoxyle

ROO° Radical peroxyle

ROOH Radical hydroxyperoxyle

ROS Reactive Oxygen Species

RPM Revolutions per minute

RPMI Roswell park memorial institute medium

RT Room temperature

S Second

SAXS Small Angle X-rays Scattering

SD Standard deviation

SEM Standard error of the mean

SGF Simulated gastric fluid

SIF Simulated intestinal fluid

SLNs Solid lipid nanoparticles

SM Sphingomyéline

SMEDDS Self Micro emulsifying drug delivery system

SOD Superoxyde dismutase

SUV Small unilamelar vesicle

TAG/TG Triacylglycérols

t1/2 Demi-vie d'élimination d'un médicament

TEM Transmission electron microscopy

TAGs Triglycerides

TMA–DPH	Trimethylammonium diphenylhexatriene
tr/min	Tour par minute
UV-Vis	Ultraviolet-visible
µg	Microgramme
µl	Microlitre
µM	Micromolaire
Vs	Vitesse de sédimentation
XTT	2,3-Bis(2-methoxy-4-nitro-5-sulfophenyl)-2H-tetrazolium-5-carbox-anilide
ζ-Potential	Zeta potential

Sommaire général

Liste des tableaux

Liste des figures

Introduction générale

I. Introduction générale

Cette étude s'inscrit dans la continuité des travaux de recherche menés au Laboratoire d'Ingénierie des Biomolécules sur les lipides polaires d'origine marine extraits par des procédés « verts » sans utilisation de solvant organique. Principale source de phospholipides très riches en acides gras polyinsaturés à longue chaîne de la série n-3, les co-produits de l'industrie de filetage et plus précisément les têtes de saumon, ont fait l'objet de nombreux travaux de recherche depuis une quinzaine d'années au laboratoire, compte tenu des effets bénéfiques des « omégas 3 » sur la santé (stress, maladie cardiovasculaire, réponses immunitaires, maladies inflammatoires…). Ces acides gras polyinsaturés à longue chaîne, dont les chefs de file sont l'acide docosahexaénoïque (DHA) et l'acide éicosapentaénoïque (EPA), jouent un rôle important au niveau du système nerveux central, sur le développement cognitif, l'apprentissage, la plasticité des neurones, la synaptogénèse ainsi que dans la transmission synaptique. Nous voyons là l'intérêt de trouver de nouveaux moyens de vectoriser ces biomolécules vers des organes cibles comme le cerveau, dans un contexte actuel où on assiste à une augmentation quasi exponentielle des maladies neurodégénératives.

Le but de notre étude, qui entre dans le cadre d'une recherche interdisciplinaire en physico-chimie et en biologie, est de mettre en œuvre des systèmes lipidiques (nanoémulsions, nanoliposomes) présentant une fluidité membranaire spécifique en raison de leur richesse en AGPI-LC. L'étude de leurs propriétés physico-chimiques (solubilité, taille, mobilité électrophorétique, efficacité d'encapsulation) sera une première étape afin de mieux maîtriser l'encapsulation et la vectoriser d'une biomolécule d'intérêt modèle, déjà étudiée au LIBio, la curcumine présentant des propriétés recherchées, tout en restant labile et peu soluble.

Aujourd'hui, nous assistons à un regain d'intérêt des consommateurs pour les produits naturels et de nombreux industriels mettent en avant les effets de principes actifs issus de matières premières végétales, tels que les flavonoïdes, les curcuminoïdes, qui présentent un pouvoir antioxydant recherché. Leurs activités antioxydantes reconnues et démontrées ne font pas de ces biomolécules que de simples antioxydants. De nombreuses études leurs sont consacrées en raison de leur propriétés anti-inflammatoires, antibactériennes et anti-cancers. La curcumine est un polyphénol de couleur jaune de faible poids moléculaire, largement

utilisé comme agent de coloration et comme épice dans de nombreux aliments. En raison de sa faible solubilité en solution aqueuse et de sa faible absorption par voie orale, de nouvelles formulations sont développées pour augmenter son absorption et renforcer son activité thérapeutique, comme la complexation avec des cyclodextrines et des phospholipides permettant une vectorisation sous forme d'émulsion, micellelaire ou liposomale.

L'objectif principal de ce travail est de mettre en évidence les effets d'une double vectorisation de molécules, faiblement bio-disponibles : ici, la curcumine dans un vecteur nanoémulsionné (nanoliposomes, nanoémulsions et nanoparticules à base de biomatériaux biodégradables), stabilisé par des lipides polaires, naturellement riches en acides gras polyinsaturés à longue chaîne comme l'EPA et le DHA.

Quant aux objectifs secondaires de ce projet, ils s'inscrivent dans un cadre d'une recherche interdisciplinaire en physico-chimie et en biologie :

- On comparera 3 systèmes de « double vectorisation » : les nanoémulsions, les nanoliposomes et les nanoliposomes enrobés de chitosane,
- Afin d'étudier l'influence de la structure sur les propriétés physicochimiques, nous allons utiliser plusieurs techniques analytiques avant de passer aux études *in vitro* sur cellules cancéreuses et neuronales,
- Une étude des interactions lipides-biomatériaux sera développée avant de présenter les résultats concernant le transfert moléculaire.

Ce travail se divise en plusieurs parties prenant en compte la formulation du vecteur, l'étude de ses propriétés physicochimiques, les interactions avec le principe actif, les cinétiques de relargage de la curcumine dans un environnement gastro-intestinal simulé, ainsi que les effets du complexe en termes de cytotoxicité sur des cellules cancéreuses et issues de neurones (études *in vitro*).

La première partie intitulée « **généralités** », présente les caractéristiques et les propriétés physicochimiques des matières premières lipidiques (huile, lécithines) et de la curcumine, choisies pour cette étude. Les différentes techniques de nanoencapsulation sont également présentées.

Une seconde partie « **matériels et méthodes** » rassemble l'ensemble des méthodes utilisées au cours de ce travail, qui se subdivise ensuite en 6 grands thèmes dont les résultats ont été publiés, présentés en congrès internationaux, en cours de publication et / ou à soumettre.

La partie résultats et discussion rassemble les différents résultats obtenus et mis en forme pour être publiés.

La première étude, intitulée **"Enhancing anti-cancer activity of curcumin on MCF7 cells through O/W nanoemulsions based on marine and plant lipids"**, présente les résultats obtenus à partir de différentes huiles et lécithines d'origine végétale et marine. Les différentes formulations de curcumine préparées sous forme d'émulsion sont ensuite soniquées et homogénéisées sous haute pression puis caractérisées en terme de propriétés physico-chimiques. Les effets de ces complexes comme vecteur hydrophobe sont ensuite étudiés sur des lignées cellulaires de type MCF7 pour caractériser leurs propriétés cytotoxiques sur des cellules cancéreuses.

La seconde étude intitulée **« Liposome encapsulation of curcumin: physico-chemical characterizations and effects on MCF7 cancer cell proliferation »** prend en compte un mode de vectorisation sous forme liposomale uniquement basé sur des lécithines de soja, de colza et marine. L'objectif est ici d'étudier l'influence de la nature et de la longueur des chaînes carbonées des acides gras estérifiés sur un phospholipide sur la taille des nanoliposomes. Le procédé de sonication couplé à une homogénéisation haute pression permet d'obtenir des nanovecteurs multilamellaires. La solubilité de la curcumine est caractérisée en fonction de la phase lipidique et son taux d'encapsulation dépend fortement de cette dernière. La nature du vecteur et la concentration de la curcumine vectorisée seront étudiées sur la cytotoxicité et la prolifération cellulaire de cellules cancéreuses MCF7.

La troisième étude intitulée « **Chitosan-coated liposomes encapsulation of curcumin for enhanced cancer MCF7 cell destruction »** présente des résultats de nanoliposomes vectorisant de la curcumine, associés à un biopolymère naturel, le chitosane. Cette association lipides polaires / chitosane sous forme de coating, est rendu possible par la charge globale négative de surface des vecteurs face aux charges cationiques du biopolymère. Ces

interactions permettent une stabilité du complexe qui lui confère de nouvelles propriétés protectrices et une libération des biomolécules encapsulées, mieux maitrisée.

La morphologie du complexe liposome / curcumine / chitosane est aussi étudiée par microscopie électronique à transmission de manière globale mais aussi au niveau membranaire, où la fluidité dépend fortement du coating de chitosane.

La quatrième étude intitulée « **Curcumin-loaded natural salmon nanoliposomes with high effect on primary cortical neurons *in vitro*** » se focalise sur une forme liposomale principalement constituée de phosphatidylcholine, encapsulant de la curcumine. Nous nous sommes principalement attachés à caractériser son efficacité d'encapsulation, son profil de libération et ses effets sur des cellules neuronales.

Une étude, intitulée « **Chitosan-coated liposomes encapsulating curcumin: Study lipid-polysaccharide interactions and investigate the rheological properties of the systems** », porte sur l'étude des interactions entre les différents composés ainsi que sur les propriétés physico-chimiques de ce complexe. Les interactions impliquées dans la stabilité du complexe liposome / chitosane ont été analysées, notamment par analyses FTIR, avant et après encapsulation de curcumine. La taille et les charges de surface du complexe liposome / chitosane ont été suivies en fonction du pH. Les propriétés rhéologiques ont également été mesurées dans cet environnement. L'influence du coating de chitosane sur les nanoliposomes et la présence de curcumine dans la membrane lipidique ont été étudiées par diffusion aux petits angles des rayons X (SAXS) et les résultats ont permis d'apporter des informations sur la structure, la localisation et les phénomènes de diffusion de la curcumine.

La dernière partie de ce travail, intitulé « **Chitosan-coated liposomes encapsulating curcumin: physicochemical characterizations and study the release kinetics of encapsulated curcumin in simulated environment** », s'est focalisée sur les cinétiques de relargage de la curcumine dans un environnement gastro-intestinal simulé. L'effet du coating de chitosane et les différentes propriétés physico-chimiques, préalablement étudiées, ont été suivies afin de connaître la stabilité du complexe liposome / curcumine au cours des principales étapes de digestion.

Synthèse bibliographique

II. Synthèse bibliographique

II.1 Les lipides

II.1.1 Généralités

Le terme “lipides” n’a pas, à ce jour, une définition fixe et précise. En 1986, Kates définit les lipides comme des substances présentes dans les organismes vivants végétaux et animaux, insolubles dans l’eau mais solubles dans les solvants organiques comme le chloroforme, l’éther ou le benzène, et pouvant présenter de longues chaînes hydrocarbonées.

La classification des lipides peut se baser sur leurs propriétés physicochimiques en prenant en compte leurs propriétés d’écoulement à température ambiante (les huiles sont liquides et les graisses restent cristallisées), leur polarité (lipides polaires ou neutres), leur structure (lipides simples ou complexes). Les lipides peuvent être divisés en différentes classes et la présence d’acides gras essentiels et / ou indispensables pourra jouer un rôle sur la biodisponibilité de ces derniers.

- **les lipides simples** comprennent les acides gras, les acylglycérols, les stérols et leurs esters ainsi que les cires,
- **les lipides complexes** sont constitués de phospholipides, de glycolipides et de sphingolipides (Gbogouri, 2005).

II.1.2 Les acides gras

Les acides gras sont des molécules organiques qui présentent une seule fonction acide organique (carboxyle) à une extrémité. Ils sont formés d’une chaîne carbonée à nombre généralement pair d’atomes de carbone compris entre 4 et 30, avec à l’extrémité terminale, un groupement méthyle. La structure de cette chaîne carbonée peut comporter ou non une liaison éthylénique permettant de les classer en :

- Acides gras saturés (AGS) qui comportent que des simples liaisons,
- Acides gras monoinsaturés (AGMI) possédant une double liaison,
- Acides gras polyinsaturés (AGPI) comportant de deux à six doubles liaisons.

Les principaux acides gras sont couramment désignés par des noms usuels qui s'appliquent aux isomères présents à l'état naturel (Tableau 1).

Différentes nomenclatures sont utiliséees pour désigner le nombre et la position des doubles liaisons sur la chaîne carbonée. La nomenclature chimique fait appel à une numérotation à partir du carboxyle terminal (carbone 1) vers le groupement méthyle (carbone n). La double liaison est indiquée par le symbole Δ suivi d'un chiffre correspondant au premier atome de carbone présent dans la double liaison. La nomenclature biochimique (n – x) tient compte de la position de cette première double liaison à partir du groupement méthyle terminal et du nombre d'atomes de carbone existants jusqu'à cette double liaison (Figure 1) (Gbogouri, 2005).

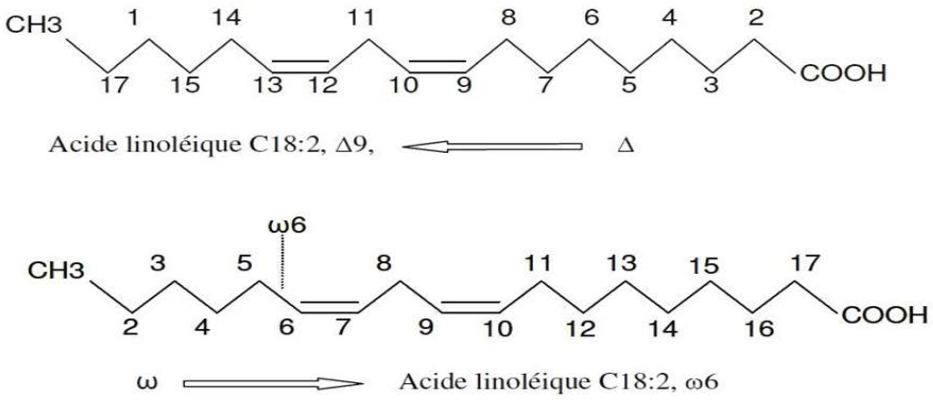

Figure 1. Nomenclatures des acides gras insaturés (Gbogouri, 2005).

II.1.1 Les acylglycérols

Ce sont des esters formés de glycérol et d'acides gras. Les trois fonctions alcooliques du glycérol peuvent être estérifiées pour donner des mono-, di- ou des triacylglycérols. Les lipides sont constitués de mélanges de ces esters où les triacylglycérols sont largement prépondérants. Ce sont des molécules non chargées et qui sont pour cette raison appelés lipides neutres. Le nom systématique des acylglycérols reprend le radical de chaque acide gras suivi du numéro de l'atome de carbone du glycérol auquel il est estérifié.

Tableau 1. Principaux acides gras saturés, monoinsaturés et polyinsaturés issus de différentes sources (Linder, 2003).

Acide gras	Nom systématique	Nom courant	Principales sources
C4:0	Acide butanoïque	Acide butyrique	Matière grasse laitière
C6:0	Acide hexanoïque	Acide caproïque	
C8:0	Acide octanoïque	Acide caprylique	Orme
C10:0	Acide décanoïque	Acide caprique	
C12:0	Acide dodécanoïque	Acide laurique	Cannelle, noix de coco, amande de palme et palmier ; noix de muscade
C14:0	Acide tétradécanoïque	Acide myristique	
C16:0	Acide hexadécanoïque	Acide palmitique	Poisson, lait, graisses de réserve des animaux d'élevage, huiles végétales
C18:0	Acide octadécanoïque	Acide stéarique	Beurre de cacao, suif ruminant
C20:0	Acide eicosanoïque	Acide arachidique	Graines
C22:0	Acide docosanoïque	Acide béhénique	
C24:0	Acide tétracosanoïque	Acide lignocérique	Cires des plantes, bactéries et insectes
C26:0	Acide hexacosanoïque	Acide cérotique	
C28:0	Acide octacosanoïque	Acide montanique	
C30:0	Acide triacontanoïque	Acide mélissique	
C5:0	Acide pentanoïque	Acide valérique	
C7:0	Acide heptanoïque	Acide énanthique	
C9:0	Acide nonanoïque	Acide pélargonique	
C11:0	Acide undécanoïque	Acide undécanoïque	
C15:0	Acide pentadécanoïque	Acide pentadécanoïque	
C17:0	Acide heptadécanoïque	Acide margarique	
C16:1 (n-7)	Acide palmitoléique		Très répandu
C18:1 (n-9)	Acide oléique		
C18:1 (n-7)	Acide vaccénique		Bactéries
C18:2 (n-6)	Acide linoléique		Graines
C18:3 (n-3)	Acide α-linolénique		Graines
C18:4 (n-3)	Acide stéaridonique		
C20:4 (n-6)	Acide arachidonique		Produits animaux
C20:5 (n-3)	Acide eicosapentaénoïque		Huiles marines
C22:5 (n-6)	Acide docosapentaénoïque		Huiles marines
C22:6 (n-3)	Acide docosahexaénoïque		Huiles marines

Si une même chaîne est présente plus d'une fois, le nom de son radical est précédé de di (ou tri) et suivi des numéros du carbone auxquels ce type de chaîne est rattaché. A titre d'exemple : palmitoyl-1, stéroyl-2, linoléoyl-3 glycérol ; dipalmitoléoyl-1,3, arachidonoyl-2 glycérol ; trioléoyl glycérol.

Il est intéressant de signaler que les acides gras insaturés estérifient le plus souvent la fonction alcool portée par le carbone médian (Gbogouri, 2005).

Les acylglycérols constituent la classe la plus importante des lipides neutres (Gontier *et al.*, 2004) et représentent de 95 à 98 % de l'apport en lipides alimentaires (Carey *et al.*, 1983).

La structure des triacylglycérols joue un rôle déterminant à tous les niveaux du processus d'assimilation des acides gras, leur absorption et leur métabolisme. La nature et la position des acides gras estérifiés sur la molécule de glycérol influence leur biodisponibilité.

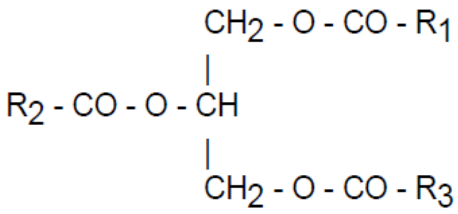

Figure 2. Structure d'un triacylglycérol (R1, R2, R3 représentant des groupements d'acides gras qui peuvent être identiques ou différents).

Les huiles végétales sont principalement riches en acides palmitique, stéarique pour les acides gras saturés, ainsi qu'en acides oléique, linoléique et alpha-linolénique pour les classes mono et polyinsaturées (Tableau 2). Les acides gras avec un nombre de double-liaisons supérieur à 3 se retrouvent majoritairement présents dans les huiles d'origine marine (Tableau 3).

Tableau 2. Composition en acides gras majeurs de quelques huiles et beurre d'origine végétale (%) (Dubois *et al.,* 2007c ; Pieszka *et al.,* 2013a ; Zhu *et al.,* 2013b).

Acide gras	Colza (a)	Soja (b)	Tournesol (c)	Maïs (c)	Olive (c)	Palme (c)	Beurre de cacao (c)
C8:0	nd	nd	nd	nd	nd	0,1	nd
C10:0	nd	nd	nd	nd	nd	0,1	nd
C12:0	nd	nd	nd	nd	nd	0,4	nd
C14:0	0,3	0,1	0,1	nd	nd	1,1	nd
C16:0	4,5	11,4	6,2	11,4	12,1	43,8	25,1
C18:0	2,7	4,4	4,3	1,9	2,6	4,4	36,4
C20:0	nd	nd	0,3	nd	0,4	0,3	1,2
C22:0	0,6	nd	0,8	nd	0,1	0,1	0,2
C24:0	nd	nd	0,3	nd	0,1	0,1	nd
Somme des acides gras saturés	8,1	15,9	12,0	13,3	15,4	50,4	62,9
C16:1	0,2	nd	0,1	0,1	0,5	0,2	nd
C17:1	nd	nd	nd	nd	0,2	nd	nd
C18:1	59,1	23,2	20,2	25,3	72,5	39,1	34,1
C20:1	nd	0,2	nd	nd	10,3	0,1	nd
C22:1	0,64	nd	nd	nd	nd	nd	nd
Somme des acides gras monoinsaturés	60,0	23,4	20,3	25,4	83,8	39,4	34,1
C18:2n-6	21,1	54,0	63,2	60,7	9,4	10,2	2,8
C18:3n-3	11,3	7,0	0,1	nd	0,6	0,3	0,2
Somme des acides gras polyinsaturés	32,4	61,0	63,3	60,7	10,0	10,5	3,0

nd : non déterminé.

Tableau 3. Composition en acide gras des huiles de différentes espèces de poissons (%)(Belhaj *et al.,* 2012a ; Gbogouri, 2005b ; Klaypradit and Huang, 2008d ; Park *et al.,* 2012e ; Velioglu *et al.,* 2015c).

Acide gras	Tête de saumon (a)	Tête de Bonite (b)	Sardine (b)	Saumon (b)	Rouget (c)	Thon (d)	Calmar (e)
C14:0	3,7	3,2	8,9	2,5	2,5	3,8	2,7
C16:0	12,1	12,2	18,4	7,3	23,0	21,2	9,9
C17:0	nd	0,5	0,4	nd	0,2	nd	0,4
C18:0	3,0	1,7	2,5	1,8	5,2	6,5	1,4
C24:0	nd	nd	nd	nd	2.7	nd	nd
Somme des acides gras saturés	18,8	17,6	30,2	11,6	33,6	31,5	14,4
C16:1 n-9	4,0	nd	nd	3,8	10,4	5,9	4,7
C18:1 n-7	2,6	3,0	3,3	2,6	4,7	nd	nd
C18:1 n-9	33,7	15,5	10,9	11,2	23,2	14,9	11,5
C20:1 n-9	1,1	1,0	2,3	11,5	1,8	6,1	3,3
C22:1 n-9	nd	0,1	0,8	1,4	0,3	nd	0,3
Somme des acides gras mono insaturés	41,4	19,6	17,3	30,5	40,4	26,9	19,8
C18:2 n-6	10,8	2,4	1,2	1,8	0,6	1,6	1,6
C18:3 n-3	5,2	0,7	0,9	nd	0,2	1,1	1,3
C18:4 n-3	2,9	1,2	2,8	nd	nd	nd	nd
C20: 2 n-6	3,0	0,2	0,1	nd	nd	2,1	3,0
C20:5 n-3 (EPA)	4,6	8,7	12,4	10,2	6,0	6,7	15,3
C22:5 n-3	2,4	1,6	1,4	2,9	nd	nd	nd
C22:6 n-3 (DHA)	6,0	31,4	9,8	18,5	3,9	21,6	30,5
Somme des acides gras polyinsaturés	34,9	46,2	28,6	33,4	10,7	33,1	51,7
DHA/EPA	1,3	3,6	0,8	1,8	0,7	3,2	2

nd : non déterminé.

II.1.2 Les phospholipides

Les phospholipides sont des molécules amphiphiles constituées d'un ester de glycérol où les fonctions alcool en position *sn-1* et *sn-2* sont estérifiées par des acides gras. L'acide gras en position *sn-2* est généralement insaturé. La troisième position *sn-3* est estérifiée par un acide phosphorique lui-même associé à un sucre (inositol) ou à une amine (choline, éthanolamine, sérine) et détermine les différentes classes de phospholipides : phosphatidylcholines (PC), phosphatidyléthanolamines (PE), phosphatidylsérines (PS), phosphatidylinositols (PI) et phosphatidylglycérols (PG). L'hydrolyse enzymatique par une phospholipase A_2 d'une liaison ester avec un acide gras en position *sn*-2 aboutit à la formation d'un lyso-phospholipide.

En raison des fonctions amphipathiques des phospholipides, recherchées dans les domaines de l'alimentaire, de la cosmétique et de la nutraceutique (Horn *et al.,* 2012 ; Lu *et al.,* 2012b), ces composés sont de plus en plus étudiés pour leurs propriétés émulsifiantes et leur capacité à former des vecteurs, suceptibles d'encapsuler des molécules d'intérêt. Les phospholipides jouent un rôle majeur dans la constitution des membranaires cellulaires et dans le transport d'acides gras. Certains phospholipides, notamment la phosphatidylcholine, possèderaient des actions cytotoxiques et anti-prolifératives recherchées dans la lutte contre le cancer (Arnoult *et al.,* 2001 ; Paris *et al.,* 2010 ; Podo, 1999). Des études sur des personnes atteintes de troubles cognitifs modérés, supplémentées par des capsules de phosphatidylsérine, ont montré une diminution significative des symptômes dépressifs, et une amélioration de la mémoire et du comportement (Maggioni *et al.,* 1990).

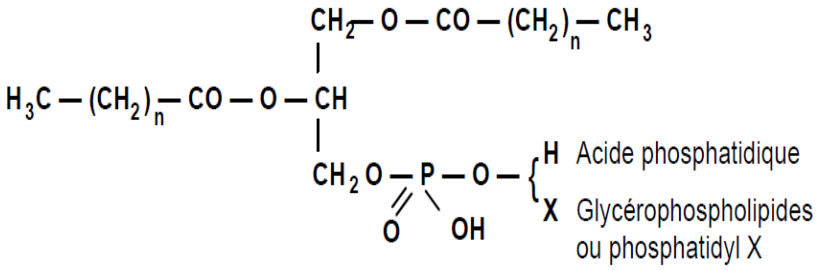

Substituant X			
Noms	**Formule chimique**	**Famille**	**Symboles**
Sérine	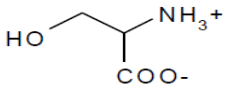	Phosphatidylsérine	PS
Ethanolamine	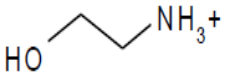	Phosphatidyléthanolamine	PE
Choline	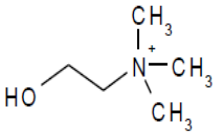	Phosphatidylcholine	PC
Inositol	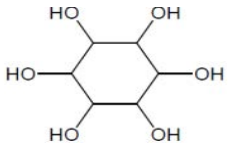	Phosphatidylinositol	PI
Glycérol	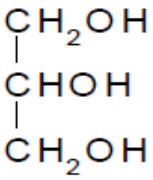	Phosphatidylglycérol	PG

Figure 3. Représentation schématique d'une molécule de phospholipide et classification en fonction des différents groupements associés (Kabri, 2013).

II.1.3 Autres constituants lipidiques

- Les **plasmalogènes** ou étherphosphoglycérides ont une structure similaire aux acides phosphatidiques à l'exception de l'acide gras en position sn-1 du glycérol qui est lié par une liaison vinyl-éther à la place d'une liaison ester. Le résidu estérifié peut être un résidu éthanolamine ou choline.
- Les **sphingolipides** présentent dans leur structure une molécule de céramide résultant de l'association par liaison amide d'un acide gras et d'une molécule de sphingosine. Les **sphingomyélines** sont des dérivés de ces bases dans lesquelles la fonction alcool primaire de la sphingosine est estérifiée par une molécule d'acide phosphorique, elle-même estérifiée à la choline. Les sphingoglycolipides dérivent de la liaison d'un sucre simple (cérébrosides) ou d'un oligosaccharide (gangliosides) à la fonction alcool primaire.
- Les **stéroïdes** sont des composés lipidiques non saponifiables. Leur structure de base est le noyau polycyclique à 17 carbones du perhydrocyclopentanophénanthrène (stérane). Parmi les stéroïdes, le **cholestérol** est le plus abondant dans les membranes des cellules animales.
- Les **glycolipides** sont, comme leur nom l'indique, constitués de glucides et de lipides. Les cérébrosides possèdent une structure semblable à celle de la sphingomyéline avec du galactose à la place de la phosphorylcholine. Les gangliosides sont également des dérivés de la sphingosine, mais dans ce cas particulier, une chaîne oligosaccharidique contenant de l'acide N-acétylneuraminique est liée à la fonction primaire de la sphingosine. Les cérébrosides sont présents en grande quantité dans les tissus nerveux, particulièrement dans la substance blanche du cerveau, tandis que les gangliosides sont majoritairement retrouvés dans la substance grise (Gbogouri, 2005 ; Sautot, 2011).

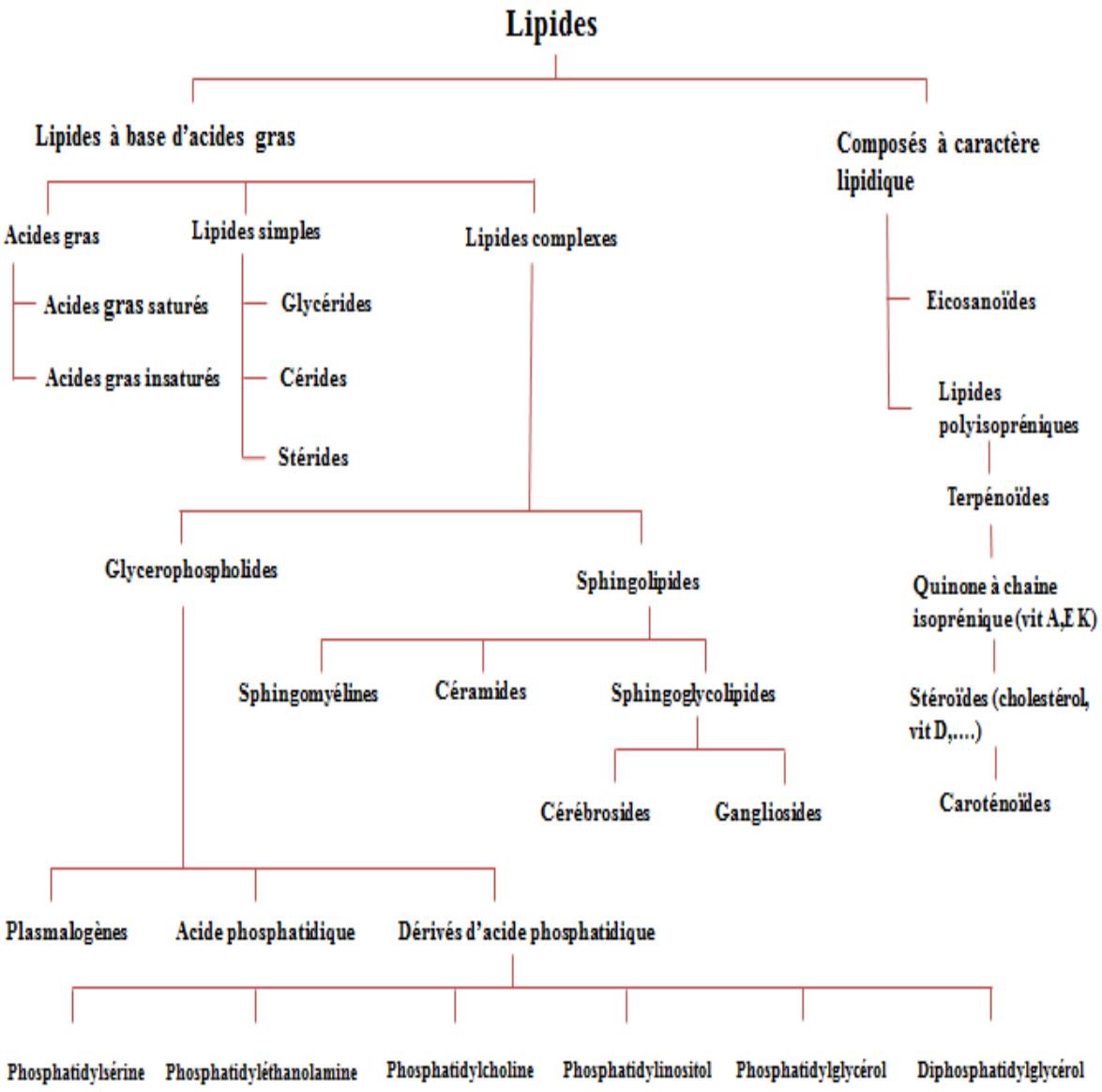

Figure 4. Classification des lipides.

II.1.4 Les lipides marins

II.1.4.1 *Synthèse des acides gras polyinsaturés à longue chaîne*

Il existe deux grandes familles d'acides gras polyinsaturés à longue chaîne (AGPI-LC). Deux acides gras sont les précurseurs de ces familles, l'acide linoléique (18:2 n-6) et l'acide alpha-linolénique (18:3n-3), précurseur des oméga-3. Ces deux acides gras sont indispensables car ils ne sont pas synthétisables par l'organisme (Dunbar *et al.,* 2014). Ils doivent donc être apportés par l'alimentation. Beaucoup d'huiles alimentaires d'origine végétale sont sources de 18:2n-6 alors que les huiles de poisson sont en général riches en 18:3n-3 (Hornstra, 2001). A partir des précurseurs que sont l'acide alpha-linolénique et l'acide linoléique, une cascade de réactions de désaturation et d'élongation se succèdent (Figure 5) pour arriver à la synthèse de deux AGPI-LC représentant les chefs de file des AGPI-LC que sont l'acide arachidonique (AA, 20:4n-6) et l'acide docosahexaénoïque (DHA, 22:6n-3). Ces deux AGPI-LC, importants en raison de leurs rôles structural et fonctionnel, sont également présents dans l'alimentation, notamment dans les produits carnés en ce qui concerne l'acide arachidonique (AA) alors que le DHA est particulièrement présent dans certains poissons gras (Hornstra, 2001).

La conversion en arachidonate, EPA et DHA à partir de AL et d'ALA respectivement, est une réaction limitée au sein du métabolisme et ne survient que dans des tissus spécifiques. Ainsi, il a été estimé que seul 10 à 15% d'ALA est converti en EPA alors que la transformation de ce dernier en DHA est encore plus limitée (Trautwein, 2001). Elle a été estimée à moins de 5% pour le DHA (Davis, 2005).

Le métabolisme de l'ALA et de LA utilise les mêmes enzymes (élongases et désaturases) et introduit ainsi la compétition entre ces deux familles d'acides gras (Burdge and Calder, 2005). Par ailleurs, ces acides gras n-3 et n-6 ne s'interconvertissent pas l'un en l'autre. Le ratio ω6 /ω3 devrait être de 1:1 à 4:1 pour une alimentation optimale équilibrée (Pickova and Morkore, 2007).

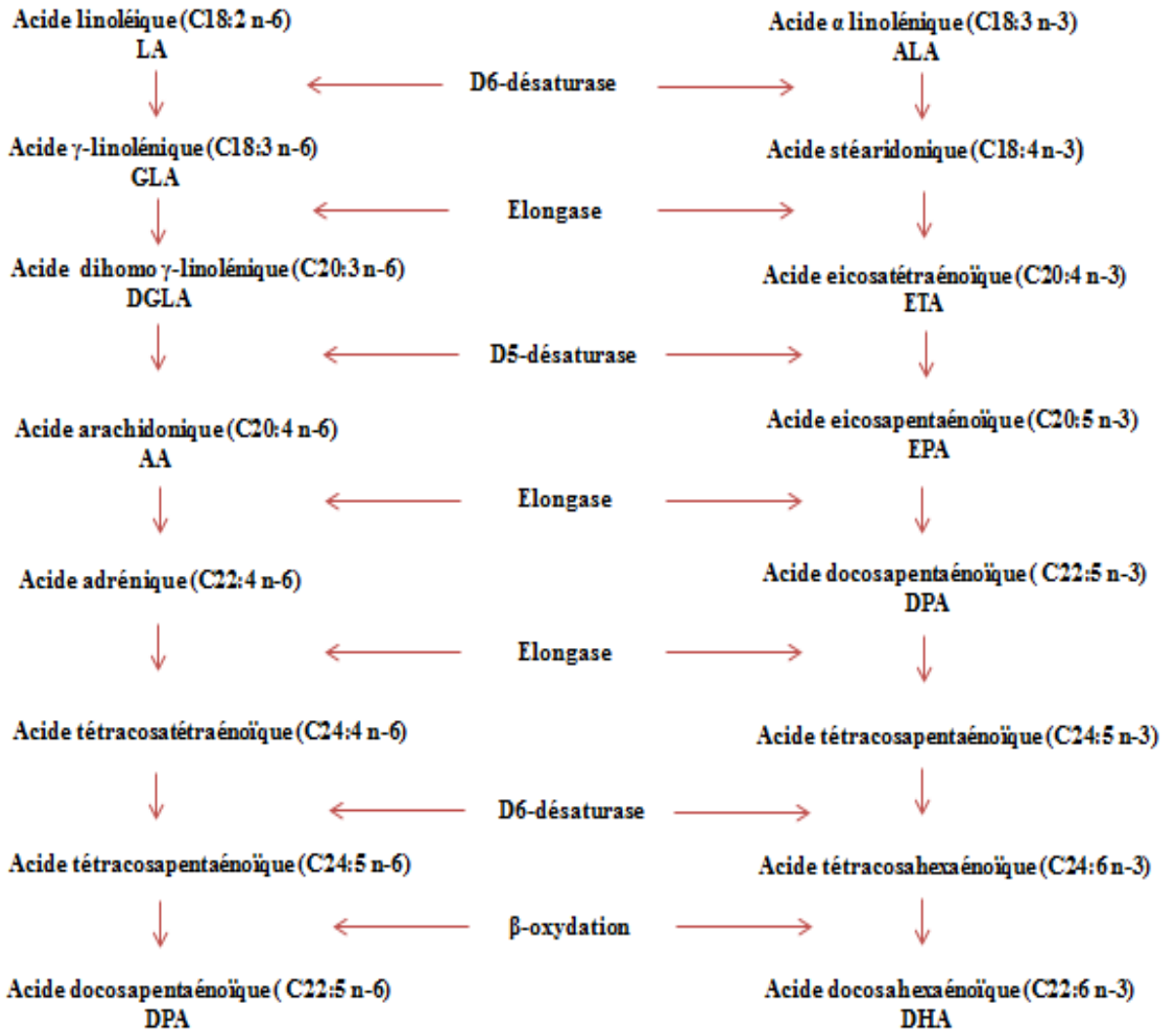

Figure 5. Biosynthèse des AGPI-LC à partir de l'acide linoléique et de l'acide alpha-linolénique (Yazdi, 2013).

II.1.4.2 *Les sources d'acides gras polyinsaturée à longue chaîne*

L'acide linoléique et alpha-linolénique sont présents en quantité notable dans les huiles végétales principalement dans les huiles de tournesol et de maïs pour l'acide linoléique et dans les huiles de colza et de soja pour l'acide alpha-linolénique. En outre, les produits animaux terrestres fournissent des quantités plus ou moins importantes en acide alpha-linolénique. Les sources marines telles que poissons et crustacés constituent les majeures sources d'acide gras polyinsaturés oméga 3. Les huiles de poisson et la chair de poissons «gras» tels que le maquereau et les sardines sont particulièrement riches en DHA. Cependant,

la teneur en huile et la nature des AGPI-LC varient en fonction des espèces, du lieu et de la saison (Schmidt *et al.,* 2006).

Même si la source la plus connue en « oméga 3 » reste l'huile extraite de poisson, le phytoplancton est le premier maillon de la chaîne alimentaire avec les micro-algues. En effet, les acides gras recherchés que sont l'EPA et le DHA proviennent essentiellement du phytoplancton marin et des micro-algues présents dans la nourriture de tous les animaux marins. Des recherches sur la composition des souches bactériennes et de microalgues montrent de fortes concentrations en EPA et DHA (40%) dans l'huile extraite à partir des intestins de poissons (Borneo *et al.,* 2007). Depuis quelques décennies, la production d'AGPI à partir de micro-algues s'est développée et l'amélioration des techniques utilisées permettent aujourd'hui de voir une augmentation croissante de la production, présentant certains avantages non négligeables par rapport aux huiles de poisson. En effet, l'absence d'odeur de poisson caractéristique, ainsi que la réduction des risques de contamination chimique leur confèrent un avantage non négligeable, mais la production reste encore limitée par des coûts d'extraction élevés (Neto *et al.,* 2013 ; Pulz and Gross, 2004 ; Tanzi *et al.,* 2012).

II.1.5 Lipides de la série n-3 et santé

Durant ces deux dernières décennies, de nombreux travaux se sont intéressés aux effets bénéfiques des AGPI-LC dans la prévention et le traitement des maladies cardiovasculaires, l'athérosclérose, certaines formes de cancer ou les maladies neurodégénératives (Gogus and Smith, 2010; Mozaffarian and Wu, 2012). Plusieurs études ont montré que la substitution dans un régime alimentaire des acides gras saturés par des acides gras polyinsaturés permet de réduire le risque d'atteintes coronaires (Dalen and Devries, 2014 ; De Lorgeril and Salen, 2012 ; Rubba and Iannuzzi, 2001), de maladies cardiovasculaires et d'athérosclerose (von Schacky, 2014). Les deux acides gras chefs de file que représente les acides arachidonique et docosahexaénoïque sont indispensables à la croissance et au développement du cerveau. En effet, le cerveau présente la teneur en lipides la plus élevée après le tissu adipeux (30 à 50% du poids sec du cerveau), essentiellement sous la forme phospholipidique. Le DHA représente à lui tout seul 10 à 20% des acides gras totaux du cerveau (Cunnane *et al.,* 2013 ; Swanson *et al.,* 2012 ; Yates *et al.,* 2014).

L'organisation ainsi que la structuration des réseaux neuronaux qui s'organisent durant la période périnatale, des trois derniers mois de la vie fœtale jusqu'à l'âge de deux ans, sont liées, durant cette période, à une accumulation active du DHA dans les structures du système nerveux (Guesnet and Alessandri, 2011 ; Judge *et al.,* 2012). Des études épidémiologiques suggèrent aussi que la consommation de DHA pourrait être associée à une diminution de l'incidence de la maladie d'Alzheimer. (Newton and McManus, 2011 ; Quinn *et al.,* 2010). Retrouvé en grande proportion dans les cellules membranaires de la rétine et des membranes de cellules neuronales post-synaptiques, le DHA joue un rôle important au niveau de la vision et du système nerveux (Igarashi *et al.,* 2013 ; Kuratko *et al.,* 2013 ; Swanson *et al.,* 2012).

L'EPA et le DHA, interviennent aussi dans la prévention de certaines maladies inflammatoires telles que l'arthrite rhumatoïde et l'inflammation du colon. La propriété anti-inflammatoire de ces AGPI est associée à leur capacité à inhiber la synthèse et la libération de médiateurs spécifiques de la pro-inflammation comme les eicosanoïdes. De même, ils interviennent dans la régulation de l'expression d'enzymes intervenant lors du processus d'inflammation, telle que la cyclooxygénase-2 (Camuesco *et al.,* 2006 ; Swanson *et al.,* 2012 ; Yates *et al.,* 2014).

Les AGPI sont également associés dans la prévention de plusieurs types de cancers. L'un des mécanismes proposés de l'action de ces acides gras sur la modulation des cellules cancéreuses et tumorales se rapporte à l'oxydation des lipides. Les AGPI-LC peuvent induire l'apoptose de cellules tumorales (Gerber, 2012 ; Ljungblad *et al.,* 2015; Wanasundara and Wanasundara, 2006). Durant ces dernières années, des études épidémiologiques ont suggéré une diminution de l'incidence des cas de cancers du sein chez des populations consommant beaucoup de poissons gras (Chajes *et al*., 2012 ; Liu and Ma, 2014).

II.2 La curcumine

La curcumine est l'une des constituants du curcuma (*Curcuma longa*), plante herbacée rhizomateuse vivace de la famille des Zingibéracées originaire du sud de l'Asie. Le curcuma est utilisé comme épice, colorant textile et alimentaire, et plante médicinale depuis 3000 ans (Cheikh Ali, 2012 ; Teuscher *et al.,* 2005). Les adultes des zones rurales indiennes consomment environ 3 à 6 g de poudre de curcuma par jour, soit 60 à 240 mg de curcumine par jour (Sanders, 2003). Les principes actifs du rhizome de curcuma sont en général des

huiles essentielles riches en cétones sesquiterpéniques composées principalement de turmérone (α-turmérone, ar-turmérone et curlone), des sesquiterpénes comme le zingibérène (Figure 6). D'autres constituants du rhizome de curcuma comme les curcuminoïdes, sont des colorants jaunes à rouge orangé, sensibles à la lumière, solubles dans l'éther et les lipides. Les curcuminoïdes sont de nature thermostables [1,7-bis (4-hydroxy-3-méthoxyphényl) -1, 6-heptadiène-3, 5-dione] souvant associés à la monodesméthoxy-curcumine, la bidesméthoxycurcumine et au féruloylcaféoylméthane (Figure 6). On peut noter la présence de peptides, des monosaccharides (glucose, fructose) et des polysaccharides (amidon) dans le curcuma (Teuscher *et al.,* 2005).

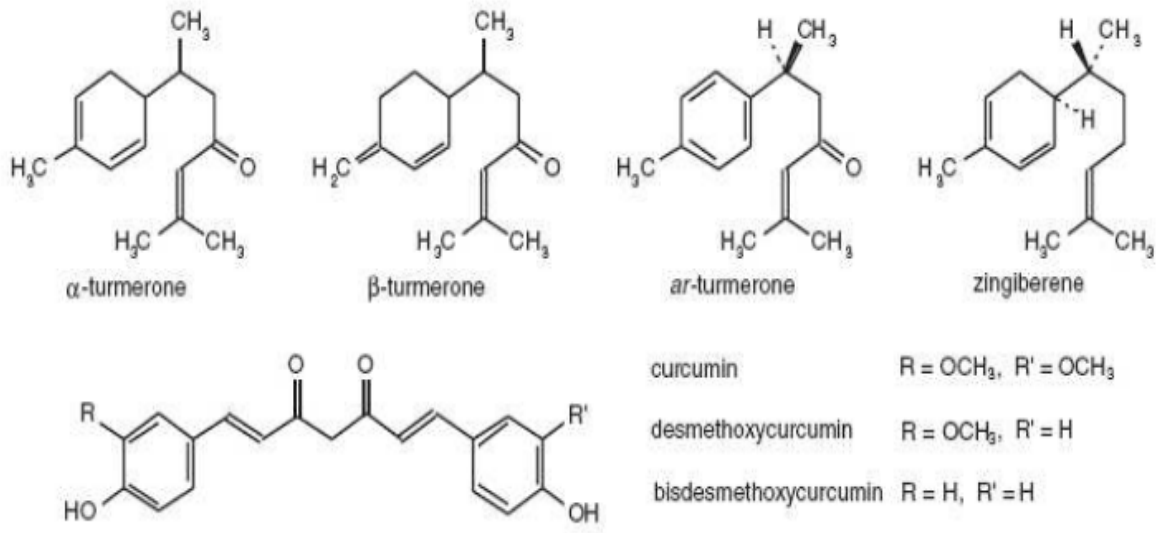

Figure 6. Structures chimiques des principaux composés présents dans la poudre de Curcuma longa (Vaquier, 2010).

Les curcuminoïdes ont généralement été isolés à partir d'espèces du genre curcuma (C. *phaeocaulis Val*., C. *aromatica Salisb*., C. *mangga Val*. et C. *xanthorrhiza Roxb*). Elles contiennent une quantité assez importante de curcumine a priori alors qu'aucun des curcuminoïdes n'est retrouvé chez C. *wenyujin Y. H. Chen*., C. *kwangsiensis S.G.Lee*. et C. *zedoaria Roxb* (Figure 7) (Tohda *et al.,* 2006).

Plusieurs genres de Zingiberaceae n'appartenant pas au genre Curcuma : *Aframomum, Alpinia.* C. *longa* et C. *xantorrhiza* ont permis d'isoler des curcuminoides et représentent des espèces médicinales en France et en Europe. Le rhizome des deux espèces est inscrit sur la

liste des plantes médicinales de la pharmacopée française, et des monographies de contrôle existent également pour les deux espèces à la pharmacopée européenne (Cheikh Ali, 2012).

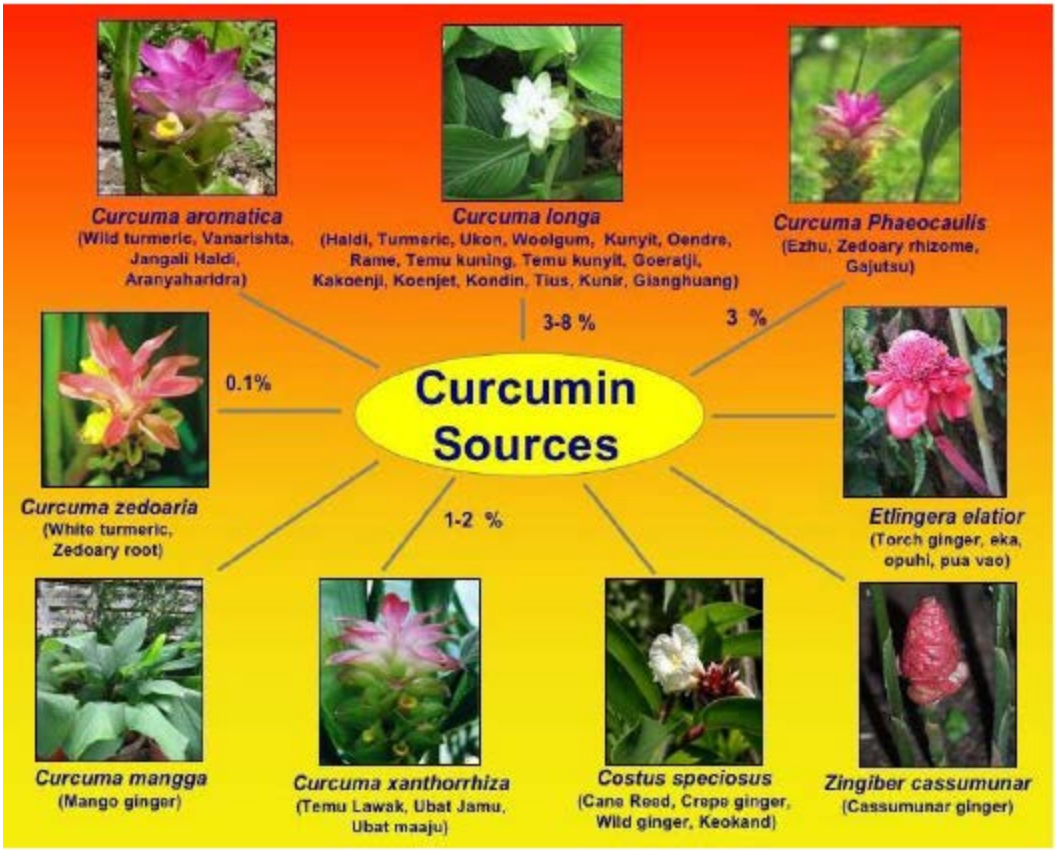

Figure 7. Sources de curcuminoïdes (Aggarwal *et al.*, 2007).

II.2.1 Les propriétés physiques et chimiques de la curcumine

La curcumine ou diferuloylméthane présente une absorption maximale dans le méthanol à 430 nm et dans l'acétone à 415-420 nm (Aggarwal *et al.*, 2003). Une solution de curcumine à 1% contient 1650 unités d'absorbance. La curcumine est jaune-orange à pH compris entre 2,5 et 7, et rouge à pH supérieur à 7 (Goel *et al.*, 2008). A pH neutre et acide, la curcumine se comporte comme un donneur de proton et à pH basique comme un donneur d'électron à l'origine de ses propriétés anti-oxydantes. La curcumine est insoluble dans l'eau, instable à pH basique et présente un poids moléculaire de 368,37 Da ainsi qu'un point de fusion de 183°C (Sharma *et al.*, 2005). C'est une molécule hydrophobe dont la valeur logP est proche de 3 (Priyadarsini, 2014).

II.2.2 Solubilité de la curcumine

La curcumine est une poudre jaune-orange presque insoluble dans l'eau (4,38 µg / mL) (Shelma and Sharma, 2013) et l'éther, mais soluble dans l'éthanol, le méthanol, le diméthylsulfoxyde (DMSO), l'acide acétique glacial ainsi que les lipides. Le fait que la forme énolique prédomine en solution est un point important à souligner. En effet, la curcumine présente la propriété de capter les radicaux libres (Shen and Ji, 2007) (Figure 8).

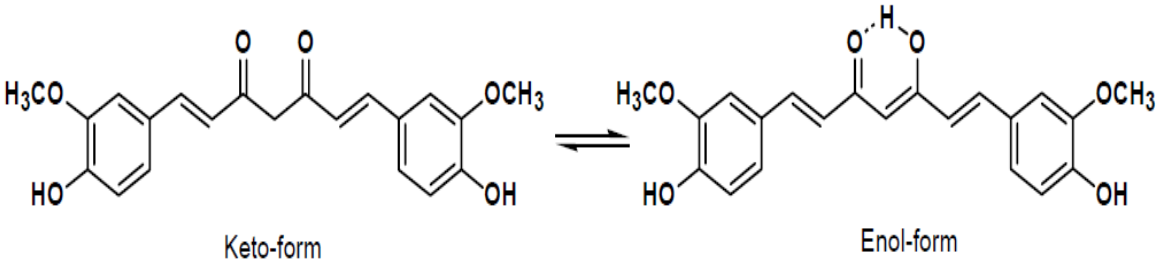

Figure 8. Tautomérie céto-énolique de la curcumine (Yanagisawa *et al.,* 2010).

II.2.3 Stabilité de la curcumine

La curcumine est plus stable à pH acide qu'à pH neutre ou alcalin. Dans des conditions physiologiques *in vitro* (tampon phosphate 0,1 M ; pH 7,2), elle est dégradée à plus de 90 % en 30 minutes en féruloylméthane, en acide férulique et en vanilline, par des mécanismes qui ont été étudiés et présentés par Tonnesen et Karlsen (1985) (Tonnesen and Karlsen, 1985), (Balasubramanian, 1991) et Wang *et al.,*1997(Wang *et al.,* 1997) (Figure 9). A pH 10,8, la demi-vie de la curcumine est d'environ une minute (Ravindran *et al.,* 2007). La stabilité accrue de la curcumine en condition acide est rendu possible par la présence des dienes conjugués. En condition de neutralité, l'enlevement d'un proton du groupe phénolique conduit à la destruction de la structure (Wang *et al.,* 1997). La tétrahydrocurcumine, principal métabolite de la curcumine, est à l'inverse, stable en milieu neutre ou alcalin, tout en gardant ses propriétés antioxydantes (Wang *et al.,* 1997).

La curcumine est également photosensible et les produits de dégradation (vanilline, acide ferulique) se décolorent lors d'une exposition à la lumière naturelle (Khurana and Ho, 1988 ; Priyadarsini, 2009). Toutefois, cette dégradation est considérablement limitée lorsque la curcumine est en présence de lipides, de liposomes, d'albumines, de cyclodextrine, de tensioactifs et de nombreux autres systèmes macromoléculaires (Jangle and Thorat, 2013 ; Priyadarsini, 2009).

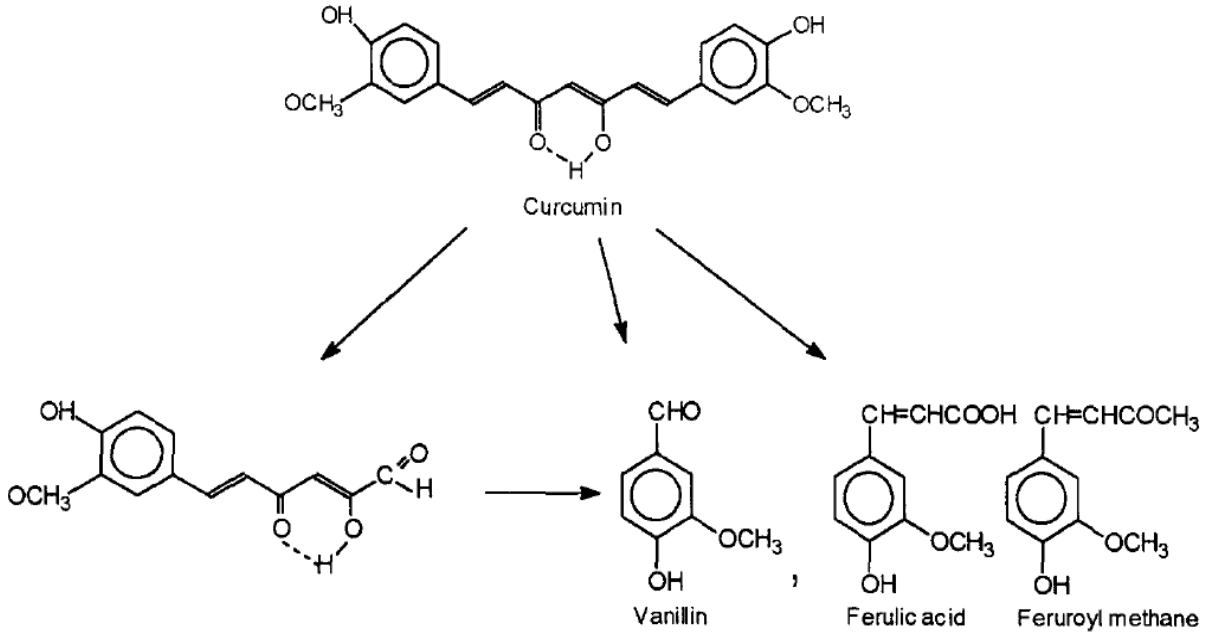

Figure 9. Les structures chimiques des produits obtenus par dégradation de la curcumine dans 0,1 M de tampon phosphate, pH 7,2 à 37 °C (Wang *et al.,* 1997).

II.2.4 Métabolisme de la curcumine

Le métabolisme de la curcumine chez les rats et les humains conduit à deux principales voies identifiées, où on retrouve différents produits de O-conjugaison comme le glucuronide de curcumine et le sulfate de curcumine (Asai and Miyazawa, 2000 ; Garcea *et al.,* 2004 ; Hoehle *et al.,* 2006 ; Ireson *et al.,* 2002 ; Singh *et al.,* 2010 ; Wahlstrom and Blennow, 1978). Les produits de réduction conduisent à des produits comme la tétrahydrocurcumine, l'hexahydrocurcumine et l'octahydrocurcumine. La figure 10 présente les différentes voies métaboliques de la curcumine.

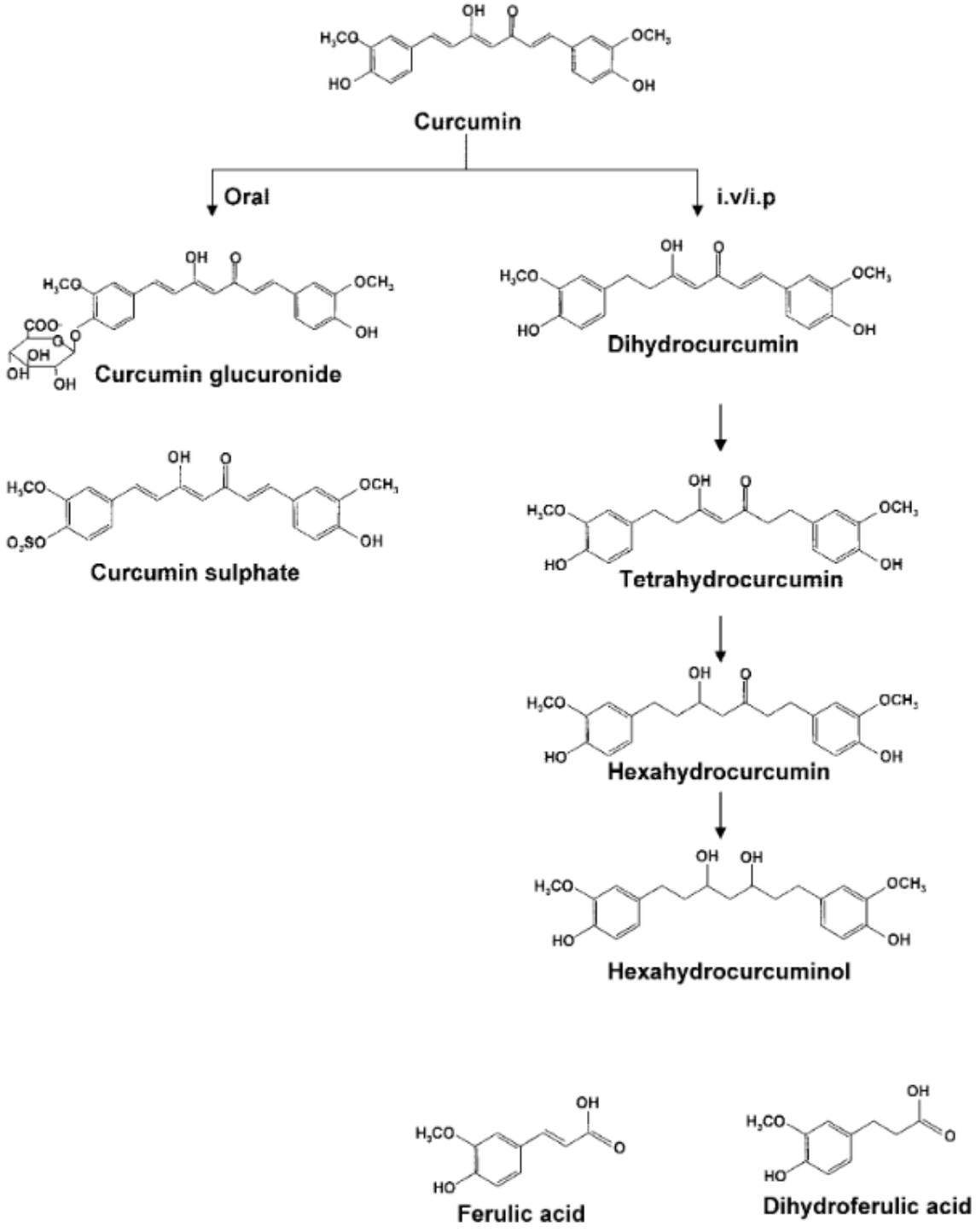

Figure 10. Structures de la curcumine et de ses métabolites (Anand *et al.*, 2007).

II.2.5 Élimination de la curcumine

Les études réalisées sur la curcumine ont montré que son administration orale aboutit à des concentrations sériques extrêmement réduites.

Yang et ses collaborateurs ont montré que l'administration orale de la curcumine chez les rats conduit à une biodisponibilité de la molécule de l'ordre de 1% (Yang *et al.,* 2012). Après administration orale d'une dose de 1 g / kg de curcumine, plus de 75% de la molécule est excrété dans les fèces et une quantité négligeable de curcumine est détectée dans l'urine (Wahlstrom and Blennow, 1978). Le temps de demi-vie est également un facteur important affectant la biodisponibilité de la curcumine. Shoba et ses collaborateurs (Shoba *et al.,* 1998) ont montré que l'absorption et l'élimination ($t_{1/2}$) de la curcumine administrée par voie orale à une dose de 2 g / kg chez le rat conduisait à 0,31 ± 0,07 et 1,7 ± 0,5 heures respectivement avec un niveau non détectable dans le sérum, chez l'homme. Cependant, Yang et ses collaborateurs (Yang *et al.,* 2007) ont montré que la phase d'élimination ($t_{1/2}$) d'une injection intraveineuse (10 mg / kg) et d'une prise par voie orale (500 mg / kg) de curcumine chez des rats conduisaient à des temps de demi-vie de 28,1 ± 5,6 et 44,5 ± 7,5 heures, respectivement. Les concentrations atteintes par voie intrapéritonéale ne sont pas sensiblement différentes de celles obtenues par voie orale (Anand *et al.,* 2007).

De façon générale, la curcumine administrée par voie orale chez l'animal ou chez l'homme est majoritairement excrétée dans les fèces sous forme inchangée. L'excrétion urinaire a lieu sous forme de glucurono- et sulfo-conjugués. Cependant, après l'administration par voie intraveineuse et intrapéritonéale, de grandes quantités de curcumine et de ses métabolites sont excrétées dans la bile, principalement sous forme de glucuronides, de tétrahydrocurcumine et d'hexahydrocurcumine. Suite à l'administration intrapéritonéale, la curcumine semble transformée tout d'abord en dihydrocurcumine et en tétrahydrocurcumine, ces composés étant ensuite convertis en monoglucurono-conjugués (Figure 10) (Anand *et al.,* 2007).

II.2.6 Les propriétés fonctionnelles de la curcumine

II.2.6.1 *Les propriétés antioxydantes de la curcumine*

Les propriétés antioxydantes et antiradicalaires des curcuminoïdes proviennent de leur capacité à intervenir dans le mécanisme d'oxydo-réduction, lors des échanges d'électrons. Un tel processus est indispensable pour notre organisme, puisque l'oxygène est nécessaire pour produire de l'énergie sous forme d'adénosine tri-phosphate (ATP) par l'intermédiaire des chaînes mitochondriales de transport d'électrons. Cependant, dans le cas où il y a transfert d'un nombre d'électrons impair, cela aboutit à la formation d'espèces réactives de l'oxygène, appelées radicaux libres (Chebil, 2006 ; Mongens, 2013). En général, un radical libre est une espèce chimique (atome ou molécule), contenant un électron non apparié, extrêmement instable, pouvant réagir avec les molécules les plus stables pour apparier son électron. Il peut soit arracher un électron (se comportant comme un oxydant), soit en céder un (agissant alors comme un réducteur). La première réaction conduit généralement à la formation en chaîne de nouveaux radicaux, expliquant ainsi que que la production d'un premier radical libre puisse entrainer des perturbations dans une cellule.

L'appellation ROS (Reactive Oxygen Species) inclut les radicaux libres de l'oxygène : le radical peroxyle ($ROO^{\bullet}$), alcoxyle ($RO^{\bullet}$), anion superoxyde ($O_2^{\bullet -}$) et radical hydroxyle ($HO^{\bullet}$) mais aussi certains dérivés oxygénés non radicalaires pouvant produire des radicaux libres tels que le peroxyde d'hydrogène. Ces radicaux centrés sur l'oxygène qui porte l'électron célibataire, sont reconnus par leur grande réactivité et font partie des espèces oxygénées réactives (Garait, 2006). Ces espèces radicalaires sont produites spontanément au sein de notre organisme et ne concernent qu'un faible pourcentage de l'oxygène capté par la respiration. Ces composés sont nécessaires à l'organisme en participant à divers processus vitaux tels que : la transduction de signaux cellulaires, la régulation des gènes et le fonctionnement de certaines enzymes, la défense immunitaire contre les agents pathogènes et la destruction par apoptose de certaines cellules tumorales (Garait, 2006). Cependant, les radicaux libres peuvent aussi avoir des effets néfastes, notamment sur le vieillissement de la peau, et seraient impliqués dans de nombreuses pathologies comme certains cancers, les maladies cardiaques et neurodégénératives.

Pour lutter contre ces radicaux libres, notre organisme possède des systèmes enzymatiques de défense qui agissent en synergie ou non comme le superoxyde dismutase (SOD), la catalase, la glutathion peroxydase et la glutathion réductase. En effet, l'enzyme SOD catalyse la dismutation du superoxyde ($O_2^{\bullet-}$) en peroxyde d'hydrogène (H_2O_2), tandis que la catalase transforme ce dernier en une molécule d'eau et une autre d'oxygène. Contrairement aux enzymes antioxydantes, la plupart des composants non-enzymatiques ne sont pas synthétisés par l'organisme et doivent être apportés par l'alimentation (Chebil, 2006 ; Garait, 2006). Parmi ces antioxydants, on trouve les vitamines C, E et A, ainsi que les flavonoïdes, l'ubiquinone, le glutathion réduit (GSH) et les curcuminoïdes.

De nombreuses recherches ont été réalisées afin de déterminer l'activité antioxydante de la curcumine. Selon l'étude de Ak et Gulcin en 2008, (Ak and Gulcin, 2008) l'activité antioxydante de la curcumine a été analysée par méthode spectrométrique, dont le principe est soit le piégeage des radicaux libres en utilisant le 1,1-diphényl-2-picrylhydraxyl ($DPPH^{\bullet}$), l'acide 2,2'–azinobis (3-éthylbenzothiazoline-6-sulfonique) ($ABTS^{\bullet+}$) et le N, N, dichlorhydrate de N-diméthyl-p-phénylènediamine ($DMPD^{\bullet+}$), ou par le piégeage de l'anion superoxyde ($O_2^{\bullet-}$) pour inhiber la peroxydation des lipides en piégeant les radicaux libres oxygénés (X) par transfert d'un électron ou d'un hydrogène :

$$X^{\cdot} + ArOH \rightarrow XH + ArO^{\cdot}$$

$$X^{\cdot} + ArOH \rightarrow X^{-} + ArOH^{+}$$

D'autre part, la curcumine a un pouvoir réducteur des ions ferriques (Fe^{3+}) en ions ferreux (Fe^{2+}) et possède des activités de chélation des ions ferreux (Fe^{2+}). En effet, ces métaux accélèrent la formation d'espèces oxygénées réactives en complexant ces métaux de transition (Figure 11) (Ak and Gulcin, 2008).

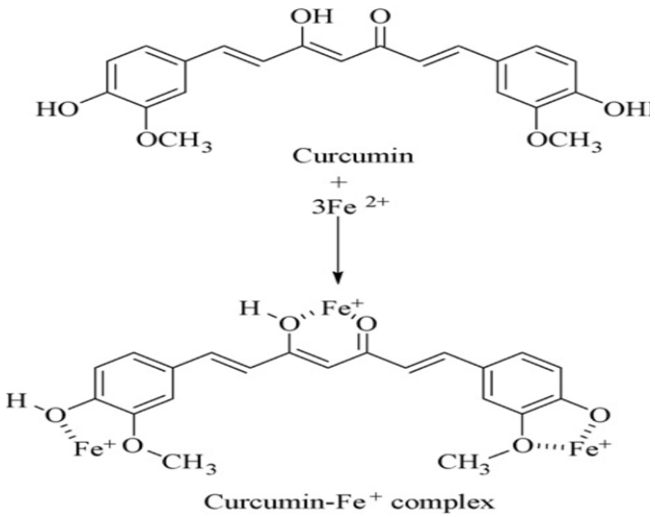

Figure 11. La chélation des ions ferreux par la curcumine (Ak and Gulcin, 2008).

Asouri et ses collaborateurs (2013) (Asouri *et al.,* 2013) ont évalué l'activité antioxydante de la curcumine par deux méthodes, dont le piégeage des radicaux libres en utilisant le 1,1-diphényl-2-picrylhydraxyl (DPPH$^{\bullet}$) et l'activité de réduction de puissance (APR), par rapport à l'acide ascorbique, un antioxydant connu. Le pourcentage de piégeage des radicaux libres de la curcumine et de l'acide ascorbique s'élève respectivement à 69 et 62%, pour une concentration de 0,1 mM. La curcumine inhibe la peroxydation lipidique et neutralise les radicaux superoxydes et hydroxyles en diminuant la génération des radicaux NO (oxyde nitrique) et des réactifs oxygénés, mais de manière dose dépendante (Borra *et al.,* 2013 ; Fujisawa and Kadoma, 2006 ; Garcea *et al.,* 2004).

Plusieurs études ont également montré l'effet pro-oxydant de la curcumine. Selon l'étude de Ahsan et ses collaborateurs (Ahsan *et al.,* 1999), la curcumine peut générer des espèces réactives de l'oxygène comme un pro-oxydant en présence de métaux de transition dans les cellules, ce qui peut entraîner des lésions de l'ADN et la mort cellulaire apoptotique. Les propriétés antioxydantes de la curcumine ont été étudiés par Banerjee *et al.,* (Banerjee *et al.,* 2008), en évaluant sa capacité à protéger les globules rouges de radicaux libres AAPH (2,2′-azobis (2-amidinopropane) hydrochloride) qui induisent des dommages oxydatifs. Les globules rouges, sensibles aux dommages oxydatifs résultant de la peroxydation des lipides membranaires, subissent une hémolyse, la libération de K^+ intracellulaire des ions et la déplétion de glutathion (GSH). Les résultats de l'étude montre que l'activité anti-oxydante / pro-oxydante de la curcumine dépend fortement de sa concentration.

II.2.6.2 *Les propriétés anti-hépatotoxiques de la curcumine*

Cette propriété des curcuminoïdes a été démontrée par des tests *in vivo*. Il s'agit d'une administration d'un composé hépatotoxique comme le tétrachlorure de carbone à des rats dans le but de provoquer des dommages hépatiques qui se traduisent par une augmentation dans le sang (de 2 à 3 fois) des taux d'aspartate-aminotransférase, de l'alanine-aminotransférase et de la phosphatase alcaline. L'ajout d'extrait de curcuma à la nourriture des animaux traités, que ce soit avant ou pendant l'administration de tétrachlorure de carbone, permet d'éviter ces dommages hépatiques (Deshpande *et al.,* 1998).

En vue d'améliorer l'activité anti-hépatotoxique des curcuminoïdes, une étude a été effectuée par Maiti et ses collaborateurs en 2007 (Maiti *et al.,* 2007). Ils ont développé une nouvelle formulation de vectorisation de la curcumine en association avec des phospholipides pour augmenter sa biodisponibilité dans l'organisme. Le complexe offre une meilleure protection du foie des rats en comparaison avec la curcumine seule utilisée en tant que contrôle (Maiti *et al.,* 2007).

Une étude plus récente a été aussi réalisée par Garcia-Nino and Pedraza-Chaverri en 2014 (Garcia-Nino and Pedraza-Chaverri, 2014), afin de déterminer l'effet protecteur de la curcumine contre les fortes lésions hépatiques induites par des métaux lourds. La curcumine réduit l'hépatotoxicité induite par l'arsenic, le cadmium, le chrome, le cuivre, le plomb et le mercure. L'effet préventif de la curcumine sur les effets nuisibles induits par des métaux lourds a été attribué à ses propriétés chélatantes.

II.2.6.3 *Les propriétés anti-inflammatoires de la curcumine*

L'activité anti-inflammatoire de la curcumine est due à son pouvoir d'inhibition de la cyclooxygénase 2 (COX-2) ainsi que de la lipoxygénase (LOX), deux enzymes impliquées dans l'inflammation. En effet, les cytokines induites par la COX-2 transforment l'acide arachidonique en prostaglandines lors des épisodes inflammatoires aiguës. La lipoxygénase transforme l'acide arachidonique en leucotriènes, qui participent aux mécanismes de l'inflammation (Duvoix *et al.,* 2005).

L'inflammation chronique est reconnue comme pouvant initier la cancérogenèse (Thangapazham *et al.,* 2006). La famille des facteurs de transcription NF-kB joue un rôle clé

dans de nombreuses fonctions cellulaires (inflammation, apoptose, survie cellulaire, la prolifération, l'angiogénèse et l'immunité innée et acquise) ainsi que dans la régulation de l'expression de plus de 500 gènes différents impliqués dans les réponses inflammatoires et immunitaires (Ghosh and Karin, 2002 ; Holt *et al.,* 2005).

La curcumine a des effets thérapeutiques bénéfiques sur les maladies inflammatoires chroniques de l'intestin (MICI). Marquées par l'inflammation chronique du colon et incluant la maladie de Crohn et la colite ulcéreuse, les MICI présentent un facteur de risque pour le cancer colorectal. Une augmentation de la production de NF-κB étant fréquemment observée lors de certaines croissances tumorales.

Une étude a été faite sur des patients atteints de rectocolite hémorragique ou de la maladie de Crohn. La curcumine, administrée quotidiennement a, pour la rectocolite hémorragique, fait diminuer la vitesse de sédimentation (Vs) et le taux de protéine CRP (protéine C réactive), qui sont des marqueurs de l'inflammation, et, pour la maladie de Crohn, une baisse de la Vs et du taux de protéine CRP, ainsi que la réduction de l'indice CDAI (Crohn's Disease Activity Index) (Holt *et al.,* 2005).

Une autre étude a été réalisée pour évaluer l'efficacité de la curcumine sur les MICI. Une étude sur 10 patients souffrant de MICI a été réalisée : cinq patients atteints de la maladie de Crohn et cinq patients affectés de proctite ulcéreuse de forme légère. Pour la forme de colite ulcéreuse, un traitement de curcumine (550 mg deux fois par jour) a été administré le premier mois de traitement et la même dose pour le deuxième mois, mais trois fois par jour. Une réduction significative à la fois des symptômes inflammatoires et des indices a été observée. Pour les patients atteints de la maladie de Crohn, 360 mg de curcumine ont été administrés trois fois par jour pendant le premier mois et quatre fois par jour pendant le deuxième et troisième mois. Une diminution de l'indice d'activité de la maladie de Crohn et des paramètres indicatifs a été observée (Lahiff and Moss, 2011).

II.2.6.4 *Les propriétés neuroprotectrices de la curcumine*

La curcumine diminue la peroxydation lipidique et augmente le taux de glutathion dans le cerveau (Teuscher *et al.,* 2005). Plusieurs études sur des modèles cellulaires et animaux indiquent également que la curcumine est un agent neuroprotecteur sur les troubles neurodégénératifs tels que la maladie d'Alzheimer (Ahmed and Gilani, 2014 ; Cheng *et al.,* 2015 ; Cole *et al.,* 2007 ; Ma *et al.,* 2009 ; Thomas *et al.,* 2009) et la maladie de Parkinson (Jagatha *et al.,* 2008 ; Ji and Shen, 2014 ; Maiti *et al.,* 2014 ; Rajeswari and Sabesan, 2008).

En effet, la co-incubation de neurones préfrontaux de rat en culture primaire en présence de curcumine et du peptide β-amyloïde (Aβ) permet d'observer un effet neuroprotecteur significatif contre la toxicité de Aβ. Ainsi, la curcumine inhibe l'activation de la caspase-3 et la chute de l'expression de Bcl-2 induite par le peptide Aβ (Qin *et al.,* 2009). En effet, le peptide bêta-amyloïde est néfaste pour le système nerveux. La présence d'agrégats de bêta-amyloïde et de protéine tau sont les signes caractéristiques de la maladie d'Alzheimer (MA).

L'effet général du peptide bêta-amyloïde est d'abaisser l'efficacité de la transmission synaptique cholinergique. En se liant directement aux peptides β-amyloïdes, la curcumine bloque l'agrégation et la formation des plaques séniles, que l'on retrouve dans la maladie d'Alzheimer, *in vitro* et *in vivo* (Yang *et al.,* 2005). Cependant, les propriétés thérapeutiques de la curcumine pour la maladie d'Alzheimer apparaissent multifactorielles via la régulation des facteurs de transcription, des cytokines et des enzymes associées à l'activité de NF-κB (Lee *et al.,* 2013).

Le stress oxydatif serait clairement impliqué dans le processus de cette pathologie. En 2011, une étude a réussi à montrer que la curcumine pouvait jouer un rôle dans la protection des neurones corticaux de rats contre les dommages oxydatifs induits par des métaux de transition (le cuivre) agissant comme des catalyseurs dans la chimie des dérivés réactifs oxygénés. Des petites doses de curcumine (de 5 à 10 μM) ont été capables d'abaisser le taux de stress oxydatif exacerbé par ces ions cuivre. Cependant, des hautes doses (>10 μM) de curcumine ne l'ont pas diminué. Au contraire, lorsqu'aucune dose de curcumine n'est injectée dans des neurones traités par des ions cuivre, ceux-ci ont présenté des aberrations chromosomiques et des dommages cellulaires. Ces résultats suggèrent que la curcumine,

d'une manière dose-dépendante, jouerait un rôle à la fois anti- et pro-oxydatif (Huang *et al.,* 2011).

Dans une étude récente menée par Mythri et ses collaborateurs (2011) (Mythri *et al.,* 2011), la supplémentation alimentaire chronique avec du curcuma protège de la neurotoxicité induite par la MPTP (1-méthyl-4-phényl-1,2,3,6-tétrahydropyridine) sur un modèle de souris présentant les symptômes de la maladie de Parkinson.

II.2.6.5 *Les propriétés anti-cancer de la curcumine*

Le cancer est un trouble hyperprolifératif où une cellule normale perd son homéostasie cellulaire et commence à activer de manière constitutive une multitude de gènes qui sont impliqués dans le cycle cellulaire, l'invasion, la survie, la métastase et l'angiogénèse (Shanmugam *et al.,* 2015). De nombreuses études ont rapporté les effets inhibiteurs de la curcumine sur de multiple types de cellules tumorales, tels que les cancers digestif, lymphatique, immunitaire, urinaire, pulmonaire, le système nerveux et les cancers de la peau (Aggarwal *et al.,* 2003 ; Maheshwari *et al.,* 2006 ; Shanmugam *et al.,* 2015 ; Shehzad *et al.,* 2013). Les concentrations de curcumine inhibitrices sont généralement comprises entre 1 µM et 100 µM dans ces études (Heger *et al.*, 2014).

Pour expliquer les effets anti-carcinogéniques de la curcumine sur des tumeurs différentes, une large variété de mécanismes sont impliqués, incluant l'inhibition des intermédiaires réactifs de l'oxygène, la suppression de l'inflammation, l'inhibition de la prolifération cellulaire, l'induction du glutathion GSH, l'inhibition des facteurs de transcription comme NF-κB (*nuclear factor kappa-light-chain-enhancer of activated B cells)* et le complexe AP-1 (*activated protein-1*), l'inhibition des isoenzymes du cytochrome P450, la suppression de la cyclooxygénase 2 (COX-2), la suppression de certains oncogènes (c-jun, c-fos), l'inhibition de protéines du cycle cellulaire (cycline E), l'inhibition des dommages chromosomiques, l'inhibition de l'oxydation des bases de l'ADN, l'inhibition de la formation d'adduits due au malondialdéhyde (MDA), l'inhibition de l'implantation des tumeurs, l'inhibition de protéines kinases, notamment la protéine kinase C, l'inhibition de la biotransformation des carcinogènes et l'induction de l'activité de la glutathion-S-transférase (Hombourger, 2010 ; Maheshwari *et al.,* 2006 ; Shanmugam *et al.,* 2015).

L'inactivation de p53 et l'activation de NF-κB sont couramment observés dans une variété de cancers et jouent un rôle important dans la progression du cancer (Dey *et al.,* 2008 ; Tergaonkar, 2009). Il a été démontré que la curcumine possède deux activités telles que l'activation de la p53 et l'inhibition de NF-κB qui induit l'apoptose. La curcumine induit aussi l'apoptose dépendante de p53 dans les cancers des cellules basales (Jee *et al.,* 1998). En effet, p53, un gène suppresseur de tumeur, a un rôle central dans la régulation du cycle cellulaire. C'est un gardien du génome, car lorsqu'apparait un dommage sur l'ADN, p53 entraîne l'arrêt du cycle cellulaire. De plus, p53 a un rôle dans l'apoptose car il est capable d'activer des protéines pro-apoptotiques (Hombourger, 2010).

La curcumine a été testée sur de nombreux modèles animaux de cancer et sur presque tous les types de cancers spécifiques d'organes, notamment le cancer du sein (Nagaraju *et al.,* 2012 ; Sinha *et al.,* 2012), buccal (Zlotogorski *et al.,* 2013), les cancers du cerveau, du cou (Gao *et al.,* 2012 ; Wilken *et al.,* 2011), le carcinome hépatocellulaire (Darvesh *et al.,* 2012), du pancréas (Johnson and de Mejia, 2011 ; Stan *et al.,* 2010), de la prostate (Nambiar and Singh, 2013 ; Singh and Agarwal, 2006 ; von Low *et al.,* 2007), du colon (Sareen *et al.,* 2013 ; Temraz *et al.,* 2013), gastrique (Chung *et al.,* 2013), ainsi que des cellules multi-drogues cancéreuses résistantes (Saha *et al.,* 2012). Les cellules souches cancéreuses ont aussi été étudiées (Norris *et al.,* 2013) ainsi qu'une variété d'autres cancers en chimioprévention, et chimiorésistance (Aggarwal and Gehlot, 2009 ; Aggarwal and Sung, 2009 ; Kuttan *et al.,* 2007 ; Park *et al.,* 2013 ; Schaffer *et al.,* 2011 ; Sung *et al.,* 2009). La curcumine a démontré *in vivo* et *in vitro* une capacité d'inhiber la carcinogenèse à trois stades : la promotion des tumeurs, l'angiogénèse et la croissance tumorale (Maheshwari *et al.,* 2006). La figure 12 illustre clairement le rôle potentiel de la curcumine dans la régulation négative de l'initiation d'une tumeur et la progression des métastases.

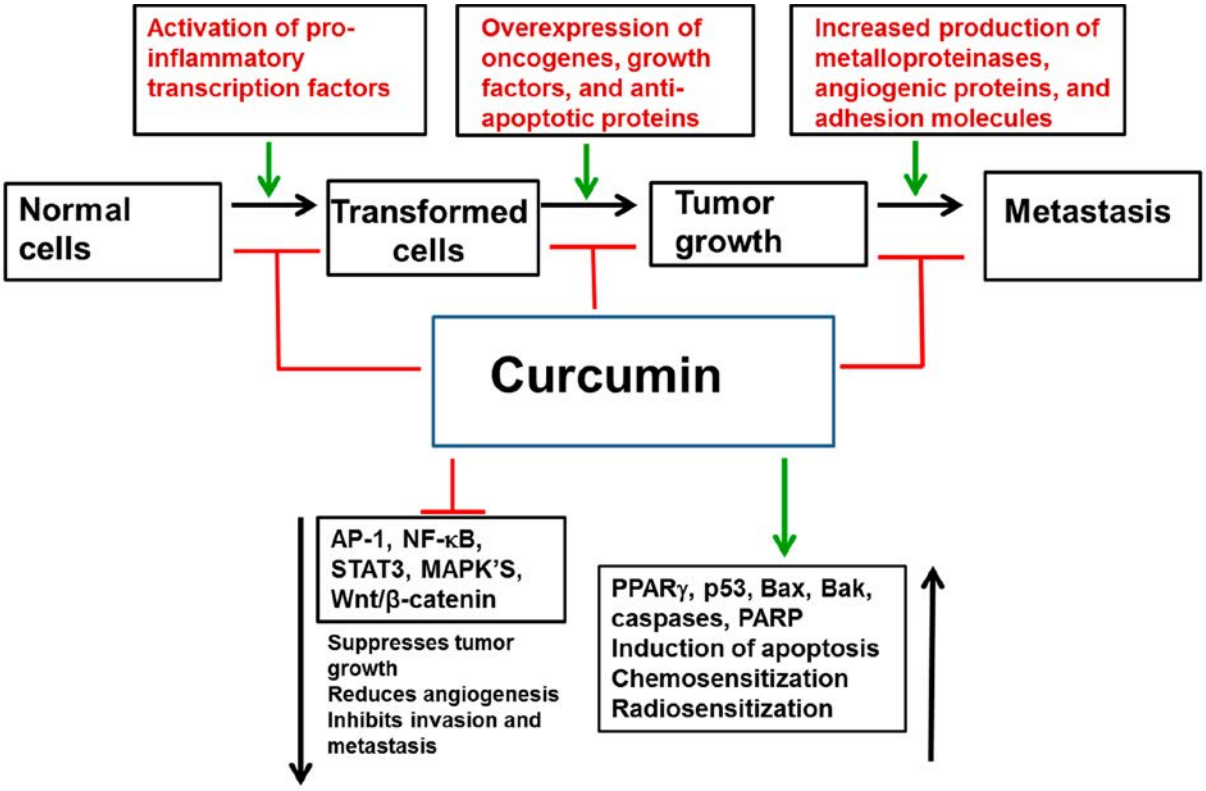

Figure 12. Fonctions anticancer potentielles de la curcumine (Shanmugam *et al.,* 2015).

Ce n'est qu'en 1987 que la propriété anticancéreuse de la curcumine sur des lésions externes a été démontrée par Kuttan et ses collaborateurs (Kuttan *et al.,* 1987), où l'application topique de la curcumine s'est avérée efficace. L'utilisation de la curcumine comme complément alimentaire a déjà été approuvée dans de nombreux pays tels que les Etats-Unis, l'Afrique du Sud, l'Inde, le Népal, le Pakistan, le Japon, la Corée, la Chine, la Thaïlande et la Turquie (Shanmugam *et al.,* 2015).

II.2.6.6 *Autres propriétés de la curcumine*

La curcumine a également des propriétés de cicatrisation, antispasmodiques, anti-coagulantes, anti-paludiques, anti-rhumatismales, anti-diabétiques, anti-bactériennes et anti-fongiques (Akbik *et al.,* 2014 ; Hombourger, 2010 ; Maheshwari *et al.,* 2006 ; Naksuriya *et al.,* 2014).

II.2.7 Effets potentiels de la curcumine sur la santé

La figure 13 résume les différentes propriétés médicinales de la curcumine. Ses effets sur la maladie d'Alzheimer et ses propriétés anti-inflammatoires, chimioprotectrices, anti-cancer sont actuellement les plus étudiés.

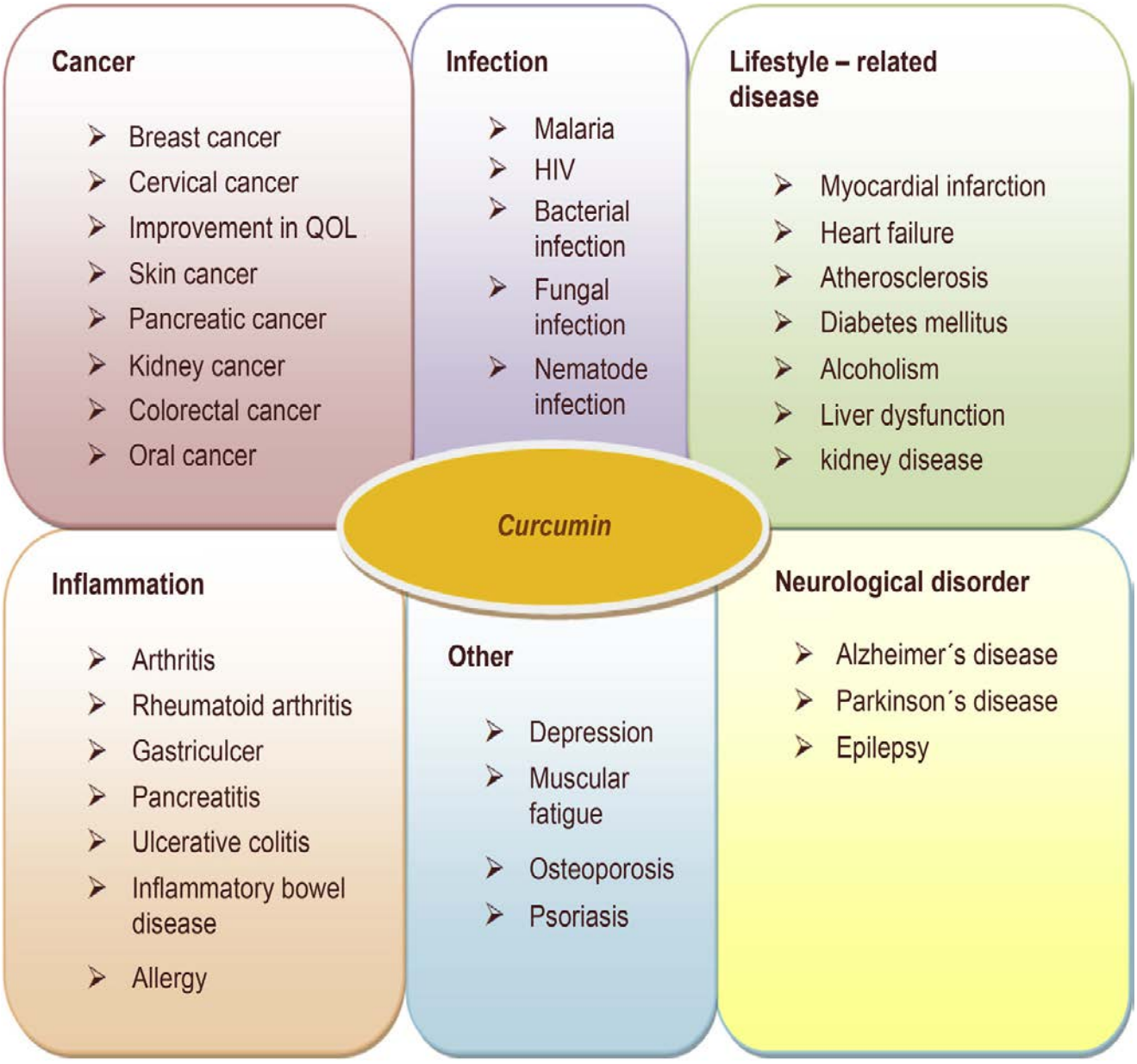

Figure 13. Usages potentiels de la curcumine et les indications pour lesquelles la curcumine a été étudiée (Naksuriya *et al.*, 2014).

II.2.8 Formulations de curcumine biodisponible

Malgré les différentes recherches montrant l'efficacité de la curcumine, de nombreux problèmes subsistent, notamment sa faible solubilité aqueuse, sa faible biodisponibilité ainsi que sa couleur intense (Prasad *et al.,* 2014). Afin d'améliorer sa biodisponibilité, de nombreuses approches ont été entreprises, faisant appel à l'utilisation d'adjuvants, de nanoparticules ou au développement d'analogues structuraux de la curcumine (Figure 14).

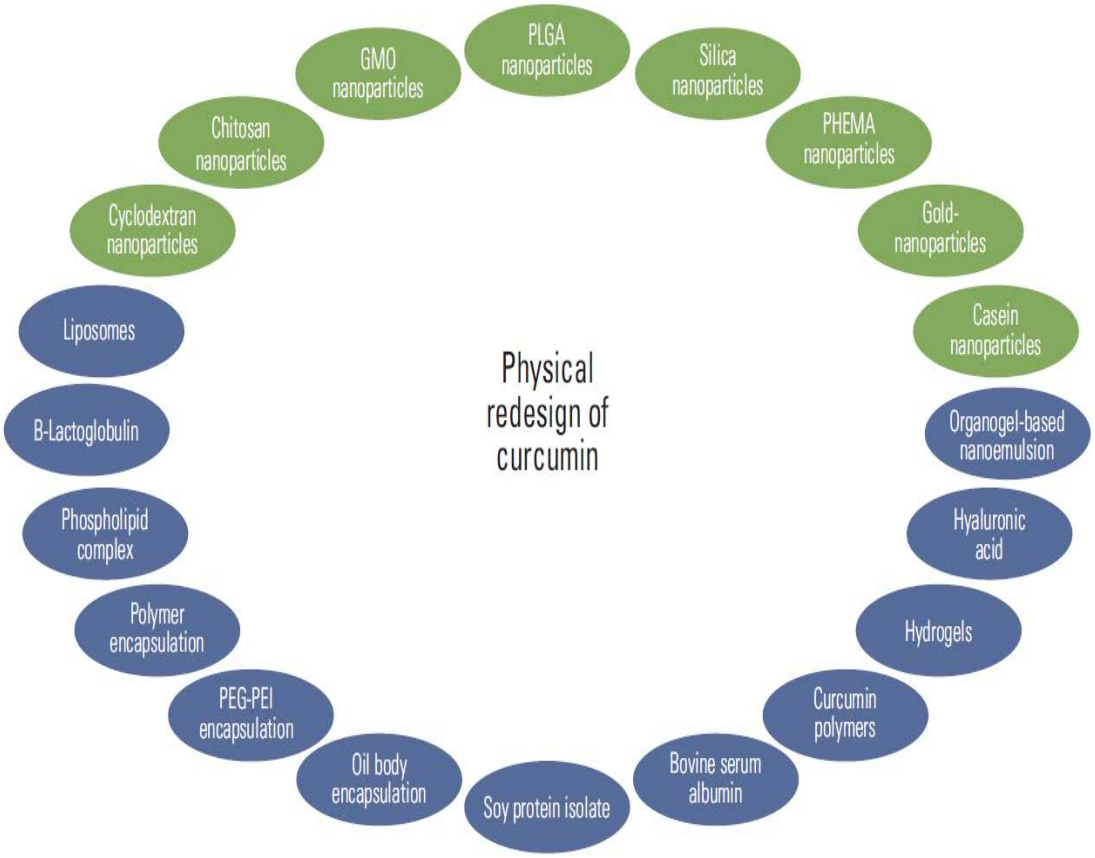

Figure 14. Diverses stratégies visant à améliorer la biodisponibilité de la curcumine, dont (GMO, glycéryl monoléate ; PLGA, polylactic-co-glycolic acid; PHEMA, poly (2-hydroxy ethyl methacrylate) ; PEG-PEI, polyethylene glycol-poly (ethylene imine) (Prasad *et al.,* 2014).

II.2.8.1 *Co-administration de la curcumine avec un adjuvant*

La pipérine a souvant été utilisée pour augmenter la biodisponibilité de la curcumine. En effet, composante majeure de poivre noir (*Piper nigrum* L.), la pipérine est connue comme inhibiteur de la glucuronidation hépatique et intestinale. Il a été démontré que

cet effet de la pipérine est plus important sur des essais cliniques que sur des essais *in vivo* (*les rats)*. La figure 15(a) montre la biodisponibilité de la curcumine chez les humains avec et sans pipérine (Anand *et al.,* 2007).

Dans cette étude où un plan croisé randomisé a été utilisé, six adultes sains volontaires masculins ont pris 2 g de curcumine avec ou sans de la pipérine (5 mg). Trois personnes ont été randomisées pour recevoir la curcumine seulement, tandis que les trois autres ont reçu la combinaison de curcumine + pipérine. Une semaine après l'administration initiale des formulations, l'absorption de la curcumine a été deux fois plus importante en présence de pipérine (Anand *et al.,* 2007 ; Dutta and Ikiki, 2013). Une autre étude a également montré que la pipérine (20 mg / kg) administrée par voie orale avec la curcumine (2 g / kg) améliore la biodisponibilité de cette dernière jusqu'à 20 fois plus chez les rats épileptiques (Sharma *et al.,* 2010). L'absorption intestinale de la curcumine s'est également avérée relativement plus élevée lorsqu'elle est administrée en association avec la pipérine et sa concentration dans les tissus de l'organisme reste élévée plus longtemps (Suresh and Srinivasan, 2010). Compte tenu de ces données, le complexe curcumine-pipérine (Cu-Pi) a été vectorisé en association avec des nanoparticules par diverses méthodes (Moorthi *et al.,* 2012).

La biodisponibilité, l'absorption cellulaire et les effets biologiques de ces nanoparticules ont étét testés. Il apparaît que que sous cette forme conjuguée, l'absorption cellulaire est plus importante, entrainant une meilleure biodisponibilité de la curcumine. Par exemple, le complex « BCM-95 curcuminoïdes », également appelé Biocurcumax, combiné avec de l'huile de curcuma (turmerons) en proportion spécifique améliore sa biodisponibilité chez l'homme (Figure 15(b)) et montre une meilleure absorption dans le sang avec un temps de rétention plus long par rapport à la curcumine seule. Ce produit a montré 700% plus d'activité et une biodisponibilité augmentée de 7 à 8 fois, confirmé par des essais cliniques (Anand *et al.,* 2007 ; Dutta and Ikiki, 2013).

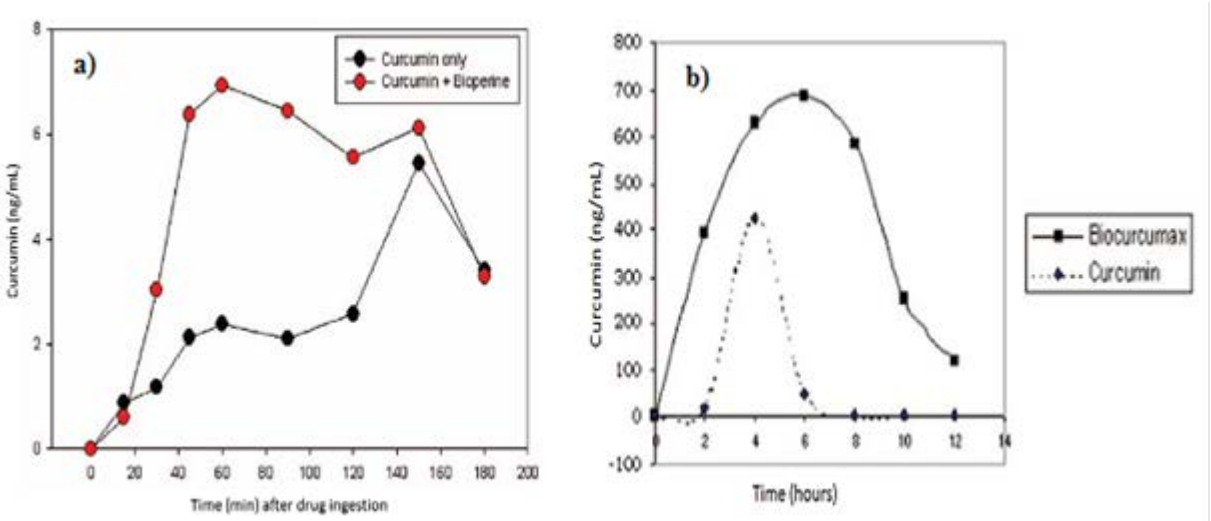

Figure 15. La biodisponibilité de la curcumine chez l'homme avec et sans pipérine (a) et en présence d'huile de curcuma (b) (Biocurcumax). D'après (Anand *et al.*, 2007).

II.2.8.2 *Encapsulation liposomale de la curcumine*

Un autre mode d'amélioration de la biodisponibilité de la curcumine est la voie liposomale. Un liposome est une vésicule artificielle formée par des bicouches lipidiques concentriques, obtenus à partir d'une grande variété de lipides amphiphiles, dont les plus couramment utilisés sont les phospholipides. De nombreuses formulations liposome / curcumine ont été développées ces dernières années (Basnet *et al.*, 2012 ; Kurzrock *et al.*, 2014 ; Li *et al.*, 2005). Ces complexes peuvent être administrés par voie intraveineuse. Des études sur l'activité antitumorale de la curcumine liposomale *in vitro* et *in vivo* sur modèle carcinomal pancréatique montrent que la curcumine liposomale inhibe *in vivo* la croissance tumorale, de manière plus importante que la curcumine seule. Ruby et ses collaborateurs (1995) (Ruby *et al.*, 1995) ont testé les activités antitumorales et antioxydantes de curcuminoïdes liposomaux *in vivo* chez les souris. D'autres études précliniques ont également montré une augmentation de la biodisponibilité de la curcumine liposomale par rapport à la curcumine administrée seule.

L'administration orale chez le rat de la curcumine encapsulée dans des liposomes a montré une biodisponibilité élevée de la curcumine et une concentration plasmatique plus élevée (Takahashi *et al.*, 2009).

Dans une étude menée au LIBio, un complexe curcumine liposomal préparé à partir de lécithine marine et végétale a permi de tester la cytotoxicité *in vitro* de ces formulations sur des cellules cancéreuses de type MCF7. Les résultats ont montré que la cytotoxicité des cellules cancéreuses augmente significativement par rapport à la curcumine non encapsulée. La vectorisation sous forme liposomale de la curcumine augmente la biodisponibilité de la molécule et améliore ses effets sur la prolifération cellulaire (Hasan *et al.,* 2014).

Des formulations de nouveaux liposomes enrobés par de la silice montrent que la disponibilité de la curcumine est respectivement 7,76 et 2,35 fois plus élevée que celle des suspensions de curcumine, pour des liposomes et des liposomes enrobés par de la silice (Li *et al.,* 2012). Afin de faciliter le transfert de la curcumine au niveau cellulaire, de nouveaux liposomes enrobés par du propylène glycol ou du chitosane sont utilisés actuellement. Les résultats montrent que ce « coating » augmente fortement l'absorption de la curcumine dans les expérimentations *in vitro* (Chen *et al.,* 2012 ; Zhang *et al.,* 2012b). La forme liposomale de la curcumine semble être la meilleure formulation pour améliorer la biodisponibilité de la curcumine pour différentes applications alimentaires (Priyadarsini, 2014).

II.2.8.3 *Complexes micellaires et complexation avec des phospholipides*

Les micelles sont des agrégats de molécules amphiphiles qui forment, à une concentration donnée (concentration micellaire critique), des agrégats sphériques possédant une tête polaire hydrophile dirigée vers le solvant et une chaîne hydrophobe dirigée vers l'intérieur. Une augmentation de l'absorption intestinale *in vitro* de la curcumine de 47 % à 56 % a été observée sous forme micellaire (Suresh and Srinivasan, 2007).

La bêta-caséine, qui peut former des nanostructures micellaires, peut être utilisée comme agent de support pour vectoriser la curcumine. Les recherches sur de la bêta-caséine de chameau utilisée pour encapsuler de la curcumine montrent une très forte augmentation de la solubilité de la curcumine (2500 fois) (Esmaili *et al.,* 2011). De nouveaux complexes chargés comme le PLGA-PEG-PLGA [PLGA : poly(acide lactique co-glycolide)] ont été synthétisés et caractérisés (Song *et al.,* 2011b). Les micelles de curcumine chargées PLGA-PEG-PLGA préparées par méthode de dialyse, permettent d'améliorer respectivement l'AUC plasmatique, $t_{1/2\alpha}$ et $t_{1/2\beta}$ de 1,31, 2,48, et 4,54 fois, par rapport à la solution témoin de curcumine.

L'utilisation de phospholipides permet d'accroître la biodisponibilité de biomolécules notamment au niveau gastro-intestinal (Liu *et al.,* 2006). Le complexe de curcumine / phospholipide a une solubilité beaucoup plus élevée dans l'eau ou le n-octanol que la curcumine ou même un mélange de curcumine et de phospholipides. Il permet d'augmenter de manière significative le taux d'absorption sérique de la curcumine (Maiti *et al.,* 2007).

II.2.8.4 *Micro-émulsions et SMEDDS (Self Micro Emulsifying Drug Delivery System)*

Les microémulsions sont des dispersions isotropes composées d'huile et d'eau stabilisées par un film interfacial composé d'agents tensioactifs, généralement associé à un co-tensioactif. En raison de leurs très petites tailles (50 à 200 nm), beaucoup plus petites que les émulsions classiques (1 à 100 µm), elles permettent de vectoriser des molécules hydrophobes comme la curcumine (Wang *et al.,* 2011). De nombreuses études ont été publiées récemment sur les profils de microémulsion de curcumine, les méthodes de préparation et l'évaluation pharmaco-cinétique (Lin *et al.,* 2009 ; Liu *et al.,* 2011 ; Setthacheewakul *et al.,* 2010 ; Wang *et al.,* 2008b). Les émulsions H/W homogénéisées en utilisant des triacylglycérols à chaîne moyenne et du Tween 20 comme émulsifiant, dont la taille moyenne des gouttelettes allant de 618,6 nm à 79,5 nm, ont été utilisées pour encapsuler de la curcumine et tester son efficacité sur un modèle d'inflammation de l'oreille, chez les souris. Des inhibitions respectives de 43% et 85% de l'œdème induite par du 12-O-tétradécanoylphorbol-13-acétate sur l'oreille de la souris pour des microémulsions de curcumine à 1% et de 618,6 nm et 79,5 nm ont été observées alors qu'un effet négligeable a été trouvé pour 1% de curcumine dans une solution à 10% de Tween 20 émulsionné en présence d'eau (Wang *et al.,* 2008b).

Des microémulsions composées de terpènes (limonène, le 1,8-cinéole et d'α-terpinéol) avec comme co-tensioactif du polysorbate 80, ont été étudiés comme vecteurs transdermiques en association avec de la curcumine. Les taux de perméation de la microémulsion de limonène étaient respectivement de 30 et 44 fois plus élevés que pour des microémulsions de 1,8-cinéole et α-terpinéol. Ces résultats indiquent que le système de microémulsion est un outil prometteur pour l'administration topique de la curcumine en association avec le limonène (Liu *et al.,* 2011).

Un mélange homogène d'huile, de surfactant, de co-surfactant et de la substance à solubiliser appelé « SMEDDS » pour Self Micro Emulsifying Drug Delivery System, peut

former une micro-émulsion ″huile dans eau″ dans les conditions gastro-intestinales après administration orale. Cette technique permet d'améliorer l'absorption de substances peu solubles dans l'eau, via l'apport de lipides. Cui et ses collaborateurs ont comparé la dissolution d'un SMEDDS contenant 20 mg de curcumine et de 20 mg de curcumine pure dans 500 mL d'un milieu aqueux à 37 °C. Alors que l'on ne parvient pas à dissoudre plus de 2 % de curcumine pure dans des solutions tampon à pH 1,2 ou 6,8, la curcumine sous forme de SMEDDS est dissoute dans le milieu à plus de 96 % après 20 minutes, indépendamment du pH. La solubilité de la curcumine sous forme de SMEDDS telle que formulée dans cette étude atteint 21 mg/g. D'après une expérience effectuée sur des intestins de rat, l'absorption de la curcumine sous forme de SMEDDS est concentration-indépendante et semble avoir lieu par diffusion passive à travers les membranes lipidiques (Cui *et al.,* 2009).

II.2.8.5 *Les niosomes*

Les niosomes sont des constructions lamellaires microscopiques de tensioactif non ionique d'alkyle ou dialkyle polyglycérol éther, qui ont d'abord été introduites dans les années 70 (Ghalandarlaki *et al.,* 2014 ; Kazi *et al.,* 2010). Les niosomes peuvent encapsuler des biomolécules avec une large gamme de solubilités due à la présence de fractions hydrophiles, amphiphiles et lipophiles dans leurs constitutions. Ils sont assimilés à des liposomes et peuvent être utilisés comme une alternative efficace aux vecteurs actuels (Azmin *et al.,* 1985) dans un certain nombre d'applications thérapeutiques potentielles, comme agents anticancéreux et anti-infectieux (Aqil *et al.,* 2013). Ils améliorent également la bio-disponibilité orale ou topique de médicaments faiblement absorbés (Jain *et al.,* 2005). Une étude *in vitro* a été effectuée pour tester des proniosomes de curcumine sur la peau de rat albinos (mélange de Span 80, de cholestérol et d'éther diéthylique) afin d'étudier un système de délivrance de médicaments transdermiques (Kumar and Rai, 2011). Les résultats ont montré que les proniosomes sont des systèmes très stables et prometteurs pour une vectorisation de biomolécules actives (Kumar and Rai, 2011).

Sur la même thématique, une étude, réalisée par Rungphanichkul et ses collaborateurs en 2011 (Rungphanichkul *et al.,* 2011), sur des niosomes de curcuminoïdes a montré une meilleure pénétration transcutanée de curcuminoïdes par rapport à une solution méthanolique des mêmes biomolécules.

II.2.8.6 *Les nanoparticules*

Les nanoparticules sont des vecteurs dont la taille varie entre 1 et 100 nm, possèdant des propriétés physiques et chimiques distinctes qui peuvent être utilisées pour vectoriser des biomolécules, l'encapsulation de médicaments afin d'améliorer leur solubilité et ou permettre un relargage ciblé et contrôlé (Malam *et al.,* 2009). De manière générale, les substances utilisées peuvent être des polymères synthétiques biodégradables (alcool polyvinylique, acide polylactique), des polymères naturels (protéines, polysaccharides) (Wang and Thanou, 2010). Parmi les différents systèmes de vectorisation de la curcumine, on retrouve des nanoparticules polymériques, des nanoparticules lipidiques solides, des nanoparticules magnétiques et des nanoparticules d'albumine (Wang *et al.,* 2011).

II.2.8.6.1 Les nanoparticules polymériques

En raison de leur petite taille, les nanoparticules de polymères présentent une excellente biocompatibilité et peuvent circuler pendant une période prolongée dans la circulation sanguine (Li *et al.,* 2009a). Les polymères synthétiques largement étudiés comprennent le chitosane (Anitha *et al.,* 2011 ; Das *et al.,* 2010) , le poly (D, L-lactide-co-glycolide) (PLGA) et de PEG (Anand *et al.,* 2010 ; Shaikh *et al.,* 2009 ; Yallapu *et al.,* 2010). Par ailleurs, d'autres matières de support tels que le poly (butyl) cyanoacrylate (Mulik *et al.,* 2009), le N-isopropylacrylamide (NIPAAm) (Bisht *et al.,* 2007) et de l'amidon modifié présentant des propriétés hydrophobes (Yu and Huang, 2010), ont été utilisés pour vectoriser de la curcumine. Les taux sanguins après l'administration orale d'une formulation nanoparticulaire de curcumine / PLGA ont été comparés avec une suspension orale de curcumine et une suspension de curcumine / pipérine comme activateur d'absorption (Figure 16).

L'admintration par voie orale de la curcumine encapsulée dans des nanoparticules de PLGA a montré une augmentation de la biodisponibilité 9 fois plus importante que la curcumine administrée avec de la pipérine comme activateur d'absorption. La concentration plasmatique de la curcumine à partir des formulations en suspension a diminué rapidement, indiquant un métabolisme rapide de la curcumine (Shaikh *et al.,* 2009).

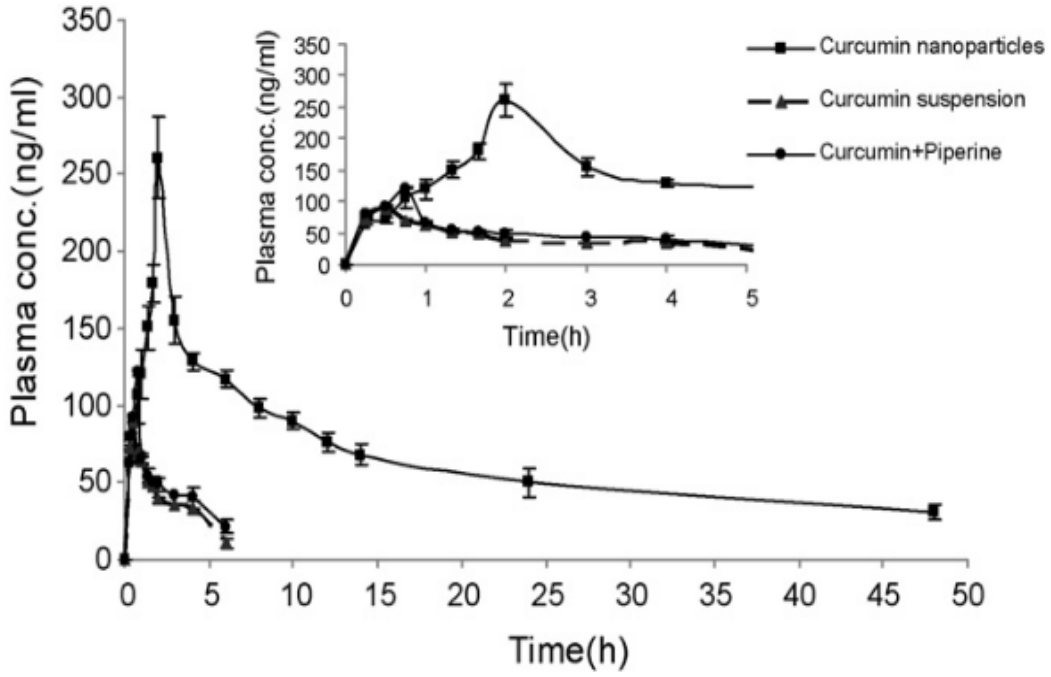

Figure 16. Les profils de concentration plasmatique *in vivo* de la curcumine en fonction du temps pour différentes formulations (Shaikh *et al.,* 2009).

Dans une autre étude, le résultat d'une expérience chez la souris a montré que les nanoparticules de curcumine / PLGA chargées améliorent l'absorption cellulaire et inhibent la prolifération des cellules tumorales. La formulation nanoparticulaire a aussi montré une meilleure biodisponibilité et une demi-vie plus longue par rapport à l'utilisation de la curcumine libre (Anand *et al.,* 2010).

II.2.8.6.2 Les nanoparticules lipidiques solides (SLNs)

Les nanoparticules lipidiques solides sont constituées de lipides naturels ou synthétiques, tels que la lécithine et certains triacyglycérols, qui sont solides à la température physiologique humaine (Pardeike *et al.,* 2009). Les nanoparticules lipidiques solides présentent de nombreux avantages potentiels. Ils protègent les composés labiles des dégradations chimiques, en permettant une libération prolongée pour améliorer la disponibilité de molécules, tout en ciblant leur efficacité (Zhu *et al.,* 2009).

Kakkar et ses collaborateurs en 2011 (Kakkar *et al.,* 2011) ont préparé des nanoparticules lipidiques solides pour encapsuler de la curcumine en utilisant la technique de

microémulsification. Ils ont obtenu une taille de particule moyenne de 134,6 nm et une teneur totale en biomolécule de 92,33 ± 1,63%.

II.2.8.6.3 Les nanoparticules magnétiques

Le ciblage de biomolécules conjuguées à un matériau magnétique sous l'action du champ magnétique externe, permet d'obtenir des résultats efficaces car ces nanoparticules magnétiques s'accumuleront dans les zones des tissus cibles sous l'action du champ magnétique externe (Yang *et al.,* 2009). Un complexe nanométrique magnéto-fluorescent dispersible dans l'eau (Fe_3O_4-curcumine), conjugué de chitosane ou d'acide oléique comme enveloppe extérieure a été élaboré par l'équipe de Lam (Lam *et al.,* 2010.). Le conjugué Fe_3O_4-curcumine présentait une absorption cellulaire élevée qui était nettement traçable par des méthodes magnétiques et fluorescentes.

II.2.8.6.4 Les nanoparticules d'albumine

L'albumine a largement été étudiée en tant que transporteur ou ligand de biomolécules hydrophobes (acides gras, hormones vitamines liposolubles) en raison de sa non-toxicité et de sa non-immunogénicité (Kim *et al.,* 2011). Elle présente d'autre part une bonne solubilité dans l'eau et l'éthanol.

Une formulation à base d'albumine sérique humaine sous forme de nanoparticules chargées en présence de curcumine (130 à 150 nm) a montré une solubilité dans l'eau beaucoup plus grande (300 fois plus élevée) et subit une perte d'activité négligeable pendant le stockage par rapport à de la curcumine libre (Kim *et al.,* 2011).

II.2.8.7 *Analogues structuraux de la curcumine*

La structure chimique de la curcumine joue un rôle essentiel dans son activité biologique et sa biodisponibilité. En effet, la tautomérie céto-énolique joue un rôle important sur l'activité antioxydante de la molécule (Shen and Ji, 2007). Aujourd'hui, un des objectifs actuels est de parvenir à obtenir de meilleures activités biologiques de la curcumine, améliorant sa biodisponibilité, par des modifications structurales. De nombreuses études se focalisent sur la recherche d'activité biologique accrue de dérivés de la curcumine et/ou d'analogues (Anand *et al.,* 2007). Une série d'analogues de la curcumine, comprenant des

composés 1,5- diarylpentadienone symétriques dont les deux cycles aromatiques possédent une substitution alcoxy, ont été synthétisés et criblés pour une activité anticancéreuse. Ces nouveaux analogues présentent une activité suppressive de croissance 30 fois plus importante que celle de la curcumine. De plus, ces analogues ne présentent pas de toxicité *in vivo* (Ohori *et al.,* 2006).

Pour améliorer l'activité biologique de la curcumine, une autre stratégie consiste à la chélater avec des métaux. En effet, la présence de deux groupes phénoliques et d'un groupe méthylène actif dans une molécule de curcumine en fait un excellent ligand pour une chélation. Plusieurs chélates métalliques de la curcumine présentent une activité biologique supérieure par rapport à celle de la curcumine libre (John *et al.,* 2002). Ces auteurs ont étudié les activités antitumorales de la curcumine, piperonylcurcumine, 2-hydroxynaphthyl-curcumine, cinnamylcurcumine, et leurs complexes de cuivre. Les complexes de cuivre de la curcumine et ses dérivés se sont révélés être de meilleurs agents anti-tumoraux que les composés de base (John *et al.,* 2002).

Shim *et al*. (2002) (Shim *et al.,* 2002) ont synthétisé des dérivés de la curcumine, de type hydrazinocurcumine (hydrazinocurcumine (a) et hydrazinobenzoylcurcumine(b)) (Figure 17). Le composé hydrazinocurcumine inhibe fortement la prolifération des cellules endothéliales aortiques bovines à une concentration nanomolaire (*CI50* = 520 nM), bien inférieure à celle de la curcumine (*CI50* = 15000 nM), sans cytotoxicité. Des tests *in vivo* et *in vitro* ont montré que l'hydrazinocurcumine peut aussi être considérée comme prometteur pour son activité anti-angiogénique (Shim *et al.,* 2002).

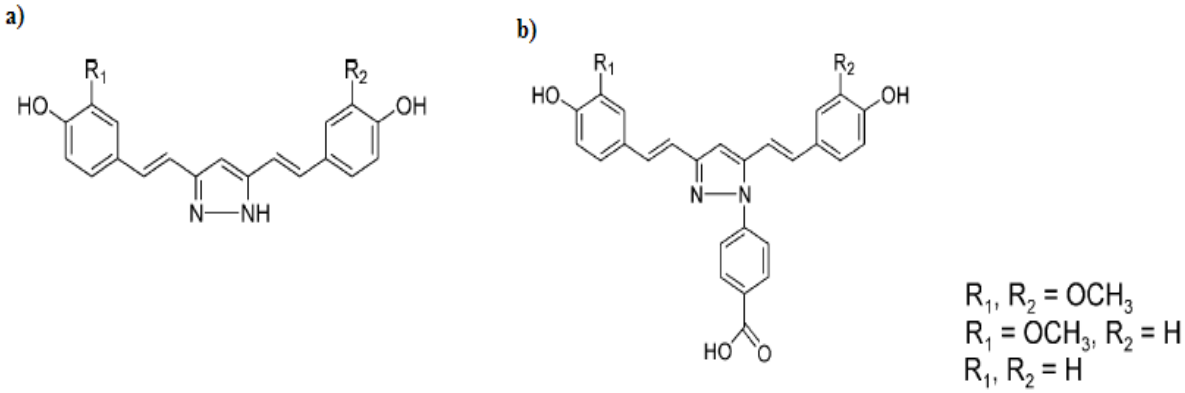

Figure 17. Dérivés de la curcumine synthétisés par shim *et al*., 2002 (Shim *et al.,* 2002).

II.3 Les différentes méthodes de vectorisation

Nous avons développé au cours de ce travail plusieurs modes de vectorisation impliquant des émulsions, des liposomes et des liposomes enrobés de chitosane. Différents lipides d'origine marine et végétale ont servi à la préparation de ces vecteurs par procédé de sonication ou par homogénéisation haute pression.

- **Homogénéisation à haute pression**

L'homogénéisation est un procédé entièrement mécanique qui entraîne une rupture et la dispersion des particules liquides ou solides en suspension aboutissant à un mélange homogène des composants. Les particules obtenues, présentent alors des dimensions extrêmement réduites, et confèrent une uniformité au produit homogénéisé. Ceci empêche de possibles phénomènes de flottation et de décantation.

Principe : Un homogénéisateur permet d'obtenir des éléments dispersés ayant une taille de 0,1 à 0,5 µm sous l'action de hautes pressions qui entraînent des turbulences, un laminage intense et des phénomènes de cavitation aboutissant à une réduction considérable de la taille des particules. Il est nécessaire d'avoir un mélange des deux phases avant d'homogénéiser le système.

- **Sonication**

La sonication à haute ou basse fréquence permet également d'homogénéiser 2 phases pour former une émulsion.

Principe : Un générateur ultrason convertit la tension du secteur en énergie électrique qui est transmise à un transducteur piézo-électrique dans le convertisseur où elle est transformée en vibrations mécaniques. Les vibrations du convertisseur intensifiées par la sonde, créent des ondes de compression dans le liquide, génèrant des millions de bulles microscopiques qui se propagent pendant la phase de pression négative, et qui implosent violemment pendant la phase de pression positive. Ce phénomène, appelé cavitation, dissipe une énergie considérable au niveau du point d'implosion, permettant ainsi une agitation intense à la pointe de la sonde.

II.3.1 Les émulsions

II.3.1.1 *Définition*

Les émulsions sont des dispersions de gouttelettes d'un liquide dans un autre liquide partiellement ou totalement immiscible. Ces systèmes sont instables d'un point de vue thermodynamique. Les émulsions sont stabilisées par la présence de molécules amphiphiles, dont le rôle émulsifiant va abaisser la tension à l'interface et réduire ainsi l'énergie libre du système.

Les émulsions sont constamment présentes dans notre vie quotidienne. Elles interviennent à l'état naturel (lait), comme résultat non désiré d'un procédé (extraction du pétrole et dégraissage), comme étape d'un procédé (fabrication de certains thermoplastiques) ou comme produit fini (Brochette, 1999). Dans ce dernier cas, le but est de stabiliser au maximum les émulsions avant de les commercialiser. Ces émulsions peuvent être produites en industries cosmétiques (crèmes hydratantes, crèmes solaires), en agroalimentaire (vinaigrette, mayonnaise), et dans le secteur pharmaceutique (encapsulation de principes actifs), biologique (cellules) ou autres (peintures, bitumes) (Debas, 2009).

II.3.1.2 *Catégories*

Ces systèmes sont, en effet, composés de deux phases (systèmes diphasiques), l'un des deux liquides constituant la phase dispersée, et l'autre constituant la phase continue. On distingue deux formes d'émulsions (Choplin, 2012) :

- **L'émulsion huile dans eau (H/E) ou émulsion aqueuse :** dans ce cas le milieu dispersant est l'eau,
- **L'émulsion eau dans huile (E/H) ou bien émulsion huileuse :** dans ce cas l'eau représente la phase dispersée.

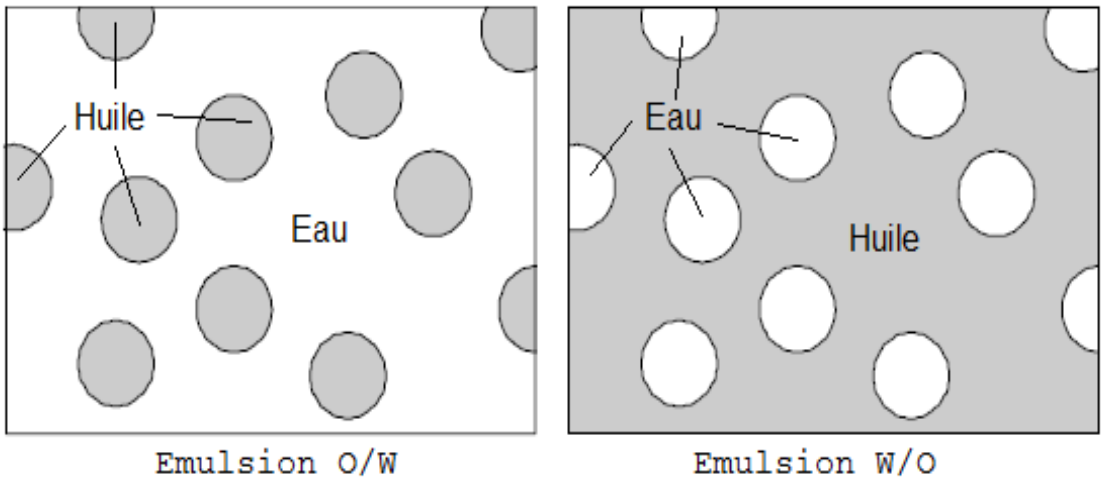

Figure 18. Représentation schématique d'une émulsion(H/E) et (E/H) (Choplin, 2012).

Généralement, la phase continue représente la fraction ayant le plus grand volume dans une émulsion. Lorsque ce volume est faible (moins de 30%), on parle alors d'une émulsion concentrée (Brochette, 1999). Selon la taille des gouttelettes de la phase dispersée, on peut distinguer différents types d'émulsions (Bou Saab, 2007):

- **Les macro-émulsions :** les gouttelettes ont un diamètre qui dépasse le micromètre,
- **Les micro-émulsions :** dans ce cas, on ne parle plus de système diphasique mais il s'agit d'un système monophasique, dans lequel les gouttelettes ne sont pas nécessairement sphériques mais sont présentes sous forme de micro-domaines. Ce type d'émulsion reste le plus stable du point de vue thermodynamique,
- **Les nano-émulsions :** les gouttelettes, cette fois-ci ont une taille comprise entre 100 nm et 500 nm.

II.3.1.3 *Stabilité des émulsions*

L'ajout de tensioactif permet également d'empêcher ou plutôt de retarder les quatre mécanismes principaux qui conduisent à une déstabilisation de l'émulsion considérée (Figure 19). Ces quatre mécanismes sont : la sédimentation ou le crémage (réversible), la floculation (réversible), le mûrissement d'Ostwald (irréversible) et la coalescence (irréversible).

- **Floculation :**

Les gouttelettes d'une émulsion sont en mouvement, appelé mouvement brownien, qui induit des chocs entre gouttelettes. Lorsque les forces d'attraction entre les gouttes dépassent les forces de répulsion, les gouttes adhèrent entre elles pour former des agrégats. Ce phénomène de floculation se produit sans influencer la structure du film interfacial entourant la goutte. Les amas de gouttelettes formés vont subir soit une sédimentation soit un crémage (Tadros, 2010).

- **Sédimentation et crémage :**

La pesanteur est le phénomène qui conduit soit à la sédimentation ou au crémage d'une émulsion. Les gouttes, animées par le mouvement brownien et soumises au champ de pesanteur terrestre, tendent à sédimenter (Brochette, 1999; Choplin, 2012).

- **Coalescence :**

Pendant la coalescence, deux ou plusieurs gouttes vont fusionner pour former une goutte plus grosse. La cause de ce phénomène est la tendance du système à diminuer la surface totale des gouttes. La nouvelle goutte formée par la coalescence, a une surface plus petite que les deux gouttes initiales. La coalescence dépend bien évidemment du film interfacial qui entoure les gouttelettes. Ainsi une concentration suffisante de l'émulsifiant permet de retarder cette phase de déstabilisation (Debas, 2009 ; Mendez *et al.,* 1999).

- **Mûrissement d'Ostwald :**

Le mûrissement d'Ostwald est un processus où les gouttes les plus petites disparaissent au profit des grosses, par transfert de matière à travers la phase continue. Pour des émulsions polydisperses, dans chaque classe de taille existe une pression de Laplace différente. La pression est plus grande pour les faibles tailles et une telle surpression implique que le potentiel chimique dans les petites gouttes est plus élevé que dans les grosses gouttes. Le retour vers l'équilibre thermodynamique s'accompagne d'un flux de matière des petites vers les grosses gouttes, au travers de la phase continue (Choplin, 2012). Ce phénomène constitue alors le mûrissement d'Ostwald qui est un mécanisme irréversible (Salager *et al.,* 2007).

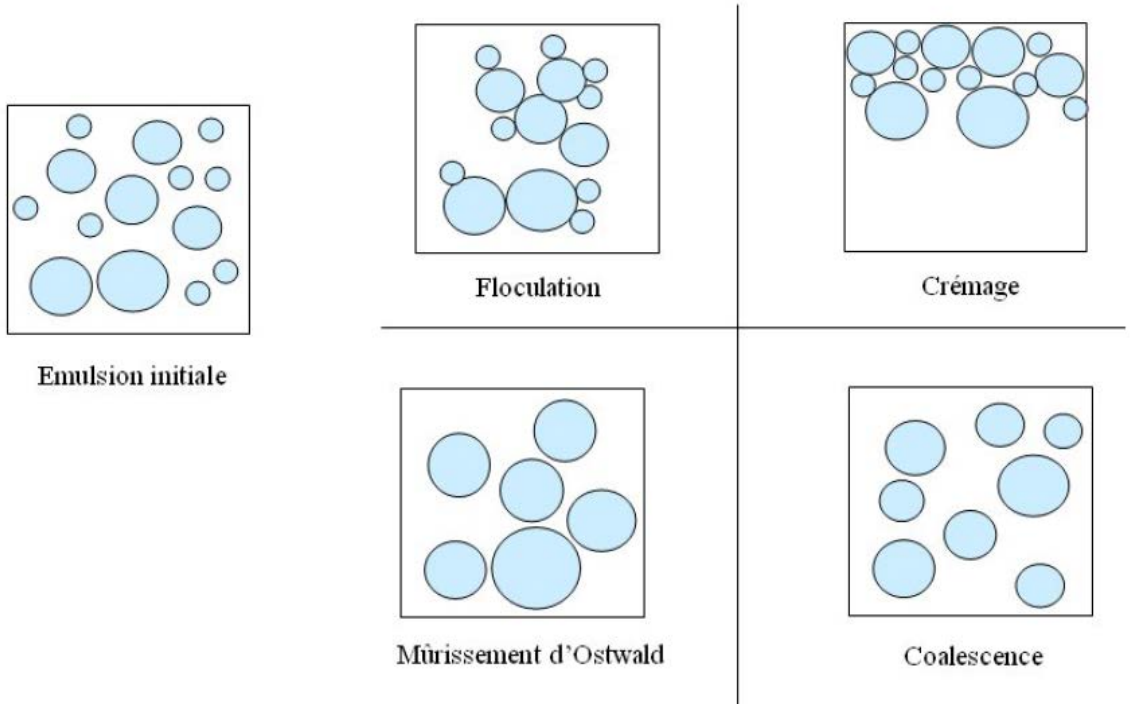

Figure 19. Mécanisme de déstabilisation d'une émulsion (Debas, 2009).

II.3.2 Les liposomes

Les liposomes sont nés il y a plus de cinquante ans où ils étaient conçus comme des modèles membranaires artificiels intéressants (Bangham *et al.,* 1965). Les premières recherches sur l'utilisation des liposomes pour encapsuler des principes actifs remontent à une quarantaine d'années (Gregoriadis, 1977).

Les liposomes sont des vésicules sphériques de quelques dizaines à quelques milliers de

nanomètres de diamètre. Ces vésicules sont composées d'une ou de plusieurs bicouches lipidiques qui permettent de séparer un milieu intra-vésiculaire d'un milieu extérieur (Lorin *et al.,* 2004).

Les liposomes possèdent des propriétés uniques du fait du caractère amphiphile des phospholipides qui composent la membrane. Le plus souvent, on retrouve les queues apolaires au centre de la bicouche, non accessibles à l'eau, et les têtes polaires exposées au milieu aqueux. Ainsi, le libre passage de macromolécules d'un compartiment à l'autre est plus difficile, contrairement aux solutés hydrophobes ou aux petits solutés hydrophiles qui diffusent librement au travers de la bicouche. Cette particularité confère aux liposomes un avantage essentiel lors de la vectorisation de molécules d'intérêt (Figure 20).

De plus, la facilité relative à leur préparation, leur biodisponibilité, leur biodégradabilité, leur large spécificité d'action, font de ces vecteurs des éléments recherchés pour la vectorisation de principes actifs dans de nombreux domaines (Bombelli *et al.,* 2005). Les liposomes peuvent véhiculer des principes actifs de nature hydrophile, sous forme dissoute dans la phase aqueuse centrale, ou de nature lipophile par insertion dans la bicouche (Mallick and Choi, 2014). Les agents bioactifs encapsulés dans des liposomes peuvent être protégés de la digestion enzymatique survenant dans l'estomac, et montrent des niveaux significatifs d'absorption dans le tractus gastro-intestinal, conduisant à l'amélioration de la bioactivité et la biodisponibilité (Takahashi *et al.,* 2006). Dans les deux cas, le principe actif peut être véhiculé dans l'organisme par simple injection. En effet, dans la circulation, les liposomes fusionnent avec les membranes cellulaires ou sont endocytés : le principe actif est alors libéré dans la cellule (Pagano and Weinstein, 1978).

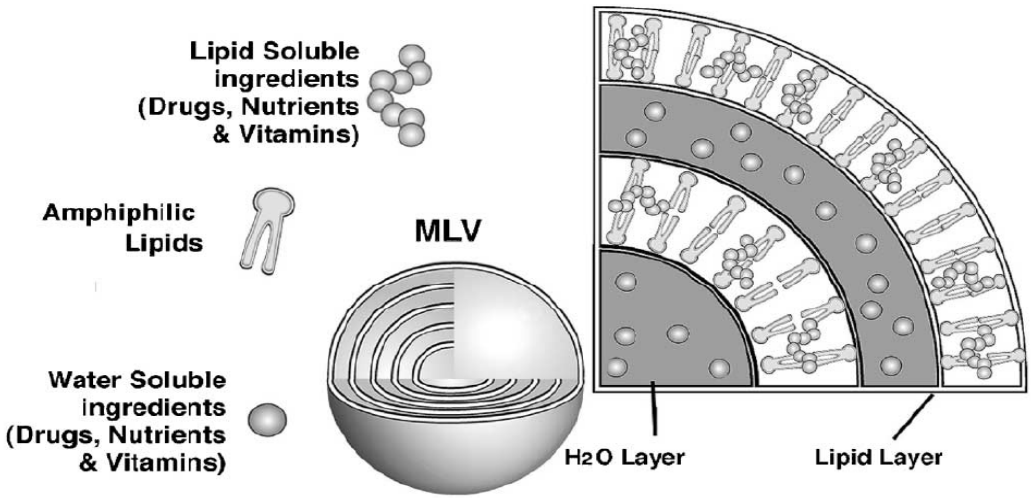

Figure 20. Schéma d'un liposome (Keller, 2001).

La conformation la plus stable des phospholipides est de se disposer en bicouches. Ce phénomène est basé sur le fait que lorsque de tels composés sont mis en présence d'un excès de solution aqueuse, ils s'organisent de manière à minimiser les interactions entre leurs chaînes hydrocarbonées et l'eau. Les têtes polaires se regroupent entre elles face à la phase aqueuse de part et d'autre de la bicouche formée et les queues apolaires, hydrophobes, se mettent au centre de la bicouche, inaccessibles à l'eau. L'effet hydrophobe constitue la force principale dirigeant la formation des bicouches lipidiques (Jesorka and Orwar, 2008).

Les phospholipides naturels forment spontanément des liposomes en milieu aqueux car l'organisation la plus stable est celle qui permet de minimiser les interactions entre les parties hydrophobes et les molécules d'eau (Lorin *et al.*, 2004). Un apport d'énergie à ces structures phospholipidiques va leur permettre de se refermer sur elles-mêmes formant une vésicule (liposome). Pendant ce processus, le piégeage des solutés présents dans le milieu aqueux survient (Mozafari *et al.*, 2008)(Figure 21).

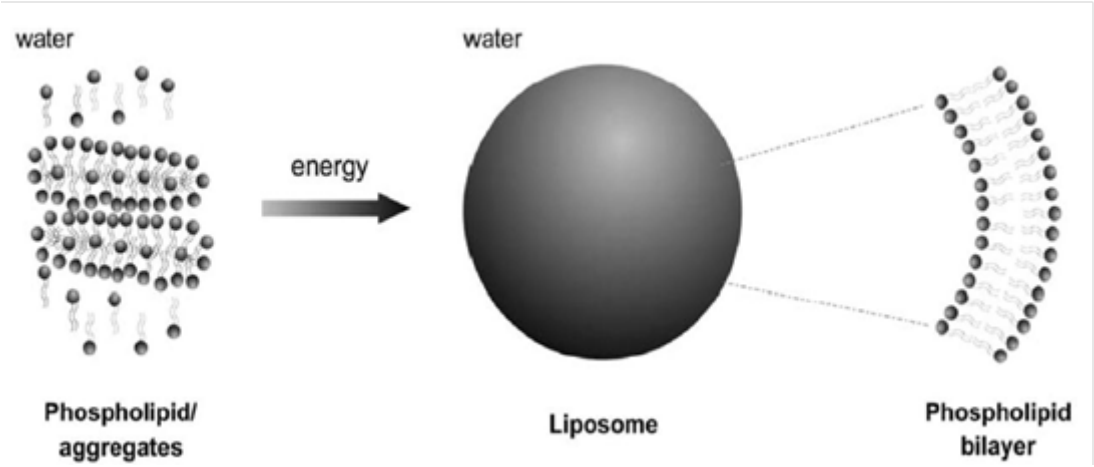

Figure 21. Mécanisme simplifié de formation de liposomes (Mozafari *et al.*, 2008).

II.3.2.1 *Classification*

Les liposomes sont classés selon leur taille et le nombre de bicouches lipidiques concentriques. On distingue :

- Les SUV (small unilamelar vesicle) ou vésicules unilamellaires de petite taille, présentent un diamètre inférieur à 200 nm,
- Les LUV (large unilamelar vesicles) ou vésicules unilamellaires de grande taille ont un diamètre compris entre 200 à 1000 nm,
- Les GUV (giant unilamelar vesicles) ou vésicules unilamellaires géantes, présentent un diamètre supérieur à 1000 nm,
- Les MLV (multilamelar vesicles) ou vésicules multilamellaires (Fathi *et al.*, 2012 ; Lorin *et al.*, 2004) (Figure 22).

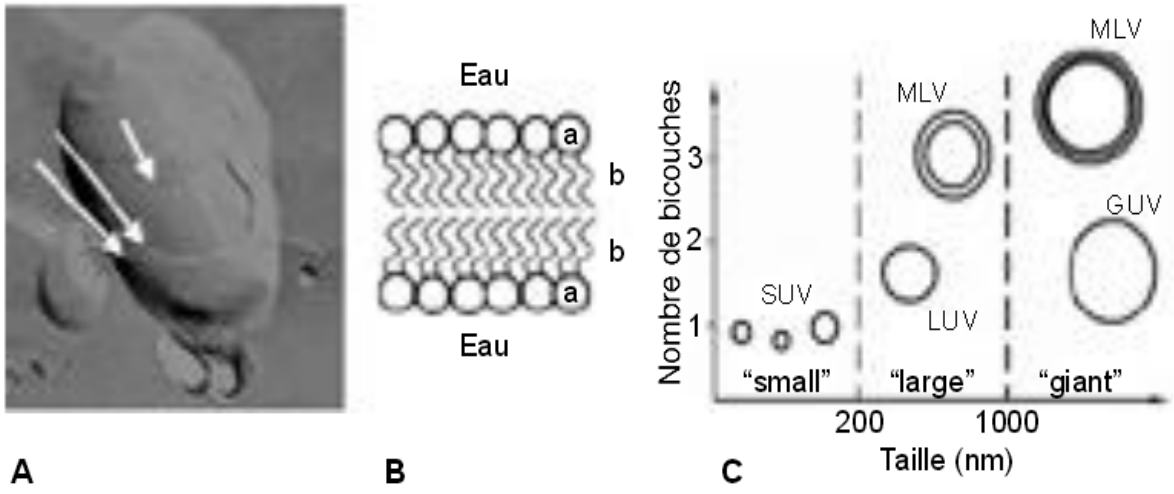

Figure 22. (A) Photographie d'un liposome multilamellaire obtenu par fracture par Gabriel Peranzi (INSERM U 410). Les flèches blanches indiquent les bicouches lipidiques; (B) Représentation d'une bicouche lipidique, (a) tête polaire, (b) queue hydrophobe; (C) Classification des liposomes selon le nombre de bicouches et leur taille, d'après (Lorin *et al.,* 2004).

II.3.3 Les liposomes enrobés par le chitosane

En dépit de présenter différents avantages, les liposomes ont aussi de nombreuses limites. La coalescence progressive des liposomes peut se produire et s'accentue dans des environnements de faible pH où les charges de surface sont réduites (Guo *et al.,* 2003). L'une des principales limitations des liposomes est le faible taux d'encapsulation des molécules, et la tendance à libérer les composants encapsulés trop rapidement (Taylor *et al.,* 2005 ; Kato *et al.,* 1993 ; Nguyen *et al.,* 2014). Ces dernières années, diverses tentatives ont été développées pour modifier la surface des liposomes afin d'améliorer leur stabilité, mais aussi pour les fonctionnaliser (Xing *et al.,* 2013 ; Nguyen *et al.,* 2014). Le revêtement avec du chitosane peut augmenter la stabilité des liposomes dans différents fluides biologiques, notamment dans le fluide gastrique et le fluide intestinal, leur confère des propriétés muco-adhésives et augmente la solubilité des médicaments (Sugihara *et al.,* 2012). Le chitosane peut être utilisé comme matériau de protection (Zaru *et al.,* 2009). En raison de sa charge positive, ce biopolymère a été utilisé précédemment pour construire des couches secondaires autour des particules dispersées telles que les gouttelettes d'émulsion ou de liposomes (Aoki *et al.,* 2005 ; Laye *et al.,* 2008 ; Ogawa *et al.,* 2003). Plusieurs études ont montré que l'enrobage des

liposomes par du chitosane fait intervenir des interactions ioniques entre le chitosane chargé positivement et le phosphate de diacétyle chargé négativement à la surface des liposomes (Laye *et al.,* 2008 ; Mady *et al.,* 2009 ; Mertins and Dimova, 2013; Nguyen *et al.,* 2014 ; Sonvico *et al.,* 2006 ; Takeuchi *et al.,* 1996). Les recherches dans les domaines pharmaceutique et agro-alimentaire ont montré que l'enrobage par le chitosane modifie la charge de surface des liposomes et augmente légèrement la taille des particules. Les liposomes ainsi protégés, montrent une libération prolongée de principes actifs *in vitro* et une stabilité accrue (Li *et al.,* 2009b ; Mazzarino *et al.,* 2012 ; Shin *et al.,* 2013).

Le chitosane (CS) est un polysaccharide cationique naturel, obtenu par désacétylation de la chitine, deuxième composant le plus abondant dans la nature après la cellulose. Ce biopolymère, extrait de l'exosquelette des crustacés, des mollusques, des insectes et de certaines familles de champignons (Al Sagheer *et al.,* 2009), est un polysaccharide linéaire formé d'unités D-glucosamines, liées entre elles par des liaisons glycosidiques et de N-acétyl-D-glucosamine. Il est obtenu à partir de la chitine par désacétylation chimique en milieu alcalin ou par voie enzymatique. Cette dernière subit au préalable une déminéralisation à l'acide chlorhydrique, une déprotéinisation par la soude ou la potasse, et enfin un blanchiment par la présence d'un agent oxydant (Figure 23). En jouant sur la durée du traitement alcalin et sur la température, il est possible d'obtenir différents chitosane à partir d'une même chitine.

Le chitosane est l'un des rares polyélectrolytes naturels cationiques. C'est une base faible présentant un pKa voisin de 6,3. Il se dissout en milieu acide par protonation des fonctions amines présentes sur la macromolécule (Sorlier *et al.,* 2001). En dessous de ce pKa, les groupements amines sont protonés et font du chitosane un polyélectrolyte cationique, soluble dans l'eau acidifiée (Shepherd *et al.,* 1997). Au-dessus du pKa, les groupements amines sont déprotonés et le chitosane est insoluble dans l'eau. Le pKa du chitosane dépend du degré de neutralisation des groupes NH_3^+ et du degré de désacétylation. En général, la valeur du pKa augmente quand le degré de désacétylation diminue (Sorlier *et al.,* 2001).

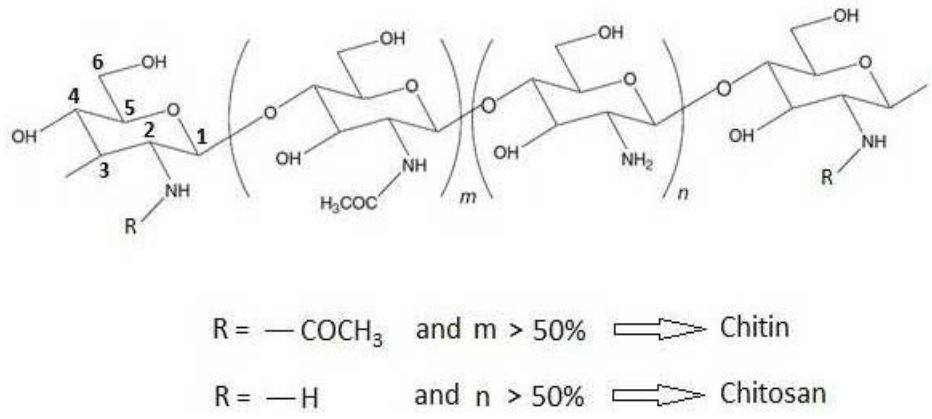

Figure 23. Structure chimique de la chitine et du chitosane d'après (Silva *et al.*, 2012)

La chitine et le chitosane présentent un intérêt dans le domaine de la libération des médicaments en raison de leurs excellentes qualités de biocompatibilité, biodégradabilité et non toxicité (Ciobanu, 2013). Le chitosane présente une capacité de fonctionnalisation très variée qui l'amène à être utilisé dans une grande gamme d'applications comme la libération de gènes (Guliyeva *et al.,* 2006), la libération contrôlée de médicaments (Sanoj Rejinold *et al.,* 2011b), comme adjuvant anti-tumoral (Menon *et al.,* 2011), en ingénierie tissulaire (Seal *et al.,* 2001). Il présente également une activité bactériostatique (Fei Liu *et al.,* 2001).

Matériels et Méthodes

III. Matériels et Méthodes/ Materials and Methods

III.1 Substrates and solvants used

III.1.1 Oils and Lecithins

Virgin rapeseed oil was purchased from Huilerie d'Ormes (France). Salmon lecithin from *Salmo salar*, was obtained by enzymatic hydrolysis. Lipidic fractions were extracted by the use of a low temperature enzymatic process without any organic solvent (Linder *et al.*, 2002). Rapeseed and soya lecithins were acquired from Solae Europe SA society (Geneva-Switzerland).

III.1.1.1 *Purification of Marine phospholipid by Acetone Precipitation*

Salmon phospholipid was isolated from salmon lecithin by using an acetone precipitation method as described by (Lu *et al.*, 2012a) and Schneider and Lovaas (Schneider and Lovaas, 2009) with a some modifications. According to Schneider and Lovaas. A total weight of 13 g salmon lecithin was dissolved in approximately 20 mL chloroform. This solution was then emptied in 100 mL of acetone (approximate ratio of 1:7.7) under vigorous stirring at ambient temperature. The ratio of lipids to solvent was according to Schneider and Lovaas (Schneider and Lovaas, 2009). The mixed solution was kept at -18°C overnight to allow phospholipid precipitation. The acetone was decanted by soft centrifugation at 1000 rpm, the precipitates were redissolved in chloroform, and the purification procedure was repeated once again. The final precipitates (purified phospholipid) were dried under nitrogen for 1 h. The residues of acetone and chloroform were further removed under vacuum at 40 °C.

III.1.1.2 *Fatty acids composition*

Fatty acid methyl esters (FAMEs) from salmon, soya and rapeseed lecithin were prepared as described by Ackman (1998) (Ackman, 1998). Then, FAMEs were analyzed using a Shimadzu 2010 gas chromatography (Shimadzu, France) system equipped with a flame-ionization detector. Separation of FAME was accomplished on a fused silica capillary column (60 m, 0.25 mm i.d. × 0.20 µm film thicknesses, SPTM2380 Supelco, Bellfonte-PA-USA). Injector and detector temperatures were settled at 250°C. The column temperature was fixed initially at 120°C for 3 min, then raised to 180°C at a rate of 2°C min^{-1} and maintained at 220°C for 25 min. Individual fatty acids were identified using Standard mixtures (PUFA1

from a marine source and PUFA2 from a vegetable source; Supelco, Sigma–Aldrich, Bellefonte, PA, USA). The results were showed as triplicate analyses.

III.1.1.3 *Characterization of lecithin for lipid classes*

Lipidic classes of salmon, rapeseed and soya lecithin were determined by Iatroscan (MK-5 TLC-FID, Iatron Laboratories Inc., Tokyo, Japan). Each sample was spotted on ten Chromarod S-III silica coated quartz rods held in a frame. The rods were developed over 20 min in hexane/diethyl ether/formic acid (80:20:0.2, v: v: v), oven dried for 1 min at 100°C and finally scanned in the Iatroscan analyzer. The Iatroscan was operated under a hydrogen flow rate of 160 ml/min and air flow rate of 2 L/min. A second migration using a polar eluent of chloroform, methanol, and ammoniac (65:35:5, v: v: v) made it possible to quantify polar lipids. The FID results were expressed as the mean value of ten separate samples. The following standards were used to identify the sample components:

- Neutral lipids: 1-monostearoyl-rac-glycerol, 1.2-dipalmitoyl-snglycerol, tripalmitin, cholesterol.

- Phospholipids: L-a-phosphatidylcholine, 3 sn-phosphatidylethanolamine, L-a-phosphatidyl-L-serine, L-a-phosphatidylinositol, lyso-phosphatidylcholine, sphingomyelin.

All standards were purchased from Sigma (Sigma–Aldrich Chemie GmbH, Germany). The recording and integration of the peaks were performed using the ChromStar internal software.

III.1.2 Curcumin

Curcumin was purchased from Sigma-Aldrich (France).

III.1.3 Solubility studies of curcumin

The solubility of curcumin in various lecithins including soya lecithin, rapeseed lecithin and salmon lecithin (lecithin aqueous solutions 3%), chitosan 1% and acetic acid 1% were determined. An excess amount of curcumin was added to 5 mL of lecithins aqueous solutions. The resultant mixture was stirred (500 rmp) at 37°C for 72 h, followed by centrifugation at 5000 rpm for 10 min to precipitate the undissolved curcumin. The supernatant was filtered through a membrane filter (0.45 µm). After the appropriate dilution with methanol, the optical

density was measured at the wavelength of 425 nm at 37 °C using a UV-Visible spectrophotometer (Shimadzu UV-1605). Samples without curcumin were used as blank and the maximum solubility of curcumin was calculated using a standard curve of curcumin in methanol.

III.1.4 Evaluation of the solubility of curcumin in salmon and rapeseed oils

Solubility of curcumin was measured at physiological temperature (37°C) (Cui *et al.*, 2009). Excess amount of curcumin was added to 2 mL of oil with stirring at 500 rpm for 72 h away from light. The mixture was then centrifuged at 10,000 rpm for 10 min to separate the insoluble curcumin. The supernatant was filtered through a 0.45 µm pore membrane filter. After the appropriate dilution with methanol, the optical density of the supernatant solution was measured at 425 nm and at 37 °C using a UV-VIS spectrophotometer (Shimadzu UV-1605,). Samples without curcumin were used as control and the maximum solubility of curcumin was calculated according to the calibration curve of curcumin in methanol. The results were presented in triplicate.

III.1.5 Chitosan

Chitosan sample (prepared from shrimp shells, practical grade) of deacetylation degree (DD) up to 75% was supplied by Sigma–Aldrich (Ref. 417963).

III.1.5.1 *pH titration of chitosan-coated liposome solution*

The chitosan-coated liposome suspension was titrated versus pH using a Multi-Purpose Titrator (MPT-Z) (Malvern Instruments, UK) linked to the Malvern Zetasizer Nano ZS (Malvern Instruments Ltd, UK). The titrants used were 0. 1 M, 1 M of NaOH and 1 M of HCl. The titration was run from pH 4 through pH 8, where size and zeta potential of the nanoparticles were measured accordingly. The experiments were done in triplicate.

III.1.6 Solvents

BF_3, (Boron trifluoride)/methanol, was obtained from Bellfonte-PA (USA). Chloroform was obtained from VMR-Prolabo (Italy). Hexane and methanol were obtained from Carlo-Erab (France). Acetonitrile and diethyl ether were purchased from Sigma-Aldrich (France).

Ammoniac was purchased from Merck KGaA (German). All organic solvents were analytical grade reagents.

III.1.7 Preparation of differents nanoemulsions containing curcumin

The emulsions contained 10 % oil phase and 90 % water according to the method used by Belhaj *et al* (Belhaj *et al.,* 2012) with slight changes. The oil phase, include 2.33 % lecithin, 7.66 % oil and curcumin with the maximum solubility in the oil phase (0.33 mg / mL salmon oil 0.18 mg / mL for rapeseed oil). We have prepared two types of emulsion: oneusing salmon oil and lecithin representing a marine emulsion and the other one using rapeseed oil and lecithin as plant emulsion. The compounds are mixed at a temperature between 55 and 60°C. After vigorously vortexed, the mixture was sonicated at 40 kHz at 40% of full power for 120s (1s on and 1s off) in an ice bath to obtain homogenous pre-nanoemulsion. The nanoemulsions were further processed in quantities of 30 mL with a high-pressure homogenizer (Emulsiflex-C3p, Sodexim S.A, France) at 1500 bar (5 cycles). Then emulsions were collected in small flasks of 40 mL and stored in the dark in an incubator at 20 °C. The same formulations without curcumin were prepared as control.

III.1.8 Preparation of nanoliposomes or chitosan-coated liposomes from different lecithins

First, we added 1.5 g of lecithin and 10 mg curcumin into 47.5 mL water, the suspension was mixed for 3-4 hours under agitation under an inert nitrogen atmosphere to prepare the liposome solution, followed by the addition of 0.5 g of chitosan and 0.5 mL of acetic acid to the liposome solution. The suspension was mixed for 3-4 h under the same conditions. Then, the droplet size of the suspension was decreased first by sonication at 40 kHz for 5 min (1s on, 1s stop) in an ice bath. Then the suspension was subjected to homogenization using high-pressure homogenizer (EmulsiFlex-C3), provided by Sodexim SA, France. The mixture was homogenized in quantities of 50 mL under a pressure of 1500 bar for 7-8 cycles. Chitosan-coated liposome samples were stored in glass bottles in the dark at 37 °C.

III.1.9 Preparation of of nanoliposomes or chitosan-coated liposomes from salmon phospholipid

In the first time, 1.5 g of salmon phospholipid and 10 mg curcumin in a completely dried round bottomed flask (RBF) dissolved in a mixture of chloroform and methanol (2:1 v/v). A thin lipid film was then formed on the wall of the RBF using Rotavapour and the organic solvent was completely evaporated by vacuum, followed by hydration with 47.5 ml Ultrapure water, the suspension was mixed for 2 hours under agitation at inert atmosphere (nitrogen) for preparation the liposome spontaneously, after we add 0.5 g of chitosan and 0.5 ml of acetic acid into the liposome already prepared. The suspension was mixed again for 4-5 at the same conditions. Then, the samples droplet size was decreased in first time by sonication at 40 KHz for 5 min (1s on, 1s stop) in an ice bath. Then the samples were subjected to homogenization using high-pressure homogenizer (EmulsiFlex-C3), provided by Sodexim SA, France. The mixture is introduced in quantities of 50 mL under a pressure of 1500 bar for 7-8 cycles. Chitosan-coated liposomes samples were stored in glass bottle in the dark at 4 and 37°C.

III.1.10 Liposome size and electrophoretic mobility measurements

The mean size and electrophoretic mobility of liposomes were measured by dynamic light scattering (DLS) using a Malvern Zetasizer Nano ZS (Malvern Instruments Ltd, UK). The apparatus was equipped with a 4 mW He/Ne laser emitting 633 nm, measurement cell, photomultiplier and correlator. Prior to measuring size and electrophoretic mobility, the samples were diluted (1:200) with ultrapure distilled water. The size distribution of particle as well as the dispersed particles electrophoretic mobility was measured to evaluate the surface net charge around droplets. Measurements were made at 25 °C with a fixed scattering angle of 173°, the refractive index (RI) at 1.471 and absorbance at 0.01. Presented sizes are the z-average mean (dz) for the liposomal hydrodynamic diameter (nm). The measurements of electrophoretic mobility were performed in standard capillary electrophoresis cells equipped with gold electrodes at the same temperature. All measurements were done at least 3 times.

III.1.11 Stability of nanoliposomes

The nanoliposomes containing curcumin and the control (nanoliposome without curcumin) ones were stored in a drying-cupboard at 37°C and at 4°C (for the chitosan-coated

liposomes) for 30 days. Mean particle size, electrophoretic mobility and polydispersity index of all formulations were analyzed every 3 days. The same protocol described previously was used for each analysis.

III.1.12 Entrapment efficiency of curcumin

The percentage of drug incorporated in the nanoliposomes was determined by centrifuging the drug-loaded nanoliposomes at 10,000 rpm for 15 min and supernatant was assayed by HPLC at 425 nm by dissolving in methanol. The concentration of curcumin was determined by a reverse-phase HPLC system (Shimadzu, Kyoto,Japan), equipped with a quaternary pump (LC-20AD), an auto-injector (SIL-20ACHT), a UV-Vis photodiode array detector (UV-Vis PDA, SPD-M20A), using a Zorbex SB-C18 column (5 µm, 4.6 mm × 250 mm) and Labsolution data software. Suspension was analyzed in isocratic mode using methanol (v/v, 5%), acetic acid 2% (v/v, 30%) and acetonitrile (v/v, 65%) at a flow rate of 0.5 $mL.min^{-1}$. 20 µL of aliquot was injected into an AlltimaTM [HP C18, 5 µm (250 x 4.6 mm i.d.) column (GRACE, Deerfield, IL, USA)] at 25 °C. Detection of curcumin was performed at 425 nm after 8 min and 49 seconds. The experiments were performed in triplicate.

The encapsulation efficiency was calculated as:

$$EE(\%) = \frac{Initial\ drug\ (mg/mL) - Free\ drug(mg/mL)}{Initial\ drug(mg/mL)} \times 100 \quad (1)$$

III.1.13 Transmission Electron Microscopy (TEM)

Transmission electron microscopy was employed to observe the structure of nanoliposomes and chitosan-coated liposome with a negative staining method according to the protocol of Colas *et al*. (2007)(Colas *et al.,* 2007). Briefly, the samples were diluted 25-folds with distilled water to reduce the concentration of the particles. Same volume of the diluted solution was mixed with an aqueous solution of ammonium molybdate (2%) as a negative staining agent. Staining was followed by a 3 min wait at room temperature, and 5 min on a copper mesh coated with carbon, then the sample was examined using a Philips CM20 Transmission Electron Microscope associated with an Olympus TEM CCD camera.

III.1.14 Membrane fluidity

Membrane fluidity of all samples was measured by fluorescence anisotropy measurements. TMA–DPH was used as fluorescent probe which is a compound that contains a cationic trimethylammonium (TMA) substitute that acts as a surface anchor to improve the localization of the fluorescent probe of membrane interiors, DPH. This measurement was carried out according to the method described by Maherani *et al* (2012) (Maherani *et al.,* 2012). Briefly, the solution of TMA–DPH (1 mM in ethanol) was added to the liposome suspension to reach finally a concentration of 4 µM and 0.2 mg/mL for the probe and the lipid, respectively. The mixture was lightly stirred for at least 1h at ambient conditions and protected from light. Then, it distributed into the wells of a 96-well black microplate at 180 µL per well. The fluorescent probe was vertically and horizontally oriented in the lipid bilayer. The fluorescent intensity of the samples was measured with Tecan INFINITE 200R PRO (Austria) equipped with fluorescent polarizers. Samples were excited at 360 nm and emission was recorded at 430 nm under constant stirring at 25 °C. The Magellan 7 software used for data analysis. The polarization value (P) of TMA–DPH was calculated using the following equation (2):

$$P = \frac{I_{II} - GI_{\perp}}{I_{II} + 2GI_{\perp}} \qquad (2)$$

Where I_{II} is the fluorescent intensity parallel to the excitation plane, $I_{\perp}$ the fluorescent intensity perpendicular to the excitation plane, and G is the factor that accounts for transmission efficiency. Membrane fluidity is defined as 1/P. The results were presented as triplicate analyses.

III.1.15 Quantification of curcumin in nanoliposomes for *in vitro* cytotoxicity test

For *in vitro* quantification of curcumin, a standard solution of curcumin in methanol was prepared by adding 5 mg of curcumin into 1 mL of methanol solution. A serial dilution from 2 to 20 $\mu g.mL^{-1}$ was done and examined at 425 nm using a UV spectrophotometer (Shimadzu UV-1605) and an HPLC. The readings were drawn to generate a calibration curve to quantify the amount of drug in the nanoliposomes.

III.1.15.1 *In vitro evaluation of the anti-cancer activity of encapsulated curcumin*

III.1.15.1.1 Cell culture

MCF-7 (Human breast cancer cell line, NCCS Pune) cells were maintained in RPMI 1640 medium supplemented with 9% (v/v) heat-inactivated fetal calf serum (FCS) (PAN Biotech GmbH, Aidenbach, Germany), 100 UmL^{-1} penicillin, 100 $mg.mL^{-1}$ streptomycin (Invitrogen, France), and 2 mM l-Glutamine (Invitrogen, France) under controlled atmosphere of 5% CO_2, 95% humidified air at 37 °C.

III.1.15.1.2 Cell proliferation assay

In vitro cellular effect of the synthesized liposome-encapsulated curcumin was investigated on MCF7 cells by using the xCELLigence system (Roche Diagnostics GmbH, Mannheim, Germany). The xCELLigence system (Real Time Cell Analyzer Single Plate, RTCA SP®) allows real-time monitoring of cell proliferation based on impedance measurement. The technology uses specific 96-well cell culture E-Plates™ with bottoms covered with microelectrodes as an electrical impedance cell sensor. The analysis is based on the measurement of electrical impedance created by attached cells across the high-density electrode array coating the bottom of the wells (Kirstein *et al.,* 2006). Impedance value is automatically converted to a dimensionless parameter Cell Index (CI) that is defined as the relative change in electrical impedance created by attached cells. As quantitative measure of cellular status, CI value represents the extend of cell-covered area and it is directly related to cell number, cell proliferation, cell size and morphology, cell viability and attachment forces (Yu *et al.,* 2005 ; Atienza *et al.,* 2005).

The proliferation of MCF7 cells in response to liposome-encapsulated curcumin exposure was analyzed by using the xCELLigence system as described recently (Benachour *et al.,* 2012). Briefly, 10^4 cells/well were cultured overnight in 96-well E-Plate. The cells were then exposed to different treatments and each condition was tested in triplicate. Three different concentrations of curcumin vectorized in nanoliposomes (5, 12 and 20 µM) were prepared by dilution with the culture medium. Nanoliposomes curcumin-free and the same concentrations of curcumin solubilized in ethanol were used as controls. The cell growth was monitored continuously for the indicated time by measuring the impedance every 15 min. CI values were automatically derived and recorded as a function of time.

III.1.16 Nanoparticle Tracking Analysis (NTA)

Suspensions containing vesicles were analyzed using a NanoSight LM10 instrument (NanoSight, Salisbury, UK). For this analysis, a monochromati laser beam at 405 nm was applied to the dilute suspension of vesicles. A video of 60 s duration was taken with a frame rate of 30 frames/s, and particle movement was analyzed by NTA software (version 2.1, NanoSight). The NTA software is optimized to first identify and then track each particle on a frame-by-frame basis, and its Brownian movement is tracked and measured from frame to frame. The velocity of particle movement is used to calculate particle size by applying the two dimensional Stokes–Einstein equation. The range of sizes that can be analyzed by NTA depends on the particle type a high refractive index (e.g., colloidal gold) or a low refractive index (e.g., cell-derived vesicles). NTA post acquisition settings were optimized and kept constant between samples, and each video was then analyzed to give the mean, mode, and median vesicle size together with an estimate of the concentration (Gercel-Taylor *et al.,* 2012).

III.1.17 Embryonic Cortical Neurons Cell Culture

Primary cortical neurons were isolated from E18 Sprague Dawley rat embryos. The cortices were collected in dissociation medium and digested with trypsin, followed by trituration. Neurons were plated on precoated poly-D-lysine (Sigma), six-well tissue culture plates. Neurons were maintained in Neurobasal Medium (Invitrogen) supplemented with B27 (2 ml/100 ml, Invitrogen) and L-glutamine (1 ml/100 ml; Invitrogen), and penicillin (50 U/ml)/streptomycin (50 µg/ml) in a 37°C humidified incubator with a 5% CO_2 in air. For biocompatibility test, neurons were directly plated on 96-well plates (15,000 cells per well) in neurobasal medium containing 2% B27 supplement, 2 mM glutamine and antibiotics.

III.1.18 XTT test

This assay is based on the ability of metabolically active cells to reduce tetrazolium salt (XTT) to color formazan compounds. The absorbance intensity can be measured at 450 nm/ 590 nm wavelengths using a spectrophotometer. The absorbance intensity is proportional to the number of active cells. Neurons were plated in 96-well plate and were exposed to different concentrations of cadmium chloride and then were washed with PBS and treated with the

reaction solution according to the manufacturer's protocol. The absorbance of the samples was measured with a multi-well plate reader (wavelength 450 nm; reference wavelength 590 nm). Results were normalized with respect to controls and were reported as a percentage.

III.1.19 Immunofluorescence assay

Cells were fixed with 4% PFA, 3% sucrose in PBS for 10 min at RT and permeabilized with 0.1%. Triton X-100 in PBS for 5 min at RT. Samples were blocked for 30 min in IF buffer (3% BSA, 2% goat serum in PBS). Primary and secondary antibodies were diluted in IF buffer and incubated for one hour at RT. Coverslips were mounted in Mowiol 4-88. Primary antibodies used: polyclonal anti-neuronal class III β-tubulin (#T2200, Sigma). Fluorescent-conjugated secondary antibodies were from Molecular Probes (Invitrogen). Images were acquired at an upright Leica TCS SP5 AOBS TANDEM confocal microscope equipped with a 60X/0.80 APO L W UVI objective.

III.1.20 Flow cytometry analysis

Flow cytometry analyses were performed as previously described (Perry *et al.,* 2009) using the annexin V-FITC apoptosis detection kit (Sigma) following the manufacturer's instructions. Cell apoptosis was measured by annexin V-FITC. Primary cortical neurons were washed and briefly trypsinized, and then washed twice with cold 1×PBS. Cells were centrifuged and resuspended in 1× binding buffer followed by incubation with staining solution (annexin V-FITC) for 10 min in the dark at 4 °C. The cells were resuspended in 1× binding buffer. Samples were kept on ice during the entire procedure and analyzed immediately by flow cytometry. Ten thousand cells from each sample were scanned and analyzed by FACS Calibur flow cytometry (Becton Dickinson) using the standard configuration and parameters. Data acquisition and analysis was performed using the Cell Quest software (BD). Apoptosis were determined by annexin V-FITC fluorescence, respectively.

III.1.21 SAXS experiments

Small Angle X-Ray Scattering (SAXS) data were collected on a SAXSess mc2 apparatus (Anton Paar KG, Graz, Austria). This instrument is attached to a ID 3003 laboratory X-Ray generator (General Electric) equipped with a sealed X-Ray tube (PANalytical, $\lambda_{Cu\ K\alpha}$ =

0.1542 nm) operating at 40 kV and 50 mA. The liposome dispersions were introduced into a 1 mm capillary before being placed inside an evacuated chamber equipped with a temperature-controlled sample holder unit maintained at 25 °C. The 2D scattering patterns were detected by a CCD camera. Using SAXSQuant software (Anton Paar), the 2D images were integrated into the 1D scattering intensities I (q) upon the magnitude of the scattering vector q ($q = (4\pi/\lambda) \sin \theta$; where 2θ is the total scattering angle). All data were collected in the q range from 0.11 to 6 nm^{-1}. Scattering data, obtained with a slit collimation, contain instrumental smearing. Therefore, the beam profile has been determined and used for the desmearing of the scattering data. All data were corrected for the background scattering from the filled capillary with solvent (water). The scattered intensities were evaluated on an absolute scale using water as a reference.

III.1.22 Fourier Transform Infrared Spectroscopy

FTIR spectra were recorded on a Tensor 27 mid-FTIR spectrometer (Bruker, Germany) equipped with a diamond ATR (Attenuated Total Reflectance) module and a DTGS (Deuterated-Triglycine Sulfate) detector. Scanning rate was fixed to 20 kHz and 128 scans were performed for both reference and samples between 400 cm^{-1} and 4000 cm^{-1} at a resolution of 2 cm^{-1} at room temperature. An initial reference spectrum was then recorded. Next, a small amount of each sample put on the diamond crystal of the optical cell and a minimum three separate experiments were done for each sample. In addition, all treatments were carried out using OPUS software (Bruker, Karlsruhe, Germany). Crude absorbance spectra were smoothed using a nine-points Savitsky-Golay smoothing functions. Then, spectra were centered and normalized using OPUS software.

III.1.23 Rheological characterization

Rheological studies were carried out using a kinexus pro rheometer (Malvern Instruments, Orsay, France). During the rheological experiments, the measuring system was covered with a humidity chamber to minimize water evaporation. Samples were allowed to rest for at least 300 s prior to analysis.

III.1.23.1 *Shear Viscosimetry*

Steady-shear viscosity and shear stress measurements were determined using a cone-and-plate geometry (50 mm, 1°). For the steady-shear viscosity measurement, the shear rate was increased from 10^{-3} to $10^{3}s^{-1}$.

In order to confirm the presence of dynamic hysteresis, shear stress was increased from 10^{-3} to 0.5 and then decreased in the same shear stress range.

III.1.23.2 *Oscillatory rheometry*

To determine the mechanical properties of the liposomes dispersions, an amplitude sweep was firstly conducted at a frequency of 0.5 Hz by changing the shear strain from 0.1% to 1000% in order to determine the linear viscoelastic region.

On the basis of this test, a value of a strain within the linear regime was then used in the subsequent frequency sweep with the change of frequency between 0.01 and 10 Hz.

For these experiments, a plate-and-plate (20 mm) and a cone-and-plate geometries were used.

III.1.24 *In vitro* Drug release

III.1.24.1 *Release in PBS solution*

The percentage of curcuminoids released was determined as described earlier with suitable modification (Aditya *et al.,* 2012). The liposomes containing curcuminoids were dispersed in PBS (pH 7.4) at a rate of 1: 2, after remove untrapped curcuminoids molecules by centrifugation at 10,000 rpm for 10 min. The dispersion was divided into 24 aliquots (1.8 ml each) in eppendorf. The eppendorfs were kept in a thermo stable water bath at 37 ºC. Since solubility of curcuminoids in aqueous solutions is exceedingly low, released curcuminoids remain in the form of crystals instead of solubilizing in the released medium. At predetermined time intervals, the sample was centrifuged also at 10,000 rpm for 10 min to separate the released curcuminoids crystals from the liposome. After centrifugation, released curcuminoids crystals formed a pellet and the supernatant contain loaded curcumin was assayed by HPLC at 425 nm by dissolving in methanol. The percentage of curcuminoids released was determined using the formula shown below (equation 3).

$$\text{Drug release}(\%) = \frac{\text{Curcumin released } (mg/mL)}{\text{Curcumin encapsulated } (mg/mL)} \times 100 \quad (3)$$

III.1.24.2 *Simulated gastric digestion*

Simulated gastric fluid (SGF) which virtually mimics the conditions in the stomach was constituted as described earlier with slight modification (Aditya *et al.,* 2013). Briefly, after remove untrapped curcuminoids molecules by centrifugation at 10,000 rpm for 10 min. sample was added in simulated gastric ((0.2 wt.% NaCl, pepsin 0.32 wt.% (from porcine stomach mucosa)) and pH was adjusted to 2 with 0.5 M HCl.

Curcumin nanoliposomes (adjusted to pH 2) were mixed with SGF in the ratio of 1:2 in a flask. The mixture was placed in a shaking water bath (170 rpm) at 37 °C. Samples were collected at different time intervals and the digestion was stopped by placing samples in cold water for 15 min, then the released curcumin measured as explained above. All the experiments were carried out in triplicate.

III.1.24.3 *Simulated intestinal digestion*

Simulated intestinal fluid (SIF) was prepared by the method given by (Singh and Sarkar, 2010 ; Tikekar *et al.,* 2013) with slight modifications. Part of the juice obtained after digestion in SGF for 2 h which represents the average duration of gastro-intestinal (GI) transit was incubated in SIF containing (30 mM CaCl2, 1.0 wt.% Pancreatin (from porcine pancreas), 0.5 wt.% Bile salts and 25 mM potassium dihydrogen phosphate, pH 6,8). The pH was adjusted to 6.8 with 0.5 M NaOH.

The mixture was placed in a shaking water bath (170 rpm) at 37°C. The samples were pipetted out at predetermined time intervals and the eppendorfs were immediately put in an ice-cold water bath for 15 min to stop the further hydrolysis. Then, the released drug determined as explained above and all the experiments were carried out in triplicate.

In the case of chitosan coated liposomes, we added in SIF 0.5% (w/v) Tween-80 to solubilize free released curcumin (Zhang *et al.,* 2013), then we followed the same digestive condition. The samples were centrifuged first at 15,000 rpm for 20 min to eliminate the participated particles, then the supernatant which contains (free curcumin dissolved in

Tween-80 solution) was separated by centrifugation at 3,300× g for 20 min using a membrane filter (Centrisart® I, MWCO 100 kDa; Sartorius,GmbH Germany)(Sun *et al.*, 2013).

III.1.25 Statistical analysis

All data are presented as mean ± standard error. Analyses were carried out with 'one-way ANOVA' (for three or more groups) with Bonferroni corrections or student t-test (for two groups). Statistical significance was determined by Student's t-tests with p value lower.

Résultats et discussion

IV. Enhancing anti-cancer activity of curcumin on MCF7 cells through O/W nanoemulsions based on marine and plant lipids.

M. Hasan[1]., N. Belhaj[1]. C. Kahn[3]., A. Tamayol[2]., E. Arab-Tehrany[1]., M. Linder[1]

[1]Université de Lorraine, Laboratoire d'ingénierie des biomolecules, TSA 40602 54518 – Vandœuvre Cedex

[2]Center for Biomedical Engineering, Department of Medicine, Brigham and Women's Hospital, Harvard Medical School, Boston, MA 02139, USA. Harvard-MIT Division of Health Sciences and Technology, Massachusetts Institute of Technology, Cambridge, MA 02139, USA. Wyss Institute for Biologically Inspired Engineering, Harvard University, Boston, MA, 02115, USA.

[3]IFSTTAR, LBA, F-13916 Marseille, France

IV.1 Résumé de la publication

L'objectif de cette première partie consiste à étudier les caractéristiques physicochimiques d'émulsions de curcumine avec des huiles végétales ou marines, puis évaluer la cytotoxicité de ces émulsions vis-à-vis d'une lignée cellulaire MCF7. Dans une première partie de ce travail, nous allons formuler des vecteurs de curcumine sous forme d'émulsion par homogénéisation haute pression et sonication.

Ces émulsions seront ensuite caractérisées en utilisant les différentes techniques analytiques notamment, le zétasizer, la chromatographie phase gaz, la chromatographie en phase liquide à haute performance HPLC, le Iatroscan (chromatographie sur couche mince couplée une détection par ionisation de flamme).

Les activités cytotoxiques de la curcumine vis-à-vis des lignées cellulaires tumorales mammaires MCF7 seront ensuite mesurées en utilisant le systeme xCELLigence (en partenariat avec le laboratoire du CRAN–CAV). L'approche était basée sur la surveillance en temps réel de l'impédance de la cellule ainsi que la caractérisation dynamique de la réponse cellulaire mesurée sur les cellules MCF7 cancéreuses.

Keywords: Nanoemulsion, Cancer cells MCF7, Drug encapsulation, curcumin.

IV.2 Introduction

Oil-in-water (O/W) nanoemulsions are commonly used in food, pharmaceutical and cosmetic industries for delivery of hydrophobic bioactive agents such as vitamins, antioxidants, antimicrobials, parenteral nutrition, phytosterols and omega-3 fatty acids (Belhaj *et al.,* 2012 ; Bouyer *et al.,* 2012 ; Joseph and Bunjes, 2012 ; Kargar *et al.,* 2011 ; Lomova *et al.,* 2010 ; Wang *et al.,* 2008b). O/W nanoemulsions are usually prepared by homogenizing an oil phase into an aqueous phase in the presence of water-soluble emulsifiers/stabilizers (McClements, 2010). Due to their small droplet size and large surface area, nanoemulsions have good stability to gravitational separation, flocculation, coalescence, and offer controlled release and/or absorption of functional ingredients (Acosta, 2009 ; McClements, 2010). On the other hand, Ostwald ripening is the major destabilization mechanism in the nanoemulsions. This problem arises due to the increased solubility of dispersed phase into the aqueous phase and can be tackled by introducing the dispersed phase with strong hydrophobic properties (Lee *et al.,* 2011).

Nanoemulsions can be prepared either using high-energy (mechanical-based) or low-energy (chemical-based) approaches depending on the underlying principle. Mechanical methods for nanoemulsions preparation include microfluidization (Jafari *et al.,* 2007 ; Qian *et al.,* 2012), high pressure homogenization (El Kinawy *et al.,* 2012 ; Yuan *et al.,* 2008), and ultrasound homogenization (Kaltsa *et al.,* 2013 ; Leong *et al.,* 2009).

Nanoemulsions are self-assembled mixtures of water, oil and surfactants and have the advantages of being optically isotropic and thermodynamically stable. It is also known that using mixed surfactants or adding can reduce the surface tension between oil and water when preparing nanoemulsion. Much attention has recently been given to the utilization of phospholipids in formulating pharmaceutically acceptable emulsions (Lundberg, 1994 ; Patel *et al.,* 2006).

Lecithin, which has two long hydrocarbon chains, is a major component of lipid bilayers of cell membranes and a natural, biological amphiphile. Furthermore, it is in many respects regarded as an ideal biological surfactant because it is biodegradable. It may be used for various purposes (Lin *et al.,* 2009).

Fish oils are a readily available source of polyunsaturated fatty acids (PUFA) which play an important role in human health and nutrition (Linder *et al.,* 2002). Eicosapentaenoic acid (EPA), *n*-3 fatty acids and docosahexaenoic acid (DHA) have been shown to be of major importance in the prevention of a number of diseases, including coronary heart disease, inflammation, hypotriglyceridemic effect, allergies and diabetes (Suarez *et al.,* 2010). Long-chain polyunsaturated fatty acids (LC-PUFAs) represent 35% of the total fatty acids (FAs) in human brain (Lauritzen *et al.,* 2001 ; Minnis *et al.,* 1998). Oil and marine lecithin from salmon head (Salmo salar) contains a high percentage of PUFAs, especially EPA and DHA (Belhaj *et al.,* 2010 ; Gbogouri *et al.,* 2006). Rapeseed lipid consist mainly of three mono- and poly-unsaturated fatty acids, namely oleic (C18:1), linoleic (C18:2), and linolenic acids (C18:3). Linoleic and linolenic acids are important to human health and are essential fatty acids as humans are unable to synthesize them (Coonrod *et al.,* 2008).

Curcumin was selected as a bioactive model compound. It is a highly lipophilic bioactive molecule isolated from the rhizomes of turmeric (i.e., *Curcuma longa*), and displays a wide variety of health promoting activities including antioxidant, anti-inflammatory, anti-carcinogenic, and antimicrobial activities (Aggarwal *et al.,* 2003 ; Anand *et al.,* 2007 ; Lin *et al.,* 2009). In the majority of research studies on curcumin, the mixtures utilized were composed of at least three major curcuminoids (Gulseren *et al.,* 2014) (Figure 24)

Curcumin is rapidly metabolized in the intestines and in the liver, quickly b-glucuronidated, and reduced to form a family of related compounds (Lin *et al.,* 2000), which makes it very challenging to trace curcumin during absorption or in the bloodstream and excretion products. However, limited water solubility and poor oxidative stability limits broad application of curcumin in diverse pharmaceutical and food products (Anand *et al.,* 2007). Therefore, there is a significant need to improve the delivery of curcumin using encapsulation strategies increase curcumin solubility and bioavailability such as O/W emulsions.

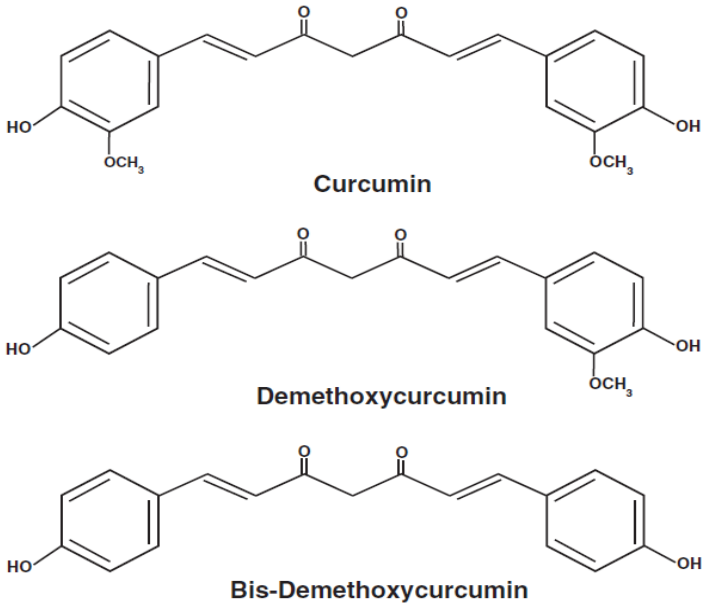

Figure 24. Chemical formula of the three major curcuminoids. Curcumin, demethoxycurcumin and Bis-demethoxycurcumin (Akhtar *et al.*, 2012).

In our study, two formulations of nanoemulsion were tested in order to improve solubility and bioavailability of curcumin, nanoemulsion based on salmon and rapeseed sources, solubilized curcumin prepared by sonication and then by high pressure homogenization methods. Nanoemulsions resulting from the latter process were characterized for the different formulations and their ability to deliver hydrophobic drugs as carrier for cancer chemotherapy was evaluated *in vitro*. The approach was based on physicochemical characterizations of nanoemulsion solutions and real-time cell impedance monitoring of MCF7 cancer cells response to curcumin nanoemulsion encapsulation exposure for cancer cell cytotoxicity.

IV.3 Results and discussion

IV.3.1 Fatty acid composition of oils and lecithins

The main fatty acid compositions are shown in Table 4. The first observations allow us to highlight the fraction of monounsaturated fatty acids that prevail regardless of the type of oil except for the salmon lecithin which polyunsaturated fatty acids were predominate (49.13%). The percentage of the fraction of monounsaturated fatty acids is followed directly by the percentage of polyunsaturated fatty acids in all samples except for the salmon lecithin

for which saturated fatty acids are higher with 26.31%. Oleic acid (C18: 1n9) is the major fatty acid of monounsaturated fatty acids in all samples and in particular oil and rapeseed lecithin 63.02 ± 0.06% and 53.75 ± 0.23% respectively. In regard to rapeseed lipid, the percentage of C18:2n6 was more important in the polyunsaturated fatty acids class with 11.46 ± 0.18% for oil and 27.95 ± 0.06%for lecithin, followed by C18:3 n-3 with 9.22 ± 0.03% and 6.54 ± 0.09% for oil and lecithin, respectively.

Marine oils contain generally long chain polyunsaturated fatty acids (LC-PUFAs) with 5 and 6 double bounds in proportion between 15% and 30% of the total fatty acids (Linder *et al.,* 2010). There is a great difference between LC-PUFA's percentage in oil and lecithin fractions, especially for eicosapentaenoïc acid (EPA) and docosahexaenoïc acid (DHA). Salmon lecithin contains about three times more DHA (23.41% ± 0.29) than salmon oil (6.43% ± 0.04), and about two times EPA (9.40% ±0.06) than salmon oil (4.94% ±0.02). Due to their high content in EPA and DHA, salmon lipids have a ratio n-3/n-6 higher than rapeseed lipids.

Table 4. Main fatty acid composition of different lecithins by gas chromatography (area %).

Fatty acids	Salmon oil		Rapeseed oil		Salmon lecithin		Rapeseed lecithin	
	%	SD	%	SD	%	SD	%	SD
C14	3.87	0.03	-	-	1.60	0.01	-	-
C16	12.67	0.13	4.54	0.00	16.14	0.09	7.65	0.02
C18	3.21	0.02	1.45	0.00	4.68	0.02	1.46	0.01
C21	0.30	0.30	-	-	1.93	0.02	-	-
C22	-	-	-	-	0.78	0.29	0.29	0.29
C23	-	-	-	-	1.18	0.07	-	-
SFA	20.05	-	5.99	-	26.31	-	9.4	-
C16:1	4.29	0.02	0.25	0.00	1.54	0.06	0.29	0.00
C17:1	0.39	0.01	-	-	1.20	0.01	-	-
C18:1n9	36.36	0.23	63.02	0.06	19.96	0.30	53.75	0.23
C20:1n11	5.17	0.12	1.21	0.01	0.42	0.10	0.68	0.01
MUFA	46.21	-	64.48	-	23.12	-	54.72	-
C18:2n6	11.46	0.18	18.81	0.07	5.81	0.07	27.95	0.06
C18:3n3	4.24	0.08	9.22	0.03	2.70	0.02	6.54	0.09
C20:2n6	1.52	0.02	0.25	0.02	0.29	0.03	0.17	0.02
C20:3n6	0.27	0.00	-	-	0.30	0.02	-	-
C20:3n3	0.40	0.00	-	-	0.31	0.04	-	-
C20:4n6	0.50	0.72	-	-	2.32	0.10	-	-
C20:5n3(EPA)	4.94	0.02	-	-	9.40	0.06	-	-
C22:4n6	0.52	0.01	-	-	1.68	0.03	-	-
C22:5n3	2.46	0.05	-	-	3.22	0.06	-	-
C22:6n3(DHA)	6.43	0.04	-	-	23.41	0.29	-	-
PUFA	32.74	-	28.28	-	49.13	-	34.66	-
n-3/n-6	1.28	-	0.51	-	3.75	-	0.23	-
DHA/EPA	1.30	-	-	-	2.49	-	-	-

IV.3.2 Analysis of different lipids

The determination of the percentage of neutral lipids, polar lipids and lipid classes was performed by using thin layer chromatography coupled with flame ionization detection

(Iatroscan). The migration of salmon and rapeseed oil revealed the presence of a single peak representing the triacylglycerol fraction (100%). The results obtained show that the oils used in this study were pure and contain no polar fraction.

In respect of lecithins, results of the migration in hexane/diethyl ether/formic acid (80:20:0.2, v:v:v) revealed the presence of two distinct peaks for the two types of lecithin (salmon and rapeseed). These two peaks correspond to the polar lipids (PL) and neutral lipids (NL) which have migrated in the apolar solvent. The neutral and polar fractions are respectively 66.54% and 33.46% for salmon lecithin (Figure 25(a)), while the percentage of polar lipids increase in rapeseed lecithin (74.81%) (Figure 25(b)). Second migration in the polar solvent (chloroform / methanol / ammonia 65: 35: 5 v / v / v) allowed us to separate the different classes of polar lipids, the results of this separation show that salmon lecithin (Figure 25(c)), contains phosphatidylcholine (PC) with 28.11% which is the majority class of phospholipid, and phosphatidylethanolamine (PE) with 13.53%. Regarding rapeseed lecithin (Figure 25(d)), the percentage of PE was relatively higher (13.89%) than PC one (11.69%).

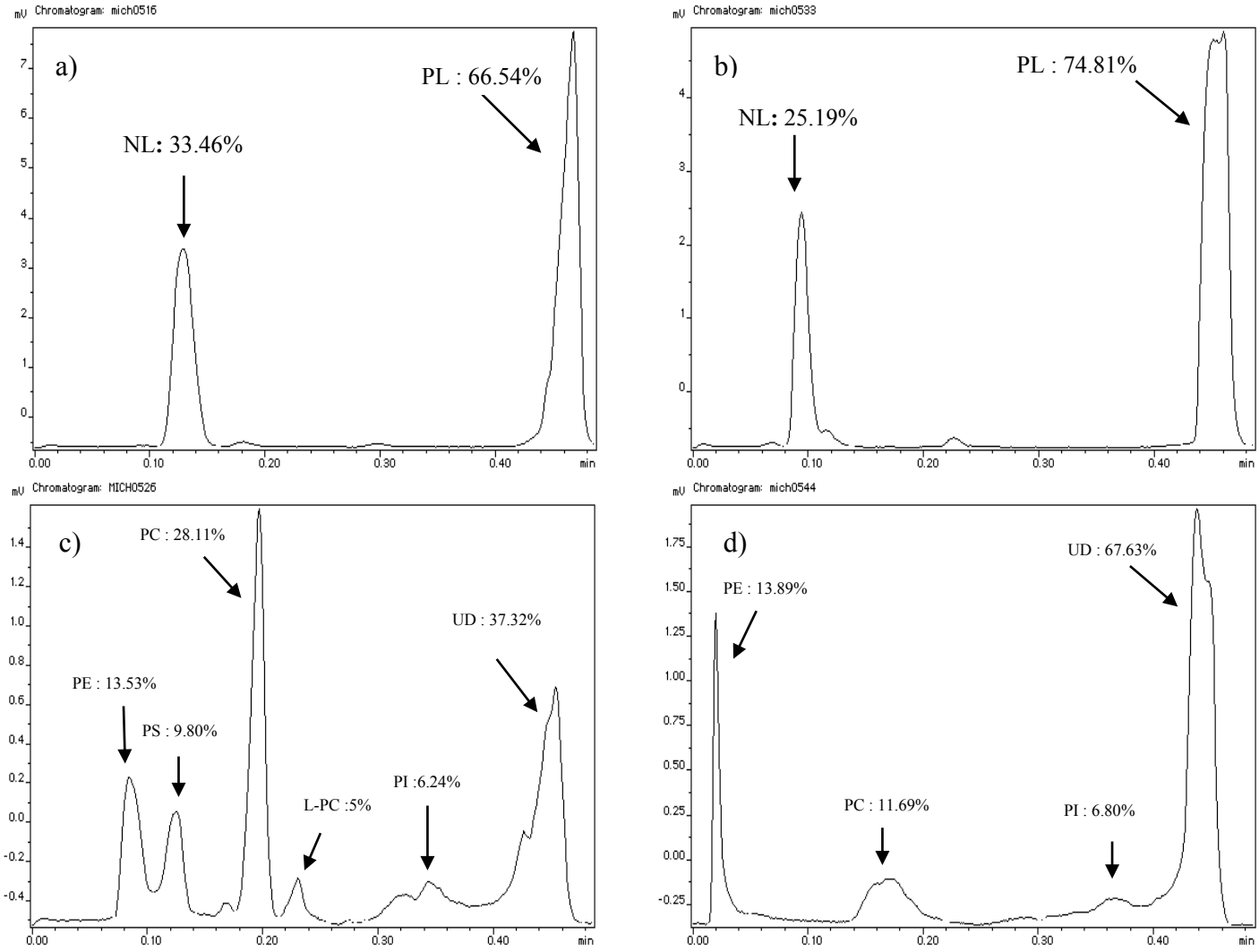

Figure 25. Lipid classes and fraction of polar lipids constituting salmon and rapeseed lecithin, (a, b) represent lipid classes of salmon and rapeseed lecithin respectively, (c, d) represent of polar lipids constituting salmon and rapeseed lecithin respectively. With: PE: Phosphatidylethanolamine, PS: Phosphatidylserine, PC: Phosphatidylcholine, L-PC: *Lysophosphatidylcholine,* PI: Phosphatidylinositol and UD: Undetermined fraction.

IV.3.3 Solubility test of curcumin in oils

Curcumin has a relatively low water-solubility (<0.005 wt.%) and a high oil–water partition coefficient (logP = 2.5)(Ahmed *et al.,* 2012 ; Fujisawa *et al.,* 2004). Thus, the maximum amount of curcumin that can be incorporated into an emulsion-based O/W delivery

system is mainly determined by the maximum amount that can be incorporated into the lipid phase. Therfore, curcumin must be dissolved within the lipid phase prior to making an O/W emulsion. The solubilization in the oil improves the transport of lipophilic molecules to the intestinal lymphatic system and this by increasing absorption from the gastrointestinal tract (Gursoy and Benita, 2004). Maximum solubility of curcumin in salmon oil (0.33±0.07 mg /mL) was found nearly twice greater time than in rapeseed oil (0.18±0.05 mg/mL). This may be explained by the composition of oils. Rapeseed oil contains a small percentage of short-chain fatty acids compared to salmon oil. The short-chain lipids have more polar groups (oxygen) per unit mass than longer chain phospholipids. Therefore, the dipole–dipole interactions between polar groups in the carrier lipid and curcumin molecules are more important (Ahmed *et al.*, 2012).

IV.3.4 Mean particle size, electrophoretic mobility and polydispersity index of nanoemulsions

Determination of vesicle size distribution is a fundamental quality control assay. The mean size and size distribution generally depend on lipid composition and preparation method, e.g. sonication time and number of homogenization process cycles. The minimum size that can be achieved generally depends on the viscosity of materials used and on applied homogenization parameters (pressure and number of cycles). The hydrodynamic diameter and electrophoretic mobility of lipid droplets were measured immediately after emulsion preparations (T0). Because emulsions have a high level of stability, we measured the size and mobility once a week. Measurement of the electrophoretic mobility is used to indicate the stability of a system consisting of particles; it corresponds to the speed at which a charged particle moves in an electric field. Indeed, the physical stability of a suspension is dependent on electrostatic repulsions droplets.

The results of size, electrophoretic mobility and polydispersity index show that the emulsions are very stable during 30 days of storage at room temperature. Indeed, the size ranges from 169.70 to 174.20 nm for the salmon emulsion without curcumin, and from 161.92 to 163.97 nm for salmon emulsion with curcumin encapsulated. In contrast, we note that for vegetable emulsion containing rapeseed oil and rapeseed lecithin, the size of the emulsions is greater and ranges from 224.00 to 228.80 nm for the rapeseed emulsion without curcumin,

and from 205.70 to 212.67 nm for the emulsion with curcumin encapsulated. Therefore, vegetable emulsions were slightly higher in size than salmon emulsions. This small difference in size is probably due to the fatty acid composition and lipid classes of lecithin. Indeed, we found more PC in lecithin salmon (28.11%) than that of rapeseed (11.69%), while the percentage of PE is practically identical, 13.53% and 13.89% respectively for salmon and rapeseed lecithin. The percentage of PC might be responsible for this difference. Thus, demonstrating that the size of the nano-droplets depends not only upon such physical parameters as number of cycles and pressure, but also on oil composition and surface-active properties of lipids used (Benedet *et al.,* 2007 ; Hasan *et al.,* 2014 ; Kabri *et al.,* 2011). The size of the curcumin-loaded emulsions was found to be smaller than the unloaded curcumin ones. Therefore, the hydrodynamic diameter of nanoemulsions decreased from 169.70 ± 0.73, 174.20 ± 1.42 nm to 161.92 ± 1.33, 163.97 ± 0.93 for salmon emulsions, and from 224.00 ± 3.16, 228.80 ± 0.98 nm to 205.70 ±0.96, 212.67 ± 1.25 for rapeseed emulsions, with and without curcumin, respectively. These results suggest a strong interaction between curcumin and oil resulting in a compaction of the core. Our results are in good agreement with the previously reported results (Hasan *et al.,* 2014 ; Mazzarino *et al.,* 2012).

The electrophoretic mobility also shows that the emulsion remains stable during the storage period. The more particle electrophoretic mobility is higher (in absolute value), the less particles will tend to aggregate. According to DLS results, the electrophoretic mobility was slightly higher in salmon lecithin with -3.70, -4.04 and -3.34, -3.60) µmcm $(Vs)^{-1}$ for rapeseed lecithin respectively than salmon lecithin with -3.21 ± 0.07 µmcm$(Vs)^{-1}$. It should be noted that the value of electrophoretic mobility was negative throughout the storage period for nanoemulsion formulation. This negative charge is due to presence of polar phospholipids in the composition of two lecithins. The salmon and rapeseed lecithin contain different type of phospholipids such as phosphatidylserine (PS), phosphatidic acid (PA), phosphatidyl-glycerol (PG), phosphatidylinositol (PI), phosphatidylethanolamine (PE), phosphatidylcholine (PC). At physiological pH, these phospho-lipids are negatively charged except the PC and PE which exhibits no net charge. So, these anionic fractions are probably responsible for the negative electrophoretic mobility (Nirmala *et al.,* 2011)

The poly-dispersity index (PI) is a dimensionless measure of the breadth of the particle size distribution (Zweers *et al.,* 2003). When the PI value is <0.3, the indication is that the sample is of narrow distribution, and when PI value is over 0.3, the sample is considered to have a broad distribution (Yen *et al.,* 2008). The polydispersity index not exceeding the value of 0.17, also supports the stability of emulsions and the fact that the population of lipid droplets does not change in terms of size with the time.

Table 5. Physicochemical properties of salmon (a) and rapeseed nanoemulsions (b), with and without curcumin, immediately after preparation (T0) and during 30 days of storage at 25 °C.

a)

Days	Mean size (nm)		Electrophoretic mobility $\mu mcm(Vs)^{-1}$		Polydispersity index	
	Salmon nanoemulsion without curcumin	Curcumin salmon nanoemulsion	Salmon nanoemulsion without curcumin	Curcumin salmon nanoemulsion	Salmon nanoemulsion without curcumin	Curcumin salmon nanoemulsion
0	169.70 ± 0.73	161.92 ± 1.33	-3.76 ± 0.02	-3.37 ± 0.07	0.16 ± 0.01	0.14 ± 0.01
7	170.47 ± 1.22	163.97 ± 0.93	-3.70 ± 0.02	-3.75 ± 0.05	0.16 ± 0.01	0.14 ± 0.02
14	174.20 ± 1.42	163.27 ± 2.11	-4.04 ± 0.08	-3.98 ± 0.10	0.17 ± 0.01	0.15 ± 0.01
22	172.57 ± 1.10	162.30 ± 0.87	-3.96 ± 0.04	-4.01 ± 0.03	0.17 ± 0.03	0.16 ± 0.01
30	172.85 ± 1.31	162.03 ± 1.01	-3.85 ± 0.03	-3.78 ± 0.06	0.17 ± 0.01	0.15 ± 0.02

b)

Days	Mean size (nm)		Electrophoretic mobility $\mu mcm(Vs)^{-1}$		Polydispersity index	
	Rapeseed anoemulsion without curcumin	Curcumin rapeseed nanoemulsion	Rapeseed nanoemulsion without curcumin	Curcumin rapeseed nanoemulsion	Rapeseed nanoemulsion without curcumin	Curcumin rapeseed nanoemulsion
0	226.07 ± 2.06	205.70 ±0.96	-3.60 ± 0.06	-3.23 ± 0.03	0.17 ± 0.01	0.14 ± 0.01
7	225.57 ± 0.76	209.37 ± 0.31	-3.56 ± 0.04	-3.47 ± 0.06	0.16 ± 0.01	0.14 ± 0.02
14	224.00 ± 3.16	210.53 ± 2.07	-3.34 ± 0.05	-3.37 ± 0.02	0.17 ± 0.01	0.15 ± 0.01
22	228.80 ± 0.98	212.67 ± 1.25	-3.40 ± 0.03	-3.50 ± 0.03	0.17 ± 0.02	0.15 ± 0.01
30	227.56 ± 1.54	211.47 ± 0.74	-3.52 ± 0.04	-3.44 ± 0.06	0.16 ± 0.03	0.15 ± 0.02

IV.3.5 Stability of nanoemulsions

Stability of both nanoemulsions with and without curcumin was performed at room temperature (25 °C), and was evaluated by monitoring the mean particle size, electrophoretic mobility and polydispersity index (Belhaj *et al.*, 2012 ; Klang *et al.*, 2012), described that small polydispersity index (lower than 0.2) indicates a narrow droplet size distribution and consequently, better stability. All these parameters remain unaffected during 30 days of storage at 25 °C, furthermore we did not observe any precipitation of curcumin (Table 5). The stability of the emulsions depends on the nature and concentration of lipids, emulsifier, and aqueous system. Emulsifier forms a layer around droplets that reduces the interfacial energy and provides a mechanical barrier to coalescence and then increases the stability of nanoemulsions (Balakrishnan *et al.*, 2009). It is known that emulsions with smaller sizes have higher kinetic stability, which is ascribed to a larger reduction in the creaming velocity, faster Brownian diffusion, and larger steric stabilization effects for emulsion droplets(Wang *et al.*, 2008b). Nanoemulsions with or without curcumin were found to have stable size distribution during 30 days of storage at 25 °C. Furthermore no precipitation or loss of encapsulation of curcumin was observed in samples.

IV.3.6 Nanoemulsion morphology

The sonication and homogenization steps were performed in order to produce homogeneous size distribution droplets. The TEM image of the nanoemulsion shown in (Figure 26) revealed that oil droplets were homogenous, spherical with good integrity

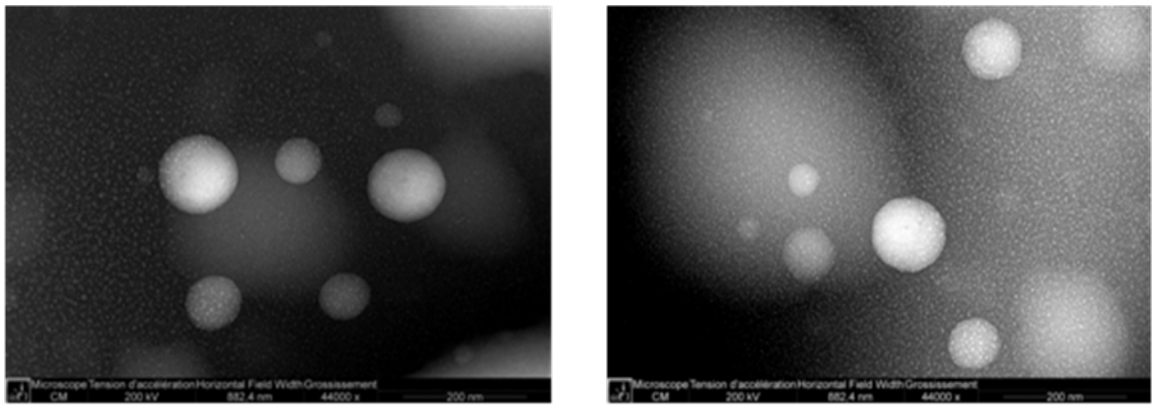

a b

Figure 26. TEM image of O/W nanoemulsion based on salmon oil and lecithin as surfactant **(**a), and nanoemulsion based on rapeseed oil (b).

IV.3.7 Cytotoxicity analysis

The cytotoxicity of nanoemulsion with and without curcumin was detected using an impedance-based analysis system. We examined the effects of composition and concentration of lipid and curcumin on toxicity of MCF7 cancer cells. The effects of vegetable (rapeseed) and marine (salmon) nanoemulsion were compared to observe the influence of the lipid composition. The samples were put in contact with the cells during the exponential phase after 24 hours of culture. Indeed, the processing time depends mainly on the rate of cell growth. Curcumin was solubilized in ethanol, and its effect at different concentrations and corresponding ethanol concentrations alone were evaluated.

In the first time, the cytotoxic effect of different concentrations of non-encapsulated curcumin (2.5 and 5 µM) on MCF7 cells was studied. Curcumin was solubilized in ethanol before analysis, and then the effect of different concentrations of ethanol was also evaluated as control. There is no significant cytotoxic effect on MCF7 cells in contact with different concentration of ethanol corresponding to 2.5, and 5 µM of curcumin dilution (Figure 27). However, curcumin have a dose-dependent effect on MCF7 cancer cells (Figure 27), but the latter effect was small compared to encapsulated curcumin effect (Figure 29). The anti-proliferative activity of curcumin has previously been attributed to curcumin-induced apoptosis (Kuo *et al.,* 1996 ; Mehta *et al.,* 1997). Two proteins have previously been shown to be involved in curcumin induced apoptosis which are Bcl-2 and BAX. Proteins of the Bcl-2

family are key regulators of apoptosis while BAX belongs to the pro-apoptotic group (Er *et al.,* 2006). Bcl-2 exerts its anti-apoptotic effects via inhibition of mitochondrial cytochrome c release. By contrast, BAX asserts a pro-apoptotic effect by interacting with membrane pore proteins to increase cytochrome c release (Murphy *et al.,* 2000). Curcumin treatment of diverse cell types has recently been shown to result in decreased Bcl-2 cellular levels and increased cellular levels of BAX (Shankar and Srivastava, 2007 ; Walters *et al.,* 2008). Hence, the anti-tumor activity of curcumin was based on two opposite mechanisms: inhibiting anti-apoptosis proteins, or activating the pro-apoptosis proteins. There are also reports which suggest that curcumin quenches ROS production (Das and Das, 2002 ; Mishra *et al.,* 2005), and thus acts as an antioxidant. Other reports suggest that curcumin quenches ROS production at low concentrations and induces ROS production at high concentrations (Chen *et al.,* 2005). Whereas the pro-oxidant mechanism mediates apoptotic effects, the antioxidant mechanism mediates NF-κB-suppressive effects (Sandur *et al.,* 2007). Other studies report that tumor cells show preferential uptake of curcumin compared to normal cells and the toxicity clearly increased with increasing curcumin uptake. Among various factors that are responsible for higher curcumin uptake in tumor cells against normal cells, the differences in membrane structure, protein composition and bigger size are the major ones (Kunwar *et al.,* 2008 ; Singer, 2004).

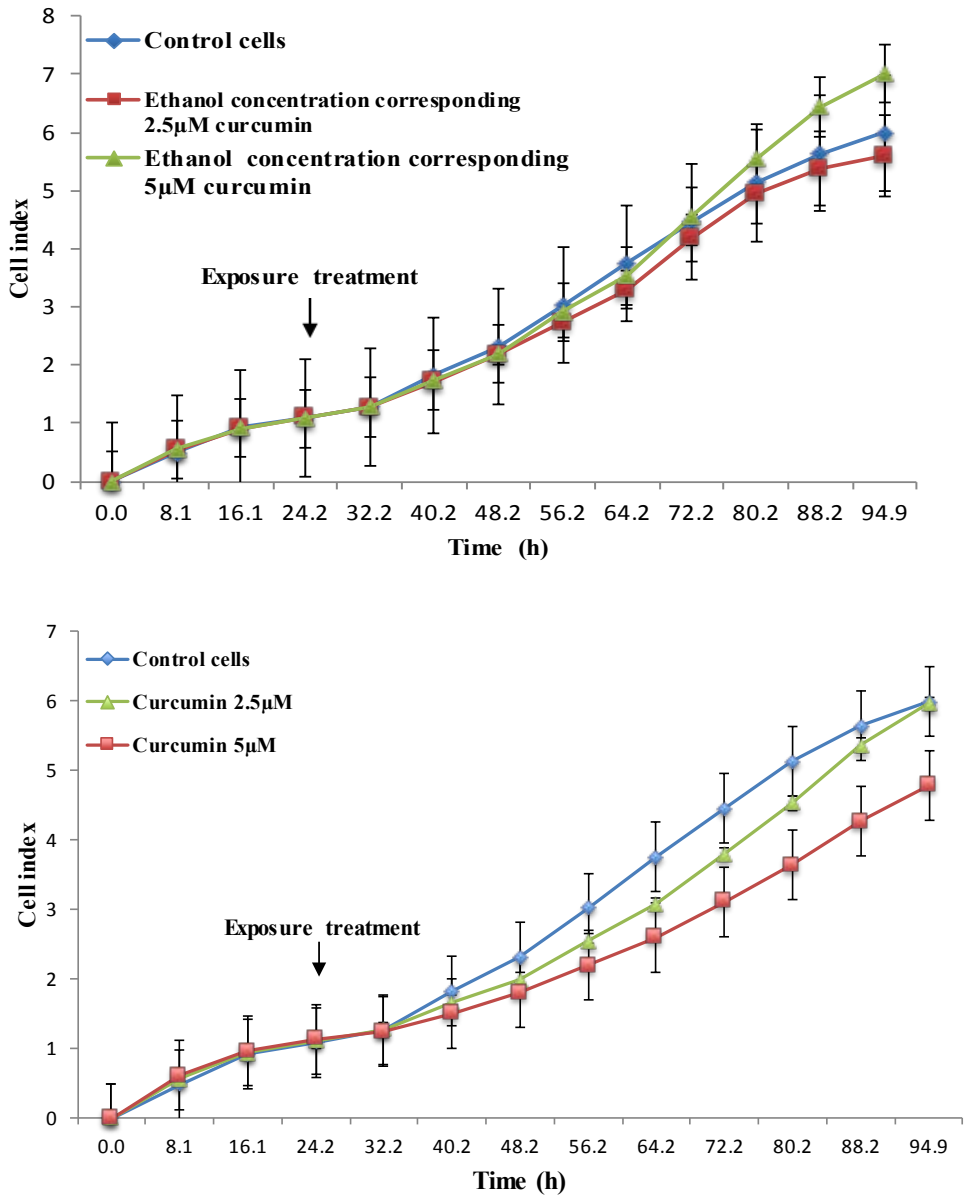

Figure 27. Cell index (CI) kinetics of the MCF-7 cells exposed to different concentrations of ethanol calculated corresponding curcumin concentration used and different concentrations of curcumin (2.5 and 5 µM). CI was monitored during 72 h after compounds exposure. Reported data are the means of three replicates.

Curcumin in its free form is poorly absorbed in the gastro intestinal tract and therefore may be limited in its clinical efficacy by oral medication. This poor oral bioavailability has been attributed to its poor aqueous solubility and extensive first-pass metabolism (Sanoj Rejinold *et al.*, 2011b).

Emulsion encapsulation of this compound would allow systemic administration. Nanoemulsions play an important role on cytotoxicity of the cancer cells depending of their concentration. Beyond the beneficial effects of long-term intake of omega-3 PUFA in cancer patients, we likewise observed rapid-onset effects in previous experimental studies. Many studies have related the cytotoxic action exerted by n-3 PUFAs on cancer cells in vitro with their pro-oxidant potential (Colquhoun and Schumacher, 2001 ; Ding *et al.,* 2004 ; Hong *et al.,* 2002). Despite generally null epidemiological findings, animal and *in vitro* experiments have demonstrated that long-chain n-3 marine fatty acids, particularly eicosapentaenoic acid (EPA) and docosahexaenoic acid (DHA), suppress the development of cancer, whereas n-6 PUFAs possibly promote carcinogenesis (Rose, 1997). Several studies have reported that a high ratio of n–6:n–3 FA is associated with an increased risk of cancer, since a risk associated with n–6 has not been demonstrated (Gerber, 2009). Biological mechanisms have been postulated for

dietary long-chain n-3 fatty acids in cancer prevention and include suppression of eicosanoid production from arachidonic acid (Larsson *et al.,* 2004 ; Terry *et al.,* 2004).

Figure 28 shows the impact of each system on cell proliferation. The nanoemulsion based on rapeseed oil decrease significantly cell proliferation at two concentration 6.49 and 12.98 mg/mL after 40 h in a concentration-dependent manner as compared to control cells. On the other hand, the cytotoxicity of nanoemulsion based on salmon lipid was significant from the low concentration 3.64 mg/mL which was more important even than the concentration nearly double 6.49 mg/mL of rapeseed lipid effect. Looking at the shape of the graph, it is clear that the lipid composition of vectors influences the cytotoxic effects on cells. Indeed, we can explain the effect more important of the salmon lipid on cytotoxicity of cancer cells is due to the presence of long chain fatty acids in the salmon lipid especially acid EPA and DHA, in a very large amount especially in the phospholid, on the one hand, and the presence of astaxanthin in the lipid suamon, which is a red pigment of the family of xanthophylls (Carotenoids), such a component known as an anti-oxidant, anti-inflammatory and anticancer (Nagendraprabhu and Sudhandiran, 2011 ; Song *et al.,* 2011a ; Tripathi and Jena, 2010).

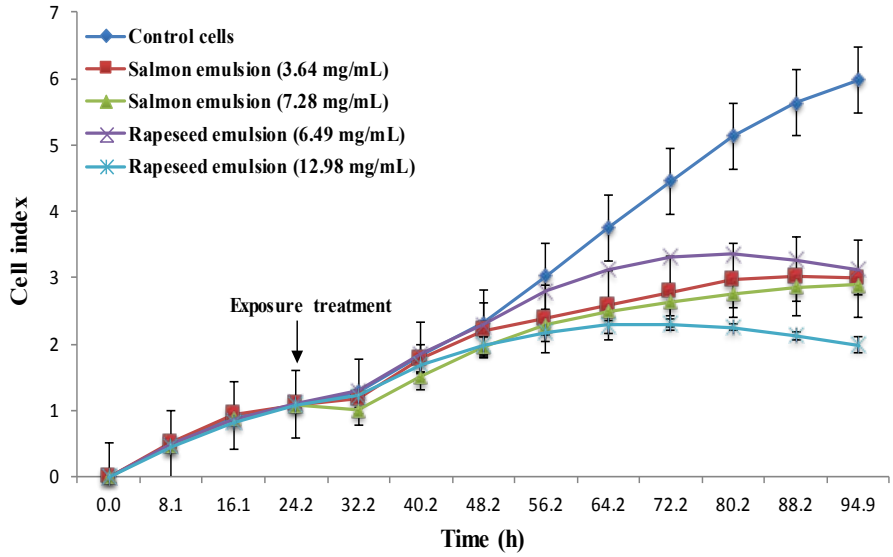

Figure 28. Cell index (CI) kinetics of the MCF-7 cells exposed to the different concentrations of salmon emulsions and rapeseed emulsions. CI was monitored during72 h after liposomes exposure. Reported data are the means of three replicates.

The current study evaluated the antitumor activity of encapsulated curcumin *in vitro* on MCF7 cancer cell. Our study showed that encapsulated curcumin in nanoemeulsion treatment significantly increases the cancer cell cytotoxicity (Figure 29), while free curcumin has a lower impact on cancer cells (Figure 27). We can conclude that emulsion encapsulation of curcumin increases curcumin's cell bioavailability and enhances their cellular effects on proliferation (Figure 29). This also suggests a synergic cytotoxic effect between curcumin and lipid in the form of emulsion. Looking at the graphs of cytotoxicity of salmon emulsion and the emulsion charged with curcumin, a synergistic effect is observed between the lipid and the curcumin gradually.

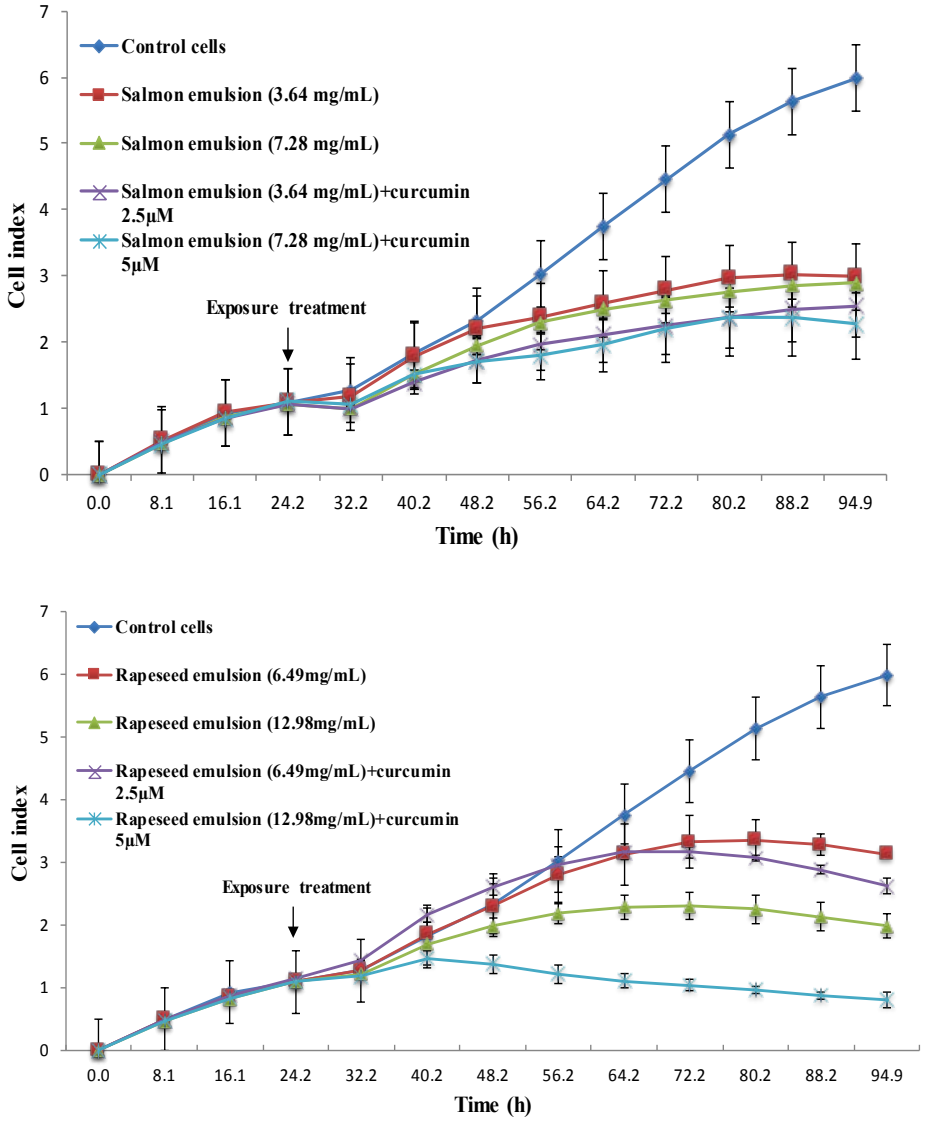

Figure 29. Effect of curcumin loaded nanoemulsion on CI kinetics in MCF7 cells exposed to different concentrations of encapsulated curcumin by xCELLigence system during 72 h afterexposure treat. Reported data are the means of three replicates.

IV.4 Conclusion

The overall objective of this study was to investigate the physicochemical properties of salmon nanoemulsion compared with rapeseed nanoemeulsion, with and without encapsulated curcumin, and assess the effect of all formulations on cell proliferation on breast tumor cell line MCF7.

Maximum solubility of curcumin in salmon oil (0.33±0.07 mg/mL) was found nearly twice fold greater than in rapeseed oil (0.18±0.05 mg/mL). This may be explained by the composition of rapeseed oil which contains a small percentage of short-chain fatty acids compared to salmon oil.

All nanoemulsions were stables over 30 days at 25°C, with 170 nm droplet mean size for salmon emulsion and 220 nm for rapeseed one due to the fatty acid composition and lipid classes of lecithin. Moreover, the size of the curcumin-loaded emulsions was found to be smaller than the unloaded curcumin ones suggesting a strong interaction between curcumin and lipid. The fatty acid composition of the vectors is the main reason that justifies the observed differences. For example, the vectors based on oil and salmon lecithin are the most toxic due to their high content in EPA and DHA, unlike lecithin and rapeseed oil which does not contain them.

Thus, the encapsulation of curcumin by rapeseed or salmon lipid controlled the proliferation of breast cancer cells for a longer time than without encapsulation process at identical curcumin dose. These results are promising and could have an impact on therapeutic strategy to contain cancer evolution or as prevention.

V. Liposome encapsulation of curcumin: physico-chemical characterizations and effects on MCF7 cancer cell proliferation

Hasan, M[1]., Belhaj, N[1]., Benachour, H[2,3], Barberi-Heyob, M[2,3,4,5], Kahn, C .J.F[6,7]., Jabbari, E[8]., Linder, M[1], Arab-Tehrany, E[1]*

[1] Université de Lorraine, Laboratoire d'ingénierie des biomolecules, TSA 40602 54518 – Vandœuvre Cedex

[2] Université de Lorraine, CRAN, UMR 7039, Campus Sciences, BP 70239, Vandœuvre-lès-Nancy Cedex, 54506, France

[3] CNRS, CRAN, UMR 7039, Vandœuvre-lès-Nancy, France

[4] CNRS, GdR 3049 "Médicaments Photoactivables - Photochimiothérapie (PHOTOMED)", France

[5] Centre Alexis Vautrin, CRLCC, avenue de Bourgogne, Vandœuvre-lès-Nancy Cedex, 54519, France

[6] Aix-Marseille Univ, LBA, F-13916, Marseille, France

[7] IFSTTAR, LBA F-13916, Marseille, France

[8] Department of Chemical Engineering, SWNG Engineering center, Rm 2C02, University of South Carolina, 301 South Main Street, Columbia, SC 29208

V.1 Résumé

La curcumine (diferuloylmethane) est largement étudiée dans le traitement de certains cancers et sucite un intérêt croissant compte tenu de ses propriétés antioxydantes. Cependant sa faible biodisponibilité limite son utilisation clinique. Dans cette étude, nous avons utilisé un procédé d'encapsulation de la curcumine pour améliorer sa biodisponibilité sous forme de nanoliposome. Les résultats montrent que le complexe liposomal augmente la biodisponibilité de la molécule en raison de la présence de lipides polaires riches en acides gras polyinsaturés issus de lipides de saumon et cela de façon plus marquée par rapport à des lécithines de colza et de soja. Les mesures de la cytotoxicité des différentes préparations liposomales ont été testées *in vitro* sur des cellules cancéreuses de type MCF7 afin de déterminer les concentrations optimales à utiliser pour l'étude de ce complexe. La solubilité maximale de la

curcumine dans les différentes lécithines atteint une valeur proche de 0,28 mg/mL avec une forte interaction entre les chaînes carbonées lipidiques. La taille des nanoliposomes formés est fonction de la nature de la lécithine utilisée. Le diamètre varie de 110 à 135 nm avec un indice de polydispersité inférieur à 0,3. L'efficacité d'encapsulation de la curcumine, molécule instable à la lumière et à la température, est comprise entre 63 et 67% en fonction de la nature de la lécithine utilisée. Un traitement par homogénéisation haute pression après une étape de sonication permet d'obtenir des liposomes avec une morphologie de vésicules multilamellaires. La fluidité de la membrane du liposome dépend fortement des lipides polaires présents et de la longueur des chaînes alkyles. La présence de la curcumine dans le complexe liposomal diminue sa fluidité compte tenu de fortes interactions. Les effets cytotoxiques de la curcumine vectorisée ont été étudiés à différentes concentrations par mesure d'impédance. Les effets de la nature du vecteur et de la concentration de la curcumine vectorisée montent des différences significatives sur la cytotoxicité et la prolifération cellulaire de cellules cancéreuses MCF7.

Keywords: Nanoliposome, cancer cells, lecithin, drug encapsulation.

V.2 Introduction

Curcumin, is a yellow lipid-soluble natural pigment, a hydrophobic polyphenol derived from the rhizome of the herb *Curcuma longa*, has been identified as the active principle of turmeric (Aggarwal *et al.,* 2003). Curcumin usually refers to three molecules namely: 1,7-bis (4-hydroxy-3-methoxyphenyl)-1,6-heptadiene-3,5-dione (curcumin); 1,6-Heptadiene-3,5-dione,1-(4-hydroxy-3-methoxyphenyl)-7-(4-hydroxyphenyl) (demethoxycurcumin) and 1,7-bis (4-hydroxy phenyl) -1,6- heptadiene-3,5-dione (bis demethoxy curcumin) (Akhtar *et al.,* 2012) (Figure 24).

Curcuminoids have already become a research focus due to their numerous biological and pharmacological benefits such as antioxidant, antitumor, anti-inflammatory, antimicrobial properties (Bush *et al.,* 2001 ; Gescher *et al.,* 2001 ; Khar *et al.,* 1999 ; Lukita-Atmadja *et al.,* 2002 ; Sharma, 1976), and other desirable medicinal benefits (Aggarwal *et al.,* 2003). However, the therapeutic efficacy of curcumin is limited due to its poor oral bioavailability (Parvathy *et al.,* 2009 ; Wilart *et al.,* 2009). Various strategies have been undertaken to

overcome the limitations of the use of curcumin and to allow its therapeutic application, such as complexation with phospholipids and cyclodextrins, encapsulation in liposomes, biodegradable microsphere, hydrogels, polymeric nanoparticles, and lipid based nanoparticles (Bisht *et al.,* 2007 ; Kunwar *et al.,* 2006 ; Maiti *et al.,* 2007 ; Sou *et al.,* 2008 ; Tiyaboonchai *et al.,* 2007 ; Tønnesen *et al.,* 2002 ; Vemula *et al.,* 2006).

Liposomes as a drug delivery system can improve the therapeutic activity and safety of drugs, mainly by delivering them to their site of action and by maintaining therapeutic drug levels for prolonged periods of time (Gregoriadis and Florence, 1993). The main constituents of liposomes are phospholipids, which are amphiphilic molecules containing water soluble hydrophilic head section and a lipid-soluble hydrophobic tail section. Liposomes can protect bioactive agents from digestion in the stomach and show significant levels of absorption in the gastrointestinal tract, leading to the enhancement of bioactivity and bioavailability (Takahashi *et al.,* 2007).

Lecithin is a natural mixture of phospholipids and neutral lipids, which is a significant constituent of nervous tissue and brain substance. Phospholipids possess a positively or negatively charged head group and a hydrocarbon tail that contains various amounts of unsaturation except phosphatidylcholine (PC) and phosphatidylethanolamine (PE), which have a zwitterionic headgroup at physiological pH. It is a typical amphiphilic phospholipid with good biocompatibility (Nirmala *et al.,* 2011). Numerous studies, both in humans and in animals (Calder and Yaqoob, 2009 ; Van der Meerena *et al.,* 2009), have demonstrated that polyunsaturated fatty acids (PUFA) of the n-3 series, in particular eicosapentaenoic acid (EPA, 20:5 n-3) and docosahexaenoic acid (DHA, 22:6 n-3), are critical to several physiological processes. Oil and marine lecithin from salmon head (*Salmo salar*) contains a high percentage of PUFAs, especially EPA and DHA (Belhaj *et al.,* 2010 ; Gbogouri *et al.,* 2006).

Rapeseed and soya lecithins consist mainly of three mono- and poly-unsaturated fatty acids, namely oleic (C18:1), linoleic (C18:2), and linolenic acids (C18:3). Linoleic and linolenic acids are important to human health and are essential fatty acids as humans are unable to synthesize them (Coonrod *et al.,* 2008). The present study focused primarily on the preparation and physicochemical characterizations of different formulations of nanoliposomes

from natural sources of lecithin (soya, rapeseed and salmon head), evaluate their ability as a carrier for hydrophobic drugs in cancer chemotherapy. In addition, the *in vitro* biological effect of nanoliposome-encapsulated curcumin on cell proliferation was performed. The approach was based on real-time cell impedance monitoring, characterizing the measured dynamic cell response on MCF7 cancer cells. Cytotoxicity test of encapsulated curcumin by nanoliposomes was performed on MCF7 cancer cells.

V.3 Results and discussion

V.3.1 Fatty acid

The main fatty acid compositions are shown in Table 6. The percentage of total polyunsaturated fatty acids was the highest in soya lecithin but the variety of polyunsaturated fatty acids is higher in salmon lecithin. Ten polyunsaturated fatty acids belonging to omega 3 and omega 6 families were detected in salmon lecithin. The high proportions of fatty acids were C18:2 n6 (52.27%) in the polyunsaturated fatty acids class, C18:1 n-9 (21.49%) in the monounsaturated fatty acids class and C16:0 (17.07%) in the saturated fatty acids class for soya lecithin. The largest amount of fatty acid was a monounsaturated fatty acid, in regards to rapeseed lecithin, the percentage of C18:3 n-3 (6.60%) was important in the polyunsaturated fatty acids class. The fatty acid most present was C18:1 n-9 (56.51%) in the monounsaturated fatty acids class, in regards to salmon lecithin, the most significant proportions of fatty acids were C22:6 n-3 and C20:5 n-3, found in the polyunsaturated fatty acids class with 23.81 and 9.56%, respectively. C18:1 n-9 in the monounsaturated fatty acids class (19.58%), and C16:0 in the saturated fatty acids class (16.21%). The ratio of n-3/n-6 was higher in salmon lecithin compared to rapeseed and soya lecithin with 3.80, 0.25 and 0.10, respectively.

Table 6. Main fatty acid composition of different lecithins by gas chromatography (area %).

Fatty acids	Salmon lecithin		Rapeseed lecithin		Soya lecithin	
	%	SD	%	SD	%	SD
C14:0	1.59	0.01	-	-	-	-
C15:0	0.22	0.01	-	-	-	-
C16:0	16.21	0.01	7.41	0.01	17.07	0.48
C17:0	0.45	0.09	-	-	-	-
C18:0	4. 67	0.06	1.31	0.00	3.32	0.16
C20:0	-	-	0.36	0.01	-	-
C21:0	1.90	0.01	-	-	-	-
C22:0	0.78	0.01	0.21	0.02	0.43	0.04
C23:0	1.22	0.02	-	-	-	-
SFA	27.03	-	9.28	-	20.82	-
C15:1	0.48	0.31	-	-	-	-
C16:1	1.46	0.08	0.33	0.01	-	-
C17:1	1.21	0.10	-	-	-	-
C18:1n9	19.58	0.02	56.51	0.04	21.49	0.47
C20:1n11	0.30	0.02	0.72	0.04	-	-
C22:1n9	-	-	0.25	0.03	-	-
MUFA	23.03	-	57.80		21.49	-
C18:2n6	5.75	0.03	26.32	0.04	52.27	0.36
C18:3n3	2.68	0.01	6.60	0.01	5.41	0.04
C20:2n6	0.29	0.02	-	-	-	-
C20:3n6	0.28	0.04	-	-	-	-
C20:3n3	0.34	0.10	-	-	-	-
C20:4n6	2.43	0.08	-	-	-	-
C20:5n3 (EPA)	9.56	0.06	-	-	-	-
C22:4n6	1.62	0.02	-	-	-	-
C22:5n3	3.27	0.06	-	-	-	-
C22:6n3 (DHA)	23.81	0.29	-	-	-	-
PUFA	49.94	-	32.91	-	57.68	-
n-3/n-6	3.80	-	0.25	-	0.10	-
DHA/EPA	2.51	-	-	-	-	-

V.3.2 Lipid classes

The lipid classes of lecithins were separated by thin-layer chromatography (Iatroscan). At that stage, phosphatidylcholine represented the major class of phospholipids contained in salmon lecithin (28%), rapeseed lecithin (33%) and soya lecithin (23%). Moreover, the percentage of triacylglycerols (TAG) contained in lecithins was 24.5 ± 1.0, 37.75 ± 0.1 and 18.2 ± 0.2% for salmon, rapeseed and soya lecithins, respectively. However, the percentage of

polar fraction showed that soya lecithin was richer in polar lipids with 84.8 ± 0.6%, which was respectively 75.5 ± 0.9 and 62.3 ± 0.8% for salmon and rapeseed lecithins.

V.3.3 Solubility

Curcumin has a relatively low water-solubility (8.33 µg/ml) (Maiti *et al.,* 2007) and high oil–water partition coefficient (log P = 2.5) (Fujisawa *et al.,* 2004). The amount of a highly lipophilic material that can be dissolved in an oil phase depends on the molecular characteristics of the oil (e.g., molecular weight, polarity, and interactions). Moreover, we showed that the maximum solubility of curcumin in soya and salmon lecithin with 0.28 ± 0.03 mg/ml and 0.27 ± 0.03 mg/ml, respectively, was slightly higher than in rapeseed lecithin with 0.25 ± 0.05 mg/ml. This may explain that rapeseed lecithin contains a small percentage of short-chain fatty acids compared to soya and salmon lecithin. The short-chain phospholipids have more polar groups (oxygen) per unit mass than longer chain phospholipids. Therefore, the dipole–dipole interactions between polar groups in the carrier lipid and curcumin molecules are more important (Ahmed *et al.,* 2012).

V.3.4 Liposome size and electrophoretic mobility

Mean size, size distribution and z-potential values are physicochemical parameters that have to be modulated as a function of the proposed application for a certain liposomal system (Calvagno *et al.,* 2007). The particle sizes of nanoliposomes were measured immediately after preparation. The minimum size that can be achieved depends on the viscosity of the materials and on the applied sonication and homogenization parameters. The average liposome diameter was 110.3 ± 0.8 nm for particles from salmon lecithin. The diameter of nanoliposome for rapeseed and soya lecithin was 133.1 ± 0.8 and 135.5 ± 0.1 nm, respectively. The polydispersity index (PI) is a dimensionless measure of the breadth of the particle size distribution (Zweers *et al.,* 2003). When the PI value is <0.3, the indication is that the sample is of narrow distribution, and when PI value is over 0.3, the sample is considered to have a broad distribution (Yen *et al.,* 2008). The polydispersity index was higher for salmon lecithin with 0.25 ± 0.01 compared to soya and rapeseed lecithins with 0.18 ± 0.00 and 0.19 ± 0.01, respectively. Thus, it was clear that the size of the nanoliposome depended not only on such physical parameters but also on fatty acid composition, lipid classes and the surface-active properties of lecithin (Arab Tehrany *et al.,* 2012 ; Benedet *et*

al., 2007). The size of the curcumin-loaded liposomes was found to be smaller than the unloaded curcumin liposomes. Therefore, the hydrodynamic diameter of nanoliposomes decreased from 135.5 ± 0.1, 110.3 ± 0.8 and 133.1 ± 0.8 nm to 131.8 ± 1.3 nm, 96.8 ± 0.7 and 128.7 ± 0.6 nm for soya, salmon and rapeseed liposomes, respectively. These results suggest a strong interaction between curcumin and lecithin resulting in a compaction of the core. Our results are in good agreement with the previously reported results (Mazzarino *et al.,* 2012). Regarding polydispersity index, we observed no significant variation between curcumin loaded liposomes and unloaded liposomes.

Electrophoretic mobility values varied between -3 and -4 µmcm/Vs with a relatively high stability of the formulations, which was due to the positive and negative charge of the polar fraction of lecithin. According to the DLS results, the electrophoretic mobility was higher in soya and rapeseed lecithin with -3.34 ± 0.06 and -3.41 ± 0.05 µmcm/Vs, respectively than salmon lecithin with -3.21 ± 0.07 µmcm/Vs. It should be noted that the value of electrophoretic mobility was negative throughout the storage period for nanoliposome formulation. The salmon, soya and rapeseed lecithin contain different type of phospholipids like as phosphatidylserine (PS), phosphatidic acid (PA), phosphatidylglycerol (PG), phosphatidylinositol (PI), phosphatidylethanolamine (PE), phosphatidylcholine (PC). At physiological pH, these phospholipids are negatively charged except the PC and PE which exhibits no net charge. So, these anionic fractions are probably responsible for the negative electrophoretic mobility (Chansiri *et al.,* 1999). We measured the stability of nanoliposomes by measuring the particle size during one month at 37°C. We observed no significant variation between day 0 and day 30.

V.3.5 Entrapment efficiency

Curcumin is a highly unstable molecule; its stability is susceptible to various conditions such as light, pH, and temperature (Priyadarsini, 2009 ; Wang *et al.,* 1997). It is therefore important to establish that curcumin retains its physiochemical properties and stability after the formulation procedures. In order to study the effect of loading on the activity of curcumin, HPLC analysis was carried out after the encapsulation step. The HPLC profile of curcumin (Figure 30(a)) showed the elution of this molecule at 8.71 min along with

demethoxycurcumin and bisdemethoxycurcumin at 8.20 and 7.75 min, respectively. Extracted curcumin from nanoliposomes also showed a similar HPLC profile (Figure 30(b)).

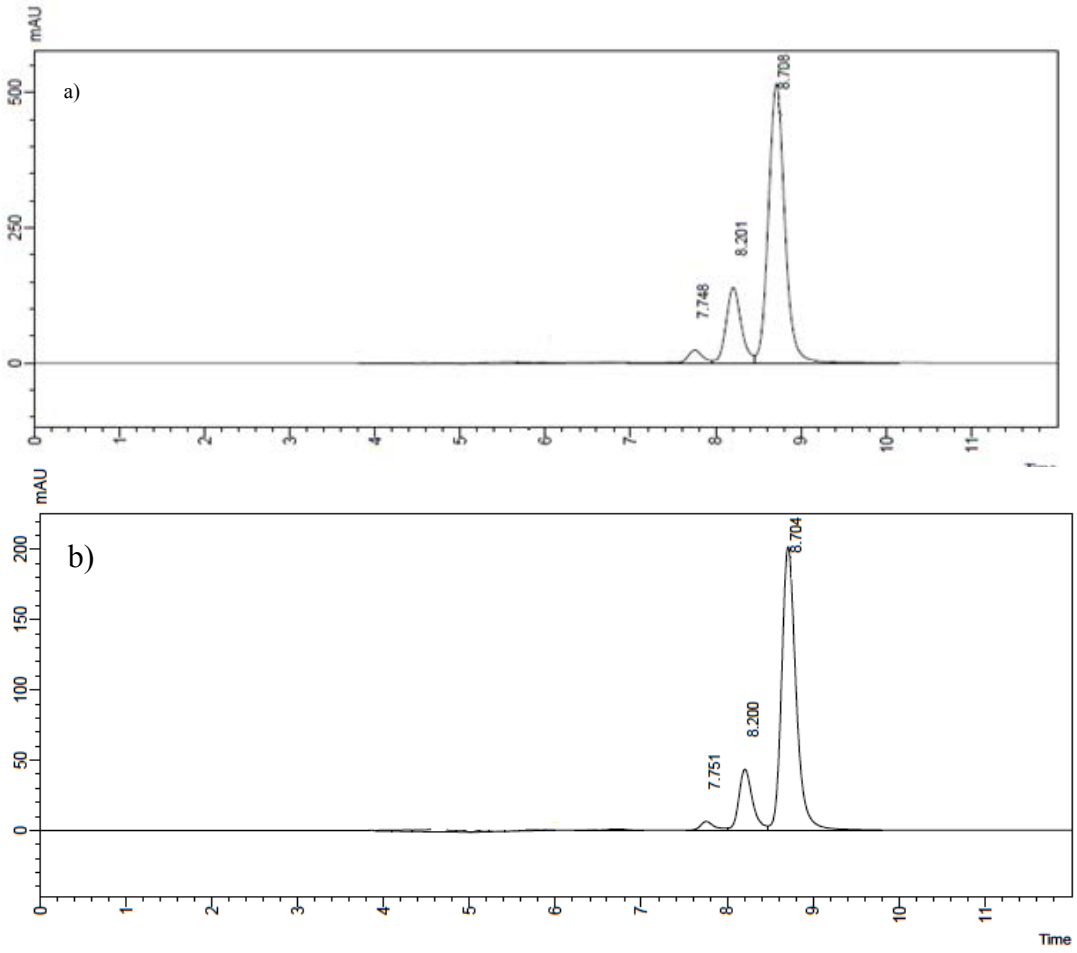

Figure 30. High-performance liquid chromatogram of (a) standard curcumin and (b) curcumin extracted from nanoliposomes.

However, the entrapment efficiency of the curcumin was 63.2 ± 0.7, 65.0 ± 1.1 and 67.3 ± 1.1% with respect to rapeseed, soya and salmon liposomes, respectively. The entrapment efficiency values were high for all formulations. We observed no significant difference in entrapment efficiency of curcumin between soya and other lecithins (rapeseed and salmon), but a significant difference was observed between salmon and rapeseed liposomes ($p<0.05$).

V.3.6 Morphology and size of the liposomes

TEM images indicated that vesicles prepared by sonication and high-pressure homogenization method were in the form of multilamellar vesicles (MLV) because of the

sonication and homogenization steps. The bilayer nature of the vesicles was clearly visible in these micrographs (Figure 31).

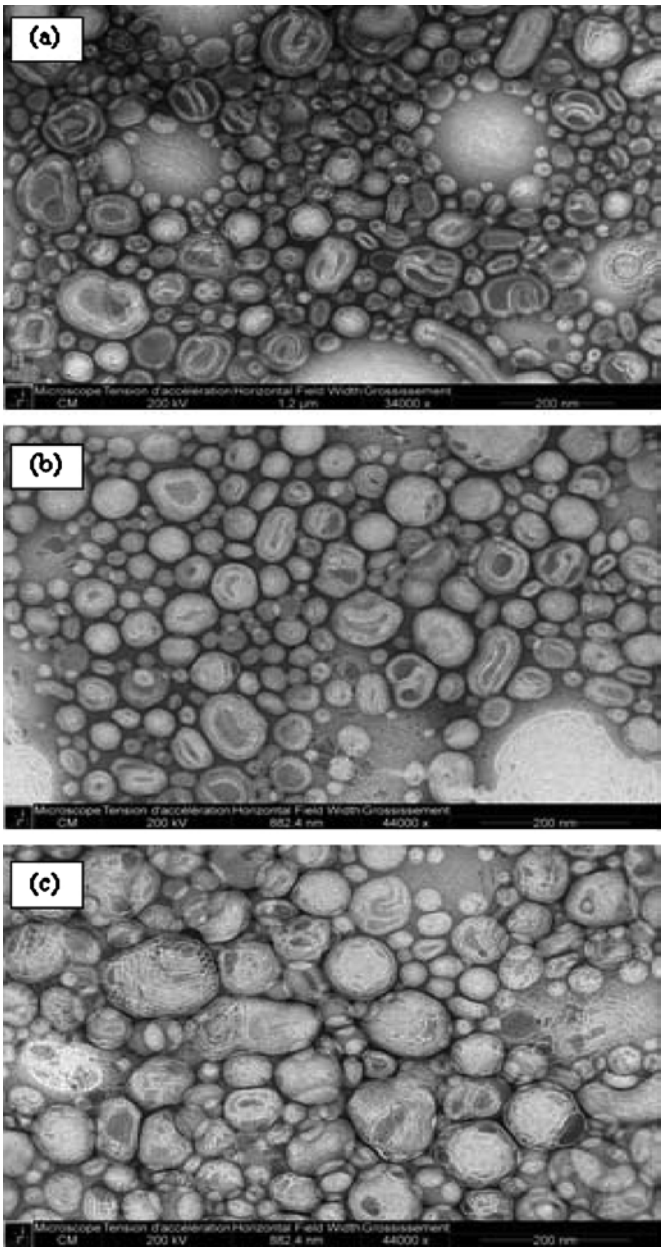

Figure 31. Transmission electron microscopic images of rapeseed (a), soya (b) and salmon (c) nanoliposomes.

We also observed some droplets in each formulation because of the presence of weak oil quantity (10%). The droplets in the three systems were found to be fine enough, even though there were large droplets with diameters higher than 200 nm.

V.3.7 Membrane fluidity

The fluidity of lipid membrane also reflects the order and dynamics of phospholipid alkyl chains in the bilayer and liposome permeation (Maherani *et al.,* 2012). The influence of liposome composition on membrane fluidity was investigates by Coderch *et al*. (Coderch *et al.,* 2000) and Calvagno *et al* (Calvagno *et al.,* 2007). They determined a significant difference in the release profiles of drugs by the presence of two factors: (i) the strength of the drug–liposomal lipid interaction and (ii) the fluidity of the bilayer, i.e. the drug leakage to the aqueous solution increased by increasing the fluidity of the bilayer. The presence of saturated FAs increased the packing between phospholipids, which expelled the water in the vicinity of the bilayer surface, which was evidence of reduced membrane fluidity. On the other hand, unsaturated FAs helped reduce the packing between phospholipids and preserved the level of hydration, thus maintaining membrane fluidity (Leekumjorn *et al.,* 2009).

To recognize the action of curcumin on membrane fluidity, it is necessary to understand the behavior of curcumin with respect to changes in solution composition. According to Table 7, we can observe that membrane fluidity depends on lipid composition of nanoliposomes. It also appears that nanoliposomes made of soya lecithin have higher membrane fluidity than nanoliposomes based on rapeseed and salmon lecithin. Soya lecithin contains a higher proportion of polyunsaturated fatty acids with short chains compared to other lecithins, and membrane fluidity was even more important when the degree of unsaturation of acyl chains increased and the chain length of decreased. The lipid fluidity is expected to increase both the diffusivity and partitioning tendency of the permeant, which yields a possible squaring effect on the enhancement factor.

Table 7. Membrane fluidity of nanoliposomes with and without curcumin.

Sample	Membrane fluidity
Salmon liposome	$3.19\pm0.08^{a,b,*}$
Curcumin loaded salmon liposome	$2.81\pm0.05^{*}$
Rapeseed liposome	$3.53\pm0.07^{a,*}$
Curcumin loaded rapeseed liposome	$2.83\pm0.04^{*}$
Soya liposome	$3.58\pm0.10^{b,*}$
Curcumin loaded soya liposome	$2.83\pm0.02^{*}$

Significant t-test ($p<0.05$) between salmon and rapeseed (a), salmon and soya (b), curcumin loaded liposome and liposome of the same lecithin.

The presence of curcumin decreased the membrane fluidity of all nanoliposomes. Such influence of curcumin is a result of its structure and its molecular interaction with liposome. Curcumin is a highly conjugated and rigid planar molecule. The presence of a curcumin molecule can weaken hydrophobic interactions among acyl chains of phospholipids.

When incorporated into the membrane, the long chain amphiphilic compound tends to decrease the membrane fluidity (Patra *et al.*, 2012). The incorporation of curcumin perturbs the packing characteristics of the phospholipid bilayer and thus enhances the packing density of the hydrocarbon moiety in the lipid bilayer.

V.3.8 Cytotoxicity analysis

The cytotoxicity of nanoliposomes with and without curcumin was detected in real-time using an impedance-based analysis system. We examined the effects of composition and concentration of lecithin and curcumin on MCF7 cells proliferation. Curcumin was solubilized in ethanol, and the effect of different concentrations of curcumin was evaluated.

As shown in (Figure 32) electrical impedance measurements from adherent MCF-7 cells, assessed by normalized cell index (NCI) kinetics, showed a significant dose-dependent effect on CI using curcumin from 12 µM, no significant difference was observed at 5 µM of curcumin.

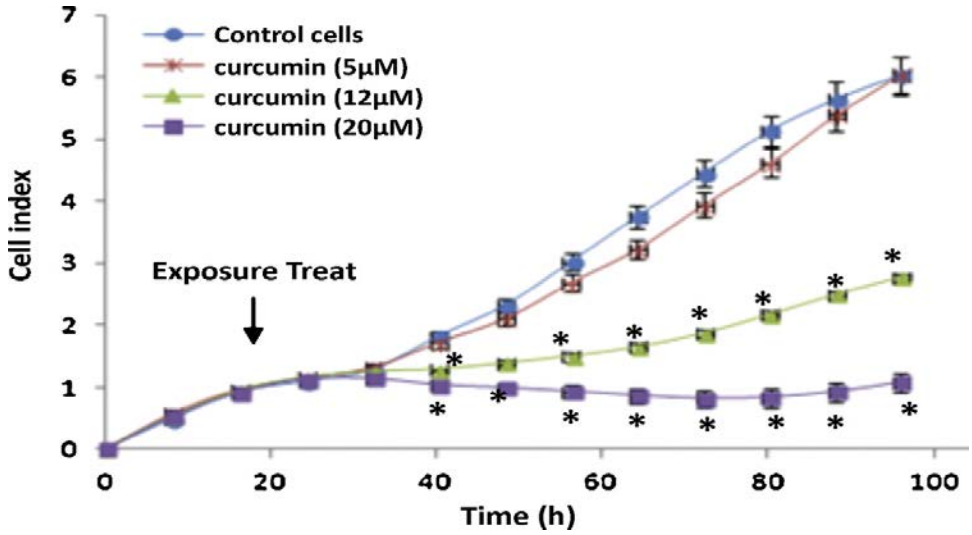

Figure 32. Cell index (CI) kinetics of the MCF-7 cells exposed to different concentrations of curcumin. CI was monitored during 72 h after compounds exposure. Reported data are the means of three replicates. Statistical differences were found after 24 hours for 12 and 20 µM of curcumin vs control cells (without curcumin) and between 12 µM and 20 µM of curcumin.

Our results are consistent with those in the literature, where curcumin has been considered as one of the most promising chemopreventive agents against a variety of human cancers (Aggarwal *et al.,* 2003). Curcumin may inhibit cancer cells proliferation in two ways; cell cycle arrest and/or inducing apoptosis (Lee *et al.,* 2010 ; Shi *et al.,* 2006). However, an antioxidant agent can become a pro-oxidant, accelerates lipid peroxidation and induces DNA damage under special conditions (Ahsan *et al.,* 1999 ; Banerjee *et al.,* 2008 ; Sakihama *et al.,* 2002). This suggested that curcumin could show selective toxicity to tumor cells. Since the cytotoxicity could be mediated through the pro-oxidant effects, the ability of curcumin to induce ROS generation and damage to critical biomolecules like DNA, and modulation in cellular redox state were evaluated in MCF7 cells (Kunwar *et al.,* 2012).

Curcumin in its free form is poorly absorbed in the gastrointestinal tract and therefore may be limited in its clinical efficacy. This poor oral bioavailability has been attributed to its poor aqueous solubility and extensive first-pass metabolism (Sanoj Rejinold *et al.,* 2011a). Liposome encapsulation of this compound would allow systemic administration. Nanoliposome plays an important role on cytotoxicity of the cancer cells depending of their concentration. Beyond the beneficial effects of long-term intake of omega-3 PUFA in cancer

patients, we likewise observed rapid-onset effects in previous experimental studies. Many studies have related the cytotoxic action exerted by n-3 PUFAs on cancer cells *in vitro* with their pro-oxidant potential (Colquhoun and Schumacher, 2001 ; Ding *et al.,* 2004 ; Hong *et al.,* 2002). The possible mechanism includes one or more of the following: oxidative stress, apoptosis, disrupted cell cycle and cell proliferation (Kunwar *et al.,* 2008). Oxidative stress is a condition associated with an increased generation of reactive oxygen species (ROS) or impaired cellular antioxidant capacity leading to an imbalance between radical generation and scavenging potential. This has been related to an impaired redox status of cancer cells and an increased level of ROS due to the activation of oncogenes and to their abnormal metabolism, as well as to mitochondrial dysfunction and DNA mutations in mitochondria (Trachootham *et al.,* 2009). During oxidative stress, polyunsaturated fatty acids of cell membranes are readily attacked by free radicals primarily from molecular oxygen to form a number of peroxidation products. These products are basically responsible for significant consequences of cell function, such as alteration of membrane fluidity plus permeability, inhibition of nucleic acid and protein synthesis up to apoptosis (Cheeseman, 1993 ; Edwards *et al.,* 1984 ; Marathe and Mishra, 2002).

Figure 33 shows the impact of each system on cell proliferation. The nanoliposomes based on vegetable lecithins such as soya (Figure 33(a)) and rapeseed (Figure 33(b)) decrease significantly cell proliferation for concentration at 20 µM and after 40 hours. On the other hand, the cytotoxicity of liposomes based on salmon lecithin was significant from the lowest concentration (5 µM) and the effect increased and began earlier with the liposome formulation (Figure 33(c)).

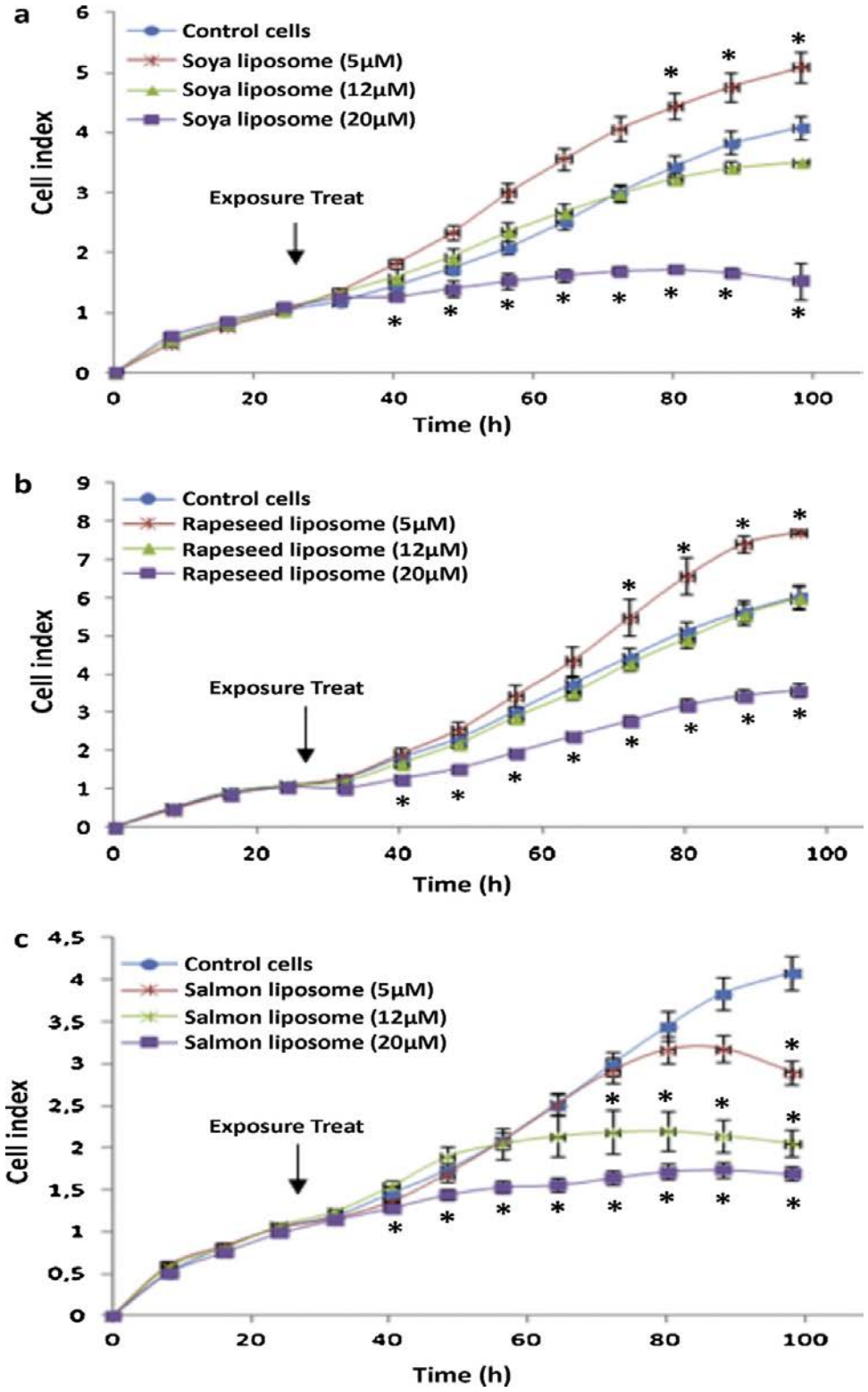

Figure 33. Cell index (CI) kinetics of the MCF-7 cells exposed to the indicated concentrations of lecithin from soya (A), rapeseed (B) or salmon (C). CI was monitored during 72 h after liposomes exposure. Reported data are the means of three replicates.

The effect may be related to the enhanced oxidative stress and cytotoxicity induced by DHA in cancer cells (DHA). As demonstrated by (Benais-Pont *et al.,* 2006), DHA increased early and late apoptosis and necrosis. Moreover, it is conceivable that EPA increases lipid peroxidation susceptibility due to its structural conformation displaying more double bonds than AA. Thus, these differences can be explained by the type of fatty acids in each lecithin. Soya and rapeseed lecithin have the same kind of fatty acids in different proportions (soya lecithin is composed of more unsaturated fatty acids than rapeseed lecithin). While salmon lecithin, which has many different fatty acids, especially DHA and EPA, have significant influence on cancer cell cytotoxicity (Arab Tehrany *et al.,* 2012).

Most of the studies used free curcumin, which is poorly absorbed in the gastrointestinal tract and is therefore limited in its clinical efficacy (Garcea *et al.,* 2004 ; Kunwar *et al.,* 2008). The highly hydrophobic nature of curcumin makes intravenous dosing impossible. Liposome encapsulation of curcumin makes this agent amenable to intravenous dosing without attenuation of its antitumor properties (Li *et al.,* 2005).The encapsulation of curcumin with biomaterials such as chitosan, PLGA and PLLA to increase the cellular delivery of curcumin has been studied by different authors (Bisht *et al.,* 2007 ; Sanoj Rejinold *et al.,* 2011a ; Yallapu *et al.,* 2010). However, the biological activity and the mechanism of action of liposomal curcumin has not been fully investigated (Li *et al.,* 2007 ; Narayanan *et al.,* 2009).

The current study evaluated the antitumor activity of liposomal curcumin *in vitro* on MCF7 cancer cell. Our study showed that liposomal curcumin treatment significantly increases the cancer cell cytotoxicity (Figure 34), while free curcumin has a lower impact on cancer cells (Figure 32). We can conclude that liposome encapsulation of curcumin increases curcumin's cell bioavailability and enhances their cellular effects on proliferation (Figure 34). This also suggests a synergic cytotoxic effect between curcumin and liposome-based-lecithins.

The effect of liposome is preponderant for curcumin encapsulated with soya lecithin which is not the case of rapeseed and salmon lecithin. Indeed, for the latter cases, there is a synergistic effect between curcumin and lecithin. Looking to rapeseed results, one can

observe a toxic effect at 12 µM after 80 h which is not observed without curcumin. Moreover, comparing to the effect of curcumin alone at the same concentration, we hypothesize that curcumin is released progressively to the media and so it might have a longer activity. Indeed, at 20 µM of curcumin encapsulated in rapeseed lecithin, the cell index augments slightly until 60 h then decreases. Likewise for curcumin encapsulated with salmon lecithin at 20 µM, the cell index reached rapidly a plateau, stopping the proliferation of breast cancer cells at a level near to one obtained by adding the curcumin directly in the media at the same concentration.

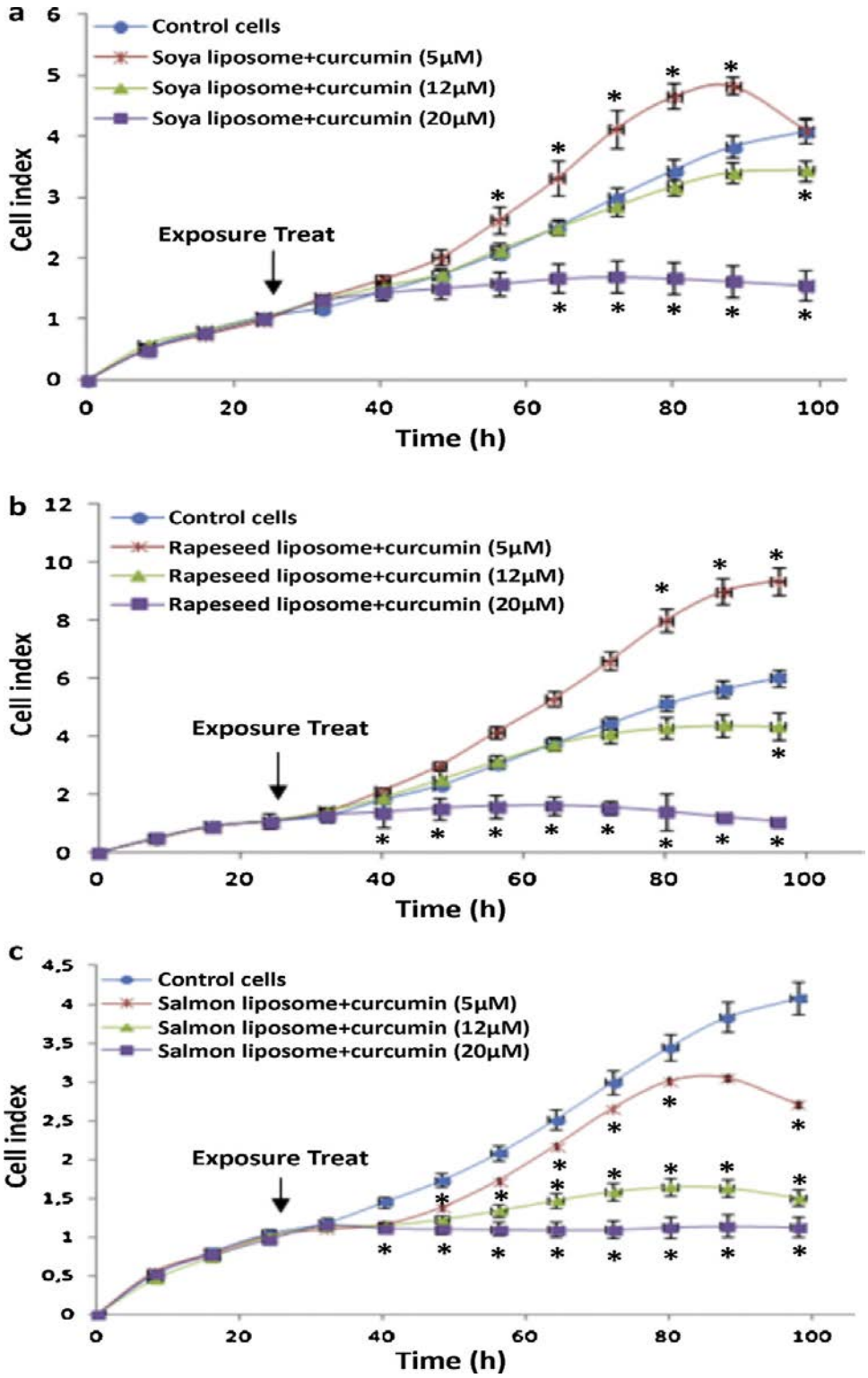

Figure 34. Effect of liposomal curcumin on CI kinetics in MCF7 cells exposed to different concentrations of encapsulated curcumin by xCELLigence system during 72 h after exposure treat. The best concentration is 20µM for all formulation.

The difference between the two systems was that for media with only curcumin, the cell index was increasing in the last part of the experiment which wasn't the case for curcumin encapsulated in liposome from salmon lecithin. Thus, the encapsulation of curcumin by rapeseed or salmon lecithin controlled the proliferation of breast cancer cells for a longer time. These results are promising and could have an impact on therapeutic strategy to contain cancer evolution or as prevention.

V.4 Conclusion

Our present studies provide information about the physico-chemical properties of liposomes before and after encapsulation of curcumin. The possibility of using liposomes as a carrier system for different applications depends on their physiochemical properties, fatty acid composition, and preparation method, which strongly influence vesicle behavior in biological systems. The results showed that soya and rapeseed lecithins are composed of the same type of fatty acids in different proportion whereas salmon lecithin which includes a wide range of fatty acids and specifically unsaturated ones known for their health benefits. The lipid fluidity is expected to increase both the diffusivity and partitioning tendency of the permeant which depends on lipid composition.

The choice of the lecithin used for encapsulate the bioactive molecule depends on the nature of the molecule and the desired final concentration. We observed that the liposomes without curcumin show an important impact in cell cytotoxicity. The results show that soya and rapeseed lecithins have comparable cellular effects for concentrations between 5 and 20 µM/mL, whereas salmon lecithin stimulated cell index decrease in a concentration-dependent manner as compared to control cells. Finally, liposomal encapsulation of curcumin can enhance cellular effect of the drug. Further studies may help to understand the mechanism of action of liposome-encapsulated curcumin and its specific effect on cancer cells.

VI. Chitosan-coated liposomes encapsulation of curcumin for enhanced cancer MCF7 cell destruction

M.Hasan[a], E. Arab-Tehrany[a*], N. Belhaj[a], W. H. EL-Reffaei[b] , H. Benachour[c,d], , C.J.F. Kahn[e], E. Jabbari[f], M. Barberi-Heyob[c,d], M. Linder[a]

[a]Université de Lorraine, Laboratoire d'ingénierie des Biomolecules, EA 4367, France

[b] Regional Centre for food and feed, Agriculture Research Center, Egypt

[c]Université de Lorraine, CRAN, UMR 7039, Campus Sciences, BP 70239, Vandœuvre-lès-Nancy Cedex 54506, France

[d]CNRS, CRAN, UMR 7039, Vandœuvre-lès-Nancy, France

[e]IFSTTAR, LBA, F-13916 Marseille, France

[f]Department of Chemical Engineering, SWNG Engineering Center, Rm 2C11, University of South Carolina, 301 Main Street, Columbia, SC 29208, United States

VI.1 Résumé

La curcumine (diferuloylmethane) présente un intérêt dans le traitement de certains cancers et fait l'objet de nombreux travaux afin d'augmenter sa biodisponibilité. Dans cette étude, nous avons encapsulé de la curcumine sous forme liposomale dans un premier temps avant de rajouter un « coating » de chitosane, biopolymère naturel chargé, afin d'augmenter la solubilité et la biodisponibilité de la curcumine. L'étude de la nature des lécithines utilisées pour élaborer le vecteur liposomal montrent des différences de comportement en fonction de la présence d'acides gras polyinsaturés à longue chaîne. Les résultats montrent une amélioration accrue de la cytotoxicité du complexe avec le chitosane sur des cellules MCF7.

Keywords: Nanoliposome, chitosan-coated liposomes; cancer cells, lecithin, curcumin, encapsulation.

VI.2 Introduction

Curcumin is a yellow natural polyphenolic compound extracted from turmeric root (Curcuma longa), it usually refers to three molecules namely: 1,7-bis (4-hydroxy-3-

methoxyphenyl)-1,6-heptadiene-3,5-dione (curcumin); 1,6-Heptadiene-3,5-dione,1-(4-hydroxy-3-methoxyphenyl)-7-(4-hydroxyphenyl) (demethoxycurcumin) and 1,7-bis (4-hydroxy phenyl) -1,6- heptadiene-3,5-dione (bis demethoxy curcumin) (Akhtar *et al.,* 2012) (Figure 24). Curcumin has been widely used as traditional medicine (Saengkrit *et al.,* 2014), due to numerous medicinal properties of these compounds, which has been subject to a multitude of investigations over the last few decades that demonstrated various health benefits such as anti-inflammatory, anti-proliferative activities, and antioxidant properties (Said *et al.,* 2012). However, the therapeutic efficiency of curcumin is limited due to its poor oral bioavailability (Parvathy *et al.,* 2009 ; Wilart *et al.,* 2009). In fact, its poor solubility in an aqueous medium and weak stability against gastrointestinal fluids or alkaline pH conditions restrict its availability to cross into the blood circulation by oral administration. Moreover, its rapid elimination from the circulation limits its bioavaibility and effectiveness (Anand *et al.,* 2007; Tønnesen, 2002). Various strategies have been undertaken to overcome limitations of the use of curcumin and to allow its therapeutic application, such as, complexation with phospholipids and cyclodextrins, encapsulation in liposomes, biodegradable microspheres, hydrogels, polymeric nanoparticles, and lipid based nanoparticles (Bisht *et al.,* 2007 ; Kunwar *et al.,* 2006 ; Maiti *et al.,* 2007 ; Sou *et al.,* 2008 ; Tiyaboonchai *et al.,* 2007 ; Tønnesen *et al.,* 2002 ; Vemula *et al.,* 2006).

Liposome is a promising delivery system due to its phospholipid bilayer structure, which is similar as a biological membrane, which can improve the therapeutic activity and safety of drugs, mainly by delivering them to their site of action and by maintaining therapeutic drug levels over prolonged periods of time (Gregoriadis and Florence, 1993). The major components of liposomes are phospholipids, which are amphiphilic molecules containing a hydrophilic head and a hydrophobic tail. Liposomes can protect bioactive agents from digestion in the stomach and show significant levels of absorption in the gastrointestinal tract, enhancing their bioactivity and bioavailability (Takahashi *et al.,* 2007). As highlighted by Kotze *et al.* (1999) and Galović Rengel *et al*. (2002), chitosan is a hydrophilic polymer with good biocompatible and biodegradable properties leading to a low toxicity level. Based on its bio-adhesive and permeation properties, chitosan has been well considered for bio-adhesive drug delivery systems, in order to improve bioavailability of drugs by increasing their time residence at absorption site.

Chitosan is obtained by alkaline deacetylation from chitin (poly-N-acetyl-D-glucosamine), the second most abundant natural polysaccharide after cellulose. Chitin is obtained from the shell of crustaceans, the cuticles of insects, the cell wall of the fungi and the yeast (Mathur and Narang, 1990). Due to the presence of amino groups, chitosan is polycationic. Because of its positive charge, it has been used previously as coating polymer for negatively charged particles such as emulsion, liposome and biopolymeric particles (Aoki *et al.,* 2005 ; Chen *et al.,* 2001 ; Laye *et al.,* 2008 ; Ogawa *et al.,* 2003). By combining chitosan and liposomes, specific, prolonged, and controlled release may be achieved (Takeuchi *et al.,* 1996). Takeuchi *et al.* (1996) showed that chitosan-coated liposomes were formed via ionic interaction between the positively charged chitosan and negatively charged diacetyl phosphate on the liposome surface (Figure 35). Research in the fields of pharmaceutical and food sciences showed that chitosan coating changed the liposome surface charge and slightly increased its particle size (Laye *et al.,* 2008 ; Li *et al.,* 2009b).

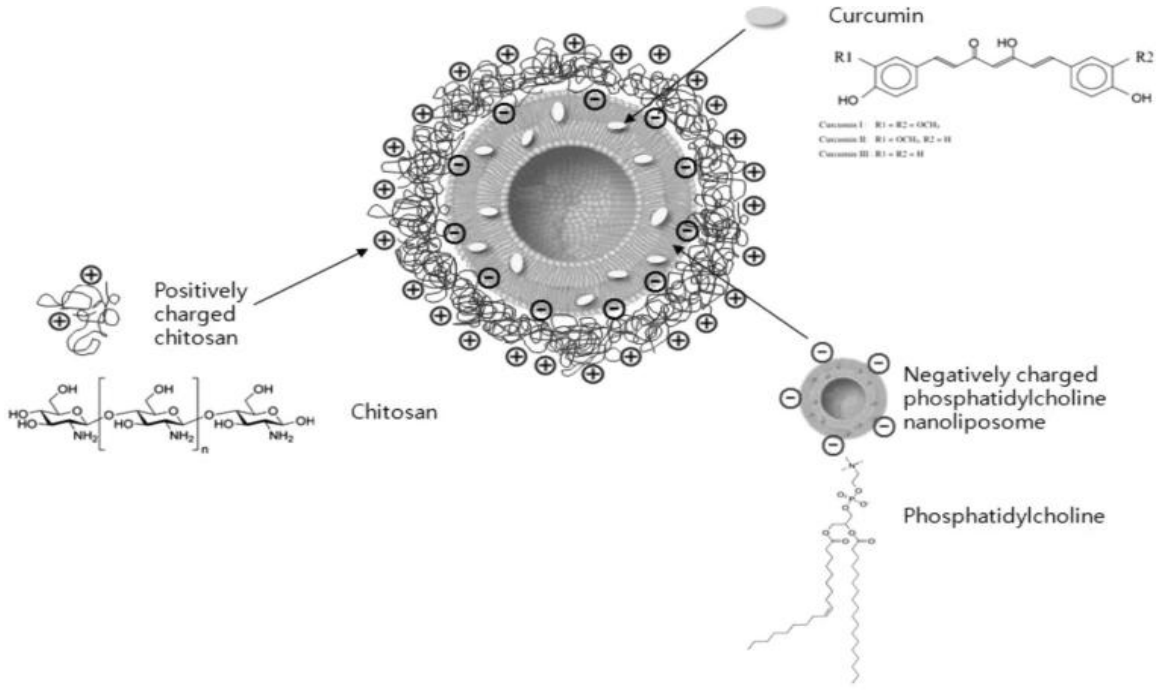

Figure 35. Schema illustrative for curcumin loaded chitosan-coated nanoliposome (Shin *et al.,* 2013).

The present study focused primarily on the preparation and physicochemical characterization of different formulations of chitosan-coated liposomes from natural sources

(soya, rapeseed and salmon lecithins), evaluate their ability as a carrier for hydrophobic drugs in cancer drug delivery applications. In addition, effects of these formulations on viability of MCF-7 cancer cells were investigated.

VI.3 Results and discussion

VI.3.1 Fatty acid analyses

The main fatty acid composition of rapeseed, soya and salmon lecithin is shown in Table 6. It can be seen that the percentage of total polyunsaturated fatty acids is higher in the soya lecithin, whereas its diversity was higher in salmon lecithin. In respect of soya lecithin, the characterized fatty acid is C18:2 n-6 found in proportions (52.27%) which belong to polyunsaturated fatty acids class. The low ratio of saturated fatty acids could be observed in rapeseed lecithin (9.28%), while its value in soya and salmon lecithin was 20.82% and 27.03%, respectively. Contrariwise, the largest amount of monounsaturated fatty acid found also in rapeseed lecithin (57.80%), where the characterized fatty acid of rapeseed lipid is C18:1n-9 found in percentage (56.51%). In regards to salmon lecithin which is rich in long chain fatty acids especially DHA (C22:6n3) and EPA (C20:5n3) with 23.81% and 9.56%, respectively. We have seen that the more significant fatty acids, in the two classes monounsaturated and saturated fatty acids, were C18:1(n-9) and C16:0 with proportion (19.58%) and (16.21%), respectively. The ratio of n-3/n-6 was observed with higher value in salmon lecithin (3.0) comparing to rapeseed (0.25) and soya lecithin (0.1).

VI.3.2 Lipid classes

The separation of lipid fractions of different lecithins was executed by thin-layer chromatography (Iatroscan). However, the results shown that the percentage of polar lipid fraction in soya lecithin (84.8%) was higher comparing to its value in salmon and rapeseed lecithin, which were 75.51% and 62.26% , respectively. Moreover, the proportion of neutral lipid represented as triacylglycerols was 37.74, 24.49, and 18.2% for rapeseed, salmon and soya lecithins, respectively. Phosphatidylcholine represented the major class of phospholipids for all lecithins with a little difference, 33 in rapeseed lecithin, 28.1% in salmon lecithin and 23.19% in soya lecithin.

VI.3.3 Solubility studies

Curcumin has a relatively low water-solubility (8.33 µg.mL^{-1}) (Maiti *et al.*, 2007) and a high oil–water partition coefficient (log P = 2.5) (Fujisawa *et al.*, 2004). The amount of a highly lipophilic material that can be dissolved in an oil phase depends on the molecular characteristics of the oil (e.g., molecular weight, polarity, and interactions). The results show that the solubility of curcumin in aqueous solution of lecithin in the presence of chitosan is four time higher in comparison with that of lecithin alone (Hasan *et al.*, 2014). This difference could be attributed to the reduced hydrogen bonding interaction of curcumin with the polymer chains (Sanoj Rejinold *et al.*, 2011b).

On the other hand the addition of 1% acetic acid in the aqueous solution to solubilize the chitosan. Chitosan has low solubility in aqueous solution at neutral and alkaline pH due to its tendency to act as a weak base with a pKa value in the 6.2–7.0 range for D-glucosamine residues. However, it is soluble in moderately acidic aqueous media due to protonation of its amino groups when pH < pKa (Akhtar *et al.*, 2012). Curcumin is also soluble in acetic acid. The results show that the solubility of curcumin in aqueous solution of lecithin and chitosan is 0.89±0.04, 0.89±0.04 and 0.88±0.02 mg.mL^{-1} for rapeseed, soya, and salmon lecithin, respectively. Thus, there is no significant difference in solubility of curcumin into the solution of the three lecithins in the presence of chitosan.

We also determined the solubility of curcumin in 1% chitosan solution and found that the maximum solubility of curcumin was 0.13 mg.mL^{-1}. These results indicate that chitosan synergistically enhances solubility of curcumin in aqueous solution in the presence of lecithins.

VI.3.4 Measurement of liposome size and electrophoretic mobility

The particle size of different chitosan coated-nanoliposomes were measured immediately after preparation. The minimum size that can be achieved depends on lipid composition as well as liposome preparation method. The average chitosan coated-liposome diameter was 317 nm, 358 and 318 nm for nanoparticles from soya, salmon and rapeseed lecithins, respectively. We observed that salmon coated with chitosan liposome was larger than the other lecithin. This increase can be explained by the interaction between lipid and

chitosan, which includes the lipid–chitosan electrostatic interactions between their head groups and the specific functional groups of chitosan NH_3^+. Hydrophobic interactions between the lipid tails and chitosan take place allowing chitosan to come up to the bilayer and fill the empty volume (Liu *et al.,* 2015). This apparently resulted in the higher expansion of the bilayers observed for the unsaturated fatty acids compared to the saturated ones, which led to the attachment of more chitosan around salmon liposomes and increases its size in comparison with the others (Wydro *et al.,* 2007).

The size of the curcumin-loaded chitosan coated nanoliposomes was greater than the unloaded curcumin ones. Therefore, the size of chitosan coated nanoliposomes increased respectively from 317 nm, 358 and 318 nm to 321 nm, 380 and 327 nm for soya, salmon and rapeseed chitosan coated nanoliposomes. The increase in size between chitosan-nanoliposomes with and without curcumin encapsulation could be attributed to the loading of curcumin in the outer layer formed by chitosan around liposomal bilayer which are in good agreement with the results of Sanoj Rejinold *et al*. (2011a).

In addition to particle size diameter, DLS also measures polydispersity index (PDI) which is a dimensionless measure of the breadth of the particle size distribution (Zweers *et al.,* 2003). When the PDI value is <0.3, the indication is that the sample is of narrow distribution, and when PDI value is over 0.3, the sample is considered to be of broad distribution (Yen *et al.,* 2008). As shown in Table 8, the PDI was, respectively, 0.23, 0.23 and 0.22 for soya, rapeseed and salmon lecithin coated with chitosan, which indicated that particle size was well controlled with a narrow dispersity. According to mean values and PDIs, there was no significant difference between the breadth of distribution of the samples. We found that PDI of the curcumin-loaded nanoparticles is slightly greater than the unloaded curcumin nanoparticles. Regarding the electrophoretic mobility, nanoliposomes prepared without chitosan showed a negative electrophoretic mobility value of -3.4 mV (Hasan *et al.,* 2014) which becomes positive with the addition of chitosan. The electrophoretic mobility of nanoparticles increased from -3.34, -3.21 and -3.41mV for soya, salmon and rapeseed liposomes, respectively, to 4.88, 5.20 and 5.19 mV by coating with chitosan, respectively.

The electrophoretic mobility of uncoated nanoliposomes was negative probably due to the anionic fractions of lecithin (Arab Tehrany *et al.,* 2012). The increase in the surface

charge of chitosan-coated nanoliposomes was attributed to the increase in positively-charged amino groups of chitosan molecules, proving that the nanoliposomes were successfully coated by chitosan (Mazzarino *et al.,* 2012). With respect to the stability of chitosan coated nanoliposome with time. We observed no significant variation in particle size up to 30 days of incubation at 37 °C.

Table 8. Mean particle size (nm), PDI, electrophoretic mobility (µmcm/Vs) and membrane fluidity of the chitosan coated liposomes (each value represents the mean of triplicates).

Sample	Particle size (nm)	Polydispersity index	Electrophoretic mobility (µmcm/Vs)	Membrane fluidity
Soya CH-LP	317±0.8	0.23 ±0.01	4.88±0.10	3.21±0.10
Curcumin loaded soya CH-LP	321±0.9	0.24±0.01	4.92±0.05	2.56±0.10
Salmon CH-LP	358±4.5	0.23±0.01	5.20 ±0.02	2.70±0.10
Curcumin loaded salmon CH-LP	380±2.8	0.24±0.02	5.23±0.04	2.62±0.20
Rapeseed CH-LP	318±3.6	0.22±0.00	5.19 ±0.10	3.21±0.10
Curcumin loaded rapeseed CH-LP	327±3.2	0.25±0.02	5.24 ±0.14	2.71±0.10

CH-LP: Chitosan-coated liposome.

VI.3.5 Encapsulation efficiency of curcumin

The entrapment efficiency of the curcumin was 87.15, 88.61 and 88.72% with respect to rapeseed, soya and salmon chitosan-coated liposome, respectively. The encapsulation efficiency values were high for all formulations, on the one hand we have incorporated an amount of curcumin in the liposomes (0.2 mg/mL) less than the maximum curcumin soluble in these systems, which was about 0.88 mg/mL. On the other hand, it is probably due to the poor water solubility of curcumin in aqueous phase surrounding the liposomes. We observed a weak difference of encapsulation efficiency of curcumin between salmon, soya and rapeseed.

These results indicate that the encapsulation efficiency of curcumin significantly increases when liposome is coated with chitosan compared to the uncoated liposome, which was 63.2, 65.0 and 67.3% with respect to rapeseed, soya and salmon liposomes, respectively (Hasan *et al.,* 2014).

VI.3.6 Morphology of the liposomes

TEM images showed that nanoliposomes prepared by sonication and high-pressure homogenization methods were in the form of multilamellar vesicles (MLV) (Figure 36, A (a)). We also observed a small quantity (10%) of oil droplets in each formulation as nanoemulsion. The morphology of the chitosan coated liposomes showed a contrasting band surrounding a liposome vesicle, as shown in Figure 36, A (b).

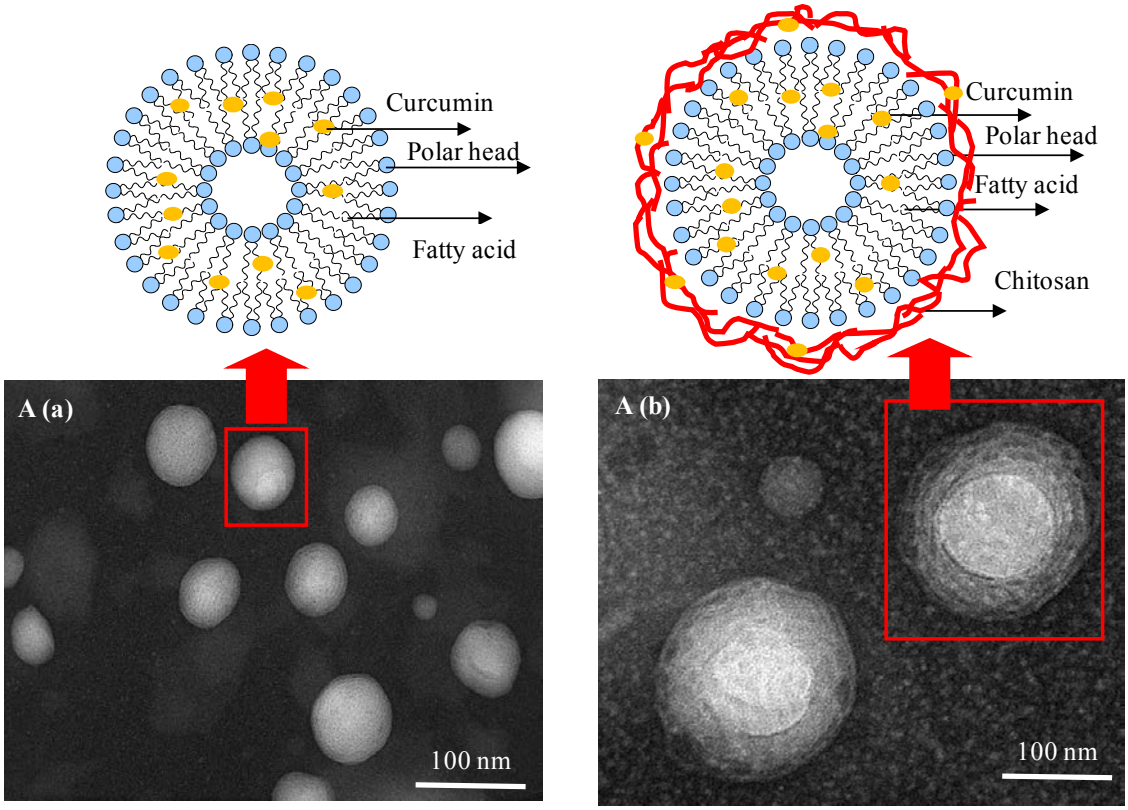

Figure 36. A. Transmission electron microscopic images of curcumin loaded-nanoliposome before (a) and after (b) coating with chitosan.

VI.3.7 Membrane fluidity

Membrane fluidity was determined for each sample by fluorescence anisotropy measurements. The fluidity of lipid membrane reflects the order and dynamics of phospholipid alkyl chains in the bilayer of vesicles (Maherani *et al.*, 2012). The influence of lipid composition on vesicle membrane fluidity was explored by Coderch *et al*. (2000) (Coderch *et al.*, 2000), and Calvagno *et al*. (2007) (Calvagno *et al.*, 2007). They determined a

significant difference in the drug release profiles by the presence of two factors: (i) the force of the drug–liposomal lipid interaction and (ii) the fluidity of the bilayer. In fact, the drug release to the aqueous medium increased by increasing the membrane fluidity of the vesicle. The FAs composition of the membrane bilayer tunes the membrane fluidity level. Indeed the presence of saturated FAs tend to reduce membrane fluidity by increasing the packing between phospholipids, which expelled the water in the proximity of the bilayer surface, whereas unsaturated FAs helped reduce the packing between phospholipids and preserved the level of membrane hydration, thus maintaining membrane fluidity (Leekumjorn *et al.,* 2009).

To recognize the action of curcumin and chitosan on membrane fluidity it is necessary to understand the behavior of curcumin and chitosan with respect to solution composition variation. Indeed, according to a previous study (Hasan *et al.,* 2014), we observed that membrane fluidity depended on lipid composition of nanoliposomes: nanoliposomes made of soya lecithin had higher membrane fluidity than nanoliposomes based on rapeseed and salmon lecithins. Soya lecithin contains a higher proportion of polyunsaturated fatty acids with short chain compared to other lecithins, and membrane fluidity is even more important when the degree of unsaturation of acyl chains increased and the length of the chain decreased.

The presence of curcumin decreased the membrane fluidity of all nanoliposomes. Such influence of curcumin is a result of its structure and its molecular interaction with liposome. The curcumin molecule can weaken hydrophobic interactions among acyl chains of phospholipids. When incorporated into the membrane, it tends to decrease the membrane fluidity (Patra *et al.,* 2012). The incorporation of curcumin perturbs the packing characteristics of the phospholipid bilayer and thus enhances the packing density of the hydrocarbon moiety in the lipid bilayer.

According to Table 8, we observed that chitosan reduced membrane fluidity of nanoliposomes. It makes a new layer around the liposome, which is probably incorporate within the membrane bilayer, causing the rigidity of bilayers, and decreasing the movement of fatty acids chains of phospholipid. Consequently, the membrane bilayer fluidity decreases. The motional freedom of phosphate group was reduced with the presence of chitosan (Shi *et al.,* 1999).

VI.3.8 Cytotoxicity by real time cell analysis

As shown in Figure 37, electrical impedance measurements from adherent MCF-7 cells, assessed by normalized cell index (NCI) kinetics, showed a significant dose-dependent effect on CI using curcumin from 12 µM, whereas no significant difference was observed at 5 µM of curcumin. Reports on the anti-tumor activity of curcumin were based on two opposite mechanisms: inhibiting anti-apoptosis proteins, or activating the pro-apoptosis proteins (Shi *et al.,* 2006). This suggested that curcumin could show selective toxicity to tumor cells. Since the cytotoxicity could be mediated through the pro-oxidant effects. The ability of curcumin to induce reactive oxygen species (ROS) (Atsumi *et al.,* 2005 ; Strasser *et al.,* 2005 ; Syng-ai *et al.,* 2004) generation and damage to critical biomolecules like DNA, and modulation in cellular redox state were evaluated in MCF7 cells (Kunwar *et al.,* 2012).

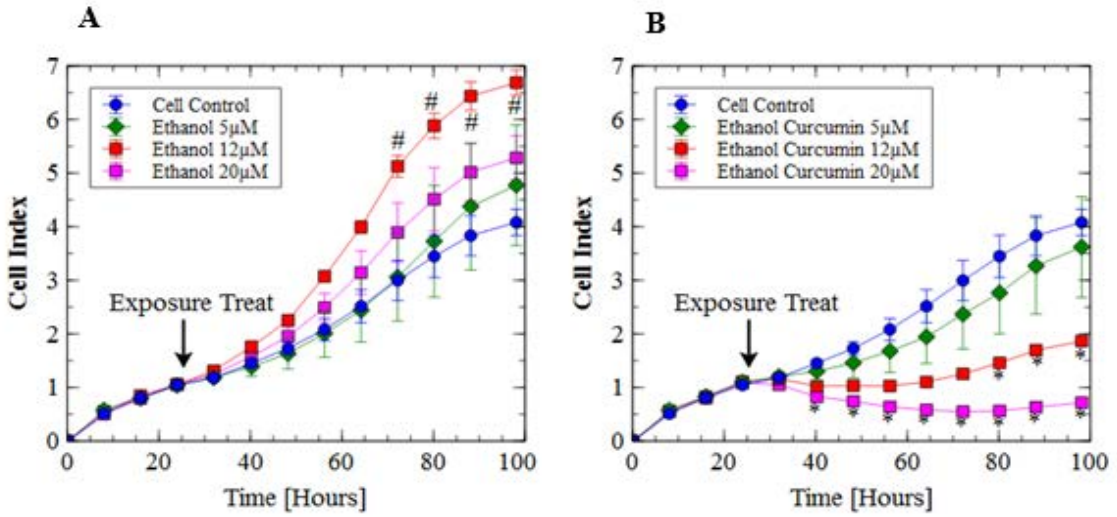

Figure 37. Cell index (CI) kinetics of the MCF-7 cells exposed to different concentrations of ethanol (A) and curcumin (B). CI was monitored during 72 h after compounds exposure. Reported data are the means of three replicates. The statistical differences toward control were presented by # for ethanol and * for curcumin in compared to cell control.

There are also studies which suggest that curcumin prevents ROS production (Das and Das, 2002 ; Mishra *et al.,* 2005), and thus acts as an antioxidant. Other studies suggest that curcumin quenches ROS production at low concentrations and induces ROS production at high concentrations (Chen *et al.,* 2005 ; Sandur *et al.,* 2007). Whereas the pro-oxidant mechanism mediates apoptotic effects, the antioxidant mechanism mediates NF-κB-suppressive effects (Sandur *et al.,* 2007). Other studies report that tumor cells show

preferential uptake of curcumin compared to normal cells and the toxicity clearly increased with increasing curcumin uptake, therefore this advantage makes it an attractive agent for cancer therapy. Among various factors that are responsible for higher curcumin uptake in tumor cells against normal cells could be their difference in membrane structure, protein composition and bigger size (Kunwar *et al.,* 2008 ; Mirgani *et al.,* 2014 ; Singer, 2004).

Curcumin in its free form is weakly absorbed in the gastrointestinal tract and therefore may be limited in its clinical efficacy. This poor oral bioavailability has been attributed to its poor aqueous solubility and extensive first-pass metabolism (Sanoj Rejinold *et al.,* 2011b). Liposome encapsulation of this compound could improve systemic administration. Nanoliposomes play an important role on cytotoxicity of the cancer cells depending of their concentration having beneficial effects for cancer patient both long-term and short-term by a rapid-onset effects previously observed. Many studies have related the cytotoxic action exerted by omega-3 PUFAs on cancer cells *in vitro* with their pro-oxidant potential (Colquhoun and Schumacher, 2001 ; Ding *et al.,* 2004 ; Hong *et al.,* 2002). The possible mechanism includes one or more of the following: oxidative stress, apoptosis, disrupted cell cycle and cell proliferation (Kunwar *et al.,* 2008). Oxidative stress is a condition associated with increased generation of ROS or impaired cellular antioxidant capacity leading to an imbalance between radical generation and scavenging potential. This has been related to an impaired redox status of cancer cells and an increased level of ROS due to the activation of genes and to their abnormal metabolism, as well as to mitochondrial dysfunction and DNA mutations in mitochondria (Trachootham *et al.,* 2009). During oxidative stress, polyunsaturated fatty acids of cell membranes are readily attacked by free radicals primarily from molecular oxygen to form a number of peroxidation products. These products are basically responsible for significant changes in cell function, such as alteration of membrane fluidity plus permeability, inhibition of nucleic acid and protein synthesis up to apoptosis (Cheeseman, 1993 ; Edwards *et al.,* 1984 ; Marathe and Mishra, 2002). According to previous studies, (Hasan *et al*., 2014) the impact of each system on cell proliferation were shown.

Nanoliposomes based on vegetable lecithins such as soya and rapeseed decrease significantly cell proliferation for concentration of 20 µM and after 40 h. On the other hand, the cytotoxicity of liposomes based on salmon lecithin was significant from the lowest

concentration (5 µM) and the effect increased and began earlier with the liposome formulation. The effect may be related to the enhanced oxidative stress and cytotoxicity induced by DHA in cancer cells. As demonstrated by Benais-Pont *et al*. (2006), DHA increased early and late apoptosis and necrosis of human colorectal adenocarcinoma cells.

Moreover, it is conceivable that EPA increases lipid peroxidation susceptibility due to its structural conformation displaying more double bonds than arachidonic acid (AA). Thus, these differences can be explained by the lecithin composition. Soya and rapeseed lecithin have the same kind of fatty acids in different proportions (soya lecithin is composed of more unsaturated fatty acids than rapeseed lecithin), while salmon lecithin, which has various polyunsaturated fatty acids, especially DHA and EPA, that can influence on cancer cell cytotoxicity (Arab Tehrany *et al.,* 2012). The current study evaluated the anti-tumor activity of liposomal curcumin *in vitro* on MCF7 cancer cell. Our study showed that liposomal curcumin treatment significantly increases the cancer cell cytotoxicity (Figure 34)(Hasan *et al.,* 2014), while free curcumin has a lower impact on cancer cells (Figure 37). We can conclude that liposome encapsulation of curcumin increases curcumin's cell bioavailability and enhances their cellular effects on proliferation. This also suggests a synergic MCF7 cytotoxic effect between curcumin and liposome-based-lecithins.

The effect of liposome is preponderant for curcumin encapsulated with rapeseed lecithin which is not the case of soya and salmon lecithin. Indeed, for the latter cases, there is a synergistic effect between curcumin and lecithin. Looking to rapeseed results, one can observe a toxic effect at 12 µM after 80 h which is not observed without curcumin. Moreover, comparing to the effect of curcumin alone at the same concentration, we hypothesize that curcumin is released progressively to the media and so it might have a longer activity. Indeed, at 20 µM of curcumin encapsulated in rapeseed lecithin, the cell index augments slightly until 60 h then decreases. Likewise for curcumin encapsulated with salmon lecithin at 20 µM, the cell index reached rapidly a plateau, stopping the proliferation of breast cancer cells at a level near to one obtained by adding the curcumin directly in the media at the same concentration. The difference between the two systems was for media with only curcumin, the cell index was increasing in the last part of the experiment which was not the case for curcumin encapsulated

in liposome from salmon lecithin. Thus, the encapsulation of curcumin by rapeseed or salmon lecithin controlled the proliferation of breast cancer cells for a longer time.

Modification of the outer surface of the liposomes with masking and targeting moieties (e.g. PEG, antibodies, and chitosan) allows their life span to be extended *in vivo* and permits accumulation of liposomes in the target sites. Because of chitosan's bioadhesive and permeation enhancing properties, it has received substantial attention in bioadhesive drug delivery systems, aimed at improving the bioavailability of drugs by prolonging their residence time at the site of absorption (Kotze *et al.,* 1999). Chitosan has great potential as a coating material for liposomes due to its positive charge in acidic aqueous solution. It is considered as biocompatible, biodegradable material and contributes a mucoadhesive property to the surface of delivery systems (Takeuchi *et al.,* 2003). The mucoadhesive properties of chitosan coated liposomes were expected to increase the probability of absorption in the intestinal tract by increasing the residence time. We observed that chitosan-coated liposomes inhibited more tumor growth compared to uncoated liposome. In case of chitosan-coated liposomes, we assumed that the positively charged chitosan may automatically coat the negatively charged liposomes, or the positively charged chitosan may stay for a longer time on the negatively charged mucosa, which results in prolonged residence time of phospholipid liposomes on the intestinal wall.

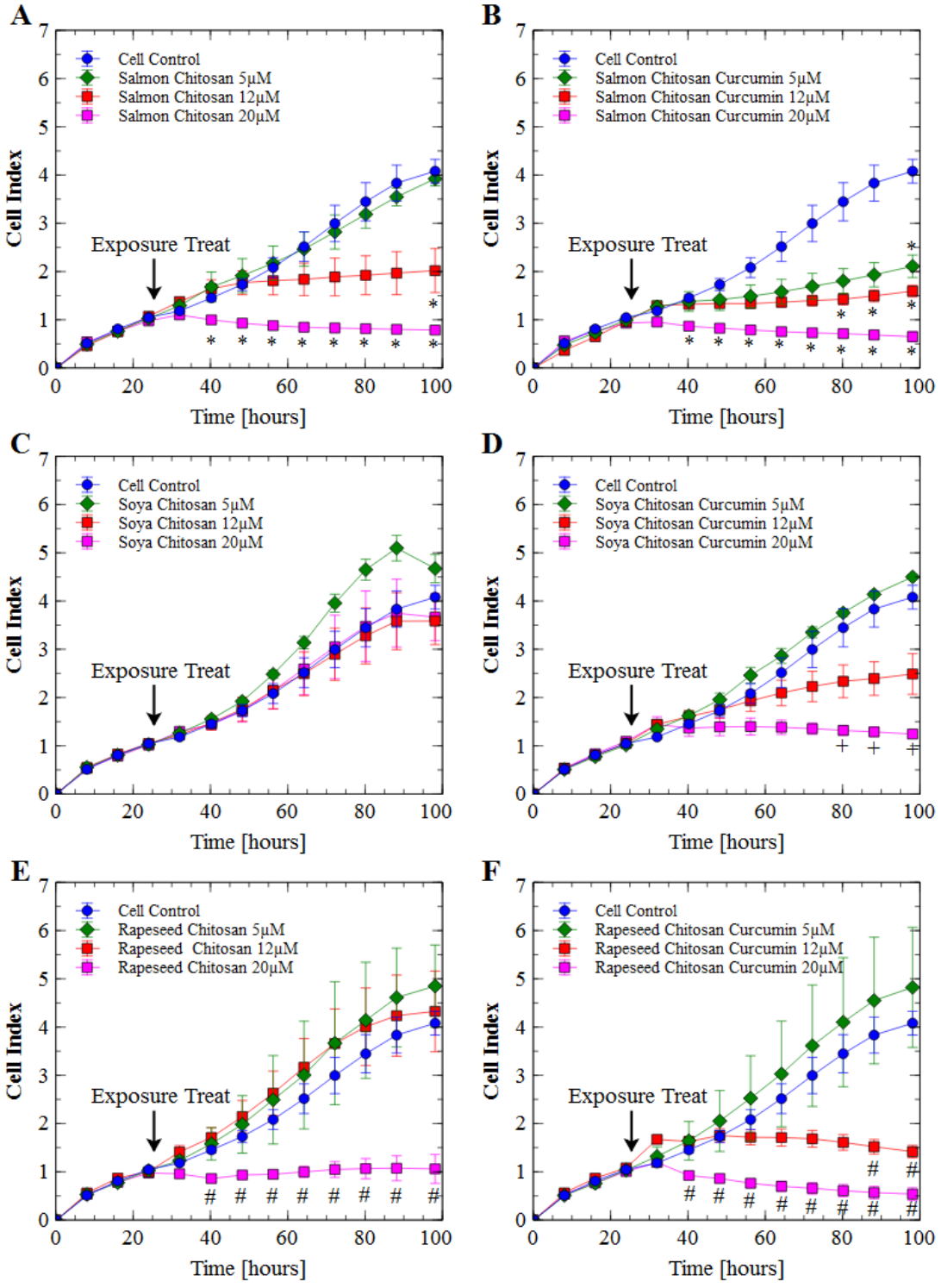

Figure 38. Cell index (CI) kinetics of the MCF-7 cells exposed to the indicated concentrations of chitosan nanoliposomes from salmon (A, B), soya (C, D) and rapeseed (E, F) lecithin with and without curcumin encapsulated. CI was monitored during 72 h after liposomes exposure. Reported data are the means of six replicates. The statistical differences toward control group were showed by * for salmon, + for soya and # for rapeseed.

The results presented in (Figure 33) (Hasan *et al.,* 2014) and in (Figure 38), indicate that cytotoxicity increases for all types of lecithin coated with chitosan. Our data indicate increased sensitivity of MCF7 cells toward curcumin-loaded chitosan-coated liposomes.The results were confirmed that coating liposome with chitosan caused the changes in particle size and electrophoretic mobility values. In addition, we showed high loading efficiency of curcumin in chitosan-coated liposomes and strong cytotoxicity towards MCF7 cells.

VI.4 Conclusion

Our present studies give the information about the physico-chemical properties of nanoliposomes before and after encapsulation of curcumin. The possibility of using liposomes as a carrier system for different applications depends on their physico-chemical properties; fatty acid composition and preparation method strongly influence vesicle behavior in biological systems.

The results showed that soya and rapeseed lecithins are composed of the same type of fatty acids in different proportion whereas salmon lecithin which includes a wide range of fatty acids and specifically unsaturated ones known for their health benefits. From TEM imaging, we observed that lecithin solutions were made largely of nanoliposomes and a little part of emulsion, in addition the result showed that chitosan coated the nanoliposome by adding a new layer at the surface of phospholipids. Generally, particle size and electrophoretic mobility are two most important properties that determine the fate of liposomes. Knowledge of the z-potential is also useful in controlling the aggregation, fusion and precipitation of liposomes, which are important factors affecting the stability of liposomal formulations. The lipid fluidity is expected to increase both the diffusivity and partitioning tendency of the permeant, which yields a possible squaring effect on the enhancement factor. This property depends on lipid composition.

The choice of the lecithin used for encapsulate the bioactive molecule will depend on the nature of the molecule and on the final concentration wanted. We observed that the nanoliposome without curcumin shows an important impact in tumor cell cytotoxicity. It results that soya and rapeseed lecithins have similar effects on tumor cell cytotoxicity with a cell index for concentration of lecithin between 0.28 and 1.1 mg/mL with an optimal

concentration at 1.1 mg/mL, whereas salmon lecithin stimulated cells index decreases with three concentrations, in particularly at 1.1 mg/mL. We can also confirm that curcumin exhibits selective cytotoxicity in MCF7 cells, and its mechanism of action proceeds through the induction of ROS, DNA damage, and mitochondrial dysfunction.

The results were confirmed that coating liposome with chitosan caused the changes in particle size and electrophoretic mobility values. In addition, we showed high loading efficiency of curcumin in chitosan-coated liposomes and strong cytotoxicity towards MCF7 cells, all results highlight that chitosan-coated liposomes enhance curcumin delivery compared to uncoated ones.

VII. Curcumin-loaded natural salmon nanoliposomes with high effect on primary cortical neurons in vitro

M. Hasan[a]†, S. Latifi[b]†, C. Kahn[c], A. Tamayol[d,e], M. Linder[a], E. Arab-Tehrany[a*]

[a]Université de Lorraine, Laboratoire d'ingénierie des biomolecules, TSA 40602 54518 – Vandœuvre Cedex.

[b]Department of Neurology, David Geffen School of Medicine, UCLA, Los Angeles, CA 90095, USA.

[c]IFSTTAR, LBA, F-13015, Marseille, France.

[d]Center for Biomedical Engineering, Department of Medicine, Brigham and Women's Hospital, Harvard Medical School, Boston, MA 02139, USA. Harvard-MIT Division of Health Sciences and Technology, Massachusetts Institute of Technology, Cambridge, MA 02139, USA. Wyss Institute for Biologically Inspired Engineering, Harvard University, Boston, MA, 02115, USA.

[e]Regenerative Medicine Program, University of Manitoba, Winnipeg, MB, Canada.

VII.1 Résumé

La curcumine (diferuloylmethane) est un composé bioactif naturel qui présente de nombreux avantages dans le domaine de la santé-promotion. Cependant, ses applications dans le domaine biomédical restent actuellement limitées en raison de ses propriétés relativement faibles de solubilité dans l'eau et de sa faible biodisponibilité. Dans cette étude, nous avons encapsulé de la curcumine sous forme liposomale issue de lécithine de saumon. Nous nous sommes attachés à caractériser son efficacité d'encapsulation ainsi que son profil de libération et ses effets sur des cellules neuronales.

La forme liposomale, constituée principalement de phosphatidylcholine, se caractérise par une taille de 120 nm avec un indice de polydispersité de 0,3. On observe une légère diminution de la taille de ce complexe curcumine-liposome à une concentration de 0,27 mg/mL (solubilité maximale de la curcumine) en raison d'une forte interaction entre les

molécules. L'efficacité d'encapsulation de la curcumine dans ce complexe (proche de 60%) permet une libération progressive de la biomolécule de 18% la première heure pour atteindre 23% au bout de 4 heures. Les propriétés neuroprotectives de la curcumine ont été étudiées sur des neurones corticaux primaires sur 9 jours à plusieurs concentrations (15 et 20 µM). Les résultats montrent une augmentation de l'activité métabolique et de la formation du réseau de neurones. Les résultats d'analyse en cytométrie de flux indiquent une diminution des cellules apoptotiques lors d'un traitement avec le complexe liposome/curcumine, comparé au témoin.

Keywords: Salmon nanoliposome, cortical neurons, lecithin, curcumin, in vitro.

VII.2 Introduction

Curcumin (CUR) is a hydrophobic polyphenolic compound derived from the rhizomes of *Curcuma longa*(Aggarwal *et al.,* 2003) . It is a derivative of turmeric which is used as a natural spice in East Asian countries. Commercial curcumin consists of a mixture of three curcuminoids [diferuloylmethane (~77%), demethoxycurcumin (~18%), and bisdemethoxycurcumin (~5%) (Yallapu *et al.,* 2013) (Figure 39(a)). Curcumin is readily soluble in organic solvents such as dimethylsulfoxide (DMSO), ethanol or acetone, but it is sparingly soluble in water. In acidic and neutral solutions as well as in the solid state, the keto form predominates, and curcumin acts as a potent donor of H-atoms. In contrast, above pH 8, the enolic form predominates, and the phenolic part of the molecule acts mainly as an electron donor (Jovanovic *et al.,* 1999) (Figure 39(b)).

a)

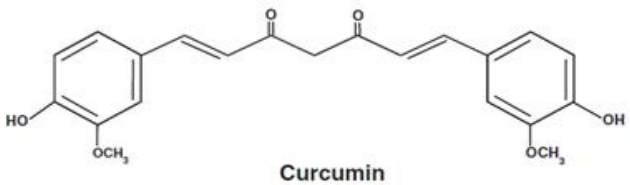

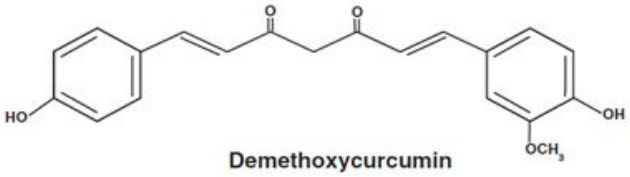

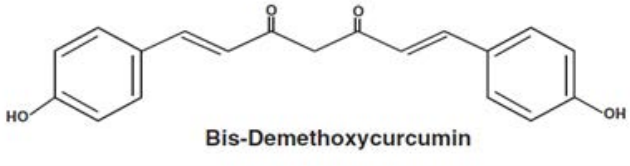

b)

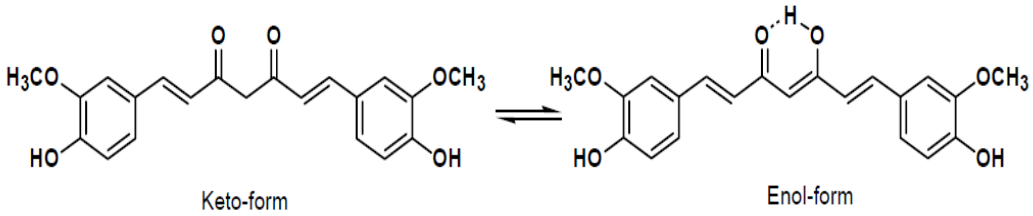

Figure 39. Chemical structure of curcuminoids (curcumin, demethoxycurcumin, bisdemethoxycurcumin) (a) and pH dependent keto- and enol- tautomeric form of curcumin (b).

Curcuminoids have already become the focus of many research activities due to their numerous biological and pharmacological benefits such as antioxidant, anti-cancerous, anti-inflammatory, antimicrobial properties (Bush *et al.*, 2001 ; Gescher *et al.*, 2001 ; Khar *et al.*, 1999 ; Lukita-Atmadja *et al.*, 2002 ; Sharma, 1976). However, curcumin has extremely low water solubility, which makes it difficult to be used as food supplement (Tonnesen *et al.*, 2002), as well as a low bioavailability, which means that its might not be beneficial even if ingested (Maiti *et al.*, 2007). Thus, many attempts have been made to improve either curcumin's water solubility or its bioavailability. These attempts involve the use of adjuvant-like piperine a known inhibitor of hepatic and intestinal glucuronidation (Shoba *et al.*, 1998), complexation with phospholipids and cyclodextrins, as well as the utilization of carriers in the form of liposomes, biodegradable microsphere, hydrogels, polymeric nanoparticles, and lipid

based nanoparticles (Bisht *et al.,* 2007 ; Kunwar *et al.,* 2006 ; Maiti *et al.,* 2007 ; Sou *et al.,* 2008 ; Tiyaboonchai *et al.,* 2007 ; Tønnesen *et al.,* 2002 ; Vemula *et al.,* 2006). Achieving high encapsulation efficiency and controlled release of curcumin are among the key challenges in utilization of micro and nanocarriers (Mainardes and Silva, 2004 ; Sharma and Sharma, 1997). The elimination process of the drug carrier from the body is also another concern that should properly study prior to its utilization.

Liposomal carriers are formed from enclosed phospholipids membranes, which are amphiphilic molecules containing both water soluble and lipid-soluble hydrophobic sections. Liposomes can not only encapsulate hydrophilic drugs within an aqueous score, but also they can entrap lipophillic drugs within their lipid bilayer (Barenholz, 2003). Liposomes can protect bioactive agents from digestion in the stomach and show significant levels of absorption in the gastrointestinal tract, leading to the enhancement of bioactivity and bioavailability (Takahashi *et al.,* 2006). Thus, liposomes have frequently employed in the literature as effective drug carriers.

Phospholipids which are the main constituent of liposomes are abundantly found in many tissues including nervous tissues and brain. This facilitates the delivery of liposomal drugs to the target tissues. Lecithin from salmon head (*Salmo salar*) contains a high percentage of polyunsaturated fatty acids (PUFA) such as eicosapentaenoic acid (EPA) and docosahexaenoic acid (DHA) which are an important constituent of neuronal membrane(Belhaj *et al.,* 2010 ; Gbogouri *et al.,* 2006). This lecithin has been proven to be biocompatible and even play positive role in neuronal network development. Thus, the present study is primarily focused on the generation and physicochemical characterizations of nanoliposomes from salmon lecithin as curcumin carriers for hydrophobic drug and *in vitro* study the neuroprotective characteristics of nanoliposome-encapsulated curcumin on neuronal cells was performed.

VII.3 Results and discussion

VII.3.1 Fatty acid analyses

The percentage of total polyunsaturated fatty acids in salmon lecithin has higher variety of polyunsaturated fatty acids (Table.9). We can observe nine polyunsaturated fatty acids of

omega 3 and omega 6 in salmon lecithin. The most significant proportions of fatty acids were C22:6 n-3 and C20:5 n-3, found in the polyunsaturated fatty acids class with 28.15 and 8.83%, respectively. C18:1 n-9 in the monounsaturated fatty acids class (19.11%), and C16:0 in the saturated fatty acids class (19.33%).The ratio of n-3/n-6 was about 10.

Table 9. Main fatty acid compositions of salmon lecithin by gas chromatography (area %).

Fatty acids	Salmon lecithin	
	%	SD
C14	2.24	0.05
C15	0.28	0.00
C16	19.33	0.26
C17	0.55	0.03
C18	4.47	0.04
C20	0.22	0.02
C22	0.58	0.02
SFA	27.67	-
C16:1n9	1.83	0.02
C18:1n9	19.11	0.35
C20:1n9	0.28	0.02
C22:1n9	2.39	0.01
MUFA	23.61	-
C18:2n6	4.41	0.08
C18:3n3	1.98	0.06
C18:4n3	2.84	0.04
C20:5n3(EPA)	8.83	0.02
C22:5n3	2.51	0.12
C22:6n3(DHA)	28.15	0.24
PUFA	48.72	-
n-3/n-6	10.06	-
DHA/EPA	3.19	-

VII.3.2 Lipid classes

The lipid classes of salmon lecithin were separated by thin-layer chromatography (Iatroscan). At that stage, phosphatidylcholine represented the major class of phospholipids contained in salmon lecithin (42.40%). Moreover, the percentage of triacylglycerols (TAG) contained in lecithin was 31.20 ± 0.4, and the percentage of polar fraction was 67.65 ± 0.9. More salmon lecithin contains a small amount of cholesterol about 1.15 + 0.1%.

VII.3.3 Liposome size and electrophoretic mobility measurements

The particle sizes of different nanoliposomes were measured immediately after sonication. The liposome size depends on the viscosity of the materials and agitation parameters including sonication amplitude and time. The size of the nanoliposome also depends on fatty acid composition, lipid classes and the surface-active properties of lecithin (Arab Tehrany *et al.,* 2012 ; Benedet *et al.,* 2007). The hydrodynamic diameter of nanoliposome for salmon lecithins was 119.97 ± 0.42 nm, and the polydispersity index was 0.31 ± 0.00. The size of the curcumin-loaded liposomes (114.37 ± 1.01 nm) was found to be slightly smaller than the unloaded curcumin liposomes. These results suggest a strong interaction between curcumin and lecithin resulting in a compaction of the core. Our results are in good agreement with the previously reported results (Mazzarino *et al.,* 2012). Regarding polydispersity index, we observed no significant variation between curcumin loaded liposomes and unloaded liposomes.

Electrophoretic mobility value was about -3.5 µmcm/Vs with a relatively high stability of the formulations, which was due to the positive and negative charge of the polar fraction of lecithins. According to the DLS results, the electrophoretic mobility in salmon lecithins was -3.51± 0.11µmcm/Vs. It should be noted that the value of electrophoretic mobility was negative throughout the storage period for nanoliposome formulation. The salmon and rapeseed lecithins contain different type of phospholipids like as phosphatidylserine (PS), phosphatidic acid (PA), phosphatidylglycerol (PG), phosphatidylinositol (PI), phosphatidylethanolamine (PE), phosphatidylcholine (PC). At physiological pH, these phospholipids are negatively charged except the PC and PE which exhibits no net charge. So, these anionic fractions are probably responsible for the negative electrophoretic mobility (Chansiri *et al.,* 1999). We measured the stability of nanoliposomes by measuring the particle size during one month at 4 °C and 37 °C. We observed no significant variation between day 0 and day 30.

The results obtained by Nanosight show clearly that the salmon liposomes are polydisperses, thus the spectra were multimodal explaining existence of many population of vesicle in the system because the salmon lecithin is not pure and contains many kinds of

phospholipids with different types of fatty acids. Indeed The mean diameter of particles obtained by NTA was highly similar to the Z-average values measured by DLS.

The small size of nanoparticle is benefit for increasing the absorption amount. Drugs delivered to mucosal surfaces are typically efficiently removed by mucus clearance mechanisms and systemic absorption, precluding prolonged drug presence locally. Encapsulation of drugs in polymeric particles offers the potential for localized and sustained delivery to mucosal tissues (Tang *et al.,* 2009). The mucus acts to entrap and remove pathogens and foreign particles, in order to protect the epithelial surface. Drug nanocarriers are nevertheless a good alternative to diffuse into the mucus layer and minimize elimination by this clearance mechanism. In addition, there is a size limit to cross the intestinal mucosal barrier since the mesh-pore spacing of the mucus layer varies from 50–1800 nm (Lai *et al.,* 2010). Many studies have shown that nanoparticles with a size under 200 nm effectively diffuse through the mucus layer (Gamboa and Leong, 2013 ; Primard *et al.,* 2010). Secondly, liposomes smaller than 70 nm are removed from the systemic circulation by liver parenchymal cells, while those larger than 300 nm accumulate in the spleen. An optimum size range of 70–200 nm has been identified to give the highest blood concentration of liposomes(Laouini *et al.,* 2011 ; Yokoyama, 2005).

TEM images indicated that vesicles prepared by sonication method were in the form of multilamellar vesicles (MLV) because of the sonication steps. The bilayer nature of the vesicles was clearly visible in these micrographs (Figure 40). We also observed some droplets in each formulation because of the presence of weak oil quantity (10%). The droplets in the three systems were found to be fine enough, even though there were large droplets with diameters higher than 200 nm.

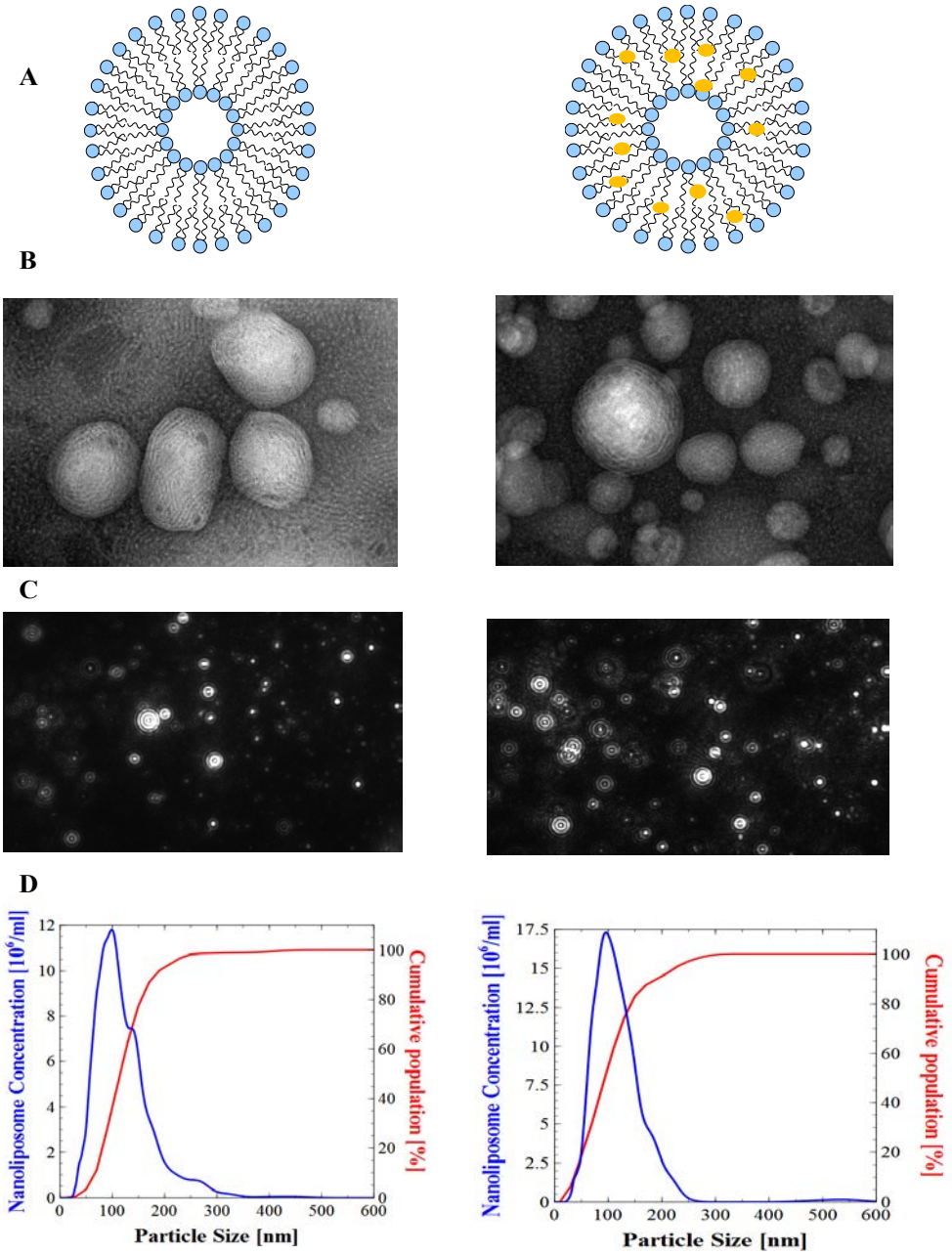

Figure 40.A, Schematic of the study, demonstrating the nanoliposomes without (left) and with curcumin (right). B, Transmission electron microscopic images of salmon nanoliposome before (left) and after (right) curcumin encapsulation. C, The size distribution of different nanoliposomes obtained from nanoparticle tracking analysis with the corresponding NTA video frame liposome (left), liposome loaded curcumin (right) and D, size distribution from NTA (E) liposome (left), liposome loaded curcumin (right).

VII.3.4 Entrapment efficiency

High encapsulation efficiency is an important factor for the selection of a proper carrier and the encapsulation method. The entrapment efficiency of the curcumin in salmon liposome (2% w/v) was 56. 2± 0.6%, which was low compared to the 67.3 ± 1.1%, % observed in the 3% solution of salmon liposome (Hasan *et al.,* 2014). This observation suggests that the entrapment efficiency was decreased as the ratio of curcumin to the lipid matrix increased, possibly due to the reduced available space for the drug to be entrapped.

Curcumin is a highly unstable molecule; its stability is susceptible to various conditions such as light, pH, and temperature (Priyadarsini, 2009 ; Wang *et al.,* 1997). It is therefore important to confirm that curcumin retains its physiochemical properties and stability after its encapsulation within liposomes. The HPLC profile of curcumin (Figure 30(a)) showed the elution of this molecule at 8.7 min with the percent of 78.2±0.16 along the demethoxycurcumin and bisdemethoxycurcumin at 8.2 and 7.75 min, with the percent of 19.2±0.1, 2.6±0.1, respectively. Extracted curcumin from nanoliposomes also showed a similar HPLC profile (Figure 30(b)).

VII.3.5 Membrane fluidity

Membrane fluidity, which reflects the order and dynamics of phospholipid alkyl chains in the bilayer is one the key factors that affects the drug release profile from liposomes (Maherani *et al.,* 2012). In fact, the drug leakage to the aqueous solution is enhanced by increasing the fluidity of the bilayer. Membrane fluidity depends on lipid composition of nanoliposomes. The presence of saturated FAs increases the packing between phospholipids, which expelles the water in the vicinity of the bilayer surface. On the other hand, unsaturated FAs help reducing the packing between phospholipids and preserve the level of hydration, thus maintaining membrane fluidity (Leekumjorn *et al.,* 2009).

It appears that nanoliposomes made of salmon lecithin have a membrane fluidity 3.20±0.03 where they contain higher proportion of polyunsaturated fatty acids, as the membrane fluidity is more important when the degree of unsaturation of acyl chains increased. The lipid fluidity is expected to increase both the diffusivity and partitioning tendency of the permeant, which yields a possible squaring effect on the enhancement factor.

The presence of curcumin decreased the membrane fluidity of liposome (2.83±0.1), which might be due to its molecular interaction with the bilayer of liposomes. As curcumin is a highly conjugated and rigid planar molecule, its presence can weaken hydrophobic interactions among acyl chains of phospholipids (Patra *et al.,* 2012). The incorporation of curcumin perturbs the packing characteristics of the phospholipid bilayer and thus enhances the packing density of the hydrocarbon moiety in the lipid bilayer.

VII.3.6 Neuronal metabolic capacity and morphology

Several studies demonstrated the importance of the nanoliposomes as natural carrier systems which are vastly applied as unique molecules in drug delivery strategies owing to their unique characteristics (Lehner *et al.,* 2013 ; Nakayama *et al.,* 2007). In addition, multiple desirable characteristics of curcumin as a neuroprotective drug have been demonstrated, including anti-inflammatory, antioxidant, and anti-protein-aggregate activities(Ringman *et al.,* 2005 ; Ryu *et al.,* 2006 ; Yang *et al.,* 2005). Based on the originality of using natural source nanoliposomes for delivery of curcumin, we treated primary cortical neurons with curcumin loaded salmon liposomes. To examine the effect of encapsulated curcumin on neuronal metabolic capacity, cortical neurons were assayed by XTT test at days 3, 5, 7, 9 after 5, 10, 15 and 20 µM curcumin encapsulated nanoliposomes or nanoliposome alone treatment. The doses were chosen based on our previous *in vitro* screening results (Hasan *et al.,* 2014).

Treatment at different concentrations was made 8h after neuronal plating. Compared to the untreated control, the metabolic activity of treated neurons with higher concentrations (15 and 20 µM) was increased significantly form DIV 3 to DIV9 and lower concentrations induced the increase at DIV5 and DIV7 in encapsulated curcumin administration (Figure 41, B). Treatment with nanoliposome alone didn't show any statistically changes at DIV3 and the maximum augmentation of activity was only observed after DIV7 in highest concentration (Figure 41, A). All these results taken together indicate that curcumin encapsulated nanoliposome induces methabolic activity of cortical neurons and has protective effect on their viability.

Results from (Figure 41, C) were obtained after the treatment of primary cortical neurons with different concentrations of curcumin as mentioned above. Cultured cortical

neurons were stained with cytoskeletal markers, anti-neuronal class III β-tubulin antibody, and DAPI for detection of nucleus at DIV5. Results showed that curcumin could promote complexity of the neuronal network morphology after treatment with high concentration. The increase in complexity of network formation was observed in treated cultures with 15 and 20 μM of encapsulated curcumin whereas at lower concentration the formation of network showed no differences compared to control cultures.

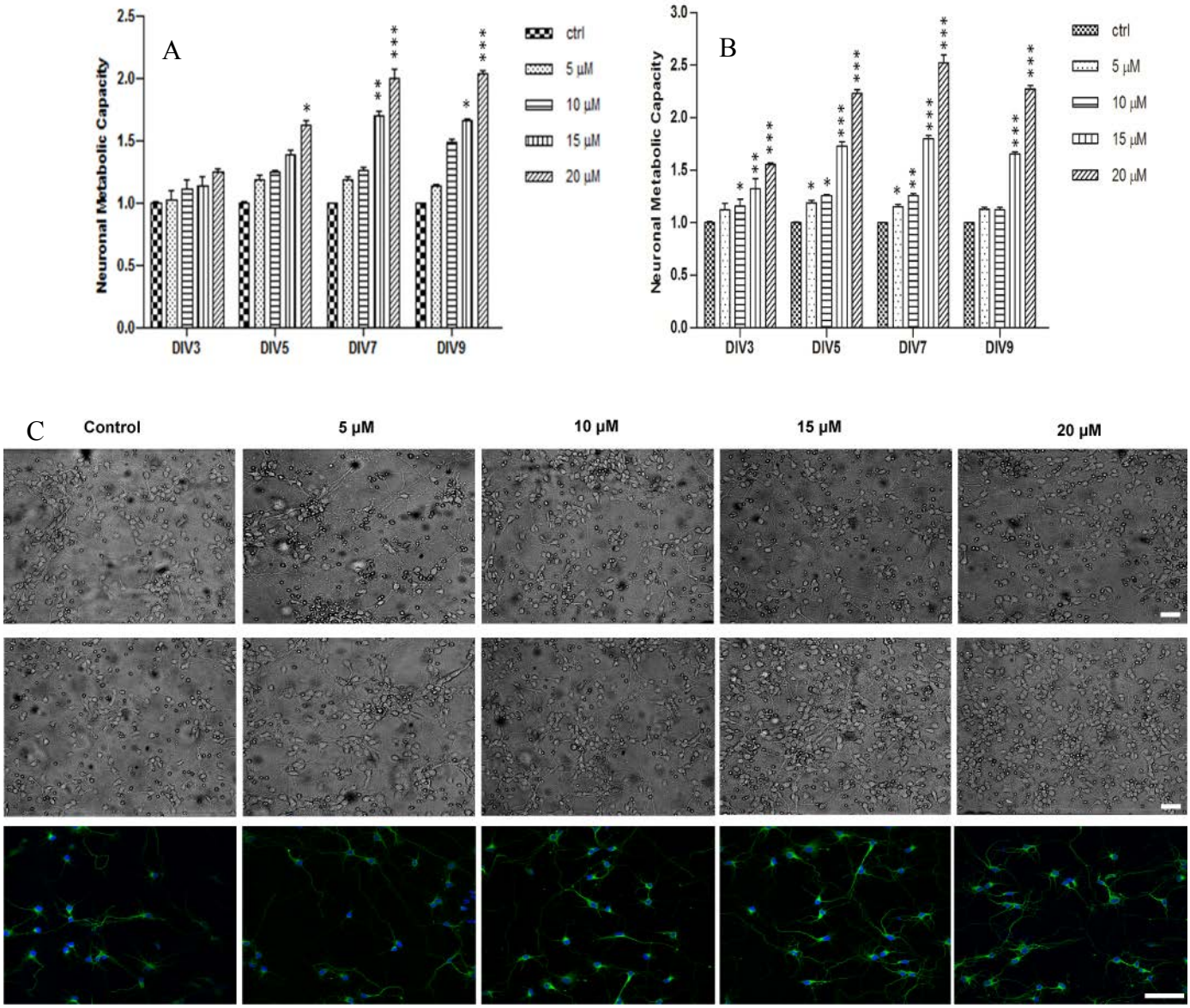

Figure 41. Curcumin increases metabolic activity and formation of neuronal network. Cortical neurons were incubated at different time-frame with the lecithin (A) or lecithin encapsulated curcumin (B) with indicated concentrations. Cell metabolic activity was checked by the XTT test. Results are expressed as normalized over control. (C) Phase contrast images of neuronal network cultures after treatment with lecithin or encapsulated curcumin at different concentration and immuno-fluorescent images of network formation from cotical neurons after treatment with curcumin. Data are mean ± standard error of three separate experiments from cells of different cultures. *p<0.05, **p<0.01, ***p<0.001.

VII.3.7 Encapsulated curcumin prevents primary cortical neurons from apoptosis

Previous studies have shown the neuroprotective role of curcumin (Thiyagarajan and Sharma, 2004; Wang *et al.*, 2008a). We therefore undertook the current studies to determine whether curcumin encapsulated liposomes could protect neurons from apoptosis.

We performed an apoptosis assay to examine the effect of curcumin in primary cortical neurons. To quantify the frequency of apoptotic cells, the cultures were incubated with FITC-labeled annexin V after treatment with different concentration of curcumin and were subsequently analyzed by flow cytometry. Figure 42 Ai-v and in panel Q4 of the density plots (high level of annexin V-FITC) indicate a decrease in the percentage of apoptotic cells in the curcumin-treated cells compared with controls. In accordance with previous results, higher concentration of curcumin prevents neuronal apoptosis significantly compared to control (2.1 folds decrease for 15 μM and 2.7 folds for 20 μM) as it was shown in (Figure 42, B).

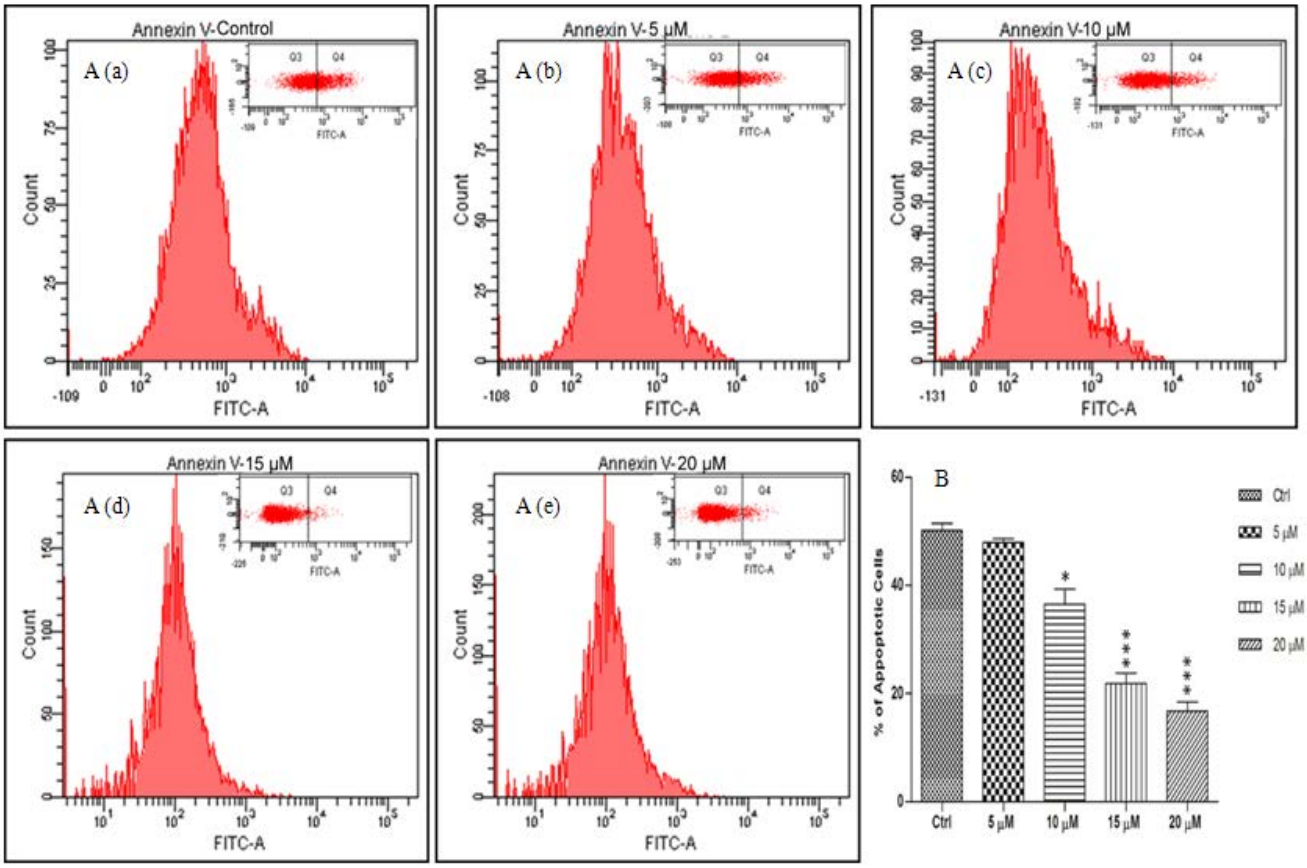

Figure 42. Curcumin encapsulated nanoliposom from natural lecithins decreases apoptosis in cortical neurons. A, Primary cortical neurons were treated with 5, 10, 15 and 20 µM curcumin after 8 h for 3 days. Percentage of apoptotic cells was determined by annexin V-FITC fluorescence staining using flow cytometry analysis and FACS analyzer. B, Quantitation of these data represents the percentage of apoptotic cells in each condition. Data are expressed as mean ± SEM from three separate treatments.

VII.4 Conclusions

The resemblance of liposomes to the model membrane makes them ideal for transportation of biomolecules through human tissues due to their broad bio-distribution and compatibility. Our present study gave rise the information about the physico-chemical properties of nanoliposomes before and after encapsulation of curcumin. The possibility of using liposomes as a carrier system for different applications depends on their physico-

chemical properties; fatty acid composition and preparation methods strongly influence vesicle behavior in biological systems.

Generally, particle size and z-potential are the most important properties that determine fate of liposomes. Knowledge of the z-potential is also useful in controlling the aggregation, fusion and precipitation of liposomes, which are important factors affecting the stability of liposomal formulations. The lipid fluidity is expected to increase both the diffusivity and partitioning tendency of the permeant. Bilayer fluidity also reflects the order and dynamics of phospholipid alkyl chains in the bilayer and is mainly dependent on its composition as liposomes composed of unsaturated lipids have more fluidity as well as ours nanoliposomes. The drug release characteristics exhibited controlled delivery of curcumins for longer duration, which may improve bioavailability of the curcumins in its active, native form.

The results showed that salmon lecithin includes a wide range of fatty acids and specifically unsaturated ones EPA and DHA which known for their health benefits. From TEM imaging, we observed that lecithin solutions were made largely of nanoliposomes and a little part of emulsion. Furthermore, the prepared salmon liposomes were stables for the period more than one month with polydisperse populations which confirmed by Nanosight and zetasizer measurement.

Curcumin, a naturally occurring polyphenolic compound has been reported to exhibit several biological and pharmacological activities such as anti-tumor and anti-cancer properties (Chan *et al.,* 1998 ; Dinkova-Kostova and Talalay, 1999 ; Fang *et al.,* 2005). Numerous studies have demonstrated the neuroprotective characteristics of curcumin, including antioxidant, anti-inflammatory and anti-protein-aggregate activities (Cole *et al.,* 2003 ; Lim *et al.,* 2001 ; Ringman *et al.,* 2005). For these characteristics, accumulating in vitro and in vivo data showed that curcumin could act as strong candidate for prevention or treatment of neurodegenerative disorders like Parkinsons, Alzheimer's and stroke (Anand *et al.,* 2007 ; Wang *et al.,* 2005). We previously demonstrated that nanoliposomes as natural carrier systems have a positive role in neuronal metabolic activity and network formation. In this regard we developed a novel curcumin carrier based on liposomal system to increase the systemic bioavailability of curcumin.

Application of nanoliposome-encapsulated curcumin in primary cortical neurons, demonstrated the effectiveness of system in viability and formation of network. Comparing to untreated or only liposome treated cultures, our results proved the advantage of using such system as neuroprotective materials. Decrease in rate of apoptosis in treated cultures achieved in this study could be beneficial for further studies *in vivo* and particularly in animal models of neurodegenerative disorders.

VIII. Chitosan-coated liposomes encapsulating curcumin: Study lipid-polysaccharide interactions and nanovesicles behavior

M. Hasan[1], G. Ben Messaouad[1], F. Michaux[1], A. Tamayol[2], C. Kahn[3], M. Linder[1], E. Arab-Tehrany[1]*

[1]Université de Lorraine, Laboratoire d'ingénierie des biomolecules, TSA 40602 54518 – Vandœuvre Cedex.

[2]Center for Biomedical Engineering, Department of Medicine, Brigham and Women's Hospital, Harvard Medical School, Boston, MA 02139, USA. Harvard-MIT Division of Health Sciences and Technology, Massachusetts Institute of Technology, Cambridge, MA 02139, USA. Wyss Institute for Biologically Inspired Engineering, Harvard University, Boston, MA, 02115, USA.

[3]IFSTTAR, LBA, F-13916 Marseille, France.

VIII.1 Résumé

La curcumine est un composé bioactif naturel provenant du curcuma, reconnu pour avoir un grand nombre de propriétés thérapeutiques. Cependant, sa biodisponibilité reste limitée en raison de sa faible solubilité en milieu acqueux. Dans cet article, la curcumine a été encapsulée dans des nanoliposomes préparés à partir de lécithine de saumon purifiée et de chitosane. Les interactions impliquées dans la stabilité du complexe liposome / chitosane ont été étudiées, notamment par analyses FTIR, avant et après encapsulation de curcumine. La taille et les charges de surface du complexe liposome chitosane ont été étudiées en fonction du pH ainsi que les propriétés rhéhologiques. L'influence du coating de chitosane sur le nanoliposome, en présence de curcumine dans la membrane lipidique a été mesurée par diffusion aux petits angles des rayons X (SAXS). Les résultats ont permis d'apporter des informations sur la structure, la localisation et les phénomènes de diffusion de la curcumine.

Keywords: Chitosan-coated liposomes, curcumin, interactions, rheology, SAXS, FTIR.

VIII.2 Introduction

Nanotechnologies supply innovations in various domains of medicine, namely therapy, diagnostics, imaging and drug delivery (Barratt, 2000 ; Freitas, 2005 ; Sonvico *et al.,* 2005). In drug delivery, colloidal carriers have been suggested for effective administration of drugs having difficulties, such as toxicity, low bioavailability or poor water solubility. For these purposes, different colloidal drug delivery systems have been fabricated such as liposomes, micelles, nanoemulsions and nanoparticles.

Curcumin (diferuloyl methane) is a natural polyphenolic phytochemical extracted from the powdered rhizomes of turmeric (Curcuma longa) spice. It has been widely used as a traditional medicine in many Asian countries, since it was reported that curcumin has antioxidant, anti-inflammatory, antimicrobial, and anticancer features, as well as wound healing characteristics (Bhawana *et al.,* 2011 ; Biswas and Mukherjee, 2003 ; Kunnumakkara *et al.,* 2008 ; Lantz *et al.,* 2005 ; Reddy and Lokesh, 1992). Although, curcumin has numerous advantages, the therapeutic application of curcumin is limited because of its low bioavailability (Parvathy *et al.,* 2009 ; Wilart *et al.,* 2009), due to its poor aqueous solubility, low stability against alkaline pH conditions, extensive first-pass metabolism and rapid systemic elimination (Anand *et al.,* 2007; Tønnesen, 2002). Therefore, a carefully designed carrier could significantly facilitate curcumin delivery and broad the range of its possible pharmaceutical applications.

Liposomes are widely used as delivery vehicles for stabilizing drugs and overcoming barriers to cellular and tissue uptake (Gregoriadis, 1988). Nanoliposomes have become very versatile tools in biology, biochemistry and medicine because of their enormous diversity of structure and com-position. Liposomes are microscopic vesicles formed essentially by phospholipids dispersed in water, which are amphiphilic molecules containing polar heads and hydrophobic hydrocarbon tails, they can associate spontaneously to form bilayer vesicles. This property of phospholipids gives liposomes unique properties, such as self-sealing, in aqueous media and make them an ideal carrier system with applications in different fields including food, cosmetics, pharmaceutics, and tissue engineering (Bangham, 1961).

Liposomes can carry both hydrophilic and hydrophobic components by encapsulation in the water phase and intercalating into the hydrophobic domains, respectively. Even hydrophobic components can be formed in a stable state in an aqueous environment by high dispersion in a liposome system. In addition, the components entrapped in liposomes can effectively penetrate and overcome biological barriers to cellular and tissue uptake because the liposome has a similar structure as the cell membrane (Brandl, 2001 ; Shin *et al.,* 2013).

Lecithin, which has two long hydrocarbon chains, is a major component of lipid bilayers of cell membranes and a natural, biological amphiphile. Furthermore, it is in many respects regarded as an ideal biological surfactant because it is biodegradable. It may be used for various purposes (Lin *et al.,* 2009). Numerous studies, both in humans and in animals (Calder and Yaqoob, 2009; Van der Meerena *et al.,* 2009), have demonstrated that polyunsaturated fatty acids (PUFA) of the n-3 series, in particular eicosapentaenoic acid (EPA, 20:5 n-3) and docosahexaenoic acid (DHA, 22:6 n-3), are known to have positive effects on human health by preventing cardiovascular diseases, cognitive decline, inflammation, hypotriglyceridemic effect and improving mental capacity. Marine lecithin from salmon head (Salmo salar) contain a high percentage of PUFAs, especially EPA and DHA, so the originality of this work is the use of these salmon's phospholipids to carry biomolecules (Belhaj *et al.,* 2010 ; Belhaj *et al.,* 2012 ; Gbogouri et al., 2006).

Polymer coating is a promising way to modify the surface characteristics of liposomes in order to improve their applicability. This can be achieved by simply mixing a liposome suspension with a polymer solution without chemically linking the two components (Takeuchi *et al.,* 1998). Among various biopolymers, chitosan has been widely studied as a mucoadhesive material that enhances the penetration of macromolecules across the intestinal and nasal barriers (Lee *et al.,* 2000).

Interestingly, the coating of lipid-based nanostructures with chitosan has been found to increase their stability (Henriksen *et al.,* 1997), and to provide them with mucoadehsive properties (Takeuchi *et al.,* 2003). Chitosan is a hydrophilic, biocompatible and biodegradable polymer with low toxicity. Because of its bioadhesive and permeation enhancing properties, chitosan has received strong attention in novel bioadhesive drug delivery systems, aimed at improving the bioavailability of drugs by prolonging their residence time at the site of

absorption (Kotze *et al.,* 1999). Chitosan is predominantly composed of β-(1,4)-linked Dglucosamine units and is obtained by deacetylation of chitin, which is the primary component of the cell walls of crustaceans, fungi, and insects (Muzzarelli *et al.,* 2012). By combining chitosan and liposomal characteristics, specific, prolonged, and controlled release may be achieved (Takeuchi *et al.,* 1996). Takeuchi and others showed that the chitosan-coated liposomes were formed via ionic interaction between the positively charged chitosan and negatively charged diacetyl phosphate on the surface of the liposomes (Figure 43).

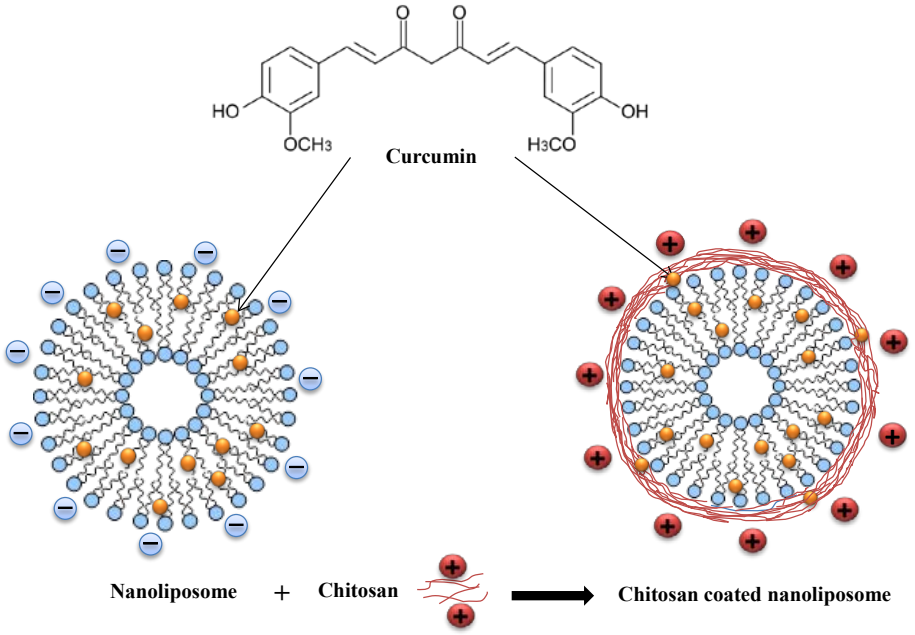

Figure 43. Schema illustrative for curcumin loaded nanoliposome and chitosan-coated curcumin nanoliposome.

Polymer-vesicle systems constitute a type of mixed colloidal system of a particular interest. In fact, the mixed biopolymer-liposome systems are good model systems for living cells since these are composed of lipidic membranes which could interact with several biopolymers (Marques *et al.,* 1999). The control of the rheological properties of liposomes dispersions is of great industrial importance (Kevelam *et al.,* 1999). The rheological behavior of type of dispersion depends on the interaction between vesicles and vesicle deformability. The interactive forces consist of a van der Waals attraction, electrostatic repulsion, and a "long-range" entropic repulsion as a result of thermal undulations (deHaas *et al.,* 1997).

Considering that the rheological response is directly related to the microstructural changes, a better understanding of the changes in microstructure under shear could provide

significant opportunities for enhancing the processing of liposomes dispersion (Berni *et al.,* 2002).

The present study focused primarily on the preparation of nanoliposomes from salmon purified phospholipid and coating them with chitosan in order to encapsulate the curcumin. The physicochemical characterization of the samples, followed by X-ray diffraction and transmission electron microscopy, infrared spectroscopic techniques, in addition, the rheological properties of systems were measured.

VIII.3 Results and discussion

VIII.3.1 Fatty acid analyses

The main fatty acid compositions are shown in Table 10. The first observations allow us to highlight the total polyunsaturated fatty acids in salmon lecithin and salmon phospholipid were predominate with 46.28% and 45.11%, respectively. The percentage of the fraction of polyunsaturated fatty acids is followed directly by the percentage of saturated fatty acids in salmon lecithin (33.40%) and salmon phospholipid (35.06%).

In general, the fatty acid composition of the phospholipid fraction and lecithin was not very different. The main difference between two was the slightly lower content of EPA and DHA, in purified phospholipid, the percentage of palmitic acid (C16:0) increased in compared to salmon lecithin, because of the oxidation phenomenon during acetone precipitation.

Where found that the amount of EPA and DHA decreased from 11.03% and 26.26% in lecithin fraction to 10.13% and 25.55% in purified phospholipid, on the other hand the amount of palmitic acid increased from 20.67% in lecithin to 22.22% in purified phospholipid. This composition was in agreement with the results presented in other study (Lu *et al.,* 2012a). Although it is known, that marine phospholipids have a higher content of eicosapentaenoic acid (EPA) and docosahexaenoic acid (DHA) as compared to fish oil in triglycerides (TAG) form (Peng *et al.,* 2003).

Table 10. Fatty acid compositions of salmon lecithin and salmon phospholipid after purified by acetone precipitatio

Fatty acids	Salmon lecithin		Salmon phospholipid	
	%	SD	%	SD
C14	2.72	0.04	2.62	0.02
C15	1.13	0.01	1.16	0.04
C16	20.67	0.15	22.22	0.15
C17	0.88	0.05	0.83	0.00
C18	6.10	0.05	6.72	0.05
C20	0.35	0.03	0.36	0.15
C22	1.55	0.06	1.15	0.21
SFA	33.40		35.06	
C14:1n9	0.33	0.02	0.33	0.03
C16:1n7	3.23	0.07	2.87	0.14
C18:1n9	13.87	0.13	14.13	0.06
C20:1n9	2.11	0.06	1.91	0.01
C22:1n9	0.79	0.08	0.59	0.09
MUFA	20.32		19.83	
C18:2n6	1.20	0.04	1.05	0.07
C18:3n3	0.35	0.01	0.34	0.09
C20:4n6	3.52	0.02	3.59	0.03
C20:5n3(EPA)	11.03	0.13	10.13	0.08
C22:5n3	3.93	0.33	4.46	0.22
C22:6n3(DHA)	26.26	0.09	25.55	0.17
PUFA	46.28		45.11	
n-3/n-6	8.88		8.73	
DHA/EPA	2.38		2.52	

VIII.3.2 Lipid classes

In this study, salmon lecithin was purified through acetone precipitation with the purpose to remove TAGs and also other nonpolar lipids and thus to increase the percentage of phospholipid. The phospholipid percentage increased from 67.65% to 100%, whereas all triglycerides and cholesterol were removed after acetone precipitation, which were with the amount of 31.20% and 1.15 % for triglycerides and cholesterol in case of lecithin (Table.11).

The results presented in Table 2 about the fraction of polar lipids in salmon lecithin and purified phospholipid showed that purified salmon phospholipid had lower contents of phosphatidycholine (PC), phosphatidylethanolamine (PE), phosphatidylserine (PS) and sphingomyelin (SPM) than untreated marine lecithin. However, purified phospholipid had a higher level of lysophosphatidycholine (LPC), phosphatidylinositol (PI) and content of other unidentified phospholipid, this probably due of hydrolysis of phospholipid during acetone precipitation. With regard to the free fatty acid (FFA), it was not detected in salmon phospholipid before and after purification.

Table 11. Lipid classes and fraction of polar lipids constituting of salmon lecithin and salmon phospholipid after purified by acetone precipitation.

Name	Salmon lecithin	Salmon phospholipid
Total phospholipids (%)	67.65±1.1	100±0.0
Phosphatidycholine, PC (%)	42.40±0.5	40.49±0.2
Phosphatidylethanolamine, PE (%)	7.73±0.1	3.58±0.1
Phosphatidylserine, PS (%)	9.09±0.1	7.95±0.2
Phosphatidylinositol, PI (%)	13.00±0.3	15.25±0.4
Sphingomyelin, SPM (%)	1.51±0.1	1.27±0.1
Lysophosphatidycholine, LPC (%)	2.75±0.1	3.23±0.2
Other phospholipids (%)	23.52±0.2	28.23±0.3
Triglycerides, TAGs (%)	31.20±0.8	nd
Cholesterol, CHO (%)	1.15±0.1	nd
Free fatty acids, FFA (%)	nd	nd

nd, not determined.

VIII.3.3 Measurement of liposome size and zeta potential

The particle sizes of nanoliposomes were measured immediately after preparation. The minimum size that can be achieved depends on lipid composition as well as liposome preparation method such as the sonication and homogenization parameters. The particle size of uncoated (typical) liposomes was found to be 88.98 nm. After coating with chitosan solution, this increased to 221.83 nm (Table. 12). This increase can be explained by the interaction between lipid and chitosan, which includes the lipid–chitosan electrostatic interactions between their head groups and the specific functional groups of chitosan $NH3^{+}$. Hydrophobic interactions between the lipid tails and chitosan take place allowing chitosan to come up to the bilayer and fill the empty volume (Wydro *et al.,* 2007). The size of the curcumin-loaded liposomes was found to be smaller than the unloaded curcumin liposomes. Therefore, the hydrodynamic diameter of nanoliposomes decreased from 88.98 nm to 79.78 nm for curcumin loaded liposome. These results suggest a strong interaction between curcumin and lecithin resulting in a core compaction. Our results are in good agreement with the previously reported (Mazzarino *et al.,* 2012). In contrast, the size of the curcumin-loaded chitosan-coated liposome was greater than the unloaded curcumin ones. Therefore, the hydrodynamic diameter of nanoparticles increased from 221.83 nm to 247.60 (Table.12). The increase in size between chitosan-nanoliposomes with and without curcumin encapsulation could be attributed to the loading of curcumin in the outer layer formed by chitosan around liposomal bilayer which are in good agreement with the results of Sanoj Rejinold *et al.,* 2011 (Sanoj Rejinold *et al.*, 2011a).

In addition to particle size diameter, DLS also measures polydispersity (PI) which is a dimensionless measure of the breadth of the particle size distribution (Zweers *et al.,* 2003). As shown in Table 2, the PIs were between 0.30 and 0.33 which indicated that particle size was well controlled with a narrow dispersity. According to mean values and PIs, there was no significant difference between the breadths of distribution of the samples. In comparing these results with the results published in our previous paper (Hasan *et al.,* 2014), we observe that the size of liposome prepared with unpurified lecithin was smaller and polydispersity index was slightly greater. This difference can be explained by the presence of triglycerides in unpurified lecithin and its absence in salmon phospholipid, which increase the flexibility of

liposomes, making the large liposomes easier to break into smaller ones caused the homogeneity of the population (Guo *et al.,* 2003).

The zeta potential has often been utilized to characterize colloidal drug delivery systems. It is a measure of the surface electrical charge of the particles. The magnitude of the zeta potential gives an indication of the stability of colloidal systems: as the potential increases, the repulsion between particles is greater, thus leading to more stable colloidal dispersions. If all the particles in the suspension have a large negative or positive zeta potential, they will repel each other, and there will be no tendency for the particles to aggregate (Mady *et al.,* 2009 ; Paolino *et al.,* 2006). This was attributed to the adsorption of the cationic polymer increasing the density of the positive charge around the liposomal surface. After adsorption, the strong electrostatic attraction between positively charged polyelectrolyte and oppositely charged surface groups of liposome forces them to come into close proximity, forming a thin layer around the surface (Guzey and McClements, 2006). It is clear from Table 3 that coating the nanoliposomes with chitosan shifted the zeta potential from negative (-45.77) to positive values (+60.93). The increase in zeta potential was attributed to the more cationic polymers adsorbed to the liposomal surface. Since chitosan carried a high positive charge, the adsorption of chitosan increased the density of the positive charge and made the positive zeta potential (Guo *et al.,* 2003). The increased particle size and zeta potential of chitosan-coated nano-liposomes reflect several changes in the surface properties of nanoliposomes due to the polymer–liposome interactions.

With respect to the stability of chitosan coated nanoliposome with time. We observed no significant variation in particle size after 30 days of incubation at 4 and 37°C.

Table 12. Mean particle size (nm), PDI, zeta potential (µm) and membrane fluidity of the liposomes and chitosan coated liposomes (each value represents the mean of triplicates).

Sample	Particle size (nm)	Polydispersity index	Zeta potential (mV)	Membrane fluidity
Salmon liposome	88.98±0.60	0.31 ±0.00	-45.77±2.40	3.24±0.05
Curcumin loaded salmon liposome	79.78±1.60	0.30±0.01	-46.03±0.76	3.04±0.01
Salmon CH-LP	221.83±2.29	0.33±0.01	+60.93 ±0.23	2.81±0.08
Curcumin loaded salmon CH-LP	247.60±2.04	0.33±0.01	+61.47±0.70	2.73±0.10

CH-LP: Chitosan-coated liposome.

VIII.3.4 Influence of pH on z-average and zeta potential of chitosan-coated liposomes

The size and surface charge of chitosan-coated liposome were evaluated in response to variations in pH degree. As shown in Figure 44, we observe that both the z-average and zeta potential of the particles were susceptible to the pH of the media. Increasing the suspension pH from 4 to 8, the zeta potential of the particles progressively decreased from about +55 mV at pH 4 near to zero mV at pH 8. The zeta potential decreased when pH increased, this can be explained by the charge neutralization of chitosan due to the addition of NaOH, which the protons H^+ of the amine group of chitosan lose when they interact with the OH^- groups of NaOH. When most of the protons in chitosan-coated liposome have been neutralized, surface charge presented a neutrality value (isoelectric point).

In parallel, the particles size of the sample still stable near pH 6.5, where the size increased rapidly especially from pH 6.8, the aggregation of particles was evidenced. These results confirmed that particles stability depends on electrostatic nature and the polysaccharide component defined the particle surface properties. In fact, the chitosan p*K*a value is around 6.5, where the particles are totally aggregated, but we observed the aggregation of particles begins at pH 6.5, when they partially deprotonated. The chitosan chains retain their affinity to the negatively charge of liposomes, which is due to a combination of various mechanisms such as adsorption, coagulation and bridging between them (Filipovic-Grcic *et al.*, 2001 ; Mertins and Dimova, 2013).

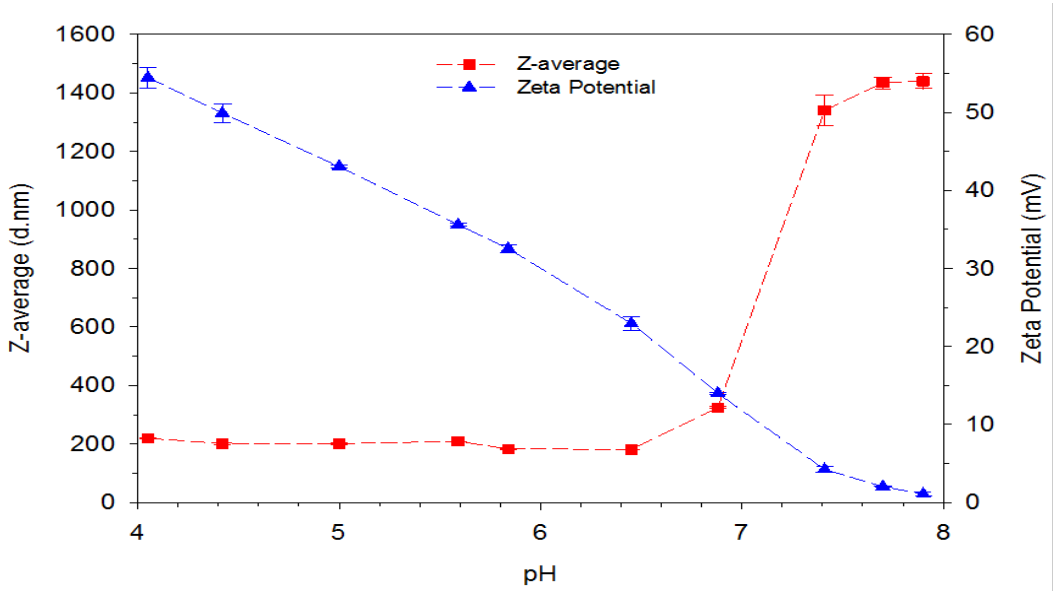

Figure 44. Effect of pH on size and zeta potential of chitosan-coated liposome.

VIII.3.5 Morphology of the liposomes

Surface morphological studies on the shape of the prepared systems using transmission electron microscopy indicated that the systems were almost spherical. TEM images indicated that liposomes prepared by sonication and high-pressure homogenization methods were in the form of multilamellar vesicles (MLV) (Figure 45(a)). The morphology of the chitosan coated liposomes showed a contrasting band surrounding a liposome vesicle, as shown in Figure 45 (b).

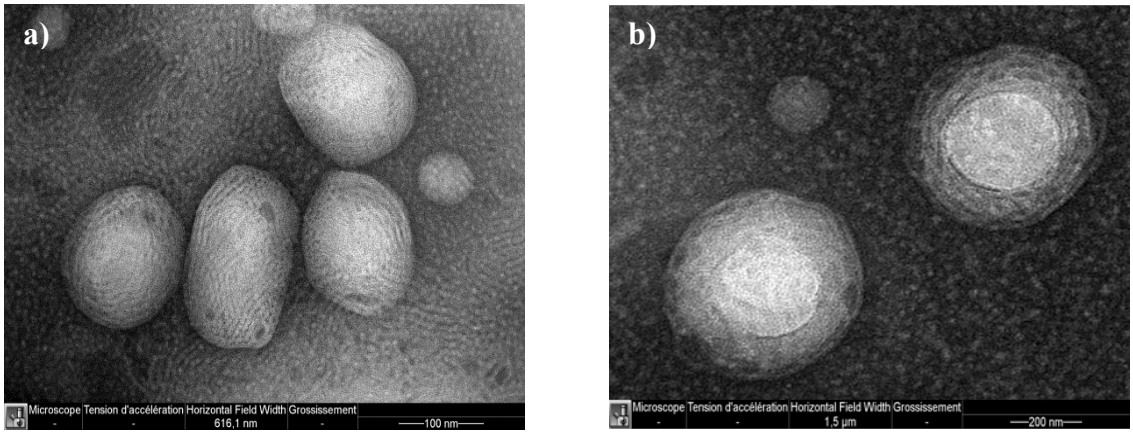

Figure 45. Transmission electron microscopic images of salmon nanoliposome before (a) and after (b) coating with chitosan.

VIII.3.6 SAXS experiments

The influence of the chitosan coating onto nanoliposomes structure has been studied by Small Angle X-ray Scattering (SAXS). Furthermore, the influence of the presence of curcumin in the lipid membrane on the scattering signal has also been investigated. Small angle scattering methods allow the investigation of the size and shape of nanoliposomes or their membrane structure depending on the employed experimental q-range. The lower the q-value is, the greater the observation window of the system. In this study, the experimental q-range ($7.5.10^{-2}$ to 4 nm^{-1}) is suitable for investigating the phospholipid bilayer structure but not the overall structure of the liposome. This q-range corresponds indeed to sizes ($d=2\pi/q$) from 84 to 1.5 nm.

Several informations are brought from scattering curves presented in Figure 46(a). At small angles (low q values; $q < 0.2$ nm^{-1}), a q^{-2} slope is detected for every samples. According to literature, this specific regime at low q values corresponds to form factor of the liposome lamellae (Kučerka *et al.,* 2011). Nevertheless, the experiment configuration does not allow to reach the plateau which should appear at lower q needful to determine the liposomes size. Since DLS experiments have been performed to measure particles diameter, we focused the SAXS experiments on a higher q-range to study the bilayer structure.

The phospholipids multilamellar arrangements of the liposome membrane usually leads to the presence of an intense diffraction peak between 0.6 and 1.6 nm^{-1} if the number of layers are sufficient. The repetition distance of the lamellar structure is deduced from the position of this peak (between 4 and 10 nm) (Sautot *et al.,* 2011). In Figure 46(a), no diffraction peaks are clearly detected in this range, and only a small diffraction line at 1.0 nm^{-1} is reported (Figure 46(b)). This tiny signal may correspond to the first reflection of the lamellar structure with a repetition distance of 6.3 nm. Nevertheless, the absence of clear diffraction peak for every samples means that the liposome membrane is composed of only a few phospholipid bilayers.

Furthermore, the presence of chitosan in the system affects the SAXS signal. The intensities of the samples coated with the polymer are indeed higher than those without chitosan. However, the curve shapes are similar which means that the bilayer structure is not

affected by the presence of chitosan around the liposome. This difference of intensities may come from the modification of the contrast term between both samples. To scatter the X-rays, a difference of electronic densities between different parts of the sample must exist and the scattered intensity depends on this difference (called contrast term) (Kučerka *et al.,* 2011). In the case of liposomes, the X-rays are scattered because water and phospholipids present different electronic densities (Figure 46(c)). The presence of chitosan around the liposomes modifies this contrast which may lead to a change in the scattered intensities (Figure 46(d)). Moreover, concerning the influence of curcumin on the liposome structure, no difference between sample with and without curcumin is reported whatever the presence of chitosan or not. The related scattering curves remain identical (Figure 46(a)).

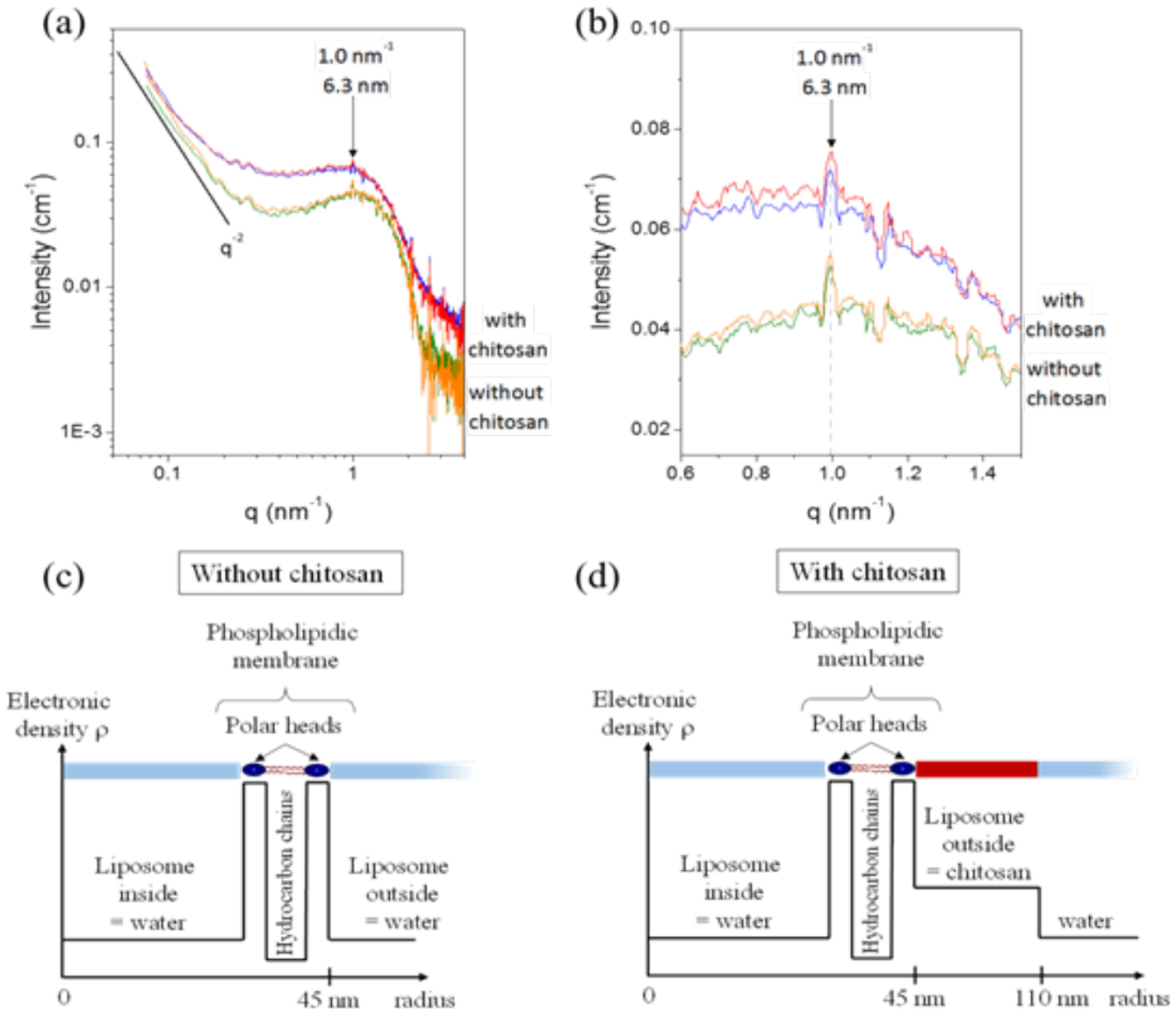

Figure 46. (a) SAXS profiles (log-log representation) of uncoated nanoliposomes (without curcumin (green line), with curcumin (orange line)) and nanoliposomes with chitosan coating (without curcumin (blue line), with curcumin (red line)). (b) Zoom on the SAXS profiles in the 0.6-1.5 nm^{-1} q-range (linear representation) to highlight to diffraction peak located at 1.0 nm^{-1}. Electronic density profiles of liposomes (c) and liposome coated by chitosan (d).

VIII.3.7 Fourier Transform Infrared Spectroscopy (FTIR)

Figure 47 shows FTIR spectra in the 4000–400 cm wave number range for salmon liposome, chitosan, curcumin each of them separately and different types of formation were presented in order to study the interaction between them. The main bands appearing in spectrum of chitosan were due to stretching vibrations of OH groups in the range from 3700 cm^{-1} to 3000 cm^{-1}, which are overlapped to the stretching vibration of N-H; and C–H bond

stretching vibration in $–CH_3$ at 2926 cm^{-1} and $–CH_2$ at 2883 cm^{-1} groups, respectively. Bending vibrations of methyl and methylene groups were also visible at 1381 cm^{-1} and 1404 cm^{-1}, respectively (Pires *et al.,* 2013 ; Mano *et al.,* 2003). The vibrations of carbonyl bonds (C=O) of the amide group CONHR (secondary amide, 1635 cm^{-1}) and to the vibrations of protonated amine group ($NH3^+$, 1541 cm^{-1}) (Marchessault *et al.,* 2006). The absorption bands at 950–1200 cm^{-1} were attributed to its saccharine structure. The sharp peaks at 1022 cm^{-1} and 1065 cm^{-1} are assigned to C-O stretching vibrations (ν (C O C)).) (Figure 47(v)) (Zhang *et al.,* 2012a).

As shown in Figure 47(i), the FTIR spectrum displays the main characteristic bands of phospholipid vesicles, especially those of the CH stretching modes with the maxima of peaks at 2854 cm^{-1} and at 2924 cm^{-1}, corresponding to the symmetric and antisymmetric stretching in the CH_2 groups of alkyl chains, respectively with minor contribution from the symmetric and antisymmetric stretching vibration in CH_3 groups at 2893 cm^{-1} and 2958 cm^{-1}, respectively. The broad band from 3750 to 3050 cm^{-1} represents the OH. The band at 1732 cm^{-1} corresponds to the stretching vibrations of the ester carbonyl groups of phospholipid, the relatively strong band centered at 1651 cm^{-1} corresponds to the stretching vibrations of alkene carbon–carbon double bond -C=C-. The scissoring vibrations of the CH_2 groups are represented by the band at 1456 cm^{-1}, and the band at 1406 cm^{-1} corresponds to (=C-H) Bending (rocking) vibrations. While the relatively weak band at 1394 cm^{-1} represents the umbrella deformation vibrations of the CH_3 groups of alkyl chains. In addition, the spectral pattern at 1086 and 1224 cm^{-1} represented the symmetric and antisymmetric $PO2^-$ stretching vibration of phospholipids, and the band representing the antisymmetric $N^+\backslash CH_3$ stretching vibrations 970 cm^{-1} (Pawlikowska-Pawlega *et al.,* 2013 ; Shimizu *et al.,* 1996 ; Yang and Irudayaraj, 2000).

The FTIR spectra for curcumin (Figure 47 (iv)), showed a sharp peak at 3508 cm^{-1} indicating the phenolic O-H stretching with a broad band at a range from 3100-3400 cm^{-1}, which is due to the ν(OH) group (in enol form), C-H (methyl) 2844 cm^{-1}, C-H (aryl) 3014 cm^{-1}. The strong peak at 1626 cm^{-1} has a predominantly mixed ν(C=C) and ν(C=O) character. Another strong band at 1601cm^{-1} is attributed to the symmetric aromatic ring stretching vibrations ν(C=C ring). The 1508 cm^{-1} peak is assigned to the ν(C=O), and the C–O–C

stretching peak of ether at 1026 cm^{-1}, and significance band was observed at 730 and 797 cm^{-1} for C=C–H aromatic stretching frequency (Hatamie *et al.,* 2012 ; Mohan *et al.,* 2012 ; Pan Ch *et al.,* 2006).

In order to disclose the structure of lipid/polysaccharide nanoparticles, the interactions between the polysaccharide and the lipid have been studied by FTIR spectrometry. The FTIR spectra of nanoparticles and of the components lecithin and chitosan alone are reproduced in Figure 47 (iii). FTIR was used, as a no perturbing technique, to analyze possible changes in the structure of phospholipid by analyzing the frequency of different functional groups of the lipid molecule in the presence or absence of chitosan. Formation of a complex between the liposomes and chitosan resulted in a considerable change in the absorption bands of OH group, which was broad is due of presence more of hydroxyls groups and possibility the formation of new intermolecular hydrogen bonds. The presence of chitosan with liposome caused also considerable change in the absorption bands acyl chains (3000–2800 cm^{-1}) toward lower wavenumbers. For example, the symmetric and antisymmetric stretching in the CH2 and CH3 groups of alkyl chains absorption bands located at 2854 cm^{-1} and 2924 cm^{-1} for CH2, and at 2893 cm−1 and 2958 cm−1 for CH3 respectively in case of free liposomes were merged into two peaks at 2852 and 2924 cm^{-1} easily distinguishable for narrow and intense in case of chitosan coated liposome (Fig. 5 (iii)). A significant shift from 2954 to 2952 cm^{-1} is also detected. We observe also a shift in the bending vibrations of acyl chains bands from 1406 cm^{-1} toward 1404 cm^{-1}, whereas the peak was more intense.The band at 1651 cm^{-1} corresponds to the stretching vibrations of alkene carbon–carbon double bond -C=C- was exposed to heavy shift towards 1641 cm^{-1}. The low frequency shifts of the absorption bands in the hydrophobic region correspond to the decrease in the acyl chain mobility in liposomes, as has been demonstrated earlier (Cieslik-Boczula and Koll, 2009 ; Hincha *et al.,* 2002). Evidently, complex formation with chitosan leads to restriction of acyl chain mobility in the bilayer structure, which implies a decrease in the membrane fluidity and thereby stabilization of the system (Biruss *et al.,* 2007).

The major potential binding site of anionic liposomes with amino polysaccharides (chitosan) via electrostatic interactions is the phosphate groups. Indeed, we found that the absorption band of liposomal phosphate groups shifted to high frequency (from 1224 to 1232

cm^{-1}), this means that the interaction with polymer ligands leads to dehydration of phosphate groups. In fact, the characteristic band of chitosan at 1539 cm^{-1}, corresponding to scissoring vibration of protonated amine group NH3, was shifted to high frequency 1549 cm^{-1}. Apparently, most hydrogen bonds of the phosphate group are broken due to electrostatic interactions with amino group of the chitosan.

Another potential binding site of chitosan conjugate on liposomes is the carbonyl group, which carries a partial negative charge on the oxygen atom. Liposome formation with chitosan was found to result in considerable changes in the region of the carbonyl group absorption. We found that the interaction between liposomes and chitosan leads to a considerable shift in the absorption band to higher frequencies (from 1732 to 1738 cm^{-1}). This position of the absorption band indicates the considerable decrease in the group hydration (Cieslik-Boczula and Koll, 2009). This evidences destruction of some of hydrogen bonds in which the carbonyl group is involved due to interaction with cationic groups of the polymer, as has been observed in the case of the liposome phosphate groups. The data prove that both carbonyl and phosphate groups act as chitosan binding sites (Deygen and Kudryashova, 2014). In respect of the characteristic band of chitosan at 1635 cm^{-1} carbonyl bonds (C=O) of the amide group CONHR (secondary amide) was not present. It was probably merged avec carbonyl groups of phospholipid resulting more important intensity of the peak at 1738 cm^{-1}.

Next, we have studied the interaction between the liposome and the encapsulated curcumin by FTIR, we found the encapsulated curcumin caused considerable change in the absorption bands of acyl chains (3000 – 2800 cm^{-1}) toward lower wavenumbers as the case of chitosan, but a lower degree kindly, for example the absorption bands located at 2854 cm^{-1} and at 2958 cm^{-1} were shifted towards lower frequency at 2852 cm^{-1} and 2956 cm^{-1}, respectively. We observed a new peak at 3011 $cm^{-1,}$ which correspond to C-H (aryl) stretching of the molecule of curcumin, found shifted also toward low frequency compared to initial vibration at 3014 cm^{-1}. The band at 1651 cm^{-1} corresponds to the stretching vibrations of alkene carbon–carbon double bond -C=C- shifted towards 1647 cm^{-1} (Figure 47 (ii)). Then, the low frequency shifts of the absorption bands in the hydrophobic region of phospholipid with encapsulated curcumin indicate the hydrophobic interaction between them and this corresponds to decrease the acyl chain mobility and an increase in the order of the bilayer

(Severcan *et al.,* 2005). In respect of the carbonyl and phosphate group of phospholipid at 1732 and 1224 cm^{-1}, respectively, we found considerable changes in the absorption of two groups, which shifted from 1732 to 1738 cm^{-1} for carbonyl group, and from 1224 to 1230 cm^{-1} for phosphate group. Additionally, the peak at 3508 cm^{-1} indicate the phenolic O-H stretching of curcumin shifted to 3295 cm^{-1}, this was possibility due of the break of hydrogen bonds and formation a intermolecular hydrogen bonds between the phenolic OH group of curcumin and the functional groups of phospholipid (phosphate and carboxyl groups) (Maiti *et al.,* 2007 ; Zhang *et al.,* 2013). The curcumin molecule was demonstrated to be anchored inside the phospholipid bilayer through the hydrogen bonding of −OH groups of phenolic rings of curcumin with the headgroup of phospholipid and the hydrophobic interactions of the aromatic rings of curcumin with phospholipid acyl chains (Barry *et al.,* 2009).

We studied the interaction between curcumin and chitosan. It was observed that the stretching vibration of CH_3 and CH_2 groups of chitosan at 2926 cm^{-1} and 2883 cm^{-1}, respectively, were shifted in presence of curcumin towards 2922 cm^{-1} and 2879 cm^{-1}, indicating the hydrophobic interaction between chitosan and hydrophobic region of curcumin. The peaks at 2922 cm^{-1} were also sharpened which could be attributed to the presence of more number of CH groups. We observed that the peak at 1541 cm^{-1} relating to the protonated amine group $NH3^+$ of the chitosan was shifted in the presence of curcumin to 1539 cm^{-1}, and the peak at 1635 cm^{-1} relating of carbonyl bonds (C=O) of the amide group CONHR was shifted in also to 1633 cm^{-1} (Figure 47 (vi)). These results suggest the formation of intermolecular hydrogen bonds between chitosan and curcumin. Then the results indicate the hydrophobic, and hydrogen bond formation between curcumin and chitosan (Erdawati and Fithriyah, 2013 ; Parize *et al.,* 2009).

In fact, these interactions between molecule of curcumin and the vector whether liposome alone or chitosan coated liposome, can help in reducing the release rate of curcumin thereby helping controlled release.

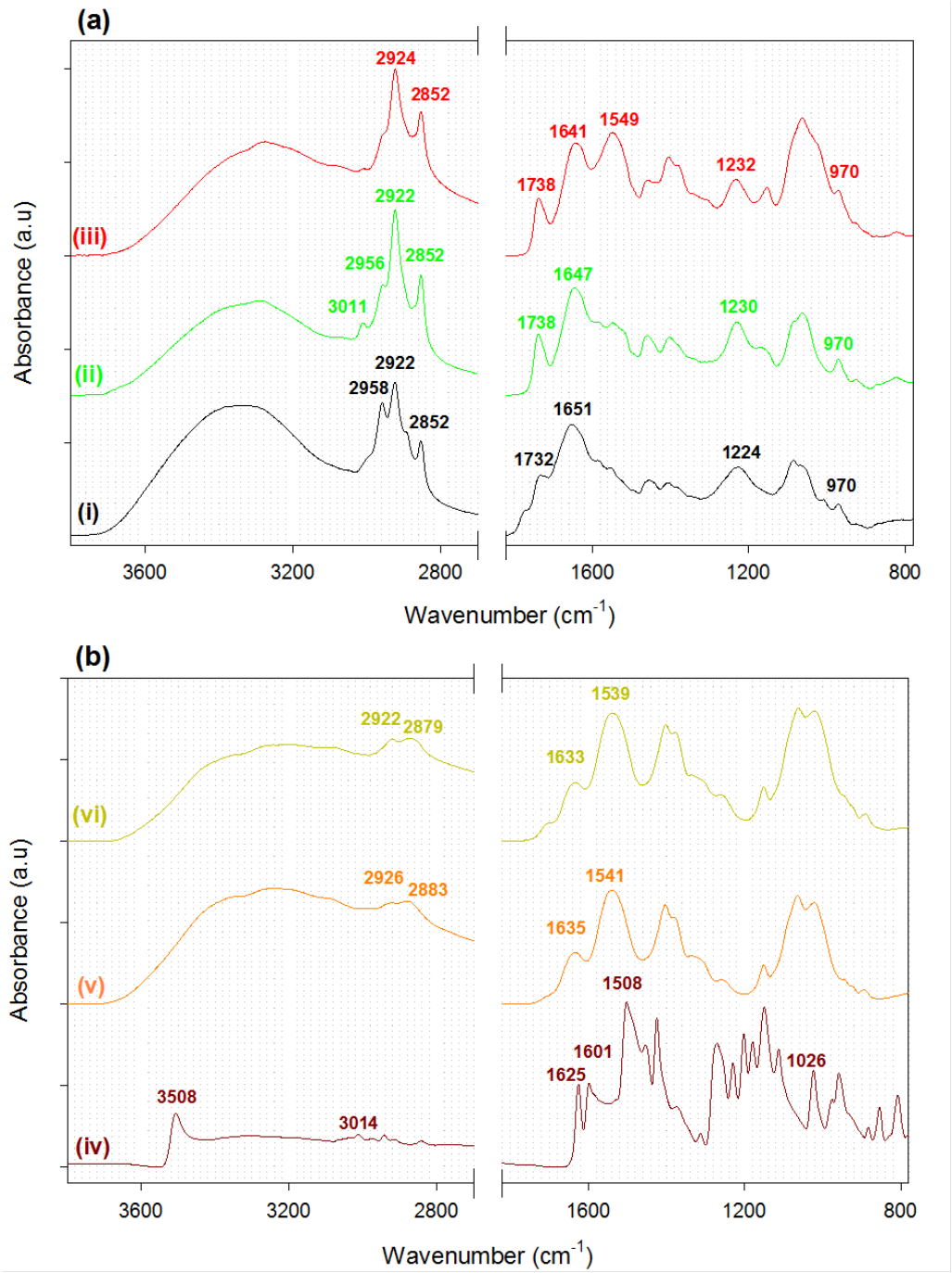

Figure 47. FTIR spectra of (i) salmon liposome, (ii) curcumin encapsulated liposome, (iii) chitosan coated liposome, (iv) curcumin, (v) chitosan, and (vi) the mixture of chitosan and curcumin.

VIII.3.8 Rheological study

VIII.3.8.1 *Steady state shear viscosity*

Figure 48(a) shows the flow curves of the different liposomal samples. The chitosan coating had an impact on the fluid rheological behavior. However no remarkable difference existed between unloaded and loaded curcumin lipid vesicles.

The flow curves of the liposomal sample are plotted in (Figure 48(a)), the solid lines represented the fits to the power law model:

$$\sigma = k\dot{\gamma}^{n} \qquad (4)$$

Where σ is the shear stress, k is the consistency index, γ is the shear rate, and n is the flow behavior index.

The consistency k is numerically equal to the viscosity at $1s^{-1}$ and could be useful as a general measure of viscosity for comparative purposes.

In order to determine the plastic viscosity and the yield stress of the different liposomal samples, the flow curve of the square root of shear stress were plotted against the square roots of shear rate (Figure 48(b)) (Sakai *et al.*, 2007).

In fact, the Casson model (Equation 5) is a structure-based model:

$$(\sigma)^{0.5} = K_{0c} + K_c\ (\dot{\gamma})^{0.5} \qquad (5)$$

Where the Casson yield stress is calculated as the square of the intercept, $\sigma_{0c} = (K_{0c})^2$ and the Casson plastic viscosity as the square of the slope, $\eta_{casson} = (K_c)^2$.

Equation 2 and 3 were used to fit the experimental data of different samples, and the rheological parameters are shown in Table 13.

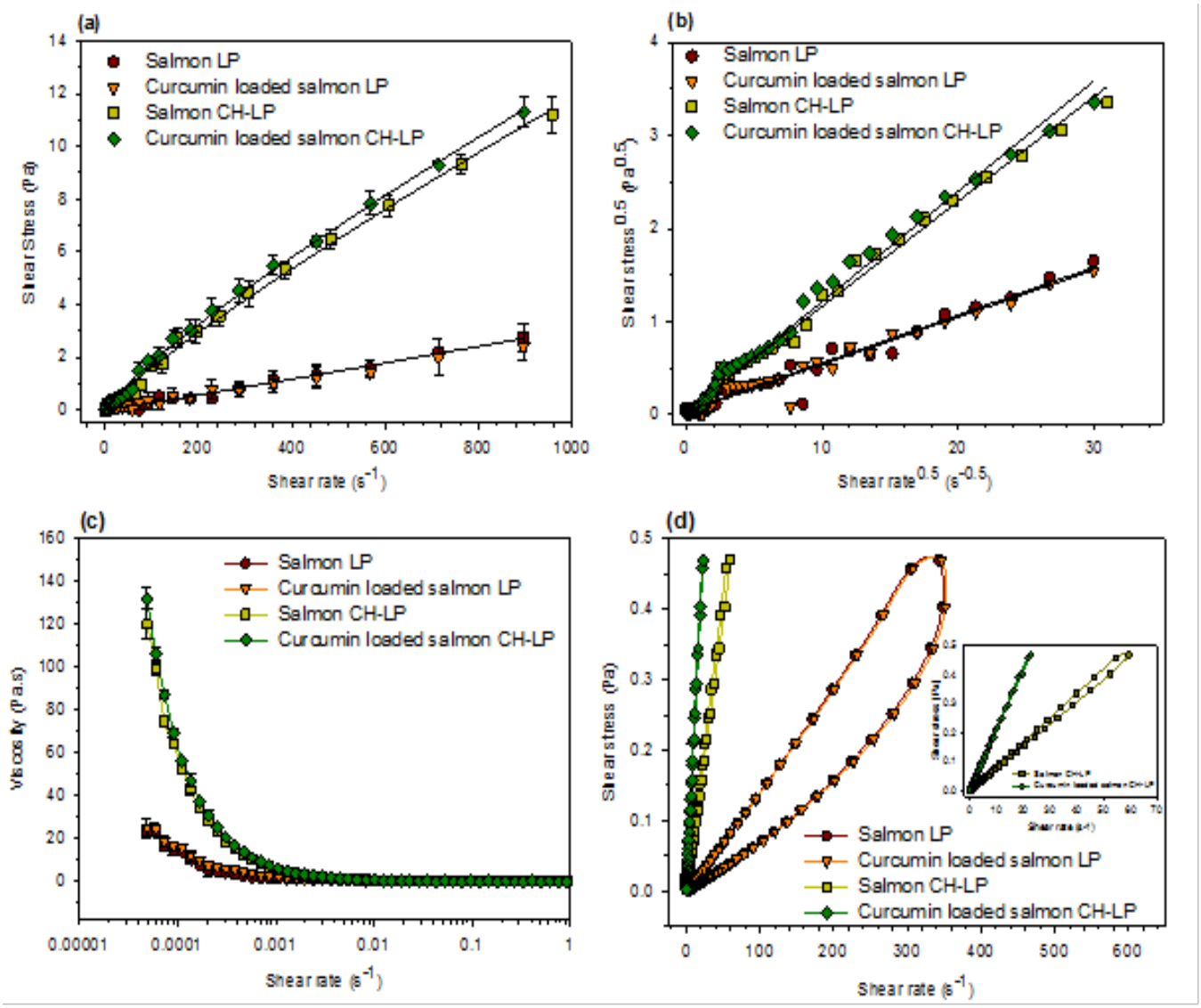

Figure 48. (a) Flow curves of the liposomal samples. The solids lines are the fit to power law model; (b) Casson plots of the square root of shear stress versus the square root of shear rate; (c) Shear viscosity evolution at low shear rates; (d) the shear stress was increased from 10^{-3} to 0.5 Pa and decreased in the same shear stress range.

Table 13. Rheological properties of the different liposomal samples.

	Power law model			Casson model		
Sample	**K**	**n**	**R^2**	**Plastic viscosity (mPa.s)**	**Yield stress (mPa)**	**R^2**
Salmon LP	0.002 ±0.0004	1.057 ±0.0683	0.9879	2.64 ± 0.53	1.79 ± 0.10	0.9668
Curcumin loaded salmon LP	0.004 ±0.0006	0.9441 ±0.0524	0.9903	2.59 ± 0.35	1.70 ± 0.12	0.9650
Salmon CH-LP	0.038 ± 0.002	0.8389 ±0.0082	0.9983	14.09 ± 2.26	3.11 ± 0.24	0.9927
Curcumin loaded salmon CH-LP	0.047 ± 0.004	0.8505 ±0.0128	0.9987	17.85 ± 2.47	3.33 ± 0.14	0.9968

The n and k values ranged from 0.83 to 1.05 and from 2×10^{-3} to 47×10^{-3}, respectively. Uncoated liposome suspension exhibited a nearly newtonian flow behavior ($n\approx1$). The chitosan coating results caused the decreasing of the flow behavior index ($n<1$) which result the shear thinning behavior (Mady *et al.,* 2009). In fact, shear-thinning behavior is generally desirable for pharmaceutical product formulation, providing the dispersion with a low viscosity when sheared, whereas at rest, the system has a certain solid-like consistency (Berni *et al.,* 2002).

The yield stress (the minimum stress needed to cause a Bingham plastic to flow) and the plastic viscosity increased respectively, from 1.70 mPa and 2.64 mPa.s for uncoated liposomes to 3.33 Pa and 17.85 mPa.s after lipid vesicles coating with chitosan. Therefore, the addition of chitosan layer allowed a better stability of the lipid vesicles dispersion at rest. It's intresting to note that the shear viscosity evolution as function of shear rates didn't show a Newtonian plateau at small shear (Figure 48(c)) which represents an infinite resistance to flow below the critical shear stress (yield stress).

The zero shear viscosity of the salmon LP increased from 23 to 123 Pa.s after lipid vesicles coating. The difference between the coated and uncoated lipid vesicles could be

related to surface charge and size. From figure 48 a, b and c, we can conclude that the inclusion of curcumin into the phospholipid bilayer, did not affect the rheological flow behavior of lipid vesicles.

In order to study the time-dependent flow behavior of the liposomal samples, the shear stress was increased from 10-3 to 0.5 Pa during 5 minutes and then decreased in the same stress range. The plots show a thixotropic behavior for all the liposomal dispersion. Nevertheless, the chitosan addition decreased significantly the hysteresis loop area which increases significantly the liposomal dispersion stability. In fact, chitosan liposomes are less thixotropic and their structure rebuild faster than uncoated liposomes after shearing which could be very useful for several applications including cosmetics where the liposomal dispersion had to recover immediately to their original structure after extrusion or applying to the skin. This observation is in a good agreement with a previous study focused on lecithin/chitosan dispersion which demonstrated that chitosan induced change on the time-dependent flow of the lecithin dispersion from rheopexic to thixotropic by allowing the transition of lecithin dispersion from planar sheets to closed structures such as vesicles (Madrigal-Carballo et al., 2008). The hysteresis loop area corresponding to the thixotropic behavior is related to the separation of vesicles from the vesicle aggregates. The chitosan layer enhanced therefore the stability of the lipid vesicles dispersion and decreased the liposomes deformation under shearing.

VIII.3.8.2 *Oscillatory rheometry*

In order to study the mechanical stability of the liposomal samples, oscillatory rheology was performed at a fixed strain within the linear viscoelastic region. The mechanical spectra of the liposomes dispersions are reported in (Figure 49).

For these experiments, two geometries were used, a plate-and-plate (20 mm) with a gap of 500 µm (Figure 7(a)) and a cone-and-plate (2°, 60mm) with a gap of 70 µm.

The complex modulus G* (G*(*w*) = G’ (*w*) + iG” (*w*)) of coated liposomes is more than one order of amplitude higher than uncoated lipid vesicles. Moreover, coated liposomes showed a low frequency dependence of G* which demonstrate a better mechanical stability due to the additional chitosan layer (Figure 49(a)). However, the encapsulated curcumin

didn't affects the general mechanical spectra of coated and uncoated lipid vesicles. In general, the viscoelastic properties of lipid vesicles is related mainly to temperature and to the volume fraction. In fact, for high volumes fractions near the maximum packing fraction, the average repulsive force is affected (deHaas *et al.,* 1997).

Several factors could be in the origin of the better stability of coated liposomes which could be related to the nanoparticles size and to the inner mechanical properties of the chitosan layer which could also act as a protective coating by reducing the phospholipid layer deformation. The interactive forces could also participate in improving the mechanical stability of the coated liposomal dispersions.

In general, the mechanical stability of a liposomal dispersion is monitored by lipid vesicles interactions types such as van der Waals attraction (w), electrostatic repulsion (e), and a "long-range" entropic repulsion (u). The total forces are assumed to be additive (Versluis *et al.,* 2001):

$$\phi = \phi_w + \phi_e + \phi_u \qquad (6)$$

In our case, the rheological experiments were performed at 25°C < T of the phase transition of liposomal dispersion (Bouarab *et al.,* 2014). When the lipid bilayers are in the gel state, the entropic repulsion (u) and van der Waals repulsion (w) are in the same order of magnitude (deHaas *et al.,* 1997). Therefore, the increase of mechanical stability could be as a result of the increase of electrostatic repulsion because the addition of the chitosan layer resulted in an increase of the absolute value of the zeta potential (from 45 to 60 mV after lipid vesicles coating) (Table 12).

The Figure 49(b) showed the frequency dependence of the elastic (G') and viscous modulus (G") using the cone-and-plate geometry at a gap of 70 µm. These experiments should be carefully monitored since the low gap and the dilute state of the liposomal samples could lead to very large phase angle (δ) and therefore the rheological test will be dominated by inertial effects.

The results showed that in the studied frequency range (0.1- 10 Hz), uncoated lipid vesicles showed several crossover points between G' and G" and therefore several relaxation process related to diffusive behavior and to the deformation of the vesicles (deHaas *et al.*, 1997). The coating of liposomes with chitosan resulted in a crossover point at a higher frequency (1 Hz) than uncoated vesicles which reflected a better resistance to shear and twist.

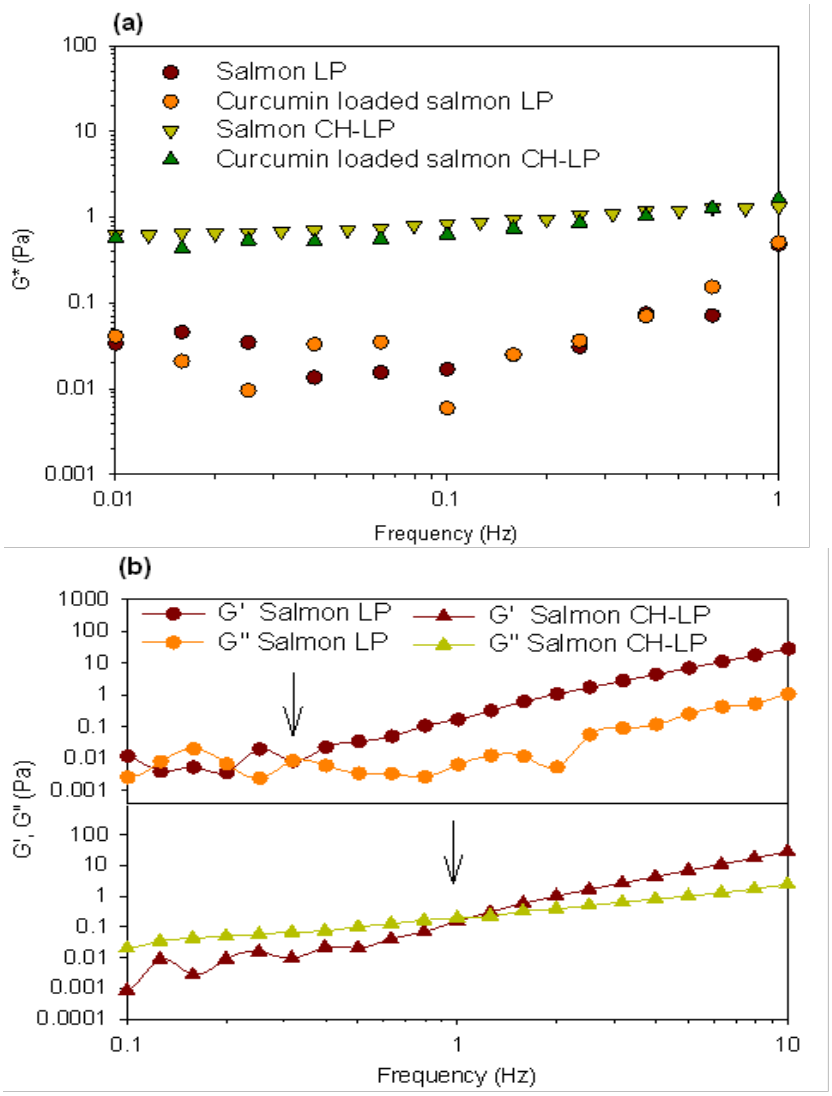

Figure 49. Frequency sweep test of liposomal samples (a) Complex modulus G* (Pa) evolution with frequency at a shear strain of 2% and (b) elastic (G') and viscous modulus (G") at a shear strain of 10%.

VIII.4 Conclusion

Our present studies give the information about the physico-chemical properties of nanoliposomes, chitosan-coated nanoliposomes before and after encapsulation of curcumin.

The particle size of the curcumin-containing liposomes increased on being coated with chitosan with forming coating layers around liposome. The zeta potential of the liposomes also demonstrated a similar trend, changing from a negative value for the uncoated, to increasingly positive values for the chitosan-coated liposomes. The coating of liposomes by a chitosan layer was confirmed by electron microscope images and the zeta potential of liposomes

FTIR results indicate electrostatic interactions between positive ammonium groups in the chitosan chain and negatively charged liposomes, and hydrophobic interactions as well as hydrogen bonding between chitosan and phospholipid were take place. While hydrophobic forces and hydrogen bonding dominated the interactions between curcumin and phospholipid as well as between curcumin and chitosan.

The flow curves of the different liposomal samples showed that the chitosan coating had an impact on the fluid rheological behavior. However no remarkable difference existed between unloaded and loaded curcumin lipid vesicles. Concerning the flow behavior, uncoated liposomes suspension exhibited a nearly newtonian behavior ($n \approx 1$), however, the chitosan coating resulted in a shear thinning behavior. In the other hand, the addition of chitosan decreased the thixotropic behavior of liposomal dispersions suggesting a significant increase in the stability of the liposomal dispersion. The mechanical properties of the liposomal samples investigated by small amplitude oscillatory shear rheology showed greater resistance to shear and twist and therefore better stability after liposomes coating with chitosan.

Small angles X-ray scattering experiments revealed that the liposomes membrane structure was not affected by the chitosan coating. Only a variation of the scattered intensity has been reported corresponding to the modification of the electronic contrast of the system induced by the presence of the polymer around the liposomes. Furthermore, with or without chitosan, curcumin did not affect the bilayer arrangement.

IX. Chitosan-coated liposomes encapsulating curcumin: physicochemical characterizations and study the release kinetics of encapsulated curcumin in simulated environment

M. Hasan[1], A. Tamayol[2], C. Kahn[3], M. Linder[1], E. Arab-Tehrany[1]*

[1]Université de Lorraine, Laboratoire d'ingénierie des biomolecules, TSA 40602 54518 – Vandœuvre Cedex.

[2]Center for Biomedical Engineering, Department of Medicine, Brigham and Women's Hospital, Harvard Medical School, Boston, MA 02139, USA. Harvard-MIT Division of Health Sciences and Technology, Massachusetts Institute of Technology, Cambridge, MA 02139, USA. Wyss Institute for Biologically Inspired Engineering, Harvard University, Boston, MA, 02115, USA.

[3]IFSTTAR, LBA, F-13916 Marseille, France.

IX.1 Résumé

L'objectif de cette étude a consisté à formuler des nanoliposomes à partir de lécithine marine purifiée dans le but de vectoriser de la curcumine dans des conditions gastro-intestinales simulées. L'efficacité d'encapsulation, la fluidité membranaire, la taille, la mobilité électrophorétique, la morphologie des vecteur avec et sans coating de chitosane ont été étudiées.

Les résultats d'une digestion gastrique simulée pendant 4h montrent que la curcumine encapsulée a été retenue à plus de 80%. Le coating de chitosane améliore légèrement la protection avec un pourcentage de rétention de 90%. Ces résultats montrent que le complexe liposomal reste stable dans un environnement gastrique simulé, contrairement à la libération plus prononcée de la curcumine lors de la réaction intestinale simulée, en raison de la rupture de la membrane liposomale, sous l'action des sels biliaires et des enzymes spécifiques.

Keywords: Chitosan-coated liposomes, curcumin, encapsulation, release, digestion.

IX.2 Introduction

The goal of drug delivery system is to administer a drug at a therapeutic concentration to a particular site of action for a specified period of time. The design of the final product for drug delivery depends on different parameters. 1) The drug must be administered by considering some factors which affect therapeutic action of the drug. These parameters include the site of action, the concentration of the drug at the time of administration, the period of time that drug must remain at a therapeutic concentration, and the initial release rate of the drug for controlled release systems. 2) The drug must remain physically and chemically stable in the formulation for a defined time. 3) The choice of delivery method must indicate the effective administration route for the drug (Barich *et al.,* 2005).

Currently, many efforts in the field of drug delivery have been made to develop the targeted delivery systems in which the drug is only active in the target site and to formulate the sustained release systems in which the drug is released over a period of time in a controlled manner (Maherani *et al.,* 2011).

Curcumin, a natural Chinese remedy, used for centuries in the traditional medicine, was recently shown to possess a broad spectrum of desirable activities(Aggarwal *et al.,* 2007). Curcumin, the bioactive component obtained by the extraction and purification of ground rhizomes of Curcuma longa has been found to exert wide range of beneficial biological and pharmacological activities including antioxidant, anti-inflammatory, antimicrobial, and anticancer features, as well as wound healing characteristics (Bhawana *et al.,* 2011 ; Biswas and Mukherjee, 2003 ; Kunnumakkara *et al.,* 2008 ; Lantz *et al.,* 2005 ; Reddy and Lokesh, 1992). But studies addressing the metabolism and uptake of curcumin had shown that either no curcumin or little amount was detected in serum or tissue after administration (Dhillon *et al.,* 2008). The main reasons attributing to the low bioavailability are supposed to be the poor solubility of curcumin in aqueous media, rapid hydrolysis followed by molecular fragmentation at physiological pH and inactivity of its metabolic products (Lin *et al.,* 2000).

Various delivery systems have been proposed as a means to improve therapeutic effects of curcumin. Among them, liposomes able to incorporate poorly soluble molecules and enable

their aqueous medium-based administration seem to be among the most promising delivery systems (Basnet and Skalko-Basnet, 2011).

Liposomes are widely used as delivery vehicles for stabilizing drugs and overcoming barriers to cellular and tissue uptake (Gregoriadis, 1988). Nanoliposomes have become very versatile tools in biology, biochemistry and medicine because of their enormous diversity of structure and com-position. The main constituents of liposomes are phospholipids, which are amphiphilic molecules containing water soluble, hydrophilic head section and a lipid-soluble, hydrophobic tail section. This property of phospholipids gives liposomes unique properties, such as self-sealing, in aqueous media and make them an ideal carrier system with applications in different fields including food, cosmetics, pharmaceutics, and tissue engineering (Bangham, 1961). Liposomes can carry both hydrophilic and hydrophobic components by encapsulation in the water phase and intercalating into the hydrophobic domains, respectively. Even hydrophobic components can be formed in a stable state in an aqueous environment by high dispersion in a liposome system. In addition, the components entrapped in liposomes can effectively penetrate and overcome biological barriers to cellular and tissue uptake because the liposome has a similar structure as the cell membrane (Brandl, 2001 ; Shin *et al.,* 2013).

Lecithin, which has two long hydrocarbon chains, is a major component of lipid bilayers of cell membranes and a natural, biological amphiphile. Furthermore, it is in many respects regarded as an ideal biological surfactant because it is biodegradable. It may be used for various purposes (Lin *et al.,* 2009). Numerous studies, both in humans and in animals (Calder and Yaqoob, 2009 ; Van der Meerena *et al.,* 2009), have demonstrated that polyunsaturated fatty acids (PUFA) of the n-3 series, in particular eicosapentaenoic acid (EPA, 20:5 n-3) and docosahexaenoic acid (DHA, 22:6 n-3), are critical to several physiological processes, particularly for decreasing high blood pressure and inflammation, lowering the risks of atherosclerosis and ischaemic heart disease (Dunbar et al., 2014 ; Gerber, 2012). Oil and marine lecithin from salmon head (*Salmo salar*) contains a high percentage of PUFAs, especially EPA and DHA (Belhaj *et al.,* 2010 ; Gbogouri *et al.,* 2006).

However, liposomes are liable to be destructed by pH, bile salts, and pancreatic lipase in the gastrointestinal tract (Kato *et al.,* 1993). Previous studies have been analyzing the

effects involved in the formation of a polymeric membrane around the liposome in order to minimize these disruptive effects (Iwanaga *et al.,* 1999). Since the discovery of polysaccharides on cell surfaces and the high affinity of chitosan to cell membranes, several researchers have been utilized chitosan as coating material for liposomes (Janes *et al.,* 2001).

Interestingly, the coating of lipid-based nanostructures with chitosan has been found to increase their stability (Henriksen *et al.,* 1997), and to provide them with mucoadehsive properties (Takeuchi *et al.,* 2003). Chitosan is a hydrophilic, biocompatible and biodegradable polymer of low toxicity. Because of its bioadhesive and permeation enhancing properties, chitosan has received substantial attention in novel bioadhesive drug delivery systems, aimed at improving the bioavailability of drugs by prolonging their residence time at the site of absorption (Kotze *et al.,* 1999). Chitosan is predominantly composed of β-(1,4)-linked D-glucosamine units and is obtained by deacetylation of chitin, which is the primary component of the cell walls of crustaceans, fungi, and insects (Muzzarelli *et al.,* 2012). By combining chitosan and liposomal characteristics, specific, prolonged, and controlled release may be achieved (Takeuchi *et al.,* 1996). Takeuchi and others showed that the chitosan-coated liposomes were formed via ionic interaction between the positively charged chitosan and negatively charged diacetyl phosphate on the surface of the liposomes.

The present study focused primarily on the preparation of nanoliposomes from salmon purified phospholipid and coating them with chitosan, and then we characterize the physico-chemical properties of the formulations such as size, electrophoretic mobility, and membrane fluidity. The release kinetics of encapsulated curcumin in simulated gastric and intestinal digestion environment were studied.

IX.3 Results and discussion

IX.3.1 Fatty acid analyses

The main fatty acid compositions are shown in Table 14. The first observations allow us to highlight the total polyunsaturated fatty acids in salmon phospholipid were predominate (45.11%). The percentage of the fraction of polyunsaturated fatty acids is followed directly by the percentage of saturated fatty acids (33.40%) salmon phospholipid.

The most significant proportions of fatty acids were C22:6 n-3 and C20:5 n-3, found in the polyunsaturated fatty acids class with 25.55 and 10.13 %, respectively. C18:1 n-9 in the monounsaturated fatty acids class (14.13%), and C16:0 in the saturated fatty acids class (22.22%).The ratio of n-3/n-6 was 8.73 and DHA/EPA was 2.52.

Table 14. Fatty acid compositions of salmon lecithin and salmon phospholipid.

Fatty acids	Salmon phospholipid	
	%	SD
C14	2.62	0.02
C15	1.16	0.04
C16	22.22	0.15
C17	0.83	0.00
C18	6.72	0.05
C20	0.36	0.15
C22	1.15	0.21
SFA	35.06	
C14:1n9	0.33	0.03
C16:1n7	2.87	0.14
C18:1n9		
C20:1n9	14.13	0.06
C22:1n9		
	1.91	0.01
	0.59	0.09
MUFA	19.83	
C18:2n6	1.05	0.07
C18:3n3	0.34	0.09
C20:4n6	3.59	0.03
C20:5n3(EPA)	10.13	0.08
C22:5n3	4.46	0.22
C22:6n3(DHA)	25.55	0.17
PUFA	45.11	
n-3/n-6	8.73	
DHA/EPA	2.52	

IX.3.1.1 Lipid classes

The lipid classes of salmon phospholipid were separated by thin-layer chromatography (Iatroscan). At that stage, phosphatidylcholine represented the major class of phospholipids

contained in salmon lecithin (40.49%), followed by phosphatidylinositol (15.25%) and phosphatidylserine (7.95%). It is interesting to note that phospholipids can enhance drug flux; they are called a sorption promoter (Wajda *et al.,* 2007). The percentage of polar lipid in salmon phospholipid was 100%, whereas it contains neither triglycerides nor other nonpolar lipid.

IX.3.2 Entrapment efficiency

In order to study the effect of loading on the activity of curcumin, HPLC analysis was carried out after the encapsulation step. However, the entrapment efficiency of the curcumin in salmon liposome was 78.2± 0.5%, which was great compared to the one shown in our previous paper (Hasan *et al.,* 2014) with 67.3 ± 1.1%. In this study, we prepared the liposome by using the formation lipid thin film, where we solubilized the phospholipid with the curcumin in the solvent, therefore the solvents were evaporated. This increase the distribution of curcumin in phospholipid and the possibility interaction between them, increased the loading efficiency. On the other hand, the encapsulation efficiency of curcumin significantly increases when liposome coated with chitosan compared to the uncoated liposome, which was 95.2±1.2%.

IX.3.3 Membrane fluidity

Bilayer fluidity reflects the order and dynamics of phospholipid alkyl chains in the bilayer. The release of the entrapped bioactive agents from nanoliposomes depends on the number of bilayers and permeability and fluidity of the bilayer (Calvagno *et al.,* 2007). The influence of lipid composition on vesicle membrane fluidity was explored by Coderch *et al.* (2000), and Calvagno *et al.* (2007)(Calvagno *et al.,* 2007 ; Coderch *et al.,* 2000). They observed a significant difference in the drug release profiles by the presence of two factors: (i) the strength of the drug–liposomal lipid interaction and (ii) the fluidity of the bilayer. In fact, the drug release to the aqueous medium increased by increasing the membrane fluidity of the vesicle. The FAs composition of the membrane bilayer tunes the membrane fluidity level. Indeed, the presence of saturated FAs increased the lipid ordering in the membrane, which excluded the water in the proximity of the bilayer surface and reduced membrane fluidity. Whereas, unsaturated FAs could reduce the packing between phospholipids and preserved a

more level of membrane hydration, thus keeping membrane fluidity (Leekumjorn *et al.,* 2009).

It appears that nanoliposomes made of salmon phospholipid have slightly high membrane fluidity 3.24±0.05 because it contains a higher proportion of polyunsaturated fatty acids, therefore membrane fluidity is more important when the degree of unsaturation of acyl chains increased. In comparing the membrane fluidity of liposome prepared with purified salmon phopholipid and unpurified lecithin which was 3.19±0.08 (Hasan *et al.,* 2014), it is clear that the fluidity increased slightly in case of pure phospholipid, probably due of absence of cholesterol after purification procedure, which is responsible for the higher stiffness of the bilayer (Karewicz *et al.,* 2011).

To recognize the action of curcumin and chitosan on membrane fluidity it is necessary to understand the behavior of curcumin and chitosan with respect to solution composition variation. Indeed, we had already studied its effects in our previous studies (Hasan *et al.,* 2014). The presence of curcumin decreased the membrane fluidity of all nanoliposomes. Such influence of curcumin is a result of its structure and its molecular interaction with liposome. Curcumin is a highly conjugated and therefore rigid planar molecule. The presence of a curcumin molecule can weaken hydrophobic interactions among acyl chains of phospholipids (Patra *et al.,* 2012). The incorporation of curcumin perturbs the packing characteristics of the phospholipid bilayer and thus enhances the packing density of the hydrocarbon moiety in the lipid bilayer.

According to Table 3, we observed that chitosan reduced membrane fluidity of nanoliposomes. It makes a new layer around the liposome, which is probably incorporate within the membrane bilayer, causing the rigidity of bilayers, and decreasing the movement of fatty acids chains of phospholipid. Consequently, the membrane bilayer fluidity decreases. The motional freedom of phosphate group was reduced with the presence of chitosan (Shi *et al.,* 1999).

The rotational motions of the probes that result in depolarization of fluorescence are tightly coupled to acyl chain orientational fluctuations and, consequently, reflect the degree of molecular packing (order) in the membrane (Lentz, 1993).

IX.3.4 *In vitro* Drug release

- **Release in PBS solution**

The *in vitro* release behavior of curcumin encapsulated in uncoated and chitosan coated liposome was studied over the course of time during 4 hours incubated in PBS at 37 °C is presented as percentage cumulative release in (Figure 50). A biphasic release was observed specially in the case of uncoated liposome charged with 0.2 mg/mL curcumin a rapid release of about 18% in the end of 1 hour followed by sustained drug release of about 22.3 % over 4 hours. Burst release characteristics suggested the drug entrapped near the surface might be the reason for initial burst release, while the sustained release characteristics suggested the diffusion of drug from the core of the liposomes.

The possible mechanism for this observation may be that during the formation of the thin lipid film some drug is entrapped within the bilayer of the liposome and some drug molecules adsorb to the surface; this may have resulted in the leading to the phenomenon of burst release (short diffusion distance for the drug adhered on the surface region of the liposome). The slow and sustained release in the latter part of the experiment may be due to time required for the drug to diffuse into the release medium from the core of the liposomes.

Whereas in the case of coated liposomes, the release is supported by the presence of chitosan coating, we observed that the release of curcumin from the colloid particles was more slowly and exhibited more pronounced sustained release. Chitosan is hydrophilic in nature and makes the surface of liposomes less hydrophobic, as in chitosan-coated liposomes. The coating layer will cause the diffusion obstacle for the drug released from the surface, resulting in the slower release (Joraholmen *et al.,* 2014). Furthermore, the coating of liposome with chitosan causing decrease of the membrane fluidity which plays an important role in the release of the entrapped drug from the liposome (Maherani *et al.,* 2013).

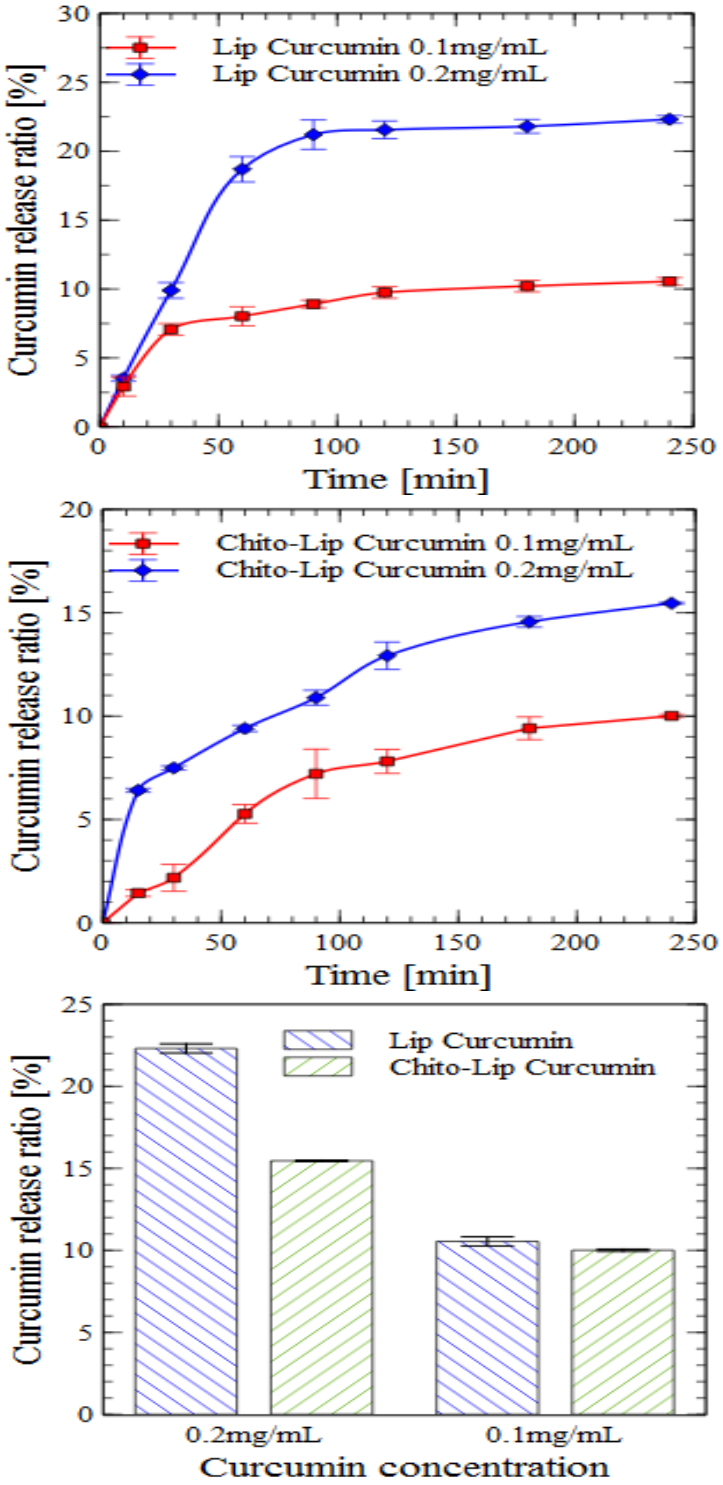

Figure 50. *In vitro* release (PBS solution) of different concentrations of encapsulated curcumin from liposome and chitosan-coated liposome (values reported are mean±SD; n = 3), and the proportions of released curcumin from liposome and chitosan-coated liposomes after 4h of incubation.

In respect to the concentration of loaded curcumin in uncoated and chitosan coated liposome, we observe that the release profile of curcumin was almost similar for two concentrations 0.1 and 0.2 mg/mL for chitosan-coated liposome on the contrary of uncoated liposome which discriminated with the burst release in initially especially for 0.2 mg/mL of curcumin concentration. Therefore, these results imply that the release profile of core material from nanocarrier systems is significantly affected by the polymer coating, then chitosan coating take over the release of drug which becomes sustained and more slowly with disappearance the burst release.

- **Digestion gastric**

The *in vitro* release profiles of curcumin from uncoated liposomesand chitosan-coated liposomes in simulated gastric digestion environment are presented in Figure 51. The digestion of encapsulated bioactives in the gastrointestinal tract is a complex process and its impact on the release of bioactive component plays a major role in the uptake, distribution as well as bioavailability of the component. The results indicated that the encapsulated curcumin was stable and not released from the delivery system by the action of pepsin. During simulated gastric digestion (4h), over 80% of the encapsulated curcumin was retained in uncoated liposome and about 90% for chitosan-coated liposome. Then the percentage of the drug released in SGF decreased for chitosan-coated liposome as compared to uncoated liposomes, which is a desirable attribute for an encapsulation system in order to protect the bioactive molecule from the harsh gastric environment (Anal and Singh, 2007; Vandenberg *et al.,* 2001). The stability of chitosan-coated liposomes in simulated gastric fluid was significantly higher as compared to uncoated liposomes (Filipovic-Grcic *et al.,* 2001).

Release profiles of curcumin during gastric incubation were almost similar to their profiles in PBS solution with slight decrease especially for uncoated liposome, where was the maximum curcumin released after 4h of incubation 23.3% in PBS versus 17.3% in simulated gastric environment.

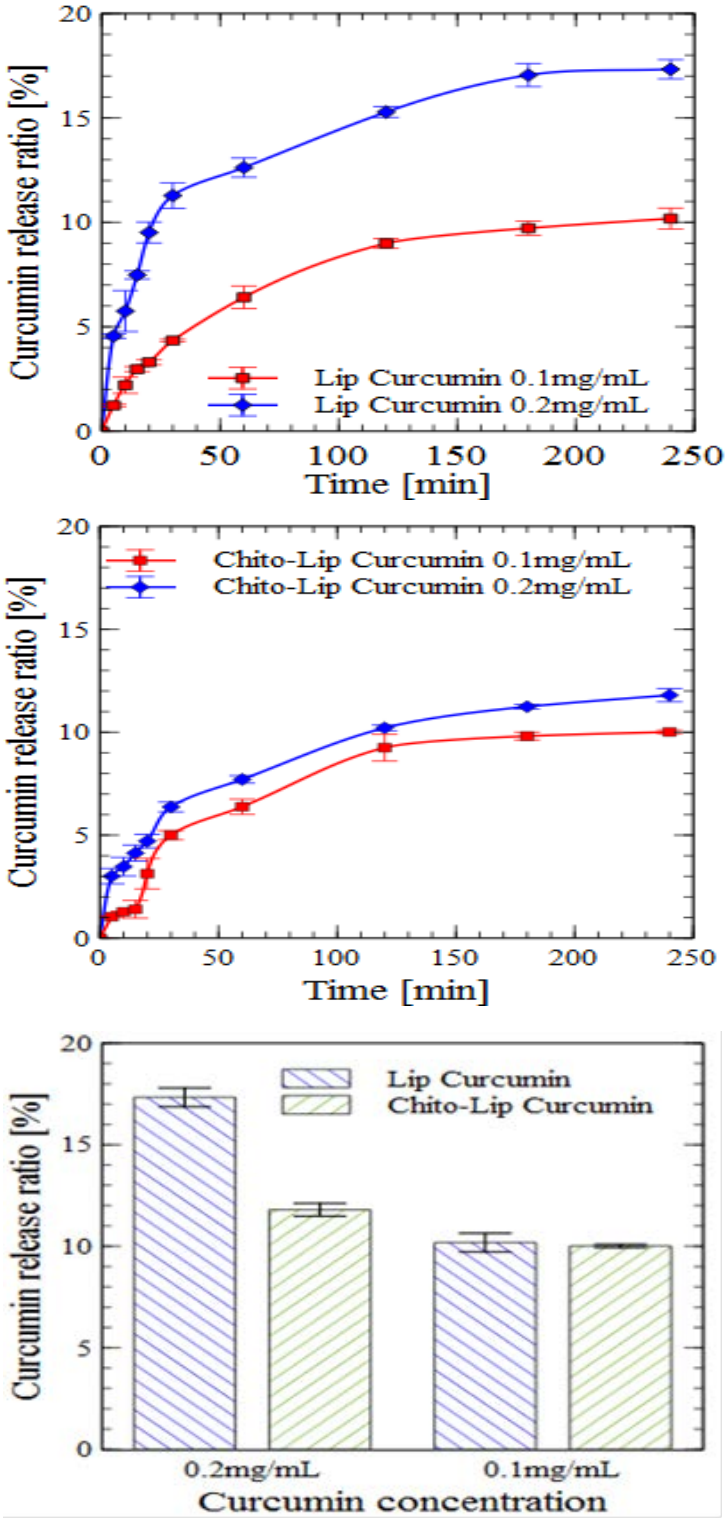

Figure 51. *In vitro* release (gastric digestion) of different concentrations of encapsulated curcumin from liposome and chitosan-coated liposome (values reported are mean±SD; n = 3), and the proportions of released curcumin from liposome and chitosan-coated liposomes after 4h of incubation.

- **Intestinal digestion**

The curcumin release rate from the liposomes was enhanced in SIF relatively to SGF. These findings are also in agreement with previous studies (Lee *et al.,* 2009 ; Liu *et al.,* 2013 ; Liu *et al.,* 2012). Liu *et al*. (Liu *et al.,* 2012) argued that liposomes released more entrapped ingredients in SIF than in SGF because of the disruption of the liposomal membrane by the pancreatic enzyme under SIF conditions.

Simulated intestinal fluid (SIF) is a mixture of pancreatin and bile salts. Bile salts may change the interface which facilitates activity of lipase present in pancreatin and helps in the release of curcumin (Sarkar *et al.,* 2010). A biphasic release was observed specially in the case of uncoated liposome charged with 0.2 mg/mL curcumin, a rapid release of about 24.5% in the end of 30 minute followed by sustained drug release of about 29.5 % over 4 hours (Figure 52).

The drug release characteristics exhibited controlled delivery of curcuminoids for longer duration, which may improve bioavailability of the curcuminoids in its active, native form. Moreover fabricated liposomes can be administered parenterally by passing the gastrointestinal route where most of the drug gets degraded and is the main cause for curcuminoids low bioavailability.

Unfortunately conventional liposomes, structured as concentric bilayers of phospholipids, are sensitive to damage caused by the harsh chemical and enzymatic GI environment, resulting in reduced oral material bioavailability (Thanki *et al.,* 2013).

In recent years, various attempts have been made to modify the liposomal surface not only to improve their stability, but also to functionalize them (Gao *et al.,* 2013 ; Xing *et al.,* 2013). Coating with chitosan can increase the stability of liposomes in various biological fluids including simulated gastric fluid (SGF) and intestinal fluid (SIF), as well as their mucoadhesive properties, cellular uptake, and the solubility of drugs (Sugihara *et al.,* 2012).

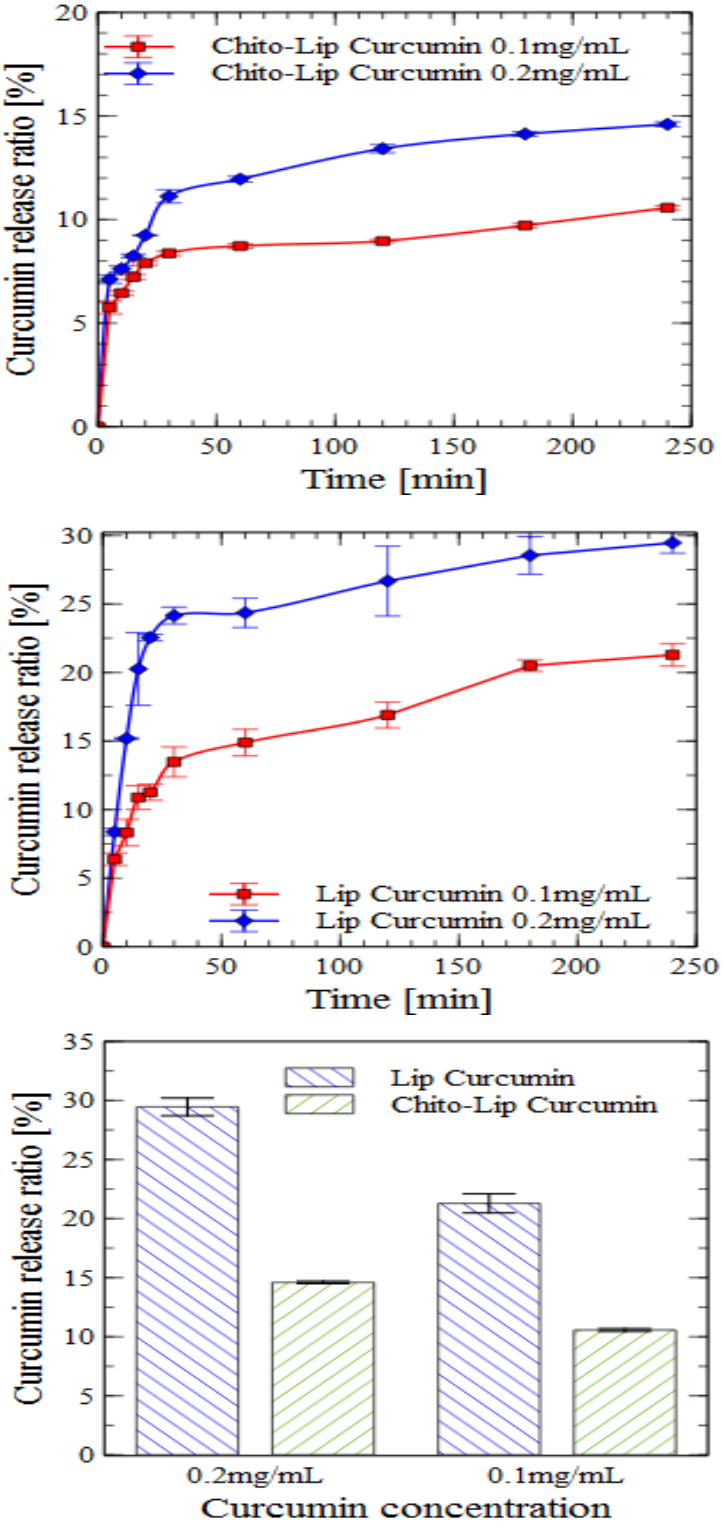

Figure 52. *In vitro* release (intestinal digestion) of different concentrations of encapsulated curcumin from liposome and chitosan-coated liposome (values reported are mean±SD; n = 3), and the proportions of released curcumin from liposome after 4h of incubation.

Major problems of such release measurements are the complicated separation of colloidal carrier and release medium as well as the warranty of sink conditions throughout the experiment. Unfortunately we have not been able to determine curcumin release from chitosan-coated liposome in simulated intestinal fluid, in view of chitosan precipitate at pH 6.8 because the chitosan pKa value is around 6.5 (Filipovic-Grcic *et al.,* 2001). For this reason we added 0.5% Tween-80 in SIF in order to solubilize released curcumin during the digestion.

The curcumin release rate from all the liposomes was higher in simulated intestinal fluid than in simulated gastric fluid. But it was much lower when coated liposomes with 14.6% compared to 29.5% for non-coated liposomes over 4 hours, which can be due to the fact that the polysaccharides have a capacity to inhibit lipid digestion, therefore they use as dietary fibers (Espinal-Ruiz *et al.,* 2014 ; Rodriguez and Albertengo, 2005).

Despite of the pancreatin enzyme from Porcine Pancreas has chitinase and chitotriosidase activities according to the literature (McConnell *et al.,* 2008 ; Shen *et al.,* 2013 ; Zhang *et al.,* 2002). It is better to complete the simulated digestion in the presence of other enzyme such as beta-glucosidase and rat or human colonic enzymes, based on the hypothesis that the chitosan is will be degraded predominantly by lysozyme and by bacterial enzymes in the colon (Kean and Thanou, 2010 ; Zhang *et al.,* 2002).

IX.4 Conclusion

Curcumin being highly unstable and hydrophobic is difficult to incorporate in aqueous systems. For this reason the curcumin was encapsulated inside liposome and chitosan coated liposome. Coating with chitosan decreased the membrane fluidity of nanoliposomes causing the rigidity of bilayers, and decreasing the movement of fatty acids chains of phospholipid as well as presence of curcumin decreased membrane fluidity. Morever the encapsulation efficiency of curcumin significantly increases when liposome is coated with chitosan compared to the uncoated liposome.

The results in the present study showed that curcumin releases slowly from all liposomes under simulated digestion. Moreover, the curcumin release rate from all the liposomes was higher in simulated intestinal fluid than in simulated gastric fluid.

Chitosan-coated liposomes were shown to exhibit more stability and prolonged release of curcumin in comparison of uncoated liposome.

These results demonstrate that the chitosan-coated samples are more efficient than uncoated samples in the oral delivery of curcumin.

Conclusion générale et perspectives

X. Conclusion générale et perspectives

L'objectif général de ce travail de thèse consistait à étudier la vectorisation d'une molécule active telle que la curcumine dans des émulsions, des liposomes et des liposomes enrobés de chitosane. La caractérisation des propriétés physicochimiques (solubilité, taille, mobilité électrophorétique, efficacité d'encapsulation, fluidité membranaire, etc…) nous ont permis d'optimiser la formulation qui a ensuite été testée *in vitro,* en culture cellulaire. Les interactions entre lipides et biomatériaux d'une part ainsi que celles entre vecteurs et principes actifs d'autre part, ont été aussi étudiées. Finalement, la cinétique de libération de la curcumine encapsulée dans un milieu de digestion simulé a été également abordée.

La première phase des travaux a été consacrée à la solubilisation de la curcumine dans des huiles végétale (huile de colza) et de poisson (huile de saumon). Le degré de solubilité maximal de la curcumine dans chacune de ces huiles a été déterminé dans le but d'encapsuler des doses de curcumine contrôlées et d'évaluer ainsi les effets de ces formulations sur la prolifération cellulaire d'une lignée tumorale mammaire de type MCF7. La vectorisation de la curcumine sous forme d'émulsion a pu être mise en œuvre grâce à l'utilisation d'un procédé d'homogénéisation à haute pression couplé à la sonication. Les résultats obtenus démontrent l'efficacité de l'association de ces deux techniques d'émulsification permettant à la fois une réduction de la taille des gouttelettes et une amélioration de la stabilité de ces dernières.

Par ailleurs, les caractéristiques physico-chimiques des émulsions ont été étudiées en utilisant différentes techniques analytiques, à savoir, la diffusion dynamique de la lumière moyennant le zetasizer, la chromatographie en phase gazeuse, le Iatroscan (chromatographie sur couche mince couplée une détection par ionisation de flamme). Il en résulte que la composition en acides gras ainsi que les différentes classes lipidiques des lécithines utilisées influencent la taille des émulsions et la solubilité de la curcumine.

L'activité anticancéreuse de la curcumine vis-à-vis des cellules MCF7 a été aussi abordée. Il apparaît que la concentration en biomolécule d'intérêt dans les émulsions joue un rôle sur la viabilité cellulaire. Pour rappel, les analyses expérimentales *in vitro* ont été effectuées en partenariat avec le laboratoire CRAN.

Dans une deuxième partie de ce travail, la préparation et la caractérisation physico-chimique des différentes formulations de nanoliposomes et nanoliposomes enrobés de chitosane ont été étudiées. Ces liposomes ont été élaborés à partir de lécithines végétales (soja, colza) et marine extraite de tête de saumon.

Des tests de cytotoxicité des liposomes renfermant la curcumine sur des cellules cancéreuses de type MCF7 ont été également effectués en ayant recours au système xCELLigence (toujours en partenariat avec le laboratoire du CRAN). L'approche était basée sur la surveillance en temps réel de l'impédance de la cellule ainsi que la caractérisation dynamique de la réponse cellulaire mesurée sur les cellules MCF7 cancéreuses. Ces études élucidant les propriétés physico-chimiques des liposomes avant et après encapsulation de la curcumine, révèlent leur potentiel d'utilisation en tant que système de support dans différentes applications qui dépendraient largement de leurs propriétés physicochimiques, leur composition en acides gras ainsi que la méthode de préparation utilisée. En effet, ces paramètres influencent fortement le comportement des vésicules dans les systèmes biologiques. Les résultats obtenus démontrent que les lécithines de soja et de colza sont constituées d'un même type d'acides gras en proportions différentes, alors que celles du saumon renferment un large éventail d'acides gras insaturés parmi lesquels on retrouve ceux connus pour leurs bienfaits santé telles que les acides gras polyinsaturés à longue chaîne (EPA et DHA). Par ailleurs, les liposomes sans curcumine présentent aussi un impact important sur la cytotoxicité des cellules tumorales soulignant l'effet similaire reporté pour les lécithines de soja et de colza avec un indice de cellule identique pour une concentration de lécithine compris entre 0,28 et 1,1 mg / mL ; la concentration optimale étant de 1,1 mg/mL. La lécithine de saumon quant à elle, a provoqué une diminution plus efficace de l'indice cellulaire. De plus, l'encapsulation liposomale de la curcumine a significativement amélioré la cytotoxicité des cellules cancéreuses en comparaison avec la curcumine solubilisée dans de l'éthanol. Par ailleurs, les résultats obtenus confirment que l'enrobage des liposomes par le chitosane provoque des changements au niveau de la taille des particules et des valeurs de potentiel zêta. L'augmentation significative en termes d'efficacité d'encapsulation de la curcumine et de cytotoxicité sur les cellules MCF7 a été également mise en évidence.

D'une façon générale, la composition en acides gras des vecteurs serait l'explication principale justifiant les différences observées. A titre d'illustration, les vecteurs à base de

lécithine et d'huile de saumon seraient les plus toxiques pour les cellules cancéreuses suite à leur richesse en EPA et DHA, contrairement à la lécithine et à l'huile de colza. Aussi, la nature des nanovecteurs (sous la forme de liposomes ou d'émulsions) influence la toxicité des cellules. La teneur en AGPI s'avère elle aussi importante. En effet, la longueur de la chaîne carbonée ainsi que le nombre d'insaturations seraient proportionnellement liés à la cytotoxicité.

Par ailleurs, l'étude de l'effet neuroprotecteur des liposomes renfermant la curcumine à base de lécithine de saumon a démontré l'efficacité du système pour la viabilité et la formation de réseau sur les cellules embryonnaires des neurones corticaux. La diminution du taux d'apoptose dans les cultures traitées, observée au cours de cette étude se révèle efficace pour d'autres modèles animaux présentant des troubles neurodégénératifs.

Dans une troisième partie de ces travaux, la purification de la lécithine de saumon, permettant d'obtenir des phospholipides purs par élimination des triglycérides et lipides neutres, a été menée grâce à une méthode de précipitation par acétone froid. La préparation de nanoliposomes à base de phospholipides purs et leur enrobage par le chitosane a été conduit afin d'étudier les interactions lipides-polysaccharides, tester le comportement rhéologique des formulations et enfin examiner l'effet de la digestion gastrique et intestinale simulées sur la cinétique de libération de la curcumine encapsulée.

Les résultats obtenus par infrarouge à transformée de Fourier décrivent l'implication d'interactions électrostatiques et hydrophobes ainsi que des liaisons hydrogènes entre les phospholipides et le chitosane. Les interactions hydrophobes et les liaisons hydrogènes s'avèrent dominantes entre la curcumine et les phospholipides d'une part et entre la curcumine et le chitosane d'autre part. Le revêtement des liposomes par la couche de chitosane a pu être confirmé par des images au microscope électronique ainsi que par la mesure de charges de surface. Ce revêtement engendre une nette diminution de la fluidité membranaire des liposomes provoquant la rigidité des bicouches (dû à une moindre mobilité des chaînes d'acides gras des phospholipides). De même, la présence de la curcumine a également diminuée la valeur de la fluidité membranaire des liposomes. Ce revêtement génère également une modification du comportement rhéologique des liposomes. Il s'avère indispensable de signaler que la curcumine n'a aucun effet sur le comportement rhéologique

des vésicules en absence et en présence d'enrobage de chitosane. Nous pourrons ainsi conclure que l'inclusion de la curcumine dans la double couche de phospholipides, n'affecte en aucun cas le comportement rhéologique des vésicules lipidiques.

Par ailleurs, les liposomes non enrobés présentaient un comportement d'écoulement presque newtonien (n≈1) ; ceux recouverts par le chitosane montraient un comportement *rhéofluidifiant,* généralement bien apprécié en pharmaceutique pour la formulation de produits offrant ainsi une dispersion à faible viscosité au cours du cisaillement et donc de son utilisation. Ce système présente néanmoins une certaine consistance et se comporte plutôt comme un solide au repos ce qui peut améliorer la stabilité de la formulation pendant le stockage.

Afin d'étudier les propriétés d'écoulement des liposomes en fonction du temps, ces derniers ont été soumis à une contrainte de cisaillement de 10^{-3} à 0,5 pascal durant 5 minutes. Les courbes obtenues témoignent d'un comportement thixotropique pour les dispersions liposomales. Néanmoins, l'ajout de chitosane s'associe à une diminution significative de la boucle d'hystérésis, suggérant ainsi une augmentation considérable de la stabilité de la dispersion liposomale et une meilleure restructuration après cisaillement. Les propriétés viscoélastiques des liposomes étudiés par la rhéologie de cisaillement oscillatoire aux faibles amplitudes ont montré une plus grande résistance au cisaillement et à la torsion, donc une meilleure stabilité après l'addition de chitosane.

Enfin, nous avons abordé *in vitro* la cinétique de libération de la curcumine encapsulée dans des liposomes non enrobés et ceux enrobés de chitosane dans des solutions de PBS et des milieux de digestion simulée.

Une libération biphasique a été observée particulièrement pour les liposomes non enrobés et chargés de 0,2 mg / mL curcumine. En effet, deux libérations, une rapide d'environ 18% à une heure suivie d'une autre plus lente de l'ordre de 22,3% à 4 heures ont été mises en évidence expliquant respectivement une décharge rapide de la curcumine piégée en surface des liposomes puis une diffusion plus lente de la molécule active à partir du cœur des liposomes.

Quant aux liposomes enrobés de chitosane, la libération de la curcumine à partir des particules colloïdales s'est déroulée plus lentement en manifestant une libération prolongée plus prononcée. La couche de revêtement constitue une barrière contre la diffusion de la curcumine en surface entrainant ainsi une libération lente. En outre, le revêtement des liposomes de chitosane induit également une nette diminution de la fluidité membranaire jouant un rôle important dans le phénomène de diffusion de la biomolécule piégée dans les liposomes.

Les expérimentations de digestion gastrique simulée indiquent une stabilité et une absence de libération de la curcumine encapsulée sous l'action de la pepsine. Après une digestion gastrique simulée de 4h, plus de 80% de curcumine encapsulée ont été conservés dans les liposomes non enrobés et environ 90% par les liposomes enrobés. Ce résultat constitue une caractéristique recherchée pour un système d'encapsulation dont le but est de protéger la molécule bioactive dans un environnement gastrique. Par ailleurs, la vitesse de libération de la curcumine des liposomes était plus importante dans le fluide intestinal en comparaison au fluide gastrique. Ce constat s'expliquerait par la rupture potentielle de la membrane liposomale sous l'action des enzymes pancréatiques de l'ordre 14,6% et 29.5% pour les liposomes enrobés et non enrobés respectivement.

Perspectives de ce travail

Des travaux complémentaires permettraient de mieux appréhender la stabilité du complexe liposomal vectorisant la curcumine :

1- L'étude de la stabilité oxydative des liposomes en absence et en présence de curcumine et de chitosane, en ayant recours aux méthodes classiques de suivi de l'oxydation, nous permettrait de déterminer le rôle protecteur du chitosane ainsi que l'effet antioxydant de la curcumine tout en déterminant la limite de concentration pour éviter l'effet pro-oxydatif.

2- Nous avons étudié au cours de ce travail les activités anticancéreuses de la curcumine vectorisée par les différents vecteurs vis-à-vis des cellules MCF7. Il serait intéressant de comparer l'effet de la curcumine sur des cellules saines.

3- Nous avons étudié l'influence d'un système liposomal de lécithine de saumon vectorisant de la curcumine, sur des cellules embryonnaires des neurones corticaux utilisés comme modèle. Il serait intéressant d'étudier l'effet de la curcumine vectorisée ainsi que celui du vecteur riche en AGPI-LC (notamment le DHA et EPA) sur des modèles de maladies neurodégénératives.

4- Dans le cadre de maladies inflammatoires chroniques de l'intestin MICI, il serait intéressant d'étudier les effets de la curcumine, connue pour son effet anti-inflammatoire, ainsi que les effets du chitosane en raison de sa bonne solubilité en milieu acide (proche du pH de l'intestin en cas de maladies MICI).

5- En raison de la faible solubilité du chitosane au pH physiologique, nous pourrons envisager l'utilisation d'oligomères du chitosane ou même de la glucosamine soluble à pH physiologique pour des applications dans les domaines médical et pharmaceutique.

6- Afin de mieux comprendre l'influence des chaînes d'acide gras et de la tête polaire des phospholipides en mélange dans la lécithine, il serait intéressant de purifier la lécithine marine permettant l'utilisation de lipides polaires purs.

7- La biodisponibilité de la curcumine vectorisée *in vivo* sur modèle murin est une étape indispensable afin de déterminer les effets des différents complexes liposome / curcumine / chitosane. Celle-ci sera mise en place afin de déterminer les constantes cinétiques et permettra l'étude du transfert de cette biomolécule.

8- Compte tenu des activités chitotriosidases de l'enzyme pancréatique retrouvées dans la littérature, il s'avère important d'aborder la digestion simulée pour les liposomes enrobés de chitosane en présence d'autres enzymes telles que la bêta-glucosidase, ou des enzymes produites par les bactéries du côlon.

Références bibliographiques

XI. Références

Ackman, R.G., 1998. Remarks on official methods employing boron trifluoride in the preparation of methyl esters of the fatty acids of fish oils. Journal of the American Oil Chemists Society; 75:541–545.

Acosta, E., 2009. Bioavailability of nanoparticles in nutrient and nutraceutical delivery. Current Opinion in Colloid & Interface Science; 14:3-15.

Aditya, N.P., Chimote, G., Gunalan, K., Banerjee, R., Patankar, S., Madhusudhan, B., 2012. Curcuminoids-loaded liposomes in combination with arteether protects against Plasmodium berghei infection in mice. Experimental Parasitology; 13:292-299.

Aditya, N.P., Shim, M., Lee, I., Lee, Y., Im, M.H., Ko, S., 2013. Curcumin and Genistein Coloaded Nanostructured Lipid Carriers: in Vitro Digestion and Antiprostate Cancer Activity. Journal of Agricultural and Food Chemistry; 61:1878-1883.

Aggarwal, B.B., Gehlot, P., 2009. Inflammation and cancer: how friendly is the relationship for cancer patients? Curr Opin Pharmacol; 9(4):351-69.

Aggarwal, B.B., Kumar, A., Bharti, A.C., 2003. Anticancer potential of curcumin: Preclinical and clinical studies. Anticancer Research; 23:363-398.

Aggarwal, B.B., Sundaram, C., Malani, N., Ichikawa, H., 2007. Curcumin: The Indian solid gold. Molecular Targets and Therapeutic Uses of Curcumin in Health and Disease; 595:1-75.

Aggarwal, B.B., Sung, B., 2009. Pharmacological basis for the role of curcumin in chronic diseases: an age-old spice with modern targets. Trends Pharmacol Sci; 30(2):85-94.

Ahmed, K., Li, Y., McClements, D.J., Xiao, H., 2012. Nanoemulsion- and emulsion-based delivery systems for curcumin: Encapsulation and release properties. Food Chemistry; 132:799-807.

Ahmed, T., Gilani, A.H., 2014. Therapeutic potential of turmeric in Alzheimer's disease: curcumin or curcuminoids? Wiley Online Library; pp. 517-525.

Ahsan, H., Parveen, N., Khan, N.U., Hadi, S.M., 1999. Pro-oxidant, anti-oxidant and cleavage activities on DNA of curcumin and its derivatives demethoxycurcumin and bisdemethoxycurcumin. Chemico-Biological Interactions; 121:161-175.

Ak, T., Gulcin, I., 2008. Antioxidant and radical scavenging properties of curcumin. Chem Biol Interact; (1):27-37.

Akbik, D., Ghadiri, M., Chrzanowski, W., Rohanizadeh, R., 2014. Curcumin as a wound healing agent. Life Sci; 116(1):1-7.

Akhtar, F., Rizvi, M.M.A., Kar, S.K., 2012. Oral delivery of curcumin bound to chitosan nanoparticles cured Plasmodium yoelii infected mice. Biotechnology Advances; 30:310-320.

Al Sagheer, F.A., Al-Sughayer, M.A., Muslim, S., Elsabee, M.Z., 2009. Extraction and characterization of chitin and chitosan from marine sources in Arabian Gulf. Elsevier; pp. 410-419.

Anal, A.K., Singh, H., 2007. Recent advances in microencapsulation of probiotics for industrial applications and targeted delivery. Trends in Food Science & Technology; 18:240-251.

Anand, P., Kunnumakkara, A.B., Newman, R.A., Aggarwal, B.B., 2007. Bioavailability of curcumin: Problems and promises. Molecular Pharmaceutics; 4:807-818.

Anand, P., Nair, H.B., Sung, B., Kunnumakkara, A.B., Yadav, V.R., Tekmal, R.R., Aggarwal, B.B., 2010. Design of curcumin-loaded PLGA nanoparticles formulation with enhanced cellular uptake, and increased bioactivity in vitro and superior bioavailability in vivo. Biochem Pharmacol; 79(3):330-8.

Anitha, A., Maya, S., Deepa, N., Chennazhi, K.P., Nair, S.V., Tamura, H., Jayakumar, R., 2011. Efficient water soluble O-carboxymethyl chitosan nanocarrier for the delivery of curcumin to cancer cells. Elsevier; pp. 452-461.

Aoki, T., Decker, E.A., McClements, D.J., 2005. Influence of environmental stresses on stability of O/W emulsions containing droplets stabilized by multilayered membranes produced by a layer-by-layer electrostatic deposition technique. Food Hydrocolloids; 19:209-220.

Aqil, F., Munagala, R., Jeyabalan, J., Vadhanam, M.V., 2013. Bioavailability of phytochemicals and its enhancement by drug delivery systems. Cancer Lett; 334(1):133-41.

Arab Tehrany, E., Kahn, C.J.F., Baravian, C., Maherani, B., Belhaj, N., Wang, X., Linder, M., 2012. Elaboration and characterization of nanoliposome made of soya; rapeseed and salmon lecithins: Application to cell culture. Colloids and Surfaces B: Biointerfaces; 95:75-81.

Arnoult, D., Petit, F., Lelievre, J., Akarid, K., Ameisen, J., Estaquier, J., 2001. Le récepteur de la phosphatidyl-sérine, un intermédiaire entre apoptose et réponse immunitaire. Sévres, FRANCE: EDK.

Asai, A., Miyazawa, T., 2000. Occurrence of orally administered curcuminoid as glucuronide and glucuronide/sulfate conjugates in rat plasma. Life Sci; 67(23):2785-93.

Asouri, M., Ataee, R., Ahmadi, A.A., Amini, A., Moshaei, M.R., 2013. Antioxidant and Free Radical Scavenging Activities of Curcumin. Asian Journal of Chemistry; 25:7593-7595.

Atienza, J.M., Zhu, J., Wang, X.B., Xu, X., Abassi, Y., 2005. Dynamic monitoring of cell adhesion and spreading on microelectronic sensor arrays. Journal of Biomolecular Screening; 10:795-805.

Atsumi, T., Fujisawa, S., Tonosaki, K., 2005. Relationship between intracellular ROS production and membrane mobility in curcumin- and tetrahydrocurcumin-treated human

gingival fibroblasts and human submandibular gland carcinoma cells. Oral Diseases; 11:236-242.

Azmin, M.N., Florence, A.T., Handjani-Vila, R.M., Stuart, J.F., Vanlerberghe, G., Whittaker, J.S., 1985.The effect of non-ionic surfactant vesicle (niosome) entrapment on the absorption and distribution of methotrexate in mice. J Pharm Pharmacol; 37(4):237-42.

Balakrishnan, P., Lee, B.J., Oh, D.H., Kim, J.O., Lee, Y.I., Kim, D.D., Jee, J.P., Lee, Y.B., Woo, J.S., Yong, C.S., Choi, H.G., 2009. Enhanced oral bioavailability of Coenzyme Q10 by self-emulsifying drug delivery systems. Int J Pharm; 374(1-2):66-72.

Balasubramanian, K., 1991. Theoretical Calculations on the Transition Energies of the Uv-Visible Spectra of Curcumin Pigment in Turmeric. Indian Journal of Chemistry Section a-Inorganic Bio-Inorganic Physical Theoretical & Analytical Chemistry; 30:61-65.

Banerjee, A., Kunwar, A., Mishra, B., Priyadarsini, K.I., 2008. Concentration dependent antioxidant/pro-oxidant activity of curcumin: Studies from AAPH induced hemolysis of RBCs. Chemico-Biological Interactions; 174:134-139.

Bangham, A.D., 1961. A Correlation between Surface Charge and Coagulant Action of Phospholipids. Nature; 192:1197-1198.

Bangham, A.D., Standish, M.M., Watkins, J.C., 1965. Diffusion of univalent ions across the lamellae of swollen phospholipids. Journal of Molecular Biology; 13:238-IN227.

Barenholz, Y., 2003. Relevancy of drug loading to liposomal formulation therapeutic efficacy. Journal of Liposome Research; 13:1-8.

Barich, D.H., Munson, E.J., Zell, M.T., 2005. Physicochemical properties, formulation, and drug delivery. John Wiley & Sons, Inc; pp. 57-71.

Barratt, G.M., 2000. Therapeutic applications of colloidal drug carriers. Pharmaceutical Science & Technology Today; 3:163-171.

Barry, J., Fritz, M., Brender, J.R., Smith, P.E.S., Lee, D.K., Ramamoorthy, A., 2009. Determining the Effects of Lipophilic Drugs on Membrane Structure by Solid-State NMR Spectroscopy: The Case of the Antioxidant Curcumin. Journal of the American Chemical Society; 131:4490-4498.

Basnet, P., Hussain, H., Tho, I., Skalko-Basnet, N., 2012. Liposomal delivery system enhances anti-inflammatory properties of curcumin. Wiley Online Library; pp. 598-609.

Basnet, P., Skalko-Basnet, N., 2011. Curcumin: An Anti-Inflammatory Molecule from a Curry Spice on the Path to Cancer Treatment. Molecules; 16:4567-4598.

Belhaj, N., Arab-Tehrany, E., Linder, M., 2010. Oxidative kinetics of salmon oil in bulk and in nanoemulsion stabilized by marine lecithin. Process Biochemistry; 45: 187-195

Belhaj, N., Dupuis, F., Arab-Tehrany, E., Denis, F.M., Paris, C., Lartaud, I., Linder, M., 2012. Formulation, characterization and pharmacokinetic studies of coenzyme Q(10) PUFA's nanoemulsions. European Journal of Pharmaceutical Sciences; 47:305-312.

Benachour, H., Bastogne, T., Toussaint, M., Chemli, Y., Sève, A., Frochot, C., Lux, F., Tillement, O., Vanderesse, R., Barberi-Heyob, M., 2012. Real-time monitoring of photocytotoxicity in nanoparticles-based photodynamic therapy: a model-based approach. PloS one; 7(11):e48617.

Benais-Pont, G., Dupertuis, Y.M., Kossovsky, M.P., Nouet, P., Allal, A.S., Buchegger, F., Pichard, C., 2006. ω-3 Polyunsaturated fatty acids and ionizing radiation: Combined cytotoxicity on human colorectal adenocarcinoma cells. Nutrition; 22:931-939.

Benedet, J.A., Umeda, H., Shibamoto, T., 2007. Antioxidant Activity of Flavonoids Isolated from Young Green Barley Leaves toward Biological Lipid Samples. Journal of Agricultural and Food Chemistry; 55:5499-5504.

Berni, M.G., Lawrence, C.J., Machin, D., 2002. A review of the rheology of the lamellar phase in surfactant systems. Advances in Colloid and Interface Science; 98:217-243.

Bhawana, Basniwal, R.K., Buttar, H.S., Jain, V.K., Jain, N., 2011. Curcumin Nanoparticles: Preparation, Characterization, and Antimicrobial Study. Journal of Agricultural and Food Chemistry; 59:2056-2061.

Biruss, B., Dietl, R., Valenta, C., 2007. The influence of selected steroid hormones on the physicochemical behaviour of DPPC liposomes. Chemistry and Physics of Lipids; 148:84-90.

Bisht, S., Feldmann, G., Soni, S., Ravi, R., Karikar, C., Maitra, A., Maitra, A., 2007. Polymeric nanoparticle-encapsulated curcumin ("nanocurcumin"): a novel strategy for human cancer therapy. Journal of Nanobiotechnology; 5(3):1-18.

Biswas, T.K., Mukherjee, B., 2003. Plant medicines of Indian origin for wound healing activity: a review. Int J Low Extrem Wounds; 2(1):25-39.

Bombelli, C., Caracciolo, G., Di Profio, P., Diociaiuti, M., Luciani, P., Mancini, G., Mazzuca, C., Marra, M., Molinari, A., Monti, D., Toccacieli, L., Venanzi, M., 2005. Inclusion of a photosensitizer in liposomes formed by DMPC/Gemini surfactant: Correlation between physicochemical and biological features of the complexes. Journal of Medicinal Chemistry; 48:4882-4891.

Borneo, R., Kocer, D., Ghai, G., Tepper, B.J., Karwe, M.V., 2007. Stability and consumer acceptance of long-chain omega-3 fatty acids (eicosapentaenoic acid, 20:5,n-3 and docosahexaenoic acid, 22 : 6, n-3) in cream-filled sandwich cookies. Journal of Food Science; 72:S049-54.

Borra, S.K., Gurumurthy, P., Mahendra, J., 2013. Antioxidant and free radical scavenging activity of curcumin determined by using different in vitro and ex vivo models. Academic Journals; pp. 2680-2690.

Bou Saab, H., 2007. Etude de la structure et de la stabilité de vecteurs d'acides gras polyinsaturés à longues chaînes. Rapport Master BANT.

Bouarab, L., Maherani, B., Kheirolomoom, A., Hasan, M., Aliakbarian, B., Linder, M., Arab-Tehrany, E., 2014. Influence of lecithin-lipid composition on physico-chemical properties of nanoliposomes loaded with a hydrophobic molecule. Colloids and Surfaces B-Biointerfaces; 115:197-204.

Bouyer, E., Mekhloufi, G., Rosilio, V., Grossiord, J.L., Agnely, F., 2012. Proteins, polysaccharides, and their complexes used as stabilizers for emulsions: Alternatives to synthetic surfactants in the pharmaceutical field? International Journal of Pharmaceutics; 436:359-378.

Brandl, M., 2001. Liposomes as drug carriers: a technological approach. Biotechnol Annu Rev; 7:59-85.

Brochette, P., 1999. Emulsification : Elaboration et étude des émulsions. Techniques de l'ingénieur : Agroalimentaire. Nancy; J2150-18p.

Burdge, G.C., Calder, P.C., 2005. Conversion of alpha-linolenic acid to longer-chain polyunsaturated fatty acids in human adults. Reproduction Nutrition Development; 45:581-597.

Bush, J.A., Cheung, K.J.J., Li, G., 2001. Curcumin induces apoptosis in human melanoma cells through a Fas receptor/caspase-8 pathway independent of p53. Experimental Cell Research; 271:305-314.

Calder, P.C., Yaqoob, P., 2009. Understanding omega-3 polyunsaturated fatty acids. Postgraduate medicine; 121:148-157.

Calvagno, M.G., Celia, C., Paolino, D., Cosco, D., Iannone, M., Castelli, F., Doldo, P., Fresta, M., 2007. Effects of lipid composition and preparation conditions on physical-chemical properties, technological parameters and in vitro biological activity of gemcitabine-loaded liposomes. Curr. Drug Delivery; 4:89–101.

Camuesco, D., Comalada, M., Concha, A., Nieto, A., Sierra, S., Xaus, J., Zarzuelo, A., Galvez, J., 2006. Intestinal anti-inflammatory activity of combined quercitrin and dietary olive oil supplemented with fish oil, rich in EPA and DHA (n-3) polyunsaturated fatty acids, in rats with DSS-induced colitis. Clinical nutrition; 25(3):466-476.

Carey, M.C., Small, D.M., Bliss, C.M., 1983. Lipid Digestion and Absorption. Annual Review of Physiology; 45:651-677.

Chajès, V., Torres- Mejía, G., Biessy, C., Ortega-Olvera, C., Angeles-Llerenas, A., Ferrari, P., Lazcano-Ponce, E., Romieu, I., 2012. Omega-3 and omega-6 polyunsaturated fatty acid intakes and the risk of breast cancer in Mexican women: impact of obesity status. Cancer Epidemiol Biomarkers Prev; 21(2):319-26.

Chan, M.M.Y., Huang, H.I., Fenton, M.R., Fong, D., 1998. In vivo inhibition of nitric oxide synthase gene expression by curcumin, a cancer preventive natural product with anti-inflammatory properties. Biochemical Pharmacology; 55:1955-1962.

Chansiri, G., Lyons, R.T., Patel, M.V., Hem, S.L., 1999. Effect of surface charge on the stability of oil/water emulsions during steam sterilization. Journal of Pharmaceutical Sciences; 88:454-458.

Chebil, L., 2006. Acylation des flavonoïdes par les lipases de *Candida antarctica* et de *Pseudomonas cepacia* : études cinétique, structurale et conformationnelle. Thèse - ENSAIA-INPL Nancy.

Cheeseman, K.H., 1993. Mechanisms and effects of lipid peroxidation. Molecular Aspects of Medicine; 14:191-197.

Cheikh Ali, Z., 2012. Études chimiques et biologiques d'Aframomum sceptrum (Zingiberaceae) et de la curcumine. Thèse - Faculté de pharmacie - Université Paris-Sud.

Chen, H.L., Wu, J., Sun, M., Guo, C.Y., Yu, A.H., Cao, F.L., Zhao, L.Y., Tan, Q., Zhai, G.X., 2012. N-trimethyl chitosan chloride-coated liposomes for the oral delivery of curcumin. Journal of Liposome Research; 22:100-109.

Chen, J., Da, W.M., Zhang, D.W., Liu, Q., Kang, J.H., 2005. Water-soluble antioxidants improve the antioxidant and anticancer activity of low concentrations of curcumin in human leukemia cells. Pharmazie; 60:57-61.

Chen, R.H., Win, H.P., Fang, H.J., 2001. Vesicle size, size distribution, stability, and rheological properties of liposomes coated with water-soluble chitosans of different molecular weights and concentrations. Journal of Liposome Research; 11:211-228.

Cheng, K.K., Chan, P.S., Fan, S., Kwan, S.M., Yeung, K.L., Wáng, Y.-X.n.J., Chow, A.H.L., Wu, E.X., Baum, L., 2015. Curcumin-conjugated magnetic nanoparticles for detecting amyloid plaques in Alzheimer's disease mice using magnetic resonance imaging (MRI). Elsevier; pp. 155-172.

Choplin, L., 2012. Alternatives de rupture d'une émulsion cationique par hétérofloculation ou par changement de pH. Thèse.Université de Lorraine-ENSIC.

Chung, M.Y., Lim, T.G., Lee, K.W., 2013. Molecular mechanisms of chemopreventive phytochemicals against gastroenterological cancer development. World J Gastroenterol; 19(7):984-93.

Cieslik-Boczula, K., Koll, A., 2009. The effect of 3-pentadecylphenol on DPPC bilayers ATR-IR and 31P NMR studies. Biophys Chem;140(1-3):51-6.

Ciobanu, B.C., 2013. De nouveaux biomatériaux polymères complexes pour la modélisation de la cinétique de libération de médicaments. Thèse, Université de PAU et des Pays de l'Adour-UFR Sciences et Techniques.

Coderch, L., Fonollosa, J., De Pera, M., Estelrich, J., De La Maza, A., Parra, J.L., 2000. Influence of cholesterol on liposome fluidity by EPR: Relationship with percutaneous absorption. Journal of Controlled Release; 68:85-95.

Colas, J.C., Shi, W.L., Rao, V., Omri, A., Mozafari, M.R., Singh, H., 2007. Microscopical investigations of nisin-loaded nanoliposomes prepared by Mozafari method and their bacterial targeting. Micron; 38:841-847.

Cole, G.M., Teter, B., Frautschy, S.A., 2007. Neuroprotective effects of curcumin. Adv Exp Med Biol; 595:197-212.

Cole, G.M., Yang, F., Lim, G.P., Cummings, J.L., Masterman, D.L., Frautschy, S.A., 2003. A Rationale for Curcuminoids for the Prevention or Treatment of Alzheimer's disease. Current Medicinal Chemistry - Immunology, Endocrine & Metabolic Agents; 3:15-25.

Colquhoun, A., Schumacher, R.I., 2001. Gamma-linolenic acid and eicosapentaenoic acid induce modifications in mitochondrial metabolism, reactive oxygen species generation, lipid peroxidation and apoptosis in Walker 256 rat carcinosarcoma cells. Biochimica et Biophysica Acta-Molecular and Cell Biology of Lipids; 1533:207-219.

Coonrod, D., Brick, M.A., Byrne, P.F., DeBonte, L., Chen, Z., 2008. Inheritance of long chain fatty acid content in rapeseed (Brassica napus L.). Euphytica; 164:583-592.

Cui, J., Yu, B., Zhao, Y., Zhu, W.W., Li, H.L., Lou, H.X., Zhai, G.X., 2009. Enhancement of oral absorption of curcumin by self-microemulsifying drug delivery systems. International Journal of Pharmaceutics; 371:148-155.

Cunnane, S.C., Chouinard-Watkins, R., Castellano, C.A., Barberger-Gateau, P., 2013. Docosahexaenoic acid homeostasis, brain aging and Alzheimer's disease: Can we reconcile the evidence? Prostaglandins Leukotrienes and Essential Fatty Acids; 88:61-70.

Dalen, J.E., Devries, S., 2014. Diets to Prevent Coronary Heart Disease 1957-2013: What Have We Learned? American Journal of Medicine; 127:364-369.

Darvesh, A.S., Aggarwal, B.B., Bishayee, A., 2012. Curcumin and Liver Cancer: A Review. Current Pharmaceutical Biotechnology; 13:218-228.

Das, K.C., Das, C.K., 2002. Curcumin (diferuloylmethane), a singlet oxygen (O-1(2)) quencher. Biochemical and Biophysical Research Communications; 295:62-66.

Das, R.K., Kasoju, N., Bora, U., 2010. Encapsulation of curcumin in alginate-chitosan-pluronic composite nanoparticles for delivery to cancer cells. Nanomedicine; 6(1):153-60.

Davis, B., 2005. Maximizing essential fatty acid status in vegetarians, in: Nutrition and Health. Current Topics, T.C.K. Descheemaeker, Ed., Garent: (Antwerp).

De Lorgeril, M., Salen, P., 2012. New insights into the health effects of dietary saturated and omega-6 and omega-3 polyunsaturated fatty acids. BioMed Central Ltd; 10(1):50.

Debas, H., 2009. Emulsification en systèmes microstructurés Thèse, Institut National Polytechnique de Lorraine-ENSIC.

DeHaas, K.H., Blom, C., vandenEnde, D., Duits, M.H.G., Haveman, B., Mellema, J., 1997. Rheological behavior of a dispersion of small lipid bilayer vesicles. Langmuir; 13:6658-6668.

Deshpande, U.R., Gadre, S.G., Raste, A.S., Pillai, D., Bhide, S.V., Samuel, A.M., 1998. Protective effect of turmeric (Curcuma longa L.) extract on carbon tetrachloride-induced liver damage in rats. Indian journal of experimental biology; 36(6):573-577.

Dey, A., Tergaonkar, V., Lane, D.P., 2008. Double-edged swords as cancer therapeutics: simultaneously targeting p53 and NF-kappaB pathways. Nat Rev Drug Discov; 7(12):1031-40.

Deygen, I.M., Kudryashova, E.V., 2014. Structure and stability of anionic liposomes complexes with PEG-chitosan branched copolymer. Russian Journal of Bioorganic Chemistry; 40:547-557.

Dhillon, N., Aggarwal, B.B., Newman, R.A., Wolff, R.A., Kunnumakkara, A.B., Abbruzzese, J.L., Ng, C.S., Badmaev, V., Kurzrock, R., 2008. Phase II trial of curcumin in patients with advanced pancreatic cancer. Clinical Cancer Research; 14:4491-4499.

Ding, W.Q., Vaught, J.L., Yamauchi, H., Lind, S.E., 2004. Differential sensitivity of cancer cells, to docosahexaenoic acid-induced cytotoxicity: The-potential importance of down-regulation of superoxide dismutase 1 expression. Molecular Cancer Therapeutics; 3:1109-1117.

Dinkova-Kostova, A.T., Talalay, P., 1999. Relation of structure of curcumin analogs to their potencies as inducers of Phase 2 detoxification enzymes. Carcinogenesis; 20:911-914. Dubois, V., Breton, S., Linder, M., Fanni, J., Parmentier, M., 2007. Fatty acid profiles of 80 vegetable oils with regard to their nutritional potential. European Journal of Lipid Science and Technology; 109:710-732.

Dunbar, B.S., Bosire, R.V., Deckelbaum, R.J., 2014. Omega 3 and omega 6 fatty acids in human and animal health: An African perspective. Molecular and Cellular Endocrinology; 398:69-77.

Dutta, A., Ikiki, E., 2013. Novel Drug Delivery Systems to Improve Bioavailability of Curcumin. Bioequivalence & Bioavailability; 6(1):001-009.

Duvoix, A., Blasius, R., Delhalle, S., Schnekenburger, M., Morceau, F., Henry, E., Dicato, M., Diederich, M., 2005. Chemopreventive and therapeutic effects of curcumin. Cancer Lett; 223(2):181-90.

Edwards, J.C., Chapman, D., Cramp, W.A., Yatvin, M.B., 1984. The effects of ionizing radiation on biomembrane structure and function. Progress in Biophysics and Molecular Biology; 43:71-93.

El Kinawy, O.S., Petersen, S., Ulrich, J., 2012. Technological Aspects of Nanoemulsion Formation of Low-Fat Foods Enriched with Vitamin E by High-Pressure Homogenization. Chemical Engineering & Technology; 35:937-940.

Er, E., Oliver, L., Cartron, P.-F., Juin, P., Manon, S., Vallette, F.M., 2006. Mitochondria as the target of the pro-apoptotic protein Bax. Biochimica Et Biophysica Acta-Bioenergetics; 1757:1301-1311.

Erdawati, Fithriyah, N.H., 2013. The Application of Chitosan for Environmentally Benign Process of Curcumin Dyeing of Silk Fabrics. Journal of Basic and Applied Scientific Research; 3(1):5-14.

Esmaili, M., Ghaffari, S.M., Moosavi-Movahedi, Z., Atri, M.S., Sharifizadeh, A., Farhadi, M., Yousefi, R., Chobert, J.M., Haertle, T., Moosavi-Movahedi, A.A., 2011. Beta casein-micelle as a nano vehicle for solubility enhancement of curcumin; food industry application. Lwt-Food Science and Technology; 44:2166-2172.

Espinal-Ruiz, M., Parada-Alfonso, F., Restrepo-Sanchez, L.P., Narvaez-Cuenca, C.E., McClements, D.J., 2014. Impact of dietary fibers [methyl cellulose, chitosan, and pectin] on digestion of lipids under simulated gastrointestinal conditions. Food & Function; 5:3083-3095.

Fang, J.G., Lu, J., Holmgren, A., 2005. Thioredoxin reductase is irreversibly modified by curcumin - A novel molecular mechanism for its anticancer activity. Journal of Biological Chemistry; 280:25284-25290.

Fathi, M., Mozafari, M.R., Mohebbi, M., 2012. Nanoencapsulation of food ingredients using lipid based delivery systems. Trends in Food Science & Technology; 23:13-27.

Fei Liu, X., Lin Guan, Y., Zhi Yang, D., Li, Z., De Yao, K., 2001. Antibacterial action of chitosan and carboxymethylated chitosan. Journal of Applied Polymer Science; 79:1324-1335.

Filipovic-Grcic, J., Skalko-Basnet, N., Jalsenjak, I., 2001. Mucoadhesive chitosan-coated liposomes: characteristics and stability. J Microencapsul; 18(1):3-12.

Freitas, R.A., Jr., 2005. What Is Nanomedicine? Disease-A-Month; 51:325-341.

Fujisawa, S., Atsumi, T., Ishihara, M., Kadoma, Y., 2004. Cyctotoxicity, ROS generation activity and radical-scavengining activity of curcumin and related compounds. Anticancer Research; 24:563-570.

Fujisawa, S., Kadoma, Y., 2006. Anti- and pro-oxidant effects of oxidized quercetin, curcumin or curcumin-related compounds with thiols or ascorbate as measured by the induction period method. In Vivo; 20:39-44.

Gamboa, J.M., Leong, K.W., 2013. In vitro and in vivo models for the study of oral delivery of nanoparticles. Advanced Drug Delivery Reviews; 65:800-810.

Gao, W., Chan, J.Y.W., Wei, W.I., Wong, T.S., 2012. Anti-cancer Effects of Curcumin on Head and Neck Cancers. Anti-Cancer Agents in Medicinal Chemistry; 12:1110-1116.

Gao, W.W., Hu, C.M.J., Fang, R.H., Zhang, L.F., 2013. Liposome-like nanostructures for drug delivery. Journal of Materials Chemistry B; 1(48):6569-6585.

Garait, B., 2006. Le stress oxydant induit par voie métabolique (régimes alimentaires) ou par voie gazeuse (hyperoxie) et effet de la GliSODin®. Thèse - Université Joseph Fourier - Grenoble.

Garcea, G., Jones, D.J.L., Singh, R., Dennison, A.R., Farmer, P.B., Sharma, R.A., Steward, W.P., Gescher, A.J., Berry, D.P., 2004. Detection of curcumin and its metabolites in hepatic tissue and portal blood of patients following oral administration. British Journal of Cancer; 90:1011-1015.

Garcia-Nino, W.R., Pedraza-Chaverri, J., 2014. Protective effect of curcumin against heavy metals-induced liver damage. Food and Chemical Toxicology 69, 182-201.

Gbogouri, G.A., 2005. Co-valorisation des protéines et des lipides riches en lécithine et en acides gras polyinsaturés oméga 3 à partir de têtes de saumon (Salmo salar) par hydrolyse enzymatique. . Thèse - ENSAIA-INPL Nancy.

Gbogouri, G.A., Linder, M., Fanni, J., Parmentier, M., 2006. Analysis of lipids extracted from salmon (Salmo salar) heads by commercial proteolytic enzymes. European journal of lipid science and technology; 108:766-775.

Gerber, M., 2009. Background Review Paper on Total Fat, Fatty Acid Intake and Cancers. Annals of Nutrition and Metabolism; 55:140-161.

Gerber, M., 2012. Omega-3 fatty acids and cancers: a systematic update review of epidemiological studies. British Journal of Nutrition; 107(S2):S228-S239.

Gercel-Taylor, C., Atay, S., Tullis, R.H., Kesimer, M., Taylor, D.D., 2012. Nanoparticle analysis of circulating cell-derived vesicles in ovarian cancer patients. Anal Biochem; 428(1):44-53.

Gescher, A.J., Sharma, R.A., Steward, W.P., 2001. Cancer chemoprevention by dietary constituents: a tale of failure and promise. The Lancet Oncology; 2:371-379.

Ghalandarlaki, N., Alizadeh, A.M., Ashkani-Esfahani, S., 2014. Nanotechnology-Applied Curcumin for Different Diseases Therapy. BioMed Research International; ID: 394264. 23 p.

Ghosh, S., Karin, M., 2002. Missing pieces in the NF-kappa B puzzle. Cell; 109:S81-S96.

Goel, A., Kunnumakkara, A.B., Aggarwal, B.B., 2008. Curcumin as "Curecumin": From kitchen to clinic. Biochemical Pharmacology; 75:787-809.

Gogus, U., Smith, C., 2010. n-3 Omega fatty acids: a review of current knowledge. International Journal of Food Science and Technology; 45:417-436.

Gontier, E., Gougeon, S., Guillot, X., Thomasset, B., Méjean, L., Tran, T., Bourgaud, F., 2004. Les plantes, sources dacides gras essentiels oméga 3. Oléagineux, Corps Gras, Lipides; 11:106-111.

Gregoriadis, G., 1977. Targeting of drugs. Nature; 265:407-411.

Gregoriadis, G., 1988. Liposomes as Drug Carriers. Recent Trend and Progress. John Wiley & Sons, New York; pp. 885.

Gregoriadis, G., Florence, A.T., 1993. Liposomes in Drug Delivery: Clinical, Diagnostic and Ophthalmic Potential; pp. 15-28.

Guesnet, P., Alessandri, J.-M., 2011. Docosahexaenoic acid (DHA) and the developing central nervous system (CNS)-Implications for dietary recommendations. Elsevier; pp. 7-12.

Guliyeva, Ü., Öner, F., Özsoy, Ş., Haziroğlu, R., 2006. Chitosan microparticles containing plasmid DNA as potential oral gene delivery system. European Journal of Pharmaceutics and Biopharmaceutics; 62:17-25.

Gulseren, I., Guri, A., Corredig, M., 2014. Effect of interfacial composition on uptake of curcumin-piperine mixtures in oil in water emulsions by Caco-2 cells. Food & Function; 5:1218-1223.

Guo, J., Ping, Q., Jiang, G., Huang, L., Tong, Y., 2003. Chitosan-coated liposomes: characterization and interaction with leuprolide. International Journal of Pharmaceutics; 260:167-173.

Gursoy, R.N., Benita, S., 2004. Self-emulsifying drug delivery systems (SEDDS) for improved oral delivery of lipophilic drugs. Biomedicine & Pharmacotherapy; 58:173-182.

Guzey, D., McClements, D.J., 2006. Formation, stability and properties of multilayer emulsions for application in the food industry. Advances in Colloid and Interface Science; 128:227-248.

Hasan, M., Belhaj, N., Benachour, H., Barberi-Heyob, M., Kahn, C.J.F., Jabbari, E., Linder, M., Arab-Tehrany, E., 2014. Liposome encapsulation of curcumin: Physico-chemical characterizations and effects on MCF7 cancer cell proliferation. International Journal of Pharmaceutics; 461:519-528.

Hatamie, S., Nouri, M., Karandikar, S.K., Kulkarni, A., Dhole, S.D., Phase, D.M., Kale, S.N., 2012. Complexes of cobalt nanoparticles and polyfunctional curcumin as antimicrobial agents. Materials Science and Engineering: C; 32:92-97.

Heger, M., van Golen, R.F., Broekgaarden, M., Michel, M.C., 2014. The Molecular Basis for the Pharmacokinetics and Pharmacodynamics of Curcumin and Its Metabolites in Relation to Cancers. Pharmacological Reviews; 66:222-307.

Henriksen, I., Vagen, S.R., Sande, S.A., Smistad, G., Karlsen, J., 1997. Interactions between liposomes and chitosan .2. Effect of selected parameters on aggregation and leakage. International Journal of Pharmaceutics; 146:193-203.

Hincha, D.K., Zuther, E., Hellwege, E.M., Heyer, A.G., 2002. Specific effects of fructo- and gluco-oligosaccharides in the preservation of liposomes during drying. Glycobiology; 12:103-110.

Hoehle, S.I., Pfeiffer, E., Solyom, A.M., Metzler, M., 2006. Metabolism of curcuminoids in tissue slices and subcellular fractions from rat liver. Journal of Agricultural and Food Chemistry; 54:756-764.

Holt, P.R., Katz, S., Kirshoff, R., 2005. Curcumin therapy in inflammatory bowel disease: A pilot study. Digestive Diseases and Sciences ; 50:2191-2193.

Hombourger, C., 2010. Le Curcuma, De l'épice au médicament. Thèse-Université Henri Poincaré Nancy 1-Faculté de Pharmacie.

Hong, M.Y., Chapkin, R.S., Barhoumi, R., Burghardt, R.C., Turner, N.D., Henderson, C.E., Sanders, L.M., Fan, Y.Y., Davidson, L.A., Murphy, M.E., Spinka, C.M., Carroll, R.J., Lupton, J.R., 2002. Fish oil increases mitochondrial phospholipid unsaturation, upregulating reactive oxygen species and apoptosis in rat colonocytes. Carcinogenesis; 23:1919-1925.

Horn, A.F., Nielsen, N.S., Jacobsen, C., 2012. Iron-mediated lipid oxidation in 70% fish oil-in-water emulsions: effect of emulsifier type and pH. International Journal of Food Science and Technology; 47:1097-1108.

Hornstra, G., 2001. Importance of polyunsaturated fatty acids of the n-6 and n-3 families for early human development. European Journal of Lipid Science and Technology; 103:379-389.

Huang, H.C., Lin, C.J., Liu, W.J., Jiang, R.R., Jiang, Z.F., 2011. Dual effects of curcumin on neuronal oxidative stress in the presence of Cu (II). Food and Chemical Toxicology; 49:1578-1583.

Igarashi, M., Chang, L., Ma, K., Rapoport, S.I., 2013. Kinetics of eicosapentaenoic acid in brain, heart and liver of conscious rats fed a high n-3 PUFA containing diet. Prostaglandins, Leukotrienes and Essential Fatty Acids (PLEFA); 89:403-412.

Ireson, C.R., Jones, D.J., Orr, S., Coughtrie, M.W., Boocock, D.J., Williams, M.L., Farmer, P.B., Steward, W.P., Gescher, A.J., 2002. Metabolism of the cancer chemopreventive agent curcumin in human and rat intestine. Cancer Epidemiol Biomarkers Prev; (1):105-11.

Iwanaga, K., Ono, S., Narioka, K., Kakemi, M., Morimoto, K., Yamashita, S., Namba, Y., Oku, N., 1999. Application of surface coated liposomes for oral delivery of peptide: Effects of

coating the liposome's surface on the GI transit of insulin. Journal of Pharmaceutical Sciences; 88:248-252.

Jafari, S.M., He, Y., Bhandari, B., 2007. Optimization of nano-emulsions production by microfluidization. European Food Research and Technology; 225:733-741.

Jagatha, B., Mythri, R.B., Vali, S., Bharath, M.M.S., 2008. Curcumin treatment alleviates the effects of glutathione depletion in vitro and in vivo: Therapeutic implications for Parkinson's disease explained via in silico studies. Free Radical Biology and Medicine; 44:907-917.

Jain, S., Singh, P., Mishra, V., Vyas, S.P., 2005. Mannosylated niosomes as adjuvant-carrier system for oral genetic immunization against hepatitis B. Immunol Lett; 101(1):41-9.

Janes, K.A., Calvo, P., Alonso, M.J., 2001. Polysaccharide colloidal particles as delivery systems for macromolecules. Advanced Drug Delivery Reviews; 47:83-97.

Jangle, R.D., Thorat, B.N., 2013. Reversed-phase High-performance Liquid Chromatography Method for Analysis of Curcuminoids and Curcuminoid-loaded Liposome Formulation. Indian Journal of Pharmaceutical Sciences; 75:60-66.

Jee, S.H., Shen, S.C., Tseng, C.R., Chiu, H.C., Kuo, M.L., 1998. Curcumin induces a p53-dependent apoptosis in human basal cell carcinoma cells. Journal of Investigative Dermatology; 111:656-661.

Jesorka, A., Orwar, O., 2008. Liposomes: Technologies and Analytical Applications, Annual Review of Analytical Chemistry; 1:801-832.

Ji, H.-F., Shen, L., 2014. The Multiple Pharmaceutical Potential of Curcumin in Parkinson's disease. Bentham Science Publishers; 13(2):369-373.

John, V.D., Kuttan, G., Krishnankutty, K., 2002. Anti-tumour studies of metal chelates of synthetic curcuminoids. J Exp Clin Cancer Res; 21(2):219-24.

Johnson, J., de Mejia, E.G., 2011. Dietary factors and pancreatic cancer: The role of food bioactive compounds. Molecular Nutrition & Food Research; 55:58-73.

Joraholmen, M.W., Vanic, Z., Tho, I., Skalko-Basnet, N., 2014. Chitosan-coated liposomes for topical vaginal therapy: Assuring localized drug effect. International Journal of Pharmaceutics; 472:94-101.

Joseph, S., Bunjes, H., 2012. Preparation of Nanoemulsions and Solid Lipid Nanoparticles by Premix Membrane Emulsification. Journal of Pharmaceutical Sciences; 101:2479-2489.

Jovanovic, S.V., Steenken, S., Boone, C.W., Simic, M.G., 1999. H-atom transfer is a preferred antioxidant mechanism of curcumin. Journal of the American Chemical Society; 121:9677-9681.

Judge, M.P., Cong, X., Harel, O., Courville, A.B., Lammi-Keefe, C.J., 2012. Maternal consumption of a DHA-containing functional food benefits infant sleep patterning: An early neurodevelopmental measure. Early Human Development ; 88 :531-537.

Kabri, T.-H., 2013. Conception raisonnée d'émulsions submicroniques vectrices d'acides gras polyinsaturés n-3-Impact de la structure moléculaire et supramoléculaire des lipides sur l'oxydation. Thèse, BIA, INRA Nantes & LiBio, Université de Lorraine.

Kabri, T.-h., Arab-Tehrany, E., Belhaj, N., Linder, M., 2011. Physico-chemical characterization of nano-emulsions in cosmetic matrix enriched on omega-3. J. Nanobiotechnol; 9:41.

Kakkar, V., Singh, S., Singla, D., Kaur, I.P., 2011. Exploring solid lipid nanoparticles to enhance the oral bioavailability of curcumin. Mol Nutr Food Res; 55(3):495-503.

Kaltsa, O., Michon, C., Yanniotis, S., Mandala, I., 2013. Ultrasonic energy input influence omicronn the production of sub-micron o/w emulsions containing whey protein and common stabilizers. Ultrason Sonochem; 20(3):881-91.

Karewicz, A., Bielska, D., Gzyl-Malcher, B., Kepczynski, M., Lach, R., Nowakowska, M., 2011. Interaction of curcumin with lipid monolayers and liposomal bilayers. Colloids and Surfaces B-Biointerfaces; 88:231-239.

Kargar, M., Spyropoulos, F., Norton, I.T., 2011. The effect of interfacial microstructure on the lipid oxidation stability of oil-in-water emulsions. Journal of Colloid and Interface Science; 357:527-533.

Kato, Y., Hosokawa, T., Hayakawa, E., Ito, K., 1993. Influence of Liposomes on Tryptic Digestion of Insulin. Biological & Pharmaceutical Bulletin; 16:457-461.

Kazi, K.M., Mandal, A.S., Biswas, N., Guha, A., Chatterjee, S., Behera, M., Kuotsu, K., 2010. Niosome: A future of targeted drug delivery systems. J Adv Pharm Technol Res; 1(4):374-80.

Kean, T., Thanou, M., 2010. Biodegradation, biodistribution and toxicity of chitosan. Advanced Drug Delivery Reviews; 62:3-11.

Keller, B.C., 2001. Liposomes in nutrition. Trends in Food Science & Technology; 12:25-31.

Kevelam, J., Hoffmann, A.C., Engberts, J., Blokzijl, W., van de Pas, J., Versluis, P., 1999. Rheology of concentrated dispersions of sterically stabilized polydisperse lamellar droplets. Langmuir; 15:5002-5013.

Khar, A., Ali, A.M., Pardhasaradhi, B.V.V., Begum, Z., Anjum, R., 1999. Antitumor activity of curcumin is mediated through the induction of apoptosis in AK-5 tumor cells. Febs Letters; 445:165-168.

Khurana, A., Ho, C.T., 1988. High-Performance Liquid-Chromatographic Analysis of Curcuminoids and Their Photo-Oxidative Decomposition Compounds in Curcuma-Longa L. Journal of Liquid Chromatography; 11:2295-2304.

Kim, T.H., Jiang, H.H., Youn, Y.S., Park, C.W., Tak, K.K., Lee, S., Kim, H., Jon, S., Chen, X., Lee, K.C., 2011. Preparation and characterization of water-soluble albumin-bound curcumin nanoparticles with improved antitumor activity. Int J Pharm; 403(1-2):285-91.

Kirstein, S.L., Atienza, J.M., Xi, B., Zhu, J., Yu, N.C., Wang, X.B., Xu, X., Abassi, Y.A., 2006. Live cell quality control and utility of real-time cell electronic sensing for assay development. Assay and Drug Development Technologies; 4:545-553.

Klang, V., Matsko, N.B., Valenta, C., Hofer, F., 2012. Electron microscopy of nanoemulsions: An essential tool for characterisation and stability assessment. Micron; 43:85-103.

Klaypradit, W., Huang, Y.W., 2008. Fish oil encapsulation with chitosan using ultrasonic atomizer. Lwt-Food Science and Technology; 41:1133-1139.

Kotze, A.F., Luessen, H.L., Thanou, M., Verhoef, J.C., de Boer, A.B.G., Junginger, H.E., Lehr, C.-M., 1999. Chitosan and chitosan derivatives as absorption enhancers for peptide drugs across mucosal epithelia. In: Mathiowitz, E., Chickering, III D.E., Lehr, C.-M. (Eds.), Bioadhesive Drug Delivery Systems Fundamentals, Novel Approaches, and Development. Marcel Dekker, New York; 341–386.

Kučerka, N., Nieh, M.-P., Katsaras, J., Ales, I., 2011. Chapter Eight - Small-Angle Scattering from Homogenous and Heterogeneous Lipid Bilayers, Advances in Planar Lipid Bilayers and Liposomes. Academic Press; pp. 201-235.

Kumar, K., Rai, A.K., 2011. Development and evaluation of proniosome- encapsulated curcumin for transdermal administration. Tropical Journal of Pharmaceutical Research; 10(6):697-703

Kunnumakkara, A.B., Anand, P., Aggarwal, B.B., 2008. Curcumin inhibits proliferation, invasion, angiogenesis and metastasis of different cancers through interaction with multiple cell signaling proteins. Cancer Lett; 269(2):199-225.

Kunwar, A., Barik, A., Mishra, B., Rathinasamy, K., Pandey, R., Priyadarsini, K.I., 2008. Quantitative cellular uptake, localization and cytotoxicity of curcumin in normal and tumor cells. Biochimica et Biophysica Acta-General Subjects; 1780:673-679.

Kunwar, A., Barik, A., Pandey, R., Priyadarsini, K.I., 2006. Transport of liposomal and albumin loaded curcumin to living cells: An absorption and fluorescence spectroscopic study. Biochimica et Biophysica Acta (BBA) - General Subjects; 1760:1513-1520.

Kunwar, A., Jayakumar, S., Srivastava, A.K., Priyadarsini, K.I., 2012. Dimethoxycurcumin-induced cell death in human breast carcinoma MCF7 cells: evidence for pro-oxidant activity, mitochondrial dysfunction, and apoptosis. Archives of Toxicology; 86:603-614.

Kuo, M.L., Huang, T.S., Lin, J.K., 1996. Curcumin, an antioxidant and anti-tumor promoter, induces apoptosis in human leukemia cells. Biochimica et Biophysica Acta (BBA)-Molecular Basis of Disease; 1317(2):95-100.

Kuratko, C.N., Barrett, E.C., Nelson, E.B., Salem, N., 2013. The Relationship of Docosahexaenoic Acid (DHA) with Learning and Behavior in Healthy Children: A Review. Nutrients; 5:2777-2810.

Kurzrock, R., Li, L., Mehta, K., Aggarawal, B.B., Helson, L., 2014. Liposomal curcumin for treatment of diseases. U.S. Patent No. 8,784,881. Washington, DC: U.S. Patent and Trademark Office.

Kuttan, G., Kumar, K.B., Guruvayoorappan, C., Kuttan, R., 2007. Antitumor, anti-invasion, and antimetastatic effects of curcumin. Adv Exp Med Biol; 595:173-84.

Kuttan, R., Sudheeran, P.C., Josph, C.D., 1987. Turmeric and curcumin as topical agents in cancer therapy. Tumori; 73(1):29-31.

Lahiff, C., Moss, A.C., 2011. Curcumin for clinical and endoscopic remission in ulcerative colitis. Inflamm Bowel Dis; 17(7):E66.

Lai, S.K., Wang, Y.Y., Hida, K., Cone, R., Hanes, J., 2010. Nanoparticles reveal that human cervicovaginal mucus is riddled with pores larger than viruses. Proceedings of the National Academy of Sciences of the United States of America; 107:598-603.

Lam, D.T., Hoang, N.M.T., Trang, T.M., al, e., 2010. . Nanosized magnetofluorescent Fe3O4-curcumin conjugate for multimodal monitoring and drug targeting. Colloids and Surfaces a-Physicochemical and Engineering Aspects; 371(1-3):104-112.

Lantz, R.C., Chen, G.J., Solyom, A.M., Jolad, S.D., Timmermann, B.N., 2005. The effect of turmeric extracts on inflammatory mediator production. Phytomedicine; 12(6-7):445-52.

Laouini, A., Jaafar-Maalej, C., Sfar, S., Charcosset, C., Fessi, H., 2011. Liposome preparation using a hollow fiber membrane contactor-Application to spironolactone encapsulation. International Journal of Pharmaceutics; 415:53-61.

Larsson, S.C., Kumlin, M., Ingelman-Sundberg, M., Wolk, A., 2004. Dietary long-chain n-3 fatty acids for the prevention of cancer: a review of potential mechanisms. American Journal of Clinical Nutrition; 79:935-945.

Lauritzen, L., Hansen, H.S., Jorgensen, M.H., Michaelsen, K.F., 2001. The essentiality of long chain n-3 fatty acids in relation to development and function of the brain and retina. Progress in Lipid Research; 40:1-94.

Laye, C., McClements, D.J., Weiss, J., 2008. Formation of biopolymer-coated liposomes by electrostatic deposition of chitosan. Journal of Food Science; 73:N7-N15.

Lee, J.-S., Kim, H.W., Chung, D., Lee, H.G., 2009. Catechin-loaded calcium pectinate microparticles reinforced with liposome and hydroxypropylmethylcellulose: Optimization and in vivo antioxidant activity. Food Hydrocolloids; 23:2226-2233.

Lee, J.W., Hong, H.M., Kwon, D.D., Pae, H.O., Jeong, H.J., 2010. Dimethoxycurcumin, a structural analogue of curcumin, induces apoptosis in human renal carcinoma caki cells through the production of reactive oxygen species, the release of cytochrome C, and the activation of caspase-3. Korean J Urol; 51:870-878.

Lee, J.W., Park, J.H., Robinson, J.R., 2000. Bioadhesive-based dosage forms: the next generation. J Pharm Sci; 89(7):850-66.

Lee, S.J., Choi, S.J., Li, Y., Decker, E.A., McClements, D.J., 2011. Protein-Stabilized Nanoemulsions and Emulsions: Comparison of Physicochemical Stability, Lipid Oxidation, and Lipase Digestibility. Journal of Agricultural and Food Chemistry; 59:415-427.

Lee, W.H., Loo, C.Y., Bebawy, M., Luk, F., Mason, R.S., Rohanizadeh, R., 2013. Curcumin and its Derivatives: Their Application in Neuropharmacology and Neuroscience in the 21st Century. Current Neuropharmacology; 11:338-378.

Leekumjorn, S., Cho, H.J., Wu, Y., Wright, N.T., Sum, A.K., Chan, C., 2009. The role of fatty acid unsaturation in minimizing biophysical changes on the structure and local effects of bilayer membranes. Biochimica et Biophysica Acta (BBA) – Biomembranes; 1788:1508-1516.

Lehner, R., Wang, X.Y., Marsch, S., Hunziker, P., 2013. Intelligent nanomaterials for medicine: Carrier platforms and targeting strategies in the context of clinical application. Nanomedicine-Nanotechnology Biology and Medicine; 9:742-757.

Lentz, B.R., 1993. Use of Fluorescent-Probes to Monitor Molecular Order and Motions within Liposome Bilayers. Chemistry and Physics of Lipids; 64:99-116.

Leong, T.S.H., Wooster, T.J., Kentish, S.E., Ashokkumar, M., 2009. Minimising oil droplet size using ultrasonic emulsification. Ultrasonics Sonochemistry; 16:721-727.

Li, C., Zhang, Y., Su, T.T., Feng, L.L., Long, Y.Y., Chen, Z.B., 2012. Silica-coated flexible liposomes as a nanohybrid delivery system for enhanced oral bioavailability of curcumin. International Journal of Nanomedicine; 7:5995-6002.

Li, D.C., Zhong, X.K., Zeng, Z.P., Jiang, J.G., Li, L., Zhao, M.M., Yang, X.Q., Chen, J., Zhang, B.S., Zhao, Q.Z., Xie, M.Y., Xiong, H., Deng, Z.Y., Zhang, X.M., Xu, S.Y., Gao, Y.X., 2009a. Application of targeted drug delivery system in Chinese medicine. J Control Release; 138(2):103-12.

Li, L., Ahmed, B., Mehta, K., Kurzrock, R., 2007. Liposomal curcumin with and without oxaliplatin: effects on cell growth, apoptosis, and angiogenesis in colorectal cancer. Molecular Cancer Therapeutics; 6:1276-1282.

Li, L., Braiteh, F.S., Kurzrock, R., 2005. Liposome-encapsulated curcumin: in vitro and in vivo effects on proliferation, apoptosis, signaling, and angiogenesis. Cancer; 104(6):1322-31.

Li, N., Zhuang, C.Y., Wang, M., Sun, X.Y., Nie, S.F., Pan, W.S., 2009b. Liposome coated with low molecular weight chitosan and its potential use in ocular drug delivery. International Journal of Pharmaceutics; 379:131-138.

Lim, G.P., Chu, T., Yang, F.S., Beech, W., Frautschy, S.A., Cole, G.M., 2001. The curry spice curcumin reduces oxidative damage and amyloid pathology in an Alzheimer transgenic mouse. Journal of Neuroscience; 21:8370-8377.

Lin, C.C., Lin, H.Y., Chen, H.C., Yu, M.W., Lee, M.H., 2009. Stability and characterisation of phospholipid-based curcumin-encapsulated microemulsions. Food Chemistry; 116:923-928.

Lin, J.K., Pan, M.H., Lin-Shiau, S.Y., 2000. Recent studies on the biofunctions and biotransformations of curcumin. Biofactors ; 13:153-158.

Linder, M., 2003. Les acides gras polyinsaturés : Des sources aux procédés d'extraction pour une meilleure maîtrise nutritionnelle. HDR.

Linder, M., Matouba, E., Fanni, J., Parmentier, M., 2002. Enrichment of salmon oil with n-3 PUFA by lipolysis, filtration and enzymatic re-esterification. European Journal of Lipid Science and Technology; 104:455-462.

Liu, A.C., Lou, H.X., Zhao, L.X., Fan, P.H., 2006. Validated LC/MS/MS assay for curcumin and tetrahydrocurcumin in rat plasma and application to pharmacokinetic study of phospholipid complex of curcumin. Journal of Pharmaceutical and Biomedical Analysis; 40:720-727.

Liu, C.H., Chang, F.Y., Hung, D.K., 2011. Terpene microemulsions for transdermal curcumin delivery: effects of terpenes and cosurfactants. Colloids Surf B Biointerfaces; 82(1):63-70.

Liu, J., Ma, D.W.L., 2014. The Role of n-3 Polyunsaturated Fatty Acids in the Prevention and Treatment of Breast Cancer. Nutrients; 6:5184-5223.

Liu, W., Liu, J., Liu, W., Li, T., Liu, C., 2013. Improved Physical and in Vitro Digestion Stability of a Polyelectrolyte Delivery System Based on Layer-by-Layer Self-Assembly Alginate-Chitosan-Coated Nanoliposomes. Journal of Agricultural and Food Chemistry; 61:4133-4144.

Liu, W., Ye, A., Liu, C., Liu, W., Singh, H., 2012. Structure and integrity of liposomes prepared from milk- or soybean-derived phospholipids during in vitro digestion. Food Research International; 48:499-506.

Liu, Y.J., Liu, D.D., Zhu, L., Gan, Q., Le, X.Y., 2015. Temperature-dependent structure stability and in vitro release of chitosan-coated curcumin liposome. Food Research International 74, 97-105.

Ljungblad, L.M., Johnsen, J-I., Wickström, M., Kogner, P., Gleissman, H., 2015. A novel approach to treat medulloblastoma: The omega-3 fatty acids DHA and EPA reduce medulloblastoma tumor growth in vitro and in vivo. AACR; 3275-3275.

Lomova, M.V., Sukhorukov, G.B., Antipina, M.N., 2010. Antioxidant Coating of Micronsize Droplets for Prevention of Lipid Peroxidation in Oil-in-Water Emulsion. Acs Applied Materials & Interfaces; 2:3669-3676.

Lorin, A., Flore, C., Thomas, A., Brasseur., R., 2004. Les liposomes : description, fabrication et applications. Biotechnology, Agronomy, Society and Environment; 8 (3):163-176.

Lu, F.S.H., Nielsen, N.S., Baron, C.P., Diehl, B.W.K., Jacobsen, C., 2012a. Oxidative Stability of Dispersions Prepared from Purified Marine Phospholipid and the Role of a-Tocopherol. Journal of Agricultural and Food Chemistry; 60:12388-12396.

Lu, F.S.H., Nielsen, N.S., Baron, C.P., Jensen, L.H.S., Jacobsen, C., 2012b. Physico-chemical Properties of Marine Phospholipid Emulsions. Journal of the American Oil Chemists Society; 89:2011-2024.

Lukita-Atmadja, W., Ito, Y., Baker, G.L., McCuskey, R.S., 2002. Effect of curcuminoids as anti-inflammatory agents on the hepatic microvascular response to endotoxin. Shock; 17:399-403.

Lundberg, B., 1994. Preparation of drug-carrier emulsions stabilized with phosphatidylcholine-surfactant mixtures. Journal of Pharmaceutical Sciences; 83:72-75.

Ma, Q.L., Yang, F., Rosario, E.R., Ubeda, O.J., Beech, W., Gant, D.J., Chen, P.P., Hudspeth, B., Chen, C., Zhao, Y., Vinters, H.V., Frautschy, S.A., Cole, G.M., 2009. Beta-amyloid oligomers induce phosphorylation of tau and inactivation of insulin receptor substrate via c-Jun N-terminal kinase signaling: suppression by omega-3 fatty acids and curcumin. J Neurosci ; 29(28):9078-89.

Madrigal-Carballo, S., Seyler, D., Manconi, M., Mura, S., Vila, A.O., Molina, F., 2008. An approach to rheological and electrokinetic behaviour of lipidic vesicles covered with chitosan biopolymer. Colloids and Surfaces a-Physicochemical and Engineering Aspects; 323:149-154.

Mady, M.M., Darwish, M.M., Khalil, S., Khalil, W.M., 2009. Biophysical studies on chitosan-coated liposomes. European Biophysics Journal with Biophysics Letters; 38:1127-1133.

Maggioni, M., Picotti, G.B., Bondiolotti, G.P., Panerai, A., Cenacchi, T., Nobile, P., Brambilla, F., 1990. Effects of Phosphatidylserine Therapy in Geriatric-Patients with Depressive-Disorders. Acta Psychiatrica Scandinavica; 81:265-270.

Maherani, B., Arab-Tehrany, E., Kheirolomoom, A., Geny, D., Linder, M., 2013. Calcein release behavior from liposomal bilayer; influence of physicochemical/mechanical/structural properties of lipids. Biochimie; 95(11):2018-33.

Maherani, B., Arab-Tehrany, E., Kheirolomoom, A., Reshetov, V., Stebe, M.J., Linder, M., 2012. Optimization and characterization of liposome formulation by mixture design. Analyst; 137:773-786.

Maherani, B., Arab-Tehrany, E., Linder, M., 2011. Mechanism of Bioactive Transfer through Liposomal Bilayers. Current Drug Targets; 12:531-545.

Maheshwari, R.K., Singh, A.K., Gaddipati, J., Srimal, R.C., 2006. Multiple biological activities of curcumin: A short review. Life Sciences; 78:2081-2087.

Mainardes, R.M., Silva, L.P., 2004. Drug delivery systems: past, present, and future. Curr Drug Targets; 5(5):449-55.

Maiti, K., Mukherjee, K., Gantait, A., Saha, B.P., Mukherjee, P.K., 2007. Curcumin-phospholipid complex: Preparation, therapeutic evaluation and pharmacokinetic study in rats. International Journal of Pharmaceutics; 330:155-163.

Maiti, P., Manna, J., Veleri, S., Frautschy, S., 2014. Molecular chaperone dysfunction in neurodegenerative diseases and effects of curcumin. Hindawi Publishing Corporation; pp. 14.

Malam, Y., Loizidou, M., Seifalian, A.M., 2009. Liposomes and nanoparticles: nanosized vehicles for drug delivery in cancer. Trends in Pharmacological Sciences; 30:592-599.

Mallick, S., Choi, J.S., 2014. Liposomes: Versatile and Biocompatible Nanovesicles for Efficient Biomolecules Delivery. Journal of Nanoscience and Nanotechnology; 14:755-765.

Mano, J.F., Koniarova, D., Reis, R.L., 2003. Thermal properties of thermoplastic starch/synthetic polymer blends with potential biomedical applicability. Journal of Materials Science-Materials in Medicine; 14:127-135.

Marathe, D., Mishra, K.P., 2002. Radiation-induced changes in permeability in unilamellar phospholipid liposomes. Radiation Research; 157: 685-692.

Marchessault, R.H., Ravenelle, F., Zhu, X.X., 2006. Polysaccharides for Drug Delivery and Pharmaceutical Applications. American Chemical Society; 934.

Marques, E.F., Regev, O., Khan, A., Miguel, M.D., Lindman, B., 1999. Interactions between catanionic vesicles and oppositely charged poly electrolytes-phase behavior and phase structure. Macromolecules; 32:6626-6637.

Mathur, N.K., Narang, C.K., 1990. Chitin and chitosan, versatile polysaccharides from marine animals. Journal of Chemical Education; 67:938-942.

Mazzarino, L., Travelet, C., Ortega-Murillo, S., Otsuka, I., Pignot-Paintrand, I., Lemos-Senna, E., Borsali, R., 2012. Elaboration of chitosan-coated nanoparticles loaded with curcumin for mucoadhesive applications. Journal of Colloid and Interface Science; 370:58-66.

McClements, D.J., 2010. Emulsion Design to Improve the Delivery of Functional Lipophilic Components. Annual Review of Food Science and Technology; 1:241-269.

McConnell, E.L., Murdan, S., Basit, A.W., 2008. An investigation into the digestion of chitosan (noncrosslinked and crosslinked) by human colonic bacteria. Journal of Pharmaceutical Sciences; 97:3820-3829.

Mehta, K., Pantazis, P., McQueen, T., Aggarwal, B.B., 1997. Antiproliferative effect of curcumin (diferuloylmethane) against human breast tumor cell lines. Anti-Cancer Drugs ; 8:470-481.

Mendez, Z., Anton, R.E., Salager, J.L., 1999. Surfactant-oil-water systems near the affinity inversion. Part XI. pH sensitive emulsions containing carboxylic acids. Journal of Dispersion Science and Technology; 20:883-892.

Menon, D., Thomas, R.T., Narayanan, S., Maya, S., Jayakumar, R., Hussain, F., Lakshmanan, V.-K., Nair, S.V., 2011. A novel chitosan/polyoxometalate nano-complex for anti-cancer applications. Carbohydrate Polymers; 84:887-893.

Mertins, O., Dimova, R., 2013. Insights on the Interactions of Chitosan with Phospholipid Vesicles. Part I: Effect of Polymer Deprotonation. Langmuir; 29:14545-14551.

Minnis, R.C., Haq, I.U., Jackson, P.R., Yeo, W.W., Ramsay, L.E., 1998. Oily fish and fish oil supplements in the prevention of coronary heart disease. Journal of Human Nutrition and Dietetics; 11:13-19.

Mirgani, M.T., Isacchi, B., Sadeghizadeh, M., Marra, F., Bilia, N.R., Mowla, S.E.J., Najafi, F., Babaei, E.S., 2014. Dendrosomal curcumin nanoformulation downregulates pluripotency genes via miR-145 activation in U87MG glioblastoma cells. International Journal of Nanomedicine; 9:403-417.

Mishra, S., Kapoor, N., Ali, A.M., Pardhasaradhi, B.V.V., Kumari, A.L., Khar, A., Misra, K., 2005. Differential apoptotic and redox regulatory activities of curcumin and its derivatives. Free Radical Biology and Medicine; 38:1353-1360.

Mohan, P.R.K., Sreelakshmi, G., Muraleedharan, C.V., Joseph, R., 2012. Water soluble complexes of curcumin with cyclodextrins: Characterization by FT-Raman spectroscopy. Vibrational Spectroscopy; 62:77-84.

Mongens, M., 2013. Origine et conséquences du stress oxydant. Thèse, École Nationale Vétérinaire d'Alfort, France.

Moorthi, C., Krishnan, K., Manavalan, R., Kathiresan, K., 2012. Preparation and characterization of curcumin-piperine dual drug loaded nanoparticles. Asian Pac J Trop Biomed; 2(11):841-8.

Mozafari, M.R., Khosravi-Darani, K., Borazan, G.G., Cui, J., Pardakhty, A., Yurdugul, S., 2008. Encapsulation of Food Ingredients Using Nanoliposome Technology. International Journal of Food Properties; 11:833-844.

Mozaffarian, D., Wu, J.H.Y., 2012. (n-3) Fatty Acids and Cardiovascular Health: Are Effects of EPA and DHA Shared or Complementary? Journal of Nutrition; 142:614S-625S.

Mulik, R., Mahadik, K., Paradkar, A., 2009. Development of curcuminoids loaded poly(butyl) cyanoacrylate nanoparticles: Physicochemical characterization and stability study. Eur J Pharm Sci; 37(3-4):395-404.

Murphy, K.M., Ranganathan, V., Farnsworth, M.L., Kavallaris, M., Lock, R.B., 2000. Bcl-2 inhibits Bax translocation from cytosol to mitochondria during drug-induced apoptosis of human tumor cells. Cell Death and Differentiation; 7:102-111.

Muzzarelli, R.A.A., Boudrant, J., Meyer, D., Manno, N., DeMarchis, M., Paoletti, M.G., 2012. Current views on fungal chitin/chitosan, human chitinases, food preservation, glucans, pectins and inulin: A tribute to Henri Braconnot, precursor of the carbohydrate polymers science, on the chitin bicentennial. Carbohydrate Polymers; 87:995-1012.

Mythri, R.B., Veena, J., Harish, G., Shankaranarayana Rao, B.S., Srinivas Bharath, M.M., 2011 Chronic dietary supplementation with turmeric protects against 1-methyl-4-phenyl-1,2,3,6-tetrahydropyridine-mediated neurotoxicity in vivo: implications for Parkinson's disease. Br J Nutr; 106(1):63-72.

Nagaraju, G.P., Aliya, S., Zafar, S.F., Basha, R., Diaz, R., El-Rayes, B.F., 2012. The impact of curcumin on breast cancer. Integrative Biology; 4:996-1007.

Nagendraprabhu, P., Sudhandiran, G., 2011. Astaxanthin inhibits tumor invasion by decreasing extracellular matrix production and induces apoptosis in experimental rat colon carcinogenesis by modulating the expressions of ERK-2, NFkB and COX-2. Investigational New Drugs; 29:207-224.

Nakayama, T., Dewa, T., Sakaguchi, M., Mochiyama, H., Nango, M., Fujimoto, H., 2007. Toward the optimal drug delivery system and cell manipulation using liposome. Nanomedicine-Nanotechnology Biology and Medicine; 3:344-345.

Naksuriya, O., Okonogi, S., Schiffelers, R.M., Hennink, W.E., 2014. Curcumin nanoformulations: A review of pharmaceutical properties and preclinical studies and clinical data related to cancer treatment. Biomaterials; 35:3365-3383.

Nambiar, D., Singh, R.P., 2013. Advances in Prostate Cancer Chemoprevention: A Translational Perspective. Nutrition and Cancer-an International Journal; 65:12-25.

Narayanan, N.K., Nargi, D., Randolph, C., Narayanan, B.A., 2009. Liposome encapsulation of curcumin and resveratrol in combination reduces prostate cancer incidence in PTEN knockout mice. International Journal of Cancer; 125:1-8.

Neto, A.M.P., de Souza, R.A.S., Leon-Nino, A.D., da Costa, J.D.A., Tiburcio, R.S., Nunes, T.A., de Mello, T.C.S., Kanemoto, F.T., Saldanha-Correa, F.M.P., Gianesella, S.M.F., 2013. Improvement in microalgae lipid extraction using a sonication-assisted method. Renewable Energy; 55:525-531.

Newton, W., McManus, A., 2011. Consumption of fish and Alzheimer's Disease. Journal of Nutrition Health & Aging; 15:551-552.

Nguyen, T.X., Huang, L., Liu, L., Abdalla, A.M.E., Gauthier, M., Yang, G., 2014. Chitosan-coated nano-liposomes for the oral delivery of berberine hydrochloride. Journal of Materials Chemistry B; 2:7149-7159.

Nirmala, R., Park, H.-M., Navamathavan, R., Kang, H.-S., El-Newehy, M.H., Kim, H.Y., 2011. Lecithin blended polyamide-6 high aspect ratio nanofiber scaffolds via electrospinning for human osteoblast cell culture. Materials Science and Engineering: C; 31:486-493.

Norris, L., Karmokar, A., Howells, L., Steward, W.P., Gescher, A., Brown, K., 2013. The role of cancer stem cells in the anti-carcinogenicity of curcumin. Mol Nutr Food Res; 57(9):1630-7.

Nguyen, T.X., Huang, L., Liu, L., Abdalla, A.M.E., Gauthier, M., Yang, G., 2014. Chitosan-coated nano-liposomes for the oral delivery of berberine hydrochloride. J. Mater. Chem. B 2, 7149–7159.

Ogawa, S., Decker, E.A., McClements, D.J., 2003. Production and characterization of O/W emulsions containing cationic droplets stabilized by lecithin-chitosan membranes. Journal of Agricultural and Food Chemistry; 51:2806-2812.

Ohori, H., Yamakoshi, H., Tomizawa, M., Shibuya, M., Kakudo, Y., Takahashi, A., Takahashi, S., Kato, S., Suzuki, T., Ishioka, C., Iwabuchi, Y., Shibata, H., 2006. Synthesis and biological analysis of new curcumin analogues bearing an enhanced potential for the medicinal treatment of cancer. Mol Cancer Ther; 5(10):2563-71.

Pagano, R.E., Weinstein, J.N., 1978. Interactions of liposomes with mammalian cells. Annu Rev Biophys Bioeng; 7:435-68.

Pan Ch, J., Tang, J.J., Weng, Y.J., Wang, J., Huang, N., 2006. Preparation, characterization and anticoagulation of curcumin-eluting controlled biodegradable coating stents. J Control Release; 116(1):42-9.

Paolino, D., Fresta, M., Sinha, D., Ferrari, M., 2006. Drug delivery systems. J.G. Webester (Ed.), Encyclopedia of medical devices and instrumentation (2nd ed.), John Wiley and Sons; pp. 437–495.

Pardeike, J., Hommoss, A., MÃ¼ller, R.H., 2009. Lipid nanoparticles (SLN, NLC) in cosmetic and pharmaceutical dermal products. International Journal of Pharmaceutics; 366:170-184.

Paris, L., Cecchetti, S., Spadaro, F., Abalsamo, L., Lugini, L., Pisanu, M.E., Iorio, E., Natali, P.G., Ramoni, C., Podo, F., 2010. Inhibition of phosphatidylcholine-specific phospholipase C downregulates HER2 overexpression on plasma membrane of breast cancer cells. Breast Cancer Research; 12:R27.

Parize, A.L., Heller, M., Favere, V.T., Laranjeira, M.C.M., Brighente, I.M.C., Micke, G.A., Souza, T.C.R., 2009. Impregnation of Chitosan Microspheres with the Natural Dye Curcuma. Latin American Journal of Pharmacy; 28:19-26.

Park, J.H., Musa-Veloso, K., Lynch, B., Leslie, H., Koo, K.H., Kim, S.B., Kang, S.N., 2012. 13-Week oral toxicity study of oil derived from squid (Todarodes pacificus) in Sprague-Dawley rats. Regulatory Toxicology and Pharmacology; 64:195-204.

Park, W., Amin, A.R., Chen, Z.G., Shin, D.M., 2013. New perspectives of curcumin in cancer prevention. Cancer Prev Res (Phila); 6(5):387-400.

Parvathy, K.S., Negi, P.S., Srinivas, P., 2009. Antioxidant, antimutagenic and antibacterial activities of curcumin-β-diglucoside. Food Chemistry; 115:265-271.

Patel, N., Schmid, U., Lawrence, M.J., 2006. Phospholipid-based microemulsions suitable for use in foods. Journal of Agricultural and Food Chemistry; 54:7817-7824.

Patra, D., El Khoury, E., Ahmadieh, D., Darwish, S., Tafech, R.M., 2012. Effect of Curcumin on Liposome: Curcumin as a Molecular Probe for Monitoring Interaction of Ionic Liquids with 1,2-Dipalmitoyl-sn-Glycero-3-Phosphocholine Liposome. Photochemistry and Photobiology; 88:317-327.

Pawlikowska-Pawlega, B., Misiak, L.E., Zarzyka, B., Paduch, R., Gawron, A., Gruszecki, W.I., 2013. FTIR, (1)H NMR and EPR spectroscopy studies on the interaction of flavone apigenin with dipalmitoylphosphatidylcholine liposomes. Biochim Biophys Acta; 1828(2):518-27.

Peng, J.L., Larondelle, Y., Pham, D., Ackman, R.G., Rollin, X., 2003. Polyunsaturated fatty acid profiles of whole body phospholipids and triacylglycerols in anadromous and landlocked Atlantic salmon (Salmo salar L.) fry. Comparative Biochemistry and Physiology B-Biochemistry & Molecular Biology; 134:335-348.

Perry, R.L.S., Yang, C., Soora, N., Salma, J., Marback, M., Naghibi, L., Ilyas, H., Chan, J., Gordon, J.W., McDermott, J.C., 2009. Direct Interaction between Myocyte Enhancer Factor 2 (MEF2) and Protein Phosphatase 1 alpha Represses MEF2-Dependent Gene Expression. Molecular and Cellular Biology; 29:3355-3366.

Pickova, J., Morkore, T., 2007. Alternate oils in fish feeds. European Journal of Lipid Science and Technology; 109:256-263.

Pieszka, M., Tombarkiewicz, B., Roman, A., Migdal, W., Niedziolka, J., 2013. Effect of bioactive substances found in rapeseed, raspberry and strawberry seed oils on blood lipid

profile and selected parameters of oxidative status in rats. Environmental Toxicology and Pharmacology; 36:1055-1062.

Pires, N.R., Cunha, P.L.R., Maciel, J.S., Angelim, A.L., Melo, V.M.M., de Paula, R.C.M., Feitosa, J.P.A., 2013. Sulfated chitosan as tear substitute with no antimicrobial activity. Carbohydrate Polymers; 91:92-99.

Podo, F., 1999. Tumour phospholipid metabolism. NMR Biomed; 12(7):413-39.

Prasad, S., Tyagi, A.K., Aggarwal, B.B., 2014. Recent Developments in Delivery, Bioavailability, Absorption and Metabolism of Curcumin: the Golden Pigment from Golden Spice. Cancer Research and Treatment; 46:2-18.

Primard, C., Rochereau, N., Luciani, E., Genin, C., Delair, T., Paul, S., Verrier, B., 2010. Traffic of poly(lactic acid) nanoparticulate vaccine vehicle from intestinal mucus to sub-epithelial immune competent cells. Biomaterials; 31:6060-6068.

Priyadarsini, K.I., 2009. Photophysics, photochemistry and photobiology of curcumin: Studies from organic solutions, bio-mimetics and living cells. Journal of Photochemistry and Photobiology C-Photochemistry Reviews; 10:81-95.

Priyadarsini, K.I., 2014. The Chemistry of Curcumin: From Extraction to Therapeutic Agent. Molecules; 19:20091-20112.

Pulz, O., Gross, W., 2004. Valuable products from biotechnology of microalgae. Applied Microbiology and Biotechnology; 65:635-648.

Qian, C., Decker, E.A., Xiao, H., McClements, D.J., 2012. Inhibition of Î²-carotene degradation in oil-in-water nanoemulsions: Influence of oil-soluble and water-soluble antioxidants. Food Chemistry; 135:1036-1043.

Qin, X.Y., Cheng, Y., Cui, J., Zhang, Y., Yu, L.C., 2009. Potential protection of curcumin against amyloid beta-induced toxicity on cultured rat prefrontal cortical neurons. Neuroscience Letters; 463:158-161.

Quinn, J.F., Raman, R., Thomas, R.G., Yurko-Mauro, K., Nelson, E.B., Van Dyck, C., Galvin, J.E., Emond, J., Jack, C.R., Weiner, M., Shinto, L., Aisen, P.S., 2010. Docosahexaenoic Acid Supplementation and Cognitive Decline in Alzheimer Disease A Randomized Trial. Jama-Journal of the American Medical Association; 304:1903-1911.

Rajeswari, A., Sabesan, M., 2008. Inhibition of monoamine oxidase-B by the polyphenolic compound, curcumin and its metabolite tetrahydrocurcumin, in a model of Parkinson's disease induced by MPTP neurodegeneration in mice. Inflammopharmacology; 16:96-99.

Ravindran, P.N., Nirmal Babu, K., Sivaraman, K., 2007. Medicinal and Aromatic Plants–Industrial Profiles: Turmeric: The Genus Curcuma. CRC Press, Washintogton; 484 p.

Reddy, A.C., Lokesh, B.R., 1992. Studies on spice principles as antioxidants in the inhibition of lipid peroxidation of rat liver microsomes. Mol Cell Biochem; 111(1-2):117-24.

Ringman, J.M., Frautschy, S.A., Cole, G.M., Masterman, D.L., Cummings, J.L., 2005. A potential role of the curry spice curcumin in Alzheimer's disease. Current Alzheimer research; 2:131-136.

Rodriguez, M.S., Albertengo, L.E., 2005. Interaction between chitosan and oil under stomach and duodenal digestive chemical conditions. Bioscience Biotechnology and Biochemistry; 69:2057-2062.

Rose, D.P., 1997. Effects of dietary fatty acids on breast and prostate cancers: evidence from in vitro experiments and animal studies. American Journal of Clinical Nutrition; 66:S1513-S1522.

Rubba, P., Iannuzzi, A., 2001. N-3 to n-6 fatty acids for managing hyperlipidemia, diabetes, hypertension and atherosclerosis: Is there evidence? European Journal of Lipid Science and Technology; 103:407-418.

Ruby, A.J., Kuttan, G., Babu, K.D., Rajasekharan, K.N., Kuttan, R., 1995. Anti-tumour and antioxidant activity of natural curcuminoids. Cancer Lett; 94(1):79-83.

Rungphanichkul, N., Nimmannit, U., Muangsiri, W., Rojsitthisak, P., 2011. Preparation of curcuminoid niosomes for enhancement of skin permeation. Pharmazie; 66(8):570-5.

Ryu, E.K., Choe, Y.S., Lee, K.-H., Choi, Y., Kim, B.-T., 2006. Curcumin and dehydrozingerone derivatives: synthesis, radiolabeling, and evaluation for beta-amyloid plaque imaging. Journal of medicinal chemistry; 49(20):6111-6119.

Saengkrit, N., Saesoo, S., Srinuanchai, W., Phunpee, S., Ruktanonchai, U.R., 2014. Influence of curcumin-loaded cationic liposome on anticancer activity for cervical cancer therapy. Colloids and Surfaces B: Biointerfaces; 114:349-356.

Saha, S., Adhikary, A., Bhattacharyya, P., Das, T., Sa, G., 2012. Death by design: where curcumin sensitizes drug-resistant tumours. Anticancer Res, 32(7):2567-84.

Said, D.E., ElSamad, L.M., Gohar, Y.M., 2012. Validity of silver, chitosan, and curcumin nanoparticles as anti-Giardia agents. Parasitology Research, 111:545-554.

Sakai, H., Sato, A., Takeoka, S., Tsuchida, E., 2007. Rheological properties of hemoglobin vesicles (artificial oxygen carriers) suspended in a series of plasma-substitute solutions. Langmuir, 23:8121-8128.

Sakihama, Y., Cohen, M.F., Grace, S.C., Yamasaki, H., 2002. Plant phenolic antioxidant and prooxidant activities: phenolics-induced oxidative damage mediated by metals in plants. Toxicology, 177:67-80.

Salager, J.L., Rondón, M., Tolosa, L., Pizzino, A., Bullón, J., 2007. Emulsion Formulation engineering for the Practitioner. Encyclopedia of Surface and Colloid Science, Second Edition. Taylor & Francis; p. 1-16.

Sanders, C.L., 2003. Prevention and therapy of cancer and other common diseases: alternative and traditional approaches. Mis à jour en 2003.

Sandur, S.K., Ichikawa, H., Pandey, M.K., Kunnumakkara, A.B., Sung, B., Sethi, G., Aggarwal, B.B., 2007. Role of pro-oxidants and antioxidants in the anti-inflammatory and apoptotic effects of curcumin (diferuloylmethane). Free Radical Biology and Medicine; 43:568-580.

Sanoj Rejinold, N., Muthunarayanan, M., Divyarani, V.V., Sreerekha, P.R., Chennazhi, K.P., Nair, S.V., Tamura, H., Jayakumar, R., 2011 b. Curcumin-loaded biocompatible thermoresponsive polymeric nanoparticles for cancer drug delivery. Journal of Colloid and Interface Science; 360:39-51.

Sanoj Rejinold, N., Sreerekha, P.R., Chennazhi, K.P., Nair, S.V., Jayakumar, R., 2011 a. Biocompatible, biodegradable and thermo-sensitive chitosan-g-poly (N-isopropylacrylamide) nanocarrier for curcumin drug delivery. International Journal of Biological Macromolecules; 49:161-172.

Sareen, R., Jain, N., Pandit, V., 2013. Curcumin: a boon to colonic diseases. Curr Drug Targets; 14(10):1210-8.

Sarkar, A., Horne, D.S., Singh, H., 2010. Pancreatin-induced coalescence of oil-in-water emulsions in an in vitro duodenal model. International Dairy Journal ; 20:589-597.

Sautot, P., 2011. Propriétés d'auto-assemblage de phospholipides riches en acides gras polyinsaturés : caractérisation physico-chimique et simulation de bicouches par dynamique moléculaire. Thèse, ENSAIA-INPL Nancy.

Sautot, P., Tarek, M., Stebe, M.J., Paris, C., Arab-Tehrany, E., Linder, M., 2011. Structural, hydration, and phase transition properties of phosphatidylcholine from salmon heads. European Journal of Lipid Science and Technology; 113:744-755.

Schaffer, M., Schaffer, P.M., Zidan, J., Bar Sela, G., 2011. Curcuma as a functional food in the control of cancer and inflammation. Curr Opin Clin Nutr Metab Care; 14(6):588-597.

Schmidt, E.B., Rasmussen, L.H., Rasmussen, J.G., Joensen, A.M., Madsen, M.B., Christensen, J.H., 2006. Fish, marine n-3 polyunsaturated fatty acids and coronary heart disease: A minireview with focus on clinical trial data. Prostaglandins Leukotrienes and Essential Fatty Acids; 75:191-195.

Schneider, M., Lovaas, E., 2009. Process for the production of phospholipids. US2009/0028989.

Seal, B.L., Otero, T.C., Panitch, A., 2001. Polymeric biomaterials for tissue and organ regeneration. Materials Science and Engineering: R: Reports; 34:147-230.

Setthacheewakul, S., Mahattanadul, S., Phadoongsombut, N., Pichayakorn, W., Wiwattanapatapee, R., 2010 Development and evaluation of self-microemulsifying liquid and pellet formulations of curcumin, and absorption studies in rats. Eur J Pharm Biopharm; 76(3): 475-85.

Severcan, F., Sahin, I., Kazanci, N., 2005. Melatonin strongly interacts with zwitterionic model membranes - evidence from Fourier transform infrared spectroscopy and differential scanning calorimetry. Biochimica et Biophysica Acta-Biomembranes; 1668:215-222.

Shaikh, J., Ankola, D.D., Beniwal, V., Singh, D., Kumar, M.N., 2009. Nanoparticle encapsulation improves oral bioavailability of curcumin by at least 9-fold when compared to curcumin administered with piperine as absorption enhancer. Eur J Pharm Sci; 37(3-4):223-30.

Shankar, S., Srivastava, R.K., 2007. Involvement of Bcl-2 family members, phosphatidylinositol 3 '-kinase/AKT and mitochondrial p53 in curcumin (diferulolylmethane)-induced apoptosis in prostate cancer. International Journal of Oncology; 30:905-918.

Shanmugam, M.K., Rane, G., Kanchi, M.M., Arfuso, F., Chinnathambi, A., Zayed, M.E., Alharbi, S.A., Tan, B.K.H., Kumar, A.P., Sethi, G., 2015. The Multifaceted Role of Curcumin in Cancer Prevention and Treatment. Molecules; 20(2):2728-2769.

Sharma, A., Sharma, U.S., 1997. Liposomes in drug delivery: progress and limitations. International Journal of Pharmaceutics; 154:123-140.

Sharma, O.P., 1976. Antioxidant activity of curcumin and related compounds. Biochemical Pharmacology; 25:1811-1812.

Sharma, R.A., Gescher, A.J., Steward, W.P., 2005. Curcumin: The story so far. European Journal of Cancer; 41:1955-1968.

Sharma, V., Nehru, B., Munshi, A., Jyothy, A., 2010. Antioxidant Potential of Curcumin against Oxidative Insult Induced by Pentylenetetrazol in Epileptic Rats. Methods and Findings in Experimental and Clinical Pharmacology; 32:227-232.

Shehzad, A., Lee, J., Lee, Y.S., 2013. Curcumin in various cancers. Biofactors; 39:56-68.

Shelma, R., Sharma, C.P., 2013. In vitro and in vivo evaluation of curcumin loaded lauroyl sulphated chitosan for enhancing oral bioavailability. Carbohydrate Polymers; 95:441-448.

Shen, C.R., Liu, C.L., Lee, H.P., Chen, J.K., 2013. The Identification and Characterization of Chitotriosidase Activity in Pancreatin from Porcine Pancreas. Molecules; 18:2978-2987.

Shen, L., Ji, H.F., 2007a. Theoretical study on physicochemical properties of curcumin. Spectrochimica Acta Part a-Molecular and Biomolecular Spectroscopy; 67:619-623.

Shepherd, R., Reader, S., Falshaw, A., 1997. Chitosan functional properties. Glycoconjugate journal; 14(4):535-542.

Shi, M., Cai, Q., Yao, L., Mao, Y., Ming, Y., Ouyang, G., 2006. Antiproliferation and apoptosis induced by curcumin in human ovarian cancer cells. Cell Biology International; 30:221-226.

Shi, X.-Y., Sun, C.-M., Wu, S.-K., 1999. Evaluation of in vitro stability of small unilamellar vesicles coated with collagen and chitosan. Polymer International; 48:212-216.

Shim, J.S., Kim, D.H., Jung, H.J., Kim, J.H., Lim, D., Lee, S.-K., Kim, K.-W., Ahn, J.W., Yoo, J.-S., Rho, J.-R., 2002. Hydrazinocurcumin, a novel synthetic curcumin derivative, is a potent inhibitor of endothelial cell proliferation. Bioorg Med Chem; 10(8):2439-44.

Shimizu, K., Maitani, Y., Takayama, K., Nagai, T., 1996. Characterization of dipalmitoylphosphatidylcholine liposomes containing a soybean-derived sterylglucoside mixture by differential scanning calorimetry, Fourier transform infrared spectroscopy, and enzymatic assay. Journal of Pharmaceutical Sciences; 85:741-744.

Shin, G.H., Chung, S.K., Kim, J.T., Joung, H.J., Park, H.J., 2013. Preparation of Chitosan-Coated Nanoliposomes for Improving the Mucoadhesive Property of Curcumin Using the Ethanol Injection Method. Journal of Agricultural and Food Chemistry; 61:11119-11126.

Shoba, G., Joy, D., Joseph, T., Majeed, M., Rajendran, R., Srinivas, P., 1998. Influence of piperine on the pharmacokinetics of curcumin in animals and human volunteers. Planta Medica; 64:353-356.

Silva, S.M.L., Braga, C.R.C., Fook, M.V.L., Raposo, C.M.O., Carvalho, L.H., Canedo, E.L., 2012. Application of infrared spectroscopy to analysis of chitosan/clay nanocomposites. Infrared spectroscopy-materials science, engineering and technology; pp. 43-62.

Singer, S.J., 2004. Some early history of membrane molecular biology. Annual Review of Physiology; 66:1-27.

Singh, H., Sarkar, A., 2010. Behaviour of protein-stabilised emulsions under various physiological conditions. Advances in Colloid and Interface Science; 165:47-57.

Singh, R.P., Agarwal, R., 2006. Mechanisms of action of novel agents for prostate cancer chemoprevention. Endocrine-Related Cancer; 13:751-778.

Singh, U., Verma, S., Ghosh, H.N., Rath, M.C., Priyadarsini, K.I., Sharma, A., Pushpa, K.K., Sarkar, S.K., Mukherjee, T., 2010. Photo-degradation of curcumin in the presence of TiO2 nanoparticles: Fundamentals and application. Journal of Molecular Catalysis a-Chemical; 318:106-111.

Sinha, D., Biswas, J., Sung, B., Aggarwal, B.B., Bishayee, A., 2012. Chemopreventive and Chemotherapeutic Potential of Curcumin in Breast Cancer. Current Drug Targets; 13:1799-1819.

Song, X.D., Zhang, J.J., Wang, M.R., Liu, W.B., Gu, X.B., Lv, C.J., 2011a. Astaxanthin Induces Mitochondria-Mediated Apoptosis in Rat Hepatocellular Carcinoma CBRH-7919 Cells. Biological & Pharmaceutical Bulletin; 34:839-844.

Song, Z.M., Feng, R.L., Sun, M., Guo, C.Y., Gao, Y., Li, L.B., Zhai, G.X., 2011b. Curcumin-loaded PLGA-PEG-PLGA triblock copolymeric micelles: Preparation, pharmacokinetics and distribution in vivo. Journal of Colloid and Interface Science; 354:116-123.

Sonvico, F., Cagnani, A., Rossi, A., Motta, S., Di Bari, M.T., Cavatorta, F., Alonso, M.J., Deriu, A., Colombo, P., 2006. Formation of self-organized nanoparticles by lecithin/chitosan ionic interaction. International Journal of Pharmaceutics; 324:67-73.

Sonvico, F., Dubernet, C., Colombo, P., Couvreur, P., 2005. Metallic colloid nanotechnology, applications in diagnosis and therapeutics. Curr Pharm Des ; 11(16):2095-105.

Sorlier, P., Denuziere, A., Viton, C., Domard, A., 2001. Relation between the degree of acetylation and the electrostatic properties of chitin and chitosan. Biomacromolecules; 2(3):765-72.

Sou, K., Inenaga, S., Takeoka, S., Tsuchida, E., 2008. Loading of curcumin into macrophages using lipid-based nanoparticles. International Journal of Pharmaceutics; 352:287-293.

Stan, S.D., Singh, S.V., Brand, R.E., 2010. Chemoprevention strategies for pancreatic cancer. Nature Reviews Gastroenterology & Hepatology; 7:347-356.

Strasser, E.M., Wessner, B., Manhart, N., Roth, E., 2005. The relationship between the anti-inflammatory effects of curcumin and cellular glutathione content in myelomonocytic cells. Biochemical Pharmacology; 70:552-559.

Suarez, E.R., Mugford, P.F., Rolle, A.J., Burton, I.W., Walter, J.A., Kralovec, J.A., 2010. C-13-NMR Regioisomeric Analysis of EPA and DHA in Fish Oil Derived Triacylglycerol Concentrates. Journal of the American Oil Chemists Society; 87:1425-1433.

Sugihara, H., Yamamoto, H., Kawashima, Y., Takeuchi, H., 2012. Effectiveness of submicronized chitosan-coated liposomes in oral absorption of indomethacin. Journal of Liposome Research; 22:72-79.

Sun, J.B., Bi, C., Chan, H.M., Sun, S.P., Zhang, Q.W., Zheng, Y., 2013. Curcumin-loaded solid lipid nanoparticles have prolonged in vitro antitumour activity, cellular uptake and improved in vivo bioavailability. Colloids and Surfaces B-Biointerfaces; 111:367-375.

Sung, B., Kunnumakkara, A.B., Sethi, G., Anand, P., Guha, S., Aggarwal, B.B., 2009. Curcumin circumvents chemoresistance in vitro and potentiates the effect of thalidomide and bortezomib against human multiple myeloma in nude mice model. Mol Cancer Ther; 8(4):959-70.

Suresh, D., Srinivasan, K., 2007. Studies on the in vitro absorption of spice principles - Curcurmin, capsaicin and piperine in rat intestines. Food and Chemical Toxicology; 45:1437-1442.

Suresh, D., Srinivasan, K., 2010. Tissue distribution & elimination of capsaicin, piperine & curcumin following oral intake in rats. Indian Journal of Medical Research; 131:682-691.

Swanson, D., Block, R., Mousa, S.A., 2012a. Omega-3 fatty acids EPA and DHA: health benefits throughout life. Advances in Nutrition: An International Review Journal; 3(1):1-7.

Syng-ai, C., Kumari, A.L., Khar, A., 2004. Effect of curcumin on normal and tumor cells: Role of glutathione and bcl-2. Molecular Cancer Therapeutics; 3:1101-1108.

Tadros, T.F., 2010. Rheology of Dispersions: Principles and Applications. Wiley-VCH.

Takahashi, M., Inafuku, K., Miyagi, T., Oku, H., Wada, K., Imura, T., Kitamoto, D., 2006. Efficient preparation of liposomes encapsulating food materials using lecithins by a mechanochemical method. Journal of Oleo Science; 56(1):35-42.

Takahashi, M., Uechi, S., Takara, K., Asikin, Y., Wada, K., 2009. Evaluation of an Oral Carrier System in Rats: Bioavailability and Antioxidant Properties of Liposome-Encapsulated Curcumin. Journal of Agricultural and Food Chemistry; 57:9141-9146.

Takeuchi, H., Matsui, Y., Yamamoto, H., Kawashima, Y., 2003. Mucoadhesive properties of carbopol or chitosan-coated liposomes and their effectiveness in the oral administration of calcitonin to rats. Journal of Controlled Release; 86:235-242.

Takeuchi, H., Yamamoto, H., Niwa, T., Hino, T., Kawashima, Y., 1996. Enteral absorption of insulin in rats from mucoadhesive chitosan-coated liposomes. Pharmaceutical Research; 13:896-901.

Takeuchi, H., Yamamoto, H., Toyoda, T., Toyobuku, H., Hino, T., Kawashima, Y., 1998. Physical stability of size controlled small unilameller liposomes coated with a modified polyvinyl alcohol. International Journal of Pharmaceutics; 164:103-111.

Tang, B.C., Dawson, M., Lai, S.K., Wang, Y.Y., Suk, J.S., Yang, M., Zeitlin, P., Boyle, M.P., Fu, J., Hanes, J., 2009. Biodegradable polymer nanoparticles that rapidly penetrate the human mucus barrier. Proceedings of the National Academy of Sciences of the United States of America; 106:19268-19273.

Tanzi, C.D., Vian, M.A., Ginies, C., Elmaataoui, M., Chemat, F., 2012. Terpenes as Green Solvents for Extraction of Oil from Microalgae. Molecules; 17:8196-8205.

Taylor, T.M., Davidson, P.M., Bruce, B.D., Weiss, J., 2005. Liposomal nanocapsules in food science and agriculture. Crit Rev Food Sci Nutr; 45(7-8):587-605.

Temraz, S., Mukherji, D., Shamseddine, A., 2013. Potential targets for colorectal cancer prevention. Int J Mol Sci; 14(9):17279-303.

Tergaonkar, V., 2009 p53 and NFkappaB: fresh breath in the cross talk. Cell Res; 19(12):1313-5.

Terry, P.D., Terry, J.B., Rohan, T.E., 2004. Long-chain (n-3) fatty acid intake and risk of cancers of the breast and the prostate: Recent epidemiological studies, biological mechanisms, and directions for future research. Journal of Nutrition; 134:3412S-3420S.

Teuscher, E., Anton, R., Lobestein, A., Rohner, C., Bernard, M., 2005. Plantes aromatiques : Epices, aromates, condiments, et huiles essentielles. ÉDITIONS TEC ET DOC / LAVOISIER; 522:216-223.

Thangapazham, R.L., Sharma, A., Maheshwari, R.K., 2006. Multiple molecular targets in cancer chemoprevention by curcumin. Aaps Journal 8, E443-E449.

Thanki, K., Gangwal, R.P., Sangamwar, A.T., Jain, S., 2013. Oral delivery of anticancer drugs: Challenges and opportunities. Journal of Controlled Release; 170:15-40.

Thiyagarajan, M., Sharma, S.S., 2004. Neuroprotective effect of curcumin in middle cerebral artery occlusion induced focal cerebral ischemia in rats. Life Sciences, 74:969-985.

Thomas, P., Wang, Y.-J., Zhong, J.-H., Kosaraju, S., O'Callaghan, N.J., Zhou, X.-F., Fenech, M., 2009. Grape seed polyphenols and curcumin reduce genomic instability events in a transgenic mouse model for Alzheimer's disease. Mutation Research-Fundamental and Molecular Mechanisms of Mutagenesis; 661:25-34.

Tikekar, R.V., Pan, Y.J., Nitin, N., 2013. Fate of curcumin encapsulated in silica nanoparticle stabilized Pickering emulsion during storage and simulated digestion. Food Research International; 51:370-377.

Tiyaboonchai, W., Tungpradit, W., Plianbangchang, P., 2007. Formulation and characterization of curcuminoids loaded solid lipid nanoparticles. International Journal of Pharmaceutics; 337:299-306.

Tohda, C., Nakayama, N., Hatanaka, F., Komatsu, K., 2006. Comparison of anti-inflammatory activities of six Curcuma rhizomes: A possible curcuminoid-independent pathway mediated by Curcuma phaeocaulis extract. Evidence-Based Complementary and Alternative Medicine; 3:255-260.

Tønnesen, H.H., 2002. Solubility, chemical and photochemical stability of curcumin in surfactant solutions: Studies of curcumin and curcuminoids, XXVIII. Pharmazie, 57:820-824.

Tonnesen, H.H., Karlsen, J., 1985. Studies on curcumin and curcuminoids. VI. Kinetics of curcumin degradation in aqueous solution. Z Lebensm Unters Forsch; 180(5):402-4.

Tønnesen, H.H., Másson, M.r., Loftsson, T., 2002. Studies of curcumin and curcuminoids. XXVII. Cyclodextrin complexation: solubility, chemical and photochemical stability. International Journal of Pharmaceutics; 244:127-135.

Trachootham, D., Alexandre, J., Huang, P., 2009. Targeting cancer cells by ROS-mediated mechanisms: a radical therapeutic approach? Nat Rev Drug Discovery; 8:579-591.

Trautwein, E.A., 2001. N-3 Fatty acids - physiological and technical aspects for their use in food. European Journal of Lipid Science and Technology; 103:45-55.

Tripathi, D.N., Jena, G.B., 2010. Astaxanthin intervention ameliorates cyclophosphamide-induced oxidative stress, DNA damage and early hepatocarcinogenesis in rat: Role of Nrf2, p53, p38 and phase-II enzymes. Mutation Research-Genetic Toxicology and Environmental Mutagenesis; 696:69-80.

Van der Meerena, G., Tlusty, M., Metzlerc, A., Van der Meerend, T., 2009. Effects of dietary DHA and EPA on neurogenesis, growth, and survival of juvenile American lobster, Homarus americanus. . New Zealand Journal of Marine and Freshwater Research; 43:225-232

Vandenberg, G.W., Drolet, C., Scott, S.L., de la Noue, J., 2001. Factors affecting protein release from alginate-chitosan coacervate microcapsules during production and gastric/intestinal simulation. Journal of Controlled Release ; 77:297-307.

Vaquier, L., 2010. Intérêt d'un nouveau nutricament à visée anti-inflammatoire dans la gestion de troubles locomoteurs chez le cheval, aspects bibliographiques et étude clinique. Doctorat vétérinaire. École nationale vétérinaire d'Alfort.

Velioglu, H.M., Temiz, H.T., Boyaci, I.H., 2015. Differentiation of fresh and frozen-thawed fish samples using Raman spectroscopy coupled with chemometric analysis. Food Chemistry; 172:283-290.

Vemula, P.K., Li, J., John, G., 2006. Enzyme catalysis: tool to make and break amygdalin hydrogelators from renewable resources: a delivery model for hydrophobic drugs. Journal of the American Chemical Society; 128:8932-8938.

Versluis, P., van de Pas, J.C., Mellema, J., 2001. Influence of salt concentration and surfactant concentration on the microstructure and rheology of lamellar liquid crystalline phases. Langmuir; 17:4825-4835.

Von Low, E.C., Perabo, F.G.E., Siener, R., Muller, S.C., 2007. Facts and fiction of phytotherapy for prostate cancer: A critical assessment of preclinical and clinical data. In Vivo; 21:189-204.

Von Schacky, C., 2014. Omega-3 Index and Cardiovascular Health. Nutrients; 6:799-814.

Wahlstrom, B., Blennow, G., 1978. A study on the fate of curcumin in the rat. Acta Pharmacol Toxicol; 43(2):86-92.

Wajda, R., Zirkel, J., Schaffer, T., 2007. Increase of bioavailability of coenzyme Q(10) and vitamin E. Journal of Medicinal Food; 10:731-734.

Walters, D.K., Muff, R., Langsam, B., Born, W., Fuchs, B., 2008. Cytotoxic effects of curcumin on osteosarcoma cell lines. Investigational New Drugs; 26:289-297.

Wanasundara, U.N., Wanasundara, J.P.D., 2006. γ-Linolenic acid: purification and functionality , in: Handbook of Functional Lipids,. C.C. Akoh, Ed., Taylor & Francis: (New York).

Wang, M., Thanou, M., 2010. Targeting nanoparticles to cancer. Pharmacol Res; 62(2):90-9.

Wang, Q., Sun, A.Y., Simonyi, A., Jensen, M.D., Shelat, P.B., Rottinghaus, G.E., MacDonald, R.S., Miller, D.K., Lubahn, D.E., Weisman, G.A., Sun, G.Y., 2005. Neuroprotective mechanisms of curcumin against cerebral ischemia-induced neuronal apoptosis and behavioral deficits. Journal of Neuroscience Research; 82:138-148.

Wang, R., Xu, Y., Wu, H.L., Li, Y.B., Li, Y.H., Guo, H.B., Li, X.J., 2008a. The antidepressant effects of curcumin in the forced swimming test involve 5-HT1 and 5-HT2 receptors. European Journal of Pharmacology; 578:43-50.

Wang, S., Tan, M., Zhong, Z., Chen, M., Wang, Y., 2011. Nanotechnologies for curcumin: an ancient puzzler meets modern solutions. . Journal of Nanomaterials ; 2011:51.

Wang, X.Y., Jiang, Y., Wang, Y.W., Huang, M.T., Ho, C.T., Huang, Q.R., 2008b. Enhancing anti-inflammation activity of curcumin through O/W nanoemulsions. Food Chemistry; 108:419-424.

Wang, Y.J., Pan, M.H., Cheng, A.L., Lin, L.I., Ho, Y.S., Hsieh, C.Y., Lin, J.K., 1997. Stability of curcumin in buffer solutions and characterization of its degradation products. Journal of Pharmaceutical and Biomedical Analysis; 15:1867-1876.

Wilart, P., Jinnantina, J., Uma, P., Samlee, M., 2009. Anti-Phytopthora capsici Activities and Potential Use as Antifungal in Agriculture of Alpinia galanga Swartz, Curcuma longa Linn, Boesenbergia pandurata Schut and Chromolaena odorata: Bioactivities Guided Isolation of Active Ingredients. American Journal of Agricultural and Biological Sciences; 4:83-91.

Wilken, R., Veena, M.S., Wang, M.B., Srivatsan, E.S., 2011. Curcumin: A review of anti-cancer properties and therapeutic activity in head and neck squamous cell carcinoma. Molecular Cancer; 10(12):1-19.

Wydro, P., Krajewska, B., Hac-Wydro, K., 2007. Chitosan as a lipid binder: A Langmuir monolayer study of chitosan - Lipid interactions. Biomacromolecules; 8:2611-2617.

Xing, H., Tang, L., Yang, X.J., Hwang, K., Wang, W.D., Yin, Q., Wong, N.Y., Dobrucki, L.W., Yasui, N., Katzenellenbogen, J.A., Helferich, W.G., Cheng, J.J., Lu, Y., 2013. Selective delivery of an anticancer drug with aptamer-functionalized liposomes to breast cancer cells in vitro and in vivo. Journal of Materials Chemistry B; 1:5288-5297.

Yallapu, M.M., Gupta, B.K., Jaggi, M., Chauhan, S.C., 2010. Fabrication of curcumin encapsulated PLGA nanoparticles for improved therapeutic effects in metastatic cancer cells. Journal of Colloid and Interface Science; 351:19-29.

Yallapu, M.M., Jaggi, M., Chauhan, S.C., 2013. Curcumin Nanomedicine: A Road to Cancer Therapeutics. Current Pharmaceutical Design; 19:1994-2010.

Yanagisawa, D., Shirai, N., Amatsubo, T., Taguchi, H., Hirao, K., Urushitani, M., Morikawa, S., Inubushi, T., Kato, M., Kato, F., Morino, K., Kimura, H., Nakano, I., Yoshida, C., Okada, T., Sano, M., Wada, Y., Wada, K.-n., Yamamoto, A., Tooyama, I., 2010. Relationship between the tautomeric structures of curcumin derivatives and their Abeta-binding activities in the context of therapies for Alzheimer's disease. Biomaterials; 31:4179-4185.

Yang, F., Lim, G.P., Begum, A.N., Ubeda, O.J., Simmons, M.R., Ambegaokar, S.S., Chen, P.P., Kayed, R., Glabe, C.G., Frautschy, S.A., Cole, G.M., 2005. Curcumin inhibits formation of amyloid beta oligomers and fibrils, binds plaques, and reduces amyloid in vivo. J Biol Chem; 280(7):5892-901.

Yang, H., Irudayaraj, J., 2000. Characterization of semisolid fats and edible oils by fourier transform infrared photoacoustic spectroscopy. Journal of the American Oil Chemists Society; 77:291-295.

Yang, K.Y., Lin, L.C., Tseng, T.Y., Wang, S.C., Tsai, T.H., 2007. Oral bioavailabilit of curcurnin in rat and the herbal analysis from Curcuma longa by LC-MS/MS. Journal of Chromatography B-Analytical Technologies in the Biomedical and Life Sciences; 853:183-189.

Yang, R.L., Zhang, S.A., Kong, D.L., Gao, X.L., Zhao, Y.J., Wang, Z., 2012. Biodegradable Polymer-Curcumin Conjugate Micelles Enhance the Loading and Delivery of Low-Potency Curcumin. Pharmaceutical Research; 29:3512-3525.

Yang, Y., Jiang, J.S., Du, B., Gan, Z.F., Qian, M., Zhang, P., 2009. Preparation and properties of a novel drug delivery system with both magnetic and biomolecular targeting. J Mater Sci Mater Med; 20(1):301-7.

Yates, C.M., Calder, P.C., Rainger, G.E., 2014. Pharmacology and therapeutics of omega-3 polyunsaturated fatty acids in chronic inflammatory disease. Pharmacology & therapeutics; 141(3):272-282.

Yazdi, P.G., 2013. A review of the biologic and pharmacological role of docosapentaenoic acid. F1000Research; 25:2:256.

Yen, F.-L., Wu, T.-H., Lin, L.-T., Cham, T.-M., Lin, C.-C., 2008. Nanoparticles formulation of Cuscuta chinensis prevents acetaminophen-induced hepatotoxicity in rats. Food and Chemical Toxicology; 46:1771-1777.

Yokoyama, M., 2005. Drug targeting with nano-sized carrier systems. J Artif Organs; 8(2):77-84.

Yu, H., Huang, Q., 2010. Enhanced in vitro anti-cancer activity of curcumin encapsulated in hydrophobically modified starch. Food Chemistry; 119:669-674.

Yu, N., Atienza, J.M., Bernard, J., Blanc, S., Zhu, J., Wang, X., Xu, X., Abassi, Y.A., 2005. Real-Time Monitoring of Morphological Changes in Living Cells by Electronic Cell Sensor Arrays: An Approach To Study G Protein-Coupled Receptors. Analytical Chemistry; 78:35-43.

Yuan, Y., Gao, Y., Zhao, J., Mao, L., 2008. Characterization and stability evaluation of β-carotene nanoemulsions prepared by high pressure homogenization under various emulsifying conditions. Food Research International; 41: 61-68.

Zaru, M., Manca, M.L., Fadda, A.M., Antimisiaris, S.G., 2009. Chitosan-coated liposomes for delivery to lungs by nebulisation. Colloids and Surfaces B-Biointerfaces; 71:88-95.

Zhang, H., Alsarra, I.A., Neau, S.H., 2002. An in vitro evaluation of a chitosan-containing multiparticulate system for macromolecule delivery to the colon. International Journal of Pharmaceutics; 239:197-205.

Zhang, H.Y., Arab Tehrany, E., Kahn, C.J.F., Ponnçot, M., Linder, M., Cleymand, F., 2012a. Effects of nanoliposomes based on soya, rapeseed and fish lecithins on chitosan thin films designed for tissue engineering. Carbohydrate Polymers; 88:618-627.

Zhang, J.F., Tang, Q., Xu, X.Y., Li, N., 2013. Development and evaluation of a novel phytosome-loaded chitosan microsphere system for curcumin delivery. International Journal of Pharmaceutics; 448:168-174.

Zhang, L., Lu, C.T., Li, W.F., Cheng, J.G., Tian, X.Q., Zhao, Y.Z., Li, X., Lv, H.F., Li, X.K., 2012b. Physical characterization and cellular uptake of propylene glycol liposomes in vitro. Drug Development and Industrial Pharmacy; 38:365-371.

Zhu, R.R., Qin, L.L., Wang, M., Wu, S.M., Wang, S.L., Zhang, R., Liu, Z.X., Sun, X.Y., Yao, S.D., 2009. Preparation, characterization, and anti-tumor property of podophyllotoxin-loaded solid lipid nanoparticles. Nanotechnology; 20(5):055702.

Zhu, X.Q., Ye, A.Q., Verrier, T., Singh, H., 2013. Free fatty acid profiles of emulsified lipids during in vitro digestion with pancreatic lipase. Food Chemistry; 139:398-404.

Zlotogorski, A., Dayan, A., Dayan, D., Chaushu, G., Salo, T., Vered, M., 2013. Nutraceuticals as new treatment approaches for oral cancer - I: Curcumin. Oral Oncology; 49:187-191.

Zweers, M.L.T., Grijpma, D.W., Engbers, G.H.M., Feijen, J., 2003. The preparation of monodisperse biodegradable polyester nanoparticles with a controlled size. Journal of Biomedical Materials Research Part B-Applied Biomaterials; 66B:559-566.

Résumé

La curcumine est un polyphénol de couleur jaune extrait du rhizome de la plante (*Curcuma longa*). Identifié comme un principe actif du curcuma, cette épice est largement consommée compte tenu de ses propriétés antioxydantes, antimicrobiennes et antitumorales. Cependant, sa solubilité et sa biodisponibilité restent limitées en raison de son hydrophobicité et diminuent de ce fait les applications potentielles dans les domaines nutraceutique et pharmaceutique. L'objectif de ce travail s'est focalisé sur l'étude des propriétés physico-chimiques de cette molécule vectorisée sous forme liposomale. Différentes formulations de nanovecteurs préparées à partir de lipides polaires plus ou moins riches en acides gras polyinsaturés à longue chaîne variables, issus de source marine ou végétale, ont été utilisées pour modifier la fluidité membranaire des vecteurs. Ces travaux ont permis d'optimiser le pourcentage d'encapsulation de cette biomolécule et d'étudier les effets de cytotoxicité et de sa biodisponibilité sur différentes lignées cellulaires (MCF7, cellules embryonnaires de neurones corticaux). Les résultats montrent des effets significatifs lors de l'utilisation de nanoliposomes formulés avec de la lécithine marine, protégés par un enrobage de polymère de chitosane. Les analyses physicochimiques de taille par diffraction de la lumière (zetasizer, nanosight), de stabilité (mesure de la taille et la mobilité électrophorétique), de structure par microscopie électronique en transmission et la libération de la molécule vectorisée, ont permis de mieux comprendre les effets des interactions polymère-phospholipides et le relargage de la curcumine encapsulée dans les conditions environnementales drastiques de digestion gastrique et intestinale. Une caractérisation multi-échelle est proposée afin d'améliorer la compréhension des différentes propriétés du nanovecteur et du principe actif qu'il vectorise, ainsi que les interactions possibles entre eux. Les techniques utilisées sont la spectroscopie infrarouge à transformée de Fourier (FTIR), les rayons X, ainsi que la microscopie électronique en transmission.

Mot clés : Vectorisation, liposome, curcumine, chitosane, propriétés physico-chimiques, transfert, cytotoxicité, lignées cellulaires, interactions.

Abstract

Curcumin, a yellow lipid-soluble natural pigment, a hydrophobic polyphenol derived from the rhizome of *Curcuma longa*, has been identified as the active principle of turmeric. Curcumin has already become a research focus due to its numerous biological and pharmacological benefits such as antioxidant, antitumor, anti-inflammatory, antimicrobial properties and other desirable medical benefits. However, due to its low absorption, the poor bioavailability of curcumin limits its clinical use. The objective of this work has focused on the study of the physicochemical properties of this molecule encapsulated in form of liposome. Different formulations of nanocarriers prepared from polar lipids more or less rich in polyunsaturated fatty acids with variable long chain, derived from vegetable or marine source, have been used to modify liposomes membrane fluidity. These works have allowed to optimize the encapsulation efficiency of the curcumin and to study its bioavailability and cytotoxicity effects on different cell lines (MCF7, embryonic cortical neurons). The results show significant effects when using nanoliposomes formulated with marine lecithin, protected by chitosan as the coating polymer. The physico-chemical analyses of the size by light scattering (Zetasizer, NanoSight), the stability (measurement of the size and the electrophoretic mobility), the structure by transmission electron microscopy and the release of the encapsulated molecule, allowed to better understand the effects of polymer-phospholipid interactions and the release of encapsulated curcumin in drastic environmental conditions of gastric and intestinal digestion. A multiscale characterization is proposed in order to improve the understanding of the various properties of the active agent (curcumin) and the nanovector, as well as the possible interactions occuring between them. The techniques used are Fourier Transform Infrared Spectroscopy (FTIR), X-rays, Rheometer and Transmission Electron Microscopy.

Keyword: Encapsulation, liposome, curcumin, chitosan, physico-chemical, cytotoxicity, cell lines, interactions.